# Development of a eukaryotic microbial fuel cell using *Arxula adeninivorans*

---

A thesis
submitted in partial fulfillment
of the requirements for the Doctorate of
Philosophy of Biochemistry

at

Lincoln University

By

N. D. Haslett

---

Lincoln University

2012

Abstract of a thesis submitted in partial fulfillment of the

requirements for the Doctorate of Philosophy of Biochemistry

**Development of a microbial fuel cell for organic waste bioremediation and simultaneous electricity generation**

**by N.D. Haslett**

The bulk of microbial fuel cell work has been conducted on prokaryotic microorganisms, with eukaryotes considered too sluggish. Access to the electron transport chain in the mitochondrion appeared to be the limiting factor. There are useful eukaryotic microorganisms yet to be investigated in the microbial fuel cell field.

*Arxula adeninivorans* is a dimorphic yeast with a large substrate range and high osmotic and temperature tolerances making it a good candidate for study in a eukaryotic microbial fuel cell. This thesis demonstrated that *A. adeninivorans* can participate in both mediated and mediator-less electron transfer in a microbial fuel cell, secreting an electrochemically active substance that contributes to the mediator-less power density when $KMnO_4$ is used in the cathode as the final electron acceptor.

A large number of physical, electrochemical and biological factors were investigated with several novel behaviours reported. Different fuel cell configurations, different electrodes, cell immobilization, different cathode

reactions, comparisons to different microorganisms, mixed culture microbial fuel cells and gene over-expression were attempted to both increase electrical output and the understanding of the limitations of eukaryotic microbial fuel cells so that they could be overcome. Research was conducted with *A. adeninivorans* in a large variety of MFC configurations and conditions to map out future work that would be required to create a model for optimal eukaryotic microbial fuel cell performance.

**Key words:** Microbial fuel cell, MFC, Yeast, Eukaryote, Electrochemistry, Biochemistry, Microbiology, Osmium Polymers, Mediators, *Arxula adeninivorans, Saccharomyces cerevisiae, Pseudomonas aerugenosa,* AFRE2, Transformation, Power Density, Model, Internal Resistance, Cyclic Voltammetry.

**Acknowledgements**

I would like to thank my supervisors Associate Professor Ravi Gooneratne, Dr Neil Pasco and Keith Baronian for their guidance, preparation and help throughout my entire PhD. I would also like to that the Marie Curie Foundation, The Enterprise Foundation, Danish Technical University, Lincoln University, Lund University, Christchurch Polytechnic Institute of Technology and the University of Canterbury for making this PhD possible. Finally thank you to all my friends, family and work colleagues for their help and support.

# Contents

# Table of Figures and Tables

# Table of Abbreviations

| | |
|---|---|
| h | Hour |
| $^{o}C$ | Degrees Celsius |
| CV | Cyclic Voltammogram |
| WP | Working Potential |
| E | Potential |
| V | Voltage |
| i | Current |
| P | Power |
| PD | Power Density |
| FC | Ferricyanide |
| FoC | Ferrocyanide |
| $mVs^{-1}$ | milli Volts per second |

# Chapter 1: Introduction

## 1.1. Background

Microbial fuel cells (MFCs) use microorganisms to generate electricity. The use of microorganisms as a biological catalyst limits the substrates used and the conditions within the MFC to those which the microorganism within it can thrive on (Bullen *et al.* 2006). As a result, the amount of electricity obtained from a MFC is small relative to other alternative energy products (MacKay 2009).

Microorganisms are also integral to bioremediation of most forms of wastewater. By incorporating MFCs into bioremediation it is possible to simultaneously generate small amounts of electricity thereby lowering the cost of bioremediation. Wastewater MFCs primarily use enriched microbial consortia originating from the bioremediation process as their biological catalyst(s) (Logan 2005). In contrast, MFCs containing monocultures are primarily used in fundamental studies of MFCs and electron transfer (Logan 2008).

A large proportion of the monoculture MFC work is conducted with prokaryotes, because eukaryote MFCs are considered ‘sluggish’ and/or ‘lethargic (Bennetto 1990; Wilkinson 2000). There are a large number of yeasts and other eukaryotes which have a wide range of growth conditions and a large substrate range which would be ideal for incorporation into a wastewater MFC that have not previously been investigated due to inadequate electricity generation.

## 1.2. Aims

The overall aim of this project was to investigate the different possible types of electron transfer in yeast MFC and to characterise how different modifications to the growth conditions, the MFC and the microorganisms, affect the power density produced by the MFC.

In addition, our goal is to increase the fundamental and practical characteristics of yeast MFC so that viable 'real world' yeast MFC can be produced.

### 1.3. Objectives

- **To characterise a MFC containing *A. adeninivorans* as the biological catalyst.**

Initially, a two-chambered MFC containing *A. adeninivorans* as the biological catalyst with potassium permanganate used in the cathode was characterised using different external loads, mediators and cyclic voltammetry (Chapter 3).

- **To investigate mediator-less power density from *A. adeninivorans* and *S. cerevisiae* in a MFC.**

Investigation into mediator-less power density of *A. adeninivorans* within a MFC were conducted through comparative studies with *S. cerevisiae* using mediators, cyclic voltammetry and different cathode reactions (Chapter 4).

- **To characterise mediated electron transfer in a MFC.**

Investigation into the mediated electron transfer of TMPD and ferricyanide within MFC were conducted using comparative studies between *A. adeninivorans* and *S. cerevisiae* using linear sweep voltammetry, cyclic voltammetry and MFC (Chapter 5).

- **To supplement ferricyanide with an osmium polymer in a double mediated poised potential MFC.**

Investigations into the possibility of replacing soluble mediators with polymers were conducted using an osmium polymer that has previously been shown to facilitate electrical wiring between a prokaryote and the electrode (Timor *et al.* 2007). Different strains of *S. cerevisiae* were used in both single and double mediated poise potential MFC. Different metabolic transformants of *S. cerevisiae* and inhibitors were used to ensure that the osmium polymer was sufficiently sensitive to detect changes in metabolic activity of the cells (Chapter 6).

- **To characterise the effect of different growth conditions and MFC configurations on power density**

The effect of varied growth and MFC configurations on power density were characterised using *A. adeninivorans* as the biological catalyst. Carbon sources, temperature, anaerobic, growth phase, and five different configurations of the MFC were investigated (Chapter 7).

- **To characterise preselected mixed cultures in a MFC**

The effect of exoelectrogens, which self-produce mediators, on power density was investigated in the MFC in pure and mixed cultures with different yeast species. The microorganisms *P. aeruginosa, A. adeninivorans* and *S. cerevisiae* where selected to be investigated when grown together and separately. Cyclic voltammetry, MFC results and observations were used to evaluate mediator production and the effect on power density (Chapter 8).

- **To characterise *A. adeninivorans* transformants containing the AFRE 2 gene in a MFC**

Investigation into increasing the mediator-less power density through genetic modification of *A. adeninivorans* was conducted through using transformants containing an amplified AFRE2 gene which should result in over-expression of a ferricyanide reducing protein. MFC, cyclic voltammetry and linear sweep voltammetry were used to characterise the transformants (Chapter 9).

### 1.4. Hypotheses

- ***A. adeninivorans* can act as a biological catalyst in a MFC**

There have been a few MFC containing different yeast species as biological catalysts reported in the literature. These include: *Candida melibiosica* (Hubenova *et al.* 2010), *S. cerevisiae* (Gunawardena *et al.* 2008; Chiao *et al.* 2006; Walker and Walker 2006; Halme & Zhang 1995; Ganguli and Dunn 2008; Potter 1911; Cohen 1931) and *Hansenula anomala*

*(Pichia anomala)* (Prasad *et al.* 2007). This is the first reported use of *A. adeninivorans* in a MFC.

- ***A. adeninivorans* uses a different mechanism for generating mediator-less power density in a MFC compared to *S. cerevisiae*.**

*A. adeninivorans* is a non-conventional yeast, with temperature dependant dimorphism, a wide substrate range and a high temperature and osmotic tolerances (Wartmann *et al.* 1995; Terentiev *et al.* 2003). It is therefore likely that the mechanism for mediator-less electron transfer will be different between *A. adeninivorans* and *S. cerevisiae.*

- **The introduction of TMPD significantly improves the power density of a MFC containing *A. adeninivorans.***

2,3,5,6-Tetramethylphenylenediamine (TMPD) is a highly stable, non-toxic, lipophilic mediator, with a low standard reaction potential which has yielded good results in electrochemical studies of *S. cerevisiae* in the past (Baronian *et al.* 2002). It is hoped that TMPD will be able to enter the mitochondrion of *A. adeninivorans*, access the NADH, and transport the electrons to the anode, thus increasing the power density of the MFC.

- **Osmium polymer can replace ferricyanide in a double mediated poised potential MFC**

Two osmium polymers have been reported to wire two different *Pseudomonas* species to electrodes (Timur *et al.* 2007). One of those polymers has a redox potential that is similar to ferricyanide and therefore is possible that it could replace it in a double mediator system.

- **Growth conditions and MFC configurations have an effect on MFC power density**

Microorganisms are able to adjust to different growth conditions through adjusting metabolism, including expression of different genes. *A. adeninivorans* has a wide range of growth conditions which it can thrive in, and many of them were tested to look for increases

in power density. There is a wide range of MFC configurations reported in the literature (see literature review) and several of these were investigated in order to achieve increases in power density.

- **Mixed cultures increase mediator-less power density in a MFC.**

*P. aeruginosa* produces a mediator like compound called pyocyanin that has been attributed to an increase in MFC power density (Rabaey *et al.* 2006). Mixed cultures of *P. aeruginosa, S. cerevisiae* and *A. adeninivorans* were tested in the MFC, along with pyocyanin added to MFC containing different cultures.

- **The AFRE 2 gene contributes to mediator-less power density in a MFC.**

The AFRE 2 gene attributed to iron oxidation was transformed into *A. adeninivorans* by the "Institut für Pflanzengenetik und Kulturpflanzenforschung" (IPK) Gatersleben, Germany. These transformants were investigated for changes in power density using the MFC and cyclic voltammetry.

# Chapter 2: Literature Review

## 2.1. Introduction to Microbial Fuel Cells

The study of MFC is a blossoming and diverse field incorporating microorganisms and power production. A MFC is difficult to define and characterise in both device and concept, due to the diversity of the field. This diversity is because every single MFC component and concept is variable except one - microorganisms must be used in at least one of processes that contribute to the generation of power. Fuel cells that use enzymes alone are called bio-fuel cells or enzymatic fuel cells and fuel cells that do not use any microorganisms or enzymes (called fuel cells) will not be discussed in this thesis. The following literature review will discuss the different manifestations of microbial fuel cells, the different types of electron transfer, provide a historical perspective of microbial fuel cells, outline and compare reported applications, and then narrow the focus to the content and questions tested and answered within the thesis.

### 2.1.1. **Physical differences between microbial fuel cells**

There are several different ways to characterise the different types of microbial fuel cells. In a physical sense there are four different types:

#### 2.1.1.1. *Poised Potential MFC*

The potential of the anode of an electrochemical cell containing a microorganism at a set potential (Figure 2.1) and measures the resulting current (Bond *et al.* 2002). The external load of a poised potential MFC is that of the potentiostat, which holds the electrochemical cell at the desired potential. The potential can be held either by electrodes in the same chamber (Dumas *et al.* 2008; Niessen 2004) or by electrodes in different chambers connected by proton/cation exchange membrane or salt bridge (Bond *et al.* 2002; Bond & Lovely 2003; Chaudhuri & Lovely 2003; Cho & Ellington 2007).

This procedure is effectively the same as a whole cell biosensor. As a result, the same electrochemical tests have been conducted on poised potential MFCs as on whole cell biosensors (Cho & Ellington 2007; Manohar & Mansfeld 2009).

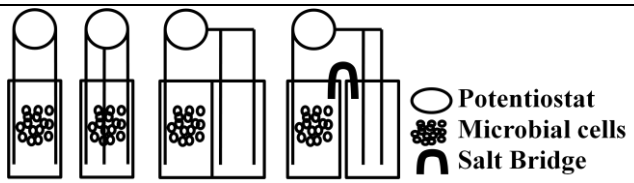


**Figure 2.1: Poised Potential Microbial Fuel Cells.** Poised potential MFC control the potential between the anode and the cathode. The potential can be controlled within a single chamber or across connected chambers (proton/cation exchange membrane or salt bridge).

2.1.1.2. *Double chambered MFC*

A double chambered MFC consists of an anode chamber and a cathode chamber. The anode chamber provides the electrons to the external circuit; the cathode chamber accepts the electrons after they have flowed through the external circuit. Both the anode and cathode participate in half of the overall reaction (half cells) where oxidation occurs at the anode and reduction occurs at the cathode. The anode and cathode can be separated by a proton exchange membrane, a cation exchange membrane, or a salt bridge. The double chambered MFC can operate with or without an external load and under batch or continuous conditions. Either chamber may contain microorganisms or the microorganisms fermented products (Figure 2.2). Logan *et al*. (2006) have comprehensively reviewed the two chamber MFC physical structures.

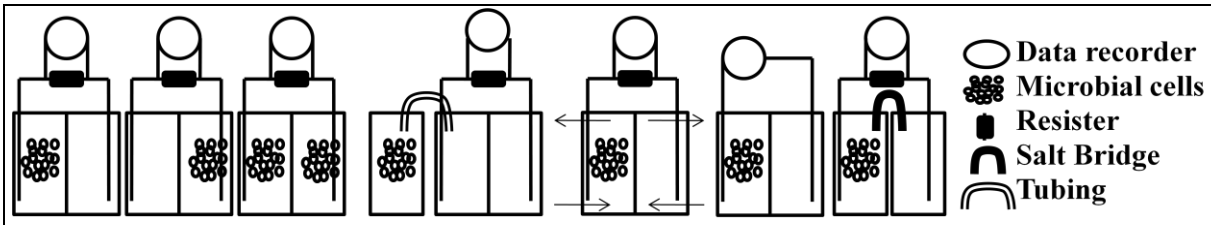


**Figure 2.2: Double Chamber Microbial Fuel Cells.** Double chambered MFCs can have the microorganisms in the anode and/or the cathode, as well as have the fermented products of microbial growth pumped in. The anode and/or the cathode can be operated under batch or continuous conditions. The double chambered MFC can be operated under external load and with a proton/cation exchange membrane or a salt bridge.

2.1.1.3. *Single chambered MFC*

Single chambered MFC consist of a single chamber with two electrodes (anode and cathode). The anode is always within the MFC, but the cathode can either be contained within the MFC or on the outside of the MFC (either separate or attached to a proton/cation exchange membrane). The single chambered MFC can operate with or without an external load and under batch or continuous conditions. The chamber may either contain microorganisms or their fermented products (Figure 2.3). The defining characteristic is the absence of a proton/cation exchange membrane/salt bridge. Logan *et al.* (2006) have comprehensively reviewed the single chamber MFC physical structures.

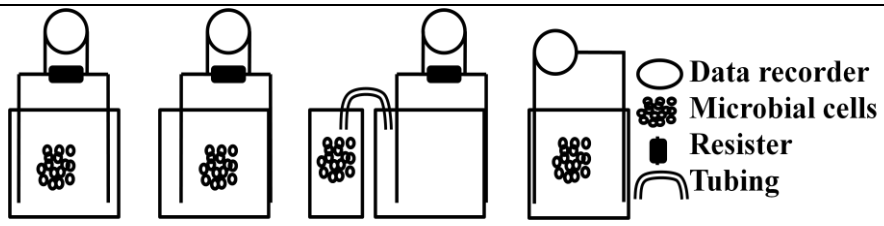


**Figure 2.3: Single Chamber Microbial Fuel Cells.** Single chamber MFC can have both the anode and cathode within the same chamber or have the cathode attached to a proton/cation exchange membrane facing the environmental air. Single chamber MFC can operate with microorganisms in the chamber or with the fermented products of their growth. They can also be operated with and without external load.

2.1.1.4. *Environmental MFC*

Environmental MFCs take advantage of environmental conditions. There are two types: The first consist of two electrodes, the anode in the anaerobic sediment of aquatic bodies (Tender *et al.* 2002; Lowy *et al.* 2006), and the cathode in the aerobic water above the sediment. The microorganism and their products that contribute to the electricity generation are those that are already present in these environments (Figure 2.4). The second type of environmental MFC consists of using photosynthetic microorganisms (*in vivo*) to harvest light (Zou *et al.* 2009).

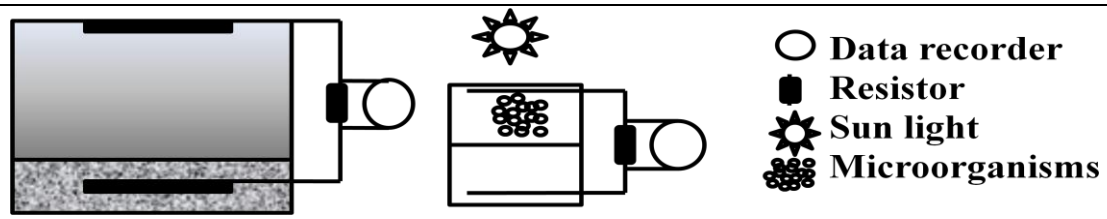


**Figure 2.4: Environmental Microbial Fuel Cells.** Environmental microbial fuel cells either consist of an anode buried in an anaerobic environment (ocean or river sediment), and a cathode suspended in the oxygenated water above, or use photosynthetic microorganisms to harvest light in their generation of electricity.

2.1.2. **Different types of electron transfer between microorganisms and the electrodes**

There are several different ways by which different types of MFCs harvest electrons from microorganisms:

*2.1.2.1. Direct electron transfer*

Electrons are transferred from the microorganisms through direct contact with the electrode surface. Prokaryotic membrane bound enzymes have been immobilized to electrodes to produce electricity (biofuel cells or enzymatic fuel cells), which indicates that direct electron transfer from prokaryotes is through an interaction between the electrode and reduction-oxidation (redox) enzymes. The enzymes attributed to this direct electron transfer in prokaryotes are electron transport chain enzymes, enzymes that reduce metals and nanowires

(Kim *et al.* 2004; Reguera *et al.* 2005; Rabaey & Verstraete 2005; Logan *et al.*2006; Zhao *et al.* 2009). However, in the case of eukaryotes the electron transport chain is contained within the mitochondrion and they do not produce nanowires. The mechanism allowing direct electron transfer between eukaryotes and the electrode is limited to metal reducing enzymes or a previously unidentified mechanism (Prasad *et al.* 2007; Zhao *et al.* 2007; Todisco *et al.* 2006; Kostesha *et al.* 2009; Avéret *et al.* 2002; Yang *et al.* 2007).

*2.1.2.2. Mediated electron transfer*

Electrons are transferred from the microorganisms through the introduction of redox molecules which are capable of acting as electron shuttles between the microorganisms and the electrode. The environment of the anode and cathode is normally aqueous to which the lipid membrane of a cell acts as a barrier. Therefore hydrophilic and lipophilic mediators are able to access electrons from microorganisms in different ways, which could prove beneficial if they were used in combination. Cohen (1931) was the first to use mediators in MFC and since then mediators have been used in probing the metabolism of eukaryotes (Zhao *et al.* 2007; Heiskanen *et al.* 2009; Baronian *et al.* 2002; Logan 2008)

2.1.2.3. *Self mediated electron transfer*

Electrons are transferred from the microorganisms through the production of redox molecules which are capable of acting as electron shuttles between the microorganisms and the electrode. These microorganisms are known as mediator producing exoelectrogens or self-mediators, and are able to produce primary (oxidisable metabolites) and/or secondary (reversibly reducible compounds) metabolites (Rabaey & Verstraete 2005)

2.1.2.4. *Fermentation products*

Electrons are transferred from the microorganisms through fermentation of a substrate by the microorganisms, then transferring the fermentation products to an electrode where it is allowed to react. Hydrogen, methane and alcohol are three examples of fermentation products

that have been used to power MFCs (Liu *et al.* 2005; Niessen *et al.* 2004; Oh & Logan 2005; Schröder *et al.* 2003)

This thesis is not application orientated (even though significant advances have been made). It is a study of the different types of electron transfer and the effects different factors have on the power generation by a MFC.

### 2.2. Historical perspective

Potter (1911) created the first microbial fuel cell. It was a double chambered microbial fuel cell, which used platinum electrodes, no external load, and a porous cylinder (salt bridge), to test two different microorganisms *Saccharomyces cerevisiae* and *Bacillus coli communis* (now called *Escherichia coli*). Because there was no external load applied to the system, an open circuit potential was observed between the two chambers, i.e. at open circuit potential the resistance is infinite, hence there is no current. Potter (1911) suggested that it is the fermentation products of these microorganisms that increased in concentration over time that created the potential difference between the two chambers and not due to direct contact between the microorganisms or the electrode surface. The microorganism and its fermented products were in the anode chamber and the cathode chamber contained a platinum electrode that was able to react with dissolved oxygen.

The next reported microbial fuel cell was also reported by Cohen (1931). It was a single chambered microbial fuel cell, which used a noble metal electrode and tested *Bacterium dysenteriae (Flexner), Corynebacterium diphtheria, Bacterium coli (*now called *Escherichia coli), Bacillus subtilis,* and *Proteus vulgaris.* They found that with the introduction of the mediators, potassium ferricyanide or benzoquinone could increase the potential to 35 volts and obtain 2 milliamps in a stacked arrangement with multiple cells linked up in series.

In the 1960's the National Aeronautics and Space Administration (NASA) attempted to convert organic waste into electricity, which increased the interest in this field (Shukla *et al.* 2004; Bullen *et al.* 2006). Manuscripts published around that time period from a variety of organisations including oil industry (Davis & Yarbrough 1962) were still exploratory in nature, testing double chambered – direct electron transfer (Davis & Yarbrough 1962) and fermentation to produce hydrogen (Rohrback *et al.* 1962). Several US patents were filed, but the literature and real world applications of MFCs were limited for the next few decades. Pant *et al.* (2010) and Berseneff (Personal Communication 2005) surveyed the number of publications containing the words "microbial fuel cell" through different search engines. They found fewer than five articles per year from 1990-1995, less than ten articles per year from 1995-1999, then an almost exponential increase from 2000 onwards. The marked increase in publications and applications of MFCs over the last decade is attributed to dwindling fossil fuel supplies (Lovely 2006; Davis & Higson 2007; Katz *et al.* 2003) and a dramatic demand for power production (Logan 2005; Rabaey & Verstraete 2005; Pant *et al.* 2010).

## 2.3. Applications of microbial fuel cells

There are many different applications for microbial fuel cells which broadly fall into either power generation and/or wastewater cleanup:

### 2.3.1. Power Generation

#### *2.3.1.1. Environmental*

In this category microbial fuel cells take advantage of environmental conditions. Two different types of environmental MFCs exist, those that use the anaerobic sediment and the oxygenated water above (Tender *et al.* 2002; Lowy *et al.* 2006), and those that use photosynthetic algae to harvest electricity from light (Zou *et al.* 2009).

#### *2.3.1.2. Medical*

Medical microbial fuel cells take advantage of conditions within the body to power medical devices, such as pacemaker implants (Han *et al.* 2010). They typically use blood to grow the microorganisms in the anode with air as the cathode.

*2.3.1.3. Batch*

There are double and single chambered MFCs that are run under batch conditions, on any substrate other than wastewater. Most fundamental studies, such as studies reported in this thesis belong to this category.

*2.3.1.4. Continuous*

Double and single camber MFCs that perform under continuous conditions on any substrate other than wastewater.

### 2.3.2. Wastewater Bioremediation

*1.3.2.1. Fermentation*

Fermentation MFC, require fermentative growth of a microorganism in a bioreactor prior to inoculation of a MFC. Fermentation products include ethanol, methanol, hydrogen, methane.

*1.3.2.2. Simultaneous power generation*

Electricity is produced at the same time, in the same chamber, as the wastewater is being digested by microorganism. This constitutes simultaneous power generation.

## 2.4. Microorganisms used in a microbial fuel cells

MFCs either use either pure cultures or a microbial consortium (community).

### 2.4.1. Pure cultures

*2.4.1.1. Aerobic*

MFCs that use microorganisms that normally grow aerobically attempt to coax the microorganisms to use the anode as the final electron acceptor instead of oxygen.

*2.4.1.2. Anaerobic*

Anaerobic MFCs use microorganisms that normally grow anaerobically, and harness the ability of microorganisms to use the anode as the final electron acceptor (Min & Angelidaki 2008).

*2.4.1.3. Fermentative*

Fermentative MFCs use a microorganism to ferment substrates, and produce power by reducing the products of this fermentation.

*2.4.1.4. Self mediating*

MFCs that use self mediating microorganisms rely on the microorganism to produce a compound that is able to react with the electrode (Rabaey *et al.* 2005).

### 2.4.2. Microbial consortia

*2.4.2.1. Enriched*

Microbial consortia using MFC studies, always originate from an environmental source. Once the microorganisms attached to the electrode from an environmental sample have been harvested and then reused, they are termed enriched. Rabaey *et al.* (2004) reported that anode compartment provides a selection pressure to select from the microorganism naturally present in the environmental sample for those best suited to the new MFC environment.

*2.4.1.5. Environmental*

Environmental consortia have been demonstrated for both the anode and the cathode by Tender *et al.* (2000), who located and identified different microbial consortia on the anode and the cathode. The anode was observed to have anaerobic consortia attached that changed with distance from the anode (Lowy *et al.* 2006). The cathode was observed to have a biofilm attached that facilitated the reduction of dissolved oxygen by the electrode.

The vast majority of MFC primarily use prokaryotic microorganisms and the microbial consortiums of anaerobic environments have demonstrated a dominance of iron, nitrogen and sulphur reducing prokaryotes. Therefore this study of eukaryotes in MFCs is quite rare.

## 2.5. Comparing power densities of microbial fuel cells

Standardisation of units of measure for MFC is a problem that has been highlighted in many reviews and several solutions have been suggested (Rabaey & Verstraete 2005; Bullen *et al.* 2006; Logan 2006; Davis & Higson 2007; Pant *et al.* 2010). For the purpose of comparison, the power density of reported MFCs will be compared (where possible) in this thesis, except for poised potential MFC which must use current density due to the potential being fixed by the potentiostat. An abridged version of these Tables (Tables 2.5.1, 2.5.2a, 2.5.2b, 2.5.3, & 2.5.4) is presented in this chapter to give a representation of the range of power densities, components, microorganisms and substrates involved in each category of MFC. A full unabbreviated version is presented in the Appendix 1-5 and will be referred to throughout this thesis. In many cases, the power density for the Tables was calculated from data reported in the materials and method section of the respective papers for the reasons discussed above, and in some cases where there were discrepancies.

**Table 2.1: Poised Potential Microbial Fuel Cells**

| Anode composition and Surface Area (SA) | Anode Contents | Poised Potential (V) | Mediators | Current Density ($Am^{-2}$) | Reference |
|---|---|---|---|---|---|
| Graphite Rod SA=0.00612 $m^2$ | *Geobacter sulfurreducens* + Acetate | 0.2 V (vs. Ag/AgCl) | N/A | 1.143 | Bond & Lovley (2003) |
| Graphite Rod SA=0.0065 $m^2$ | *Rhodoferax ferrireducens* + Glucose | 0.2 V (vs. Ag/AgCl) | N/A | 0.1 | Chaundhuri & Lovely (2003) |
| Graphite Plate SA=0.007 $m^2$ | *Shewanella oneidensis MR-1* + Lactate | 0.5 V (vs. Ag/AgCl) | N/A | 0.228 | Cho & Ellington (2007) |
| Graphite SA=0.00125 $m^2$ | *Geobacter sulfurreducens* | -0.6 V (vs. Ag/AgCl) | fumarate | 0.75 | Dumas *et al.* (2008) |
| Stainless Steel SA=0.00025 $m^2$ | *Geobacter sulfurreducens* | -0.6 V (vs. Ag/AgCl) | fumarate | 20.5 | Dumas *et al.* (2008) |
| Pt+ Polytetrafluoroaniline SA=0.0015 $m^2$ | *Clostridium butyricum* + Starch (Fermented) | 0.2 V (vs. Ag/AgCl) | N/A | 0.0011 | Niessen *et al.*(2004) |
| Pt+ Polytetrafluoroaniline SA=0.0015 $m^2$ | *Clostridium butyricum* + Molasses (Fermented) | 0.2 V (vs. Ag/AgCl) | N/A | 0.0011 | Niessen *et al.*(2004) |
| Pt + Polyaniline SA=0.0001 $m^2$ | *Escherichia coli* + glucose (Fermented) | 0.2 V (vs. Ag/AgCl) | N/A | 12 | Schröder *et al.* (2003) |
| Plain Graphite SA=0.005 $m^2$ | Domestic wastewater + Anaerobic Sludge | 0.2 V (vs. Ag/AgCl) | N/A | 0.6 | Wang *et al.* (2009) |

**Table 2.2a: Two Chambered Mediator-less Microbial Fuel cells**

| Anode composition and Surface Area (SA) | Anode Contents | Cathode composition and Surface Area (SA) | Cathode Contents | Power Density $Wm^{-2}$ | External Load Ω | Reference |
|---|---|---|---|---|---|---|
| Graphite Rod SA=0.0065 $m^2$ | *Rhodoferax ferrireducens* | Graphite Rod SA=0.0065 $m^2$ | Tris buffer ($O_2$) | 0.00171 | 1000 Ω | Chaundhuri & Lovely (2003) |
| Graphite Felt SA=0.02 $m^2$ | *Rhodoferax ferrireducens* | Graphite Felt SA=0.02 $m^2$ | Tris buffer ($O_2$) | 0.01262 | 1000 Ω | Chaundhuri & Lovely (2003) |
| Graphite Foam SA=0.0061 $m^2$ | *Rhodoferax ferrireducens* | Graphite Foam SA=0.0061 $m^2$ | Tris buffer ($O_2$) | 0.00147 | 1000 Ω | Chaundhuri & Lovely (2003) |
| Carbon Felt SA=0.0004 $m^2$ | *Candida melibiosica* | Carbon Felt SA=0.0004 $m^2$ | Ferricyanide | 0.036 | 1250 Ω | Hubenova *et al.* (2010) |
| Carbon Felt (+Ni) SA=0.0004 $m^2$ | *Candida melibiosica* | Carbon Felt SA=0.0004 $m^2$ | Ferricyanide | 0.72 | 530 Ω | Hubenova *et al.* (2010) |
| Rod Anode SA=0.005 $m^2$ | *Pseudomonas Aeruginosa* | Graphite SA=0.005 $m^2$ | Ferricyanide | 0.00121 | 20 Ω | Rabaey *et al.* (2005) |
| Rod Anode SA=0.005 $m^2$ | *Escherichia coli* | Graphite SA=0.005 $m^2$ | Ferricyanide | 0.00085 | 20 Ω | Rabaey *et al.* (2005) |
| Rod Anode SA=0.005 $m^2$ | *Lactobacillus amylovorus* | Graphite SA=0.005 $m^2$ | Ferricyanide | 0.00027 | 20 Ω | Rabaey *et al.* (2005) |
| Rod Anode SA=0.005 $m^2$ | *Alcaligenes faecalis* | Graphite SA=0.005 $m^2$ | Ferricyanide | 0.00044 | 20 Ω | Rabaey *et al.* (2005) |
| Rod Anode SA=0.005 $m^2$ | *Enterococcus faecium* | Graphite SA=0.005 $m^2$ | Ferricyanide | 0.00029 | 20 Ω | Rabaey *et al.* (2005) |
| Carbon Felt SA=0.00025 $m^2$ | *Desulfovibrio vulgaris* ($H_2$) | Carbon Felt SA=0.00025 $m^2$ | BOD + $ABTS^{2-}$ ($O_2$) | 3.6 | 1100 Ω | Tsujimura *et al.* (2001) |

**Table 2.2b : Two Chambered Meditated Microbial Fuel cells**

| Anode composition and Surface Area (SA) | Anode Contents | Mediator | Cathode composition and Surface Area (SA) | Cathode Contents | Power Density $Wm^{-2}$ | External Load Ω | Reference |
|---|---|---|---|---|---|---|---|
| Carbon fibre veil SA=0.018 $m^2$ | *Escherichia coli* + *glucose* | MB | Carbon fibre veil SA=0.018 $m^2$ | Ferricyanide | 0.001765 | 10 KΩ | Ieropoulos *et al.* (2005) |
| Carbon fibre veil SA=0.018 $m^2$ | *Escherichia coli* + *glucose* | HNQ | Carbon fibre veil SA=0.018 $m^2$ | Ferricyanide | 0.0016572 | 10 KΩ | Ieropoulos *et al.* (2005) |
| Carbon fibre veil SA=0.018 $m^2$ | *Escherichia coli* + *glucose* | Thionin | Carbon fibre veil SA=0.018 $m^2$ | Ferricyanide | 0.0016022 | 10 KΩ | Ieropoulos *et al.* (2005) |
| Carbon fibre veil SA=0.018 $m^2$ | *Escherichia coli* + *glucose* | MelB | Carbon fibre veil SA=0.018 $m^2$ | Ferricyanide | 0.0014544 | 10 KΩ | Ieropoulos *et al.* (2005) |
| Carbon fibre veil SA=0.018 $m^2$ | *Escherichia coli* + *glucose* | Neutral Red | Carbon fibre veil SA=0.018 $m^2$ | Ferricyanide | 0.0007072 | 10 KΩ | Ieropoulos *et al.* (2005) |
| Rod Anode SA=0.005 $m^2$ | *Pseudomonas Aeruginosa* | Pyocyanin | Graphite SA=0.005 $m^2$ | Ferricyanide | 0.00267 | 20 Ω | Rabaey *et al.* (2005) |
| Rod Anode SA=0.005 $m^2$ | *Escherichia coli* | Pyocyanin | Graphite SA=0.005 $m^2$ | Ferricyanide | 0.000236 | 20 Ω | Rabaey *et al.* (2005) |
| Rod Anode SA=0.005 $m^2$ | *Lactobacillus amylovorus* | Pyocyanin | Graphite SA=0.005 $m^2$ | Ferricyanide | 0.00113 | 20 Ω | Rabaey *et al.* (2005) |
| Rod Anode SA=0.005 $m^2$ | *Alcaligenes faecalis* | Pyocyanin | Graphite SA=0.005 $m^2$ | Ferricyanide | 0.000486 | 20 Ω | Rabaey *et al.* (2005) |
| Rod Anode SA=0.005 $m^2$ | *Enterococcus faecium* | Pyocyanin | Graphite SA=0.005 $m^2$ | Ferricyanide | 0.003977 | 20 Ω | Rabaey *et al.* (2005) |

Legend: Methylene Blue (MB), Neutral Red (NR), 2-hydroxy-1,4-naphthoquinone (HNQ), Meldola's blue (MelB).

**Table 2.3: Single Chamber Microbial Fuel Cells**

| Anode composition and Surface Area (SA) | Inoculum | Liquid | Cathode composition and Surface Area (SA) | Power Density $Wm^{-2}$ | External Load Ω | Reference |
|---|---|---|---|---|---|---|
| Glassy Carbon SA=0.016 $m^2$ | Activated sludge blanket | Synthetic wastewater + Glucose | Glassy Carbon SA=0.016 $m^2$ | 0.0734 | 250 Ω | Aldrovandi *et al.* (2009) |
| Carbon Cloth SA=0.0002 $m^2$ | Acetate acclimatised consortium | Glucose | Carbon Cloth + PTFE + Pt SA=0.0007 $m^2$ | 2.16 | 120 Ω | Catal *et al.* (2008) |
| Carbon Cloth SA=0.0002 $m^2$ | Acetate acclimatised consortium | Galactitol | Carbon Cloth + PTFE + Pt SA=0.0007 $m^2$ | 2.65 | 120 Ω | Catal *et al.* (2008) |
| Graphite felt SA=0.0465 $m^2$ | *Activated sludge* | Artificial wastewater ($O_2$) | Graphite felt SA=0.0089 $m^2$ | 0.0013 | 200 Ω | Huang & Logan (2008) |
| Platinum mesh SA=0.002 $m^2$ | Marine sediment | Ocean water (O2) | Platinum mesh SA=0.002 $m^2$ | 0.014 | 1500 Ω | Reimers *et al.* (2001) |
| Graphite fibre brushes SA=0.000707 | *Chlorella vulgaris* | Pt SA=0.000707 | $O_2$ | 0.98 | 350 Ω | Velasquez-Orta *et al.* (2009) |
| Graphite fibre brushes SA=0.000707 | *Ulva lactuca* | Pt SA=0.000707 | $O_2$ | 0.76 | 270 Ω | Velasquez-Orta *et al.* (2009) |
| Carbon Cloth SA=0.0006 $m^2$ | Anaerobic Sludge blanket + Glucose | Air ($O_2$) | Carbon Cloth SA=0.0006 $m^2$ (+Pt) | 0.401 | 1000 Ω | Sharma & Li (2010) |
| Carbon Cloth SA=0.0006 $m^2$ | anaerobic sludge blanket + Acetate | Air ($O_2$) | Carbon Cloth SA=0.0006 $m^2$ (+Pt) | 0.368 | 1000 Ω | Sharma & Li (2010) |
| Carbon Cloth SA=0.0006 $m^2$ | Anaerobic Sludge blanket + Ethanol | Air ($O_2$) | Carbon Cloth SA=0.0006 $m^2$ (+Pt) | 0.302 | 1000 Ω | Sharma & Li (2010) |

**Table 2.4: Environmental Microbial Fuel Cells**

| Anode composition and Surface Area (SA) | Anode Contents | Cathode composition and Surface Area (SA) | Cathode Contents | Power Density $Wm^{-2}$ | Notes | External Load Ω | Reference |
|---|---|---|---|---|---|---|---|
| AQDS modified Graphite disks SA=0.457$m^2$ | Marine sediment | Graphite disks SA=0.457 $m^2$ | Ocean water ($O_2$) | 0.098 | Immobilized Mediator | 5 Ω | Lowy *et al.* (2006) |
| GCC modified anode SA=0.183 $m^2$ | Marine sediment | Graphite disks SA=0.457 $m^2$ | Ocean water ($O_2$) | 0.105 | Immobilized Mediator | 5 Ω | Lowy *et al.* (2006) |
| Graphite Disk SA=0.183 $m^2$ | Marine sediment | Graphite Disk SA=0.183 $m^2$ | Ocean water (O2) | 0.028 | N/A | 14 Ω | Tender *et al.* (2002) |
| Carbon SA=0.005 $m^2$ | Synechocystis PCC-6803 biofilm | Carbon (+Pt) SA=0.00096 $m^2$ | Water ($O_2$) | 1.56 | Two chambered (HNQ) | 1000 Ω | Zou *et al.* (2009) |

Power density is calculated by multiplying the current with the voltage to obtain the number of watts, or power, and then dividing the result by the cross sectional surface area of the anode (Equation 1). Based on Ohm's Law the power density can be calculated only if the MFC is operated under an external load (Equation 2). It is common practice to only measure the voltage and calculate the power density by integrating Ohm's law into Equation 1 (Equation 3).

$$\text{Power Density } (Wm^{-2}) = \frac{\text{Current (A) x Voltage (V)}}{\text{Anode Surface Area (SA)}} \qquad \textbf{Equation 1}$$

$$\text{Voltage (V)} = \text{Resistance (Ω) x Current (A)} \qquad \textbf{Equation 2}$$

$$\text{Power Density } (Wm^{-2}) = \frac{\text{Voltage (V) x (Voltage (V) / Resistance (Ω))}}{\text{Surface Area (SA)}} \qquad \textbf{Equation 3}$$

It must be stressed that power density can only be calculated for MFC that are under load. If a MFC is not under load, it cannot produce a current (Ohms law). Although several papers have reported the potential and current for fuel cells that are not under load, the reality is that the

current in these system is then due to the internal resistance of the devices employed to measure the current (usually around 16,000 Ω).

For those systems that are under load, two factors must be taken into account. Firstly, the lower the external resistance, the harder the MFC has to work. This is because, at lower resistance, more electrons must be supplied from the microorganism to supply the current at the same voltage (Ohm's Law). The ability of the microorganisms to supply the current required in any MFC is dependent on the amount of substrate available, the number of microorganisms present, the type of electrodes used, the type of reaction that occurs in the cathode, and the type of MFC (Rabaey & Verstraete 2005; Bullen *et al.* 2006; Logan 2006: Davis & Higson 2007; Pant *et al.* 2010). Secondly, the external load which produces the optimal power density should be the same as the internal resistance of the microbial fuel cells:

According to Jacobi's Law, "Maximum power is transferred when the internal resistance of the source equals the resistance of the load, when the external resistance can be varied, and the internal resistance is constant" (Cartwright 2009).

Tables 2.1, 2.2a, 2.2b, 2.3, and 2.4 report and contrast the different physical types of MFC. Table 2.2 was split into two (mediated and mediator-less) because of size and ease of comparison. The general trends observed in the creation of these Tables were:

1) There are only a few truly environmental MFCs (environmental samples used in single or two chambered MFC are not considered environmental MFC in this thesis because Rabaey *et al.* 2004 demonstrated that the MFC anode exerts a selection pressure)
2) Mediated MFCs have a greater power density than equivalent mediator-less MFCs
3) Microbial consortia produce a greater power density than single culture MFCs
4) The MFCs with the highest power densities operate under the lowest external load, i.e. they have a low internal resistance (Jacobi's Law)

5) Carbon/graphite electrodes are the electrodes most commonly used
6) Ferricyanide or oxygen are the cathode molecules most commonly used

A couple of trends that are not immediately apparent from the above Tables are:

1) Prokaryotic single culture MFCs are studied more than eukaryotic MFCs
2) Mediated MFCs have not been vigorously investigated in recent years
3) Single chamber MFCs have a lower internal resistance and have only been investigated in the past 10 years.

## 2.6. Microbial fuel cell power production

In order to create electricity, a MFC must produce both voltage and current. In a two chamber MFC, a potential difference between the reactions occurring in each chamber creates the voltage. In a single chamber MFC, a potential difference between the two electrodes creates the voltage. By separating the two reactions, a two chamber MFC is able to use two completely different reactions and the potential created by each half reaction ($E^o$) can be selected for and changed, but a higher internal resistance is created by the separation of either a membrane or a salt bridge (Rabaey & Verstraete 2005).

## 2.7. A novel microbial fuel cell using *Arxula adeninivorans* as the biological catalyst

### 2.7.1. *Arxula adeninivorans*

There are many fundamental questions surrounding MFCs. In an effort to answer some of them, this thesis utilised the unconventional yeast *Arxula adeninivorans*. The reasons *A. adeninivorans* has been considered for research are:

1) It can metabolise a wide range of substrates
2) It is temperature and osmotically tolerant (Terentiev *et al.* 2003)
3) It is an eukaryote

4) It has temperature dependant dimorphism, i.e. A yeast at 37$^{o}$C and filamentous at 45$^{o}$C (Wartmann *et al.* 1995) and express different biochemical behaviours in each form

### 2.7.2. *Arxula* fuel cell design

A two chambered MFC was used for the bulk of the MFC work conducted in this thesis (Figure 2.5). The polycarbonate fuel cell design is based on that reported by Bennetto *et al.* (1990). Delaney *et al.* (1984) and Bennetto (1990) constructed with rubber gaskets to prevent leakage. A proton exchange membrane (Nafion membrane 115, DuPont, San Diego, USA, Fang *et al.* 2004) separated the 15 mL anode and cathode compartments. Four MFCs operated simultaneously in a shaking water bath at 37°C, 180 rpm, each with a 100 Ω resistor (Figure 2.6). The potential difference across the resister was measured every 5 mins (UT20B Multi-meter) and converted into power density (PD) using Equation 3.

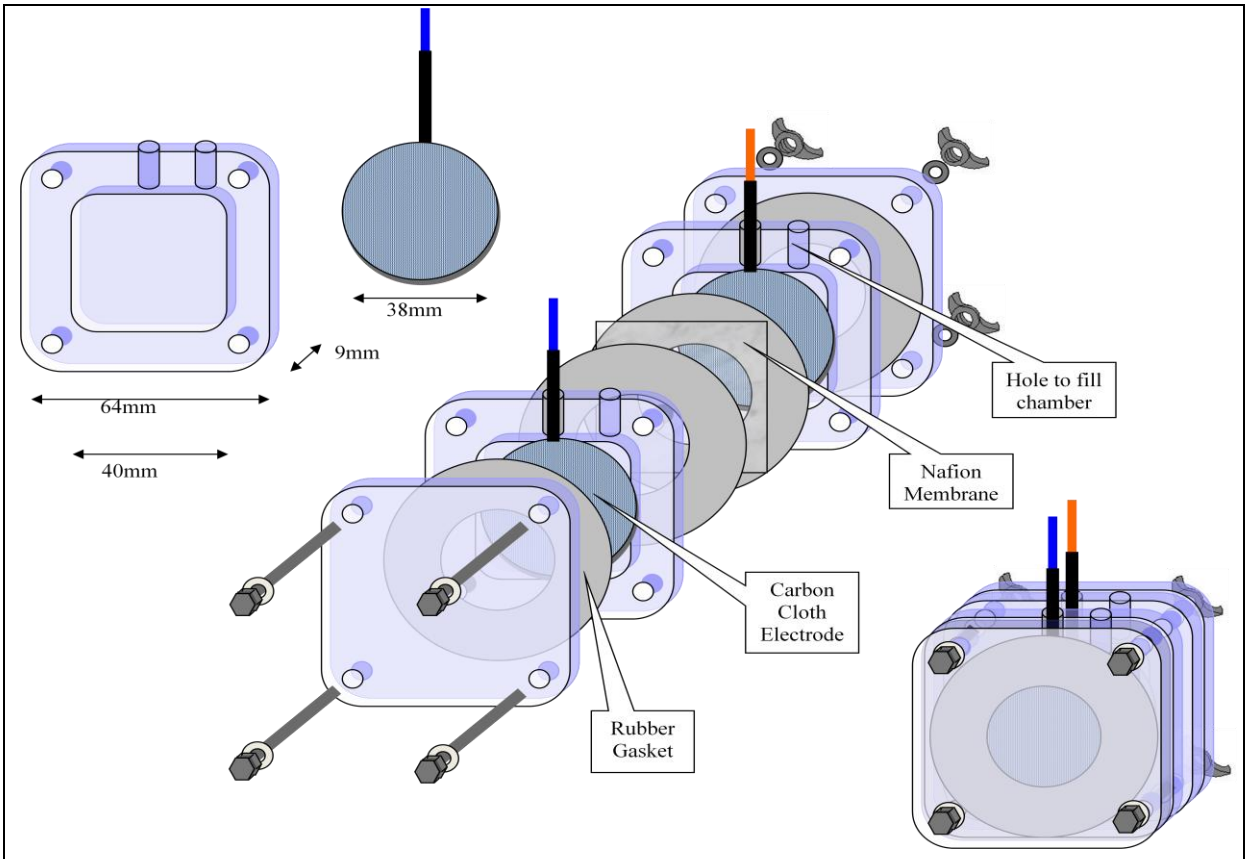


**Figure 2.5: Labelled explosion of two chambered Microbial fuel cell.** A polycarbonate external shell, fastened together using bolts and wing nuts, housed 15 mL anode and cathode chambers each containing a 0.001018 $m^2$ carbon cloth electrode. The anode and cathode chambers were separated by a nafion membrane with rubber gaskets to prevent leakage.

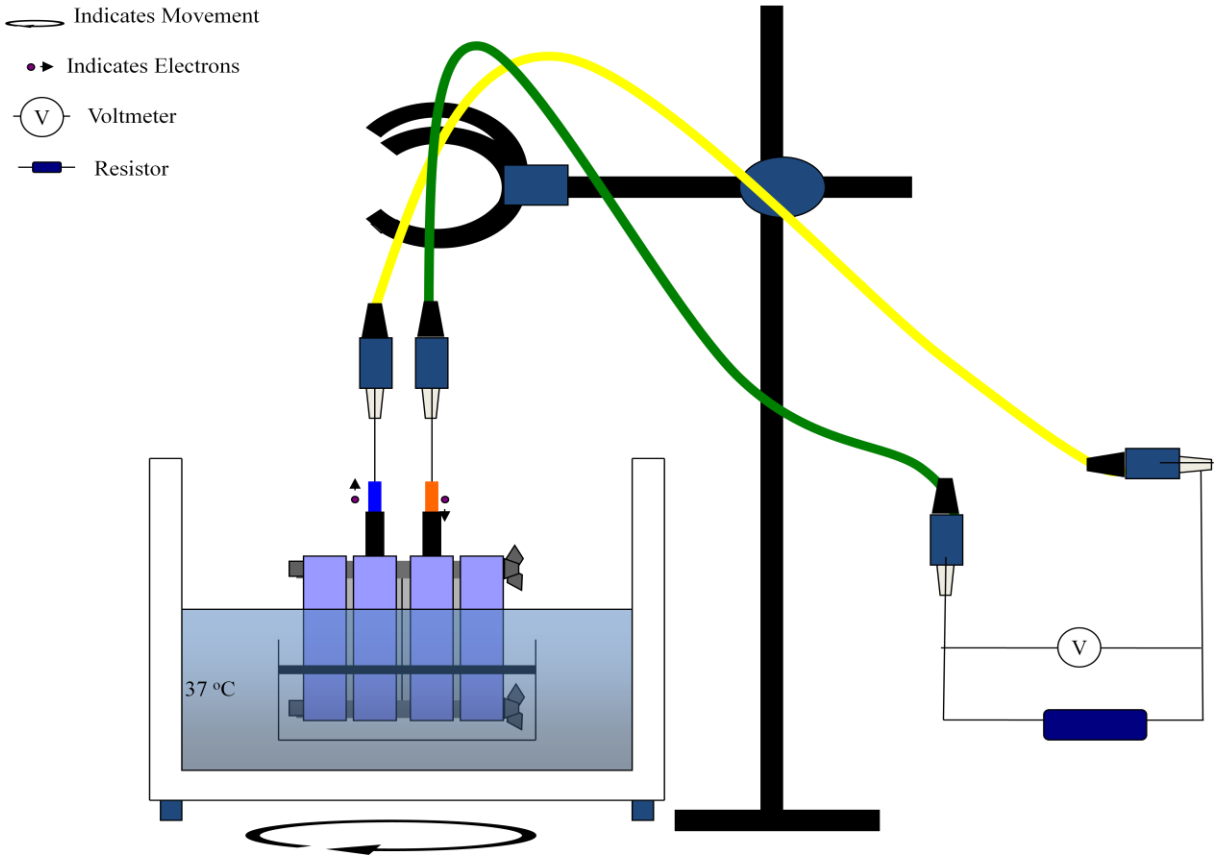


**Figure 2.6: Experimental set up of microbial fuel cells.** The MFCs were placed in a 37°C shaking water bath (180 rpm). The voltage was measured across an external resistance.

### 2.7.3. Potassium Permanganate

Ferricyanide is the preferred cathode molecule in many of the reported two chambered MFC (Table 2.5.2a & 2.5.2b) and has an $E^o$ = +0.44 V. The potential difference between the chambers is dictated by the half reactions. Therefore, by changing the cathode reaction to one at a more positive potential, should increase the power production. Potassium permanganate ($KMnO_4$) has three different possible half reactions as the electron acceptor in the cathode chamber which all posses a higher positive potential than potassium ferricyanide:

(a) $MnO_4^- + 8H^+ + 5e^- \rightarrow Mn^{2+} + 4H_2O$ $\qquad E^o$ = +1.51 V

This reaction will occur under acidic conditions, and will be maintained if the $H^+$ migrates from the anode chamber to the cathode chamber through the proton exchange membrane. However, if the production and movement of $H^+$ from the anode chamber to the cathode

chamber is not sufficient and the pH increases in the cathode chamber, then the reaction in the cathode chamber will change to the following two reactions:

(b) $MnO_4^- + 4H^+ + 3e^- \rightarrow MnO_{2(s)} + 2H_2O$ $E^o = +1.7$ V

$MnO_2 + 4H^+ + e^- \rightarrow Mn^{3+} + 2H_2O$ $E^o = +0.9$ V

If the transfer of protons is not sufficient to maintain this reaction and the pH continues to increase, then the reaction occurring in the cathode chamber will change to the following reaction:

(c) $MnO_4^- + 2H_2O + 3e^- \rightarrow MnO_{2(s)} + 4OH^-$ $E^o = + 0.6$ V

If the pH continues to increase, then the reaction will deplete $H^+$ and the electrons will stop flowing through the external circuit.

**2.8. Microbial fuel cell power production**

Electrochemistry is the branch of chemistry that involves the manipulation of chemical reactions involving the transfer of electrons, or redox reactions. A MFC is essentially a device where redox reaction occurs; one half-reaction occurring in the anode and the other half-reaction occurring in the cathode. Electroanalytical-chemistry was therefore, used as a tool to observe, characterise and understand electron-transfer between cells and the electrode (mediated and mediator-less) as well as a means to optimize different components of a microbial fuel cell.

The electrochemical experimental techniques used to observe, characterise and understand electron transfer were cyclic voltammetry (CV), linear sweep voltammetry (LSV) and fixed potential amperometry. Cyclic voltammetry and linear sweep voltammetry involves the control and change of electrode potential in order to observe the changes in current as a function of voltage, whereas chrono/amperometry only involves the control of electronic potential to observe changes in current as a function of time.

### 2.8.1. The three electrode configuration

An electrochemical cell in this thesis refers to any vessel containing a working, counter/auxiliary and reference electrode connected to a potentiostat (Figure 2.7). It is possible to use a two electrode set up. However, this was not employed in this thesis. The potentiostat controls the potential of an electrochemical cell using a three electrode set up (Kissinger & Heineman 1983), through feedback from the reference electrode (Figure 2.7). The potentiostat monitors the potential through the reference electrode and adjusts the applied potential accordingly (Kissinger & Heineman 1983; Wang 2006; Rawson 2008).

Working electrodes used in this thesis include: glassy carbon disc (28.27 $mm^2$), platinum pseudo-micro-disc (0.03142 $mm^2$), gold micro-band electrode array (0.375 $mm^2$) and carbon fibre microbial fuel cell electrode (1018 $mm^2$). The counter/auxiliary electrode was either platinum or gold. The reference electrode was either silver/silver chloride (Ag/AgCl) or gold.

A suitable reference electrode must have a high internal resistance (so that it will not participate in the reaction), be stable, and have a known standard electrode potential. The only reference electrode used to conduct CV or LSV in this work was Ag/AgCl (standard electrode potential = + 0.197 V). Therefore all voltages used in this thesis are referenced to the standard electrode potential for Ag/AgCl.

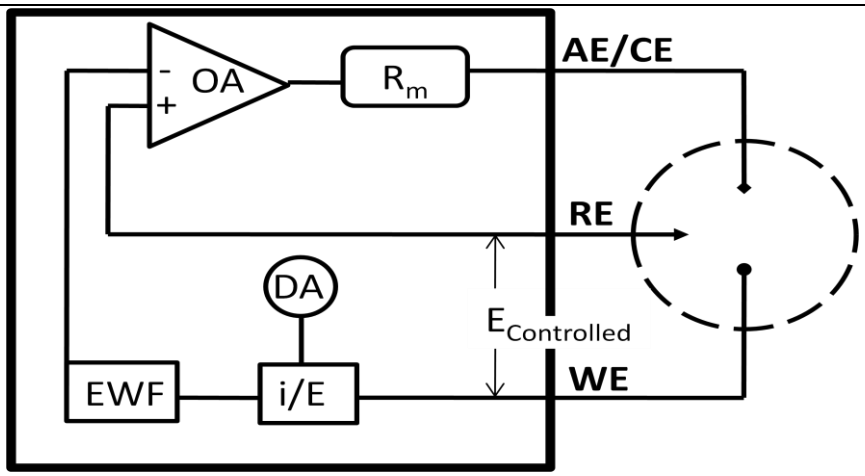


**Figure 2.7: Diagram of three electrode set up controlled by a potentiostat.** WE – working electrode, RE – reference electrode, AE/CE – auxiliary electrode/counter electrode, Rm – Resistance of machine (potentiostat), OA – operational amplifier, EWF – excitation wave formation generator (input), i/E – current to potential converter, DA – data acquisition system. Adapted from reference (Kissinger & Heineman 1983; Rawson 2008)

### 2.8.2. Ferricyanide/ferrocyanide redox couple

Ferricyanide is the oxidised form of ferrocyanide. This redox couple are a chemically reversible (Equation 4). In electrochemistry, a redox couple is considered *electrochemically reversible* based on the rate of reaction (Fast – Reversible, Medium – Quasi-reversible, Slow - irreversible).

$$\text{Oxidised} + ne^- \underset{K_r}{\overset{K_f}{\Leftrightarrow}} \text{Reduced}$$

**Equation 4**

**Equation 4: Chemically reversible redox couple.** Oxidised – Oxidised species of redox couple, Reduced – reduced species of redox couple, $ne^-$ – number of electrons involved in the reaction, $K_f$ – rate of forward reaction, $K_r$ – rate of reverse reaction and ⇔ – each species is able to be converted from one to the other in the time scale of an electrochemistry experiment.

Ferricyanide and ferrocyanide are extremely hydrophilic, stable and unable to permeate the plasma membrane (Baronian *et al.* 2002). As a result, this redox couple is used as a mediator and reporter molecule in this thesis. As a mediator, they are capable to transporting electrons from the external surface of the cell membrane to the working electrode (anode). As reporter molecules, the electrochemical detection of ferrocyanide over a period of provides information on how much extracellular electron transfer has taken place when only ferricyanide was initially added.

### 2.8.3. Electro-analytical chemistry techniques

Linear sweep voltammetry and cyclic voltammetry are electrochemical techniques that rely on the ability of the potentiostat to alter and control the potential of the electrochemical cell using the three electrode system. Each technique involves scanning a range of potentials and recording the current generated in the electrochemical cell, but where CV cycles away from a starting potential and then back again, LSV only scans away from the stating potential (Figure 2.8. and Figure 2.9.).

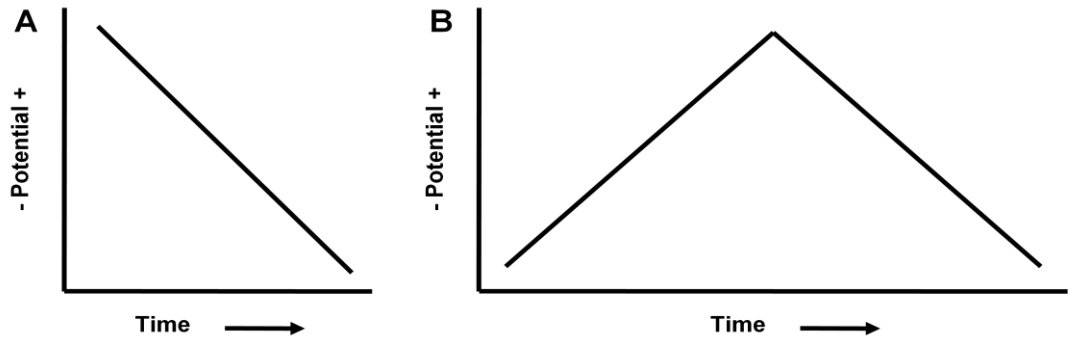


**Figure 2.8: Wave excitation forms** for (A) linear sweep voltammetry and (B) cyclic voltammetry

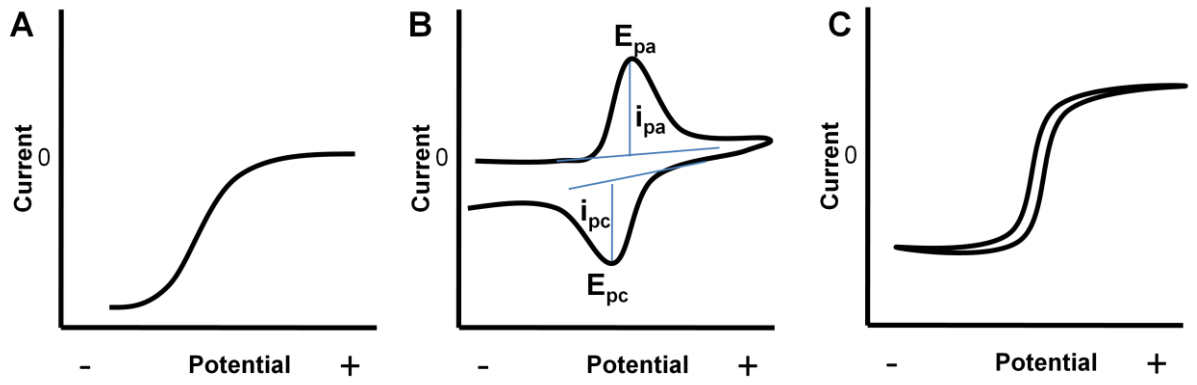


**Figure 2.9: Experimental response** to (A) linear sweep voltammetry (micro-disc electrode) and (B) cyclic voltammetry (macro-disc electrode) (C) cyclic voltammetry (micro-disc electrode). In (B) the parameters are $E_{pa}$ – potential of the anodic (oxidation) peak, $E_{pc}$ – potential of the cathodic (reduction) peak, $i_{pa}$ – current of the anodic peak, $i_{pc}$ – current of the cathode peak (Kissinger & Heineman 1983; Wang 2006; Rawson 2008)

Fixed potential amperometry differs from cyclic voltammetry in that the potential is held at a specific potential rather than scanned through a range of potentials (Figure 2.10.).

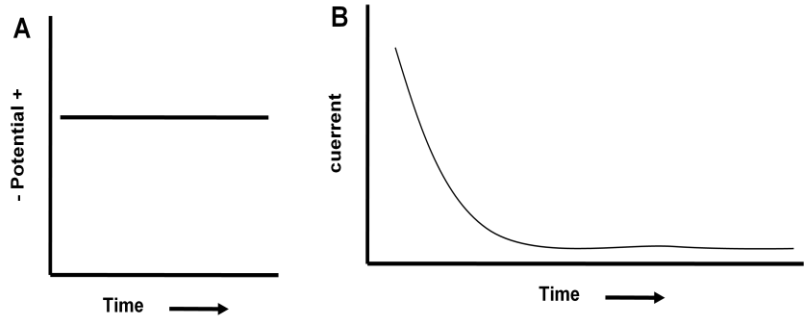


**Figure 2.10: Wave excitation form for chronoamperometry/amperometry** (A) and experimental response to wave excitation (B) with a microelectrode.

### 2.8.4. Planar and radial diffusion

Wang 3rd edition (Wang, 2006) defines a micro-electrode as "electrodes with at least one dimension not greater than 25 μm" (Wang 2006). This is because "the rate of mass transport to and from the electrode and the current density increases as the electrode size decreases". At high scan rates the electrode planar diffusion has a greater affect on the wave excitation form,

and at low scan rates the electrode is subjected to radial diffusion (Figure 2.11). Radial diffusion allows for higher mass transport and steady state behaviour for LSV and CV (Figure 2.9) (Forster 1994).

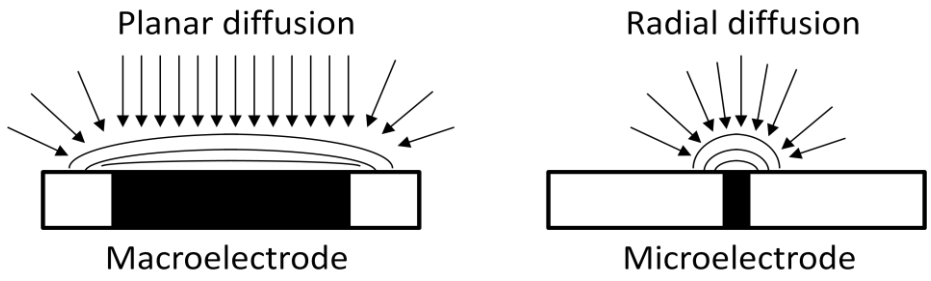


**Figure 2.11: Comparing planar diffusion to radial diffusion.** The bulk of the diffusion to a macro electrode is planar diffusion with only a small part radial. In contrast, the bulk of the diffusion to a microelectrode is radial (Wang 2006).

### 2.8.5. Faraday processes and Steady state

In Figure 2.9, two different shaped cyclic voltammograms are described; macro-disc electrode and micro-disc electrode. The shape of the two cyclic voltammograms is due to the ferricyanide ferrocyanide redox couple. When a redox couple is electrochemically reversible, the formal reduction potential ($E^o$) lies midway between $E_{pa}$ and $E_{pc}$ (Equation 5).

$$E^o = (E_{pa} + E_{pc}) / 2 \qquad \textbf{Equation 5}$$

In Figure 2.9 B & 2.9 C as the potential is changed from positive to negative the potential rises above the standard potential ($E^o$) for the redox couple resulting in the surface concentration of the reduced member of the couple to rapidly decrease (Nernst Equation - Equation 6). The current observed from this change in oxidative state at the electrode surface is called *faradic current* because it is the current that results from the transformation of the redox couple (Wang 2006).

$$E = E^o + \frac{2.3RT}{nF} \log \frac{C_o(0,t)}{C_r(0,t)} \qquad \textbf{Equation 6}$$

**Equation 6: Nernst Equation.** $E$ - potential, $E^o$ – standard reaction potential (redox reaction), $R$ - gas constant (8.314 J $K^{-1}$ $mol^{-1}$), $T$ - temperature (Kelvin), $n$ – electrons transferred (per molecule), $F$ - Faraday constant (96,487 Coulombs), $C_o(0,t)$ – Concentration oxidised species (at electrode), $C_r(0,t)$ – Concentration reduced species

The conversion from one redox molecule to the other at the working electrode surface causes a concentration gradient relative to the bulk concentration of the electrochemical cell. The change in concentration from one redox molecule to the other at the working electrode surface is caused by passing the $E^o$ of the redox couple. The region of the bulk solution affected by the working electrode is known as the *diffusion layer*. The diffusion layer is small at first but increases with time. That is, the concentration gradient is steep at first but decreases with time. With macro-electrodes (planar diffusion) the diffusion layer becomes rate-limiting as the electrode is moved to a favourable potential and the concentration of the reactant species becomes effectively zero at the surface of the electrode. In a cyclic voltammogram this causes a peak in current which can be predicted using the Randles-Sevick equation (Equation 7) (Wang 2006). After the peak, a drop in current is observed and this can be predicted using the Cottrell equation (Equation 8). From this point onward no current increase will be caused by the redox couple and an increase in potential, because the kinetics of the electrochemistry is limited by diffusion. All of these can be visualised in Figure 2.12.

$$\mathbf{i_p = (2.69 \times 10^5) n^{3/2} A D^{1/2} C^o v^{1/2}} \qquad \textbf{Equation 7}$$

**Equation 7: Randles-Sevick equation.** Variables: $i_p$ - peak current, n - number of electrons, A - electrode area ($cm^2$), D - diffusion coefficient ($cm^2\ s^{-1}$), $C^o$ - concentration of the species of interest in bulk solution ($mol\ dm^{-3}$) and v - scan rate ($V\ s^{-1}$).

$$i_t = \frac{nFAC^oD^{½}}{\pi^{½}\ t^{½}} \qquad \textbf{Equation 8}$$

**Equation 8: Cottrell equation.** Where n is the number of electrons, F is the Faraday constant, A is the electrode area ($cm^2$), $C^o$ is the bulk electrolyte concentration ($mol/cm^3$), and D is the diffusion coefficient ($cm^2/s$) and t is time (seconds).

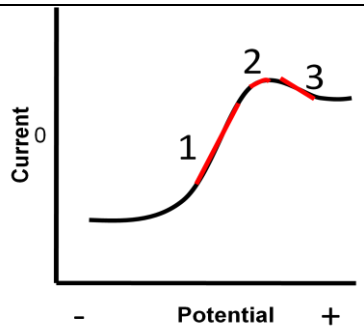


**Figure 2.12: Anatomy of macro-electrode cyclic voltammetry peak.** Using ferricyanide ferrocyanide 1 – area of peak predictable with Nernst Equation, 2 – area of curve predictable with Randles-Sevick Equation, 3 – area of curve predictable with Cottrell Equation.

For short periods of time, micro-disc electrodes are not limited by mass transport which limits the rate of electron transfer (described above) and if the scan rate remains low, the current will approach a steady state and no peak will be observed (Wang 2006).

### 2.8.6. Linear sweep voltammetry

Steady state and excellent signal-to-background currents make micro-electrodes preferable to macro-electrodes when conducting LSV. All of the experiments contained in this thesis involving LSV use the ferricyanide/ferrocyanide redox couple as reporter molecules, Ag/AgCl as reference electrode, a platinum auxiliary/counter electrode and a platinum pseudo-micro-disc working electrode (Figure 2.13.). The working electrode used to conduct

LSV in this work was a platinum pseudo-micro-disc electrode 100 µm in diameter, which is four times larger than that specified by Wang (2006). While it is too large to be considered a true micro-disc electrode, this electrode is capable of micro disc behaviour such as steady state at low scan rates (20 $mVs^{-1}$ <), the reason being that at the lower scan rates, the diffusion to the working electrode switches from by being primarily affected by planar to radial diffusion.

### 2.8.7. Cyclic voltammetry

Cyclic voltammetry involves placing the three electrodes in each solution (Figure 2.13.) and has been well described by Kissinger & Heineman (1983) and Van Denschoten (1983). Cyclic voltammetry was conducted with four different working electrodes: glassy carbon disc (28.27 $mm^2$), platinum pseudo-micro-disc (0.03142 $mm^2$), gold micro electrode array (0.375 $mm^2$) and carbon fibre microbial fuel cell electrode (1018 $mm^2$), but the reference and counter/auxiliary electrodes were always Ag/AgCl and Pt wire (respectively). Many different redox couples were used and will be discussed in later chapters.

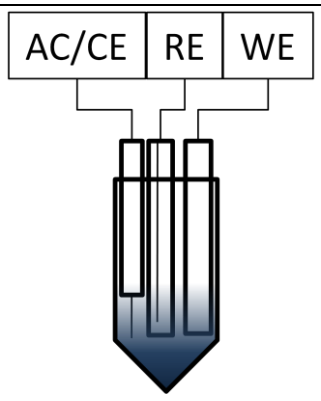


**Figure 2.13: Three electrode set up.** Used in Cyclic voltammetry and linear sweep voltammetry: WE – Working electrode, RE – reference electrode, AC/CE – auxiliary/counter electrode.

### 2.8.8. Fixed potential amperometry

All of the fixed potential amperometry conducted in my research used a three electrode set up, was unstirred and was conducted on a micro-band electrode array. The micro-band electrode array used gold as working, reference and auxiliary/counter electrodes. See chapter 6 for more details.

# Chapter 3: Mediated and mediator-less power density of a microbial fuel cell containing *Arxula adeninivorans* in the anode and $KMnO_4$ in the cathode

## 3.1. Abstract

A two chambered microbial fuel cell has been constructed and characterised. The external load was found to be optimal at 100 Ω, when TMPD was used as a mediator. Potassium permanganate ($KMnO_4$) was found to be an effective cathode reactant. However, a consistent drop in power density with time was observed when using $KMnO_4$. Mediated electron transfer from the catabolism of glucose by *A. adeninivorans* as well as from internal stores was demonstrated in the MFC. Mediator-less electron transfer from *A. adeninivorans* was also demonstrated.

## 3.2. Introduction

Two chambered MFCs were the first type of MFC created (Potter *et al.* 1911) and have been used in many fundamental studies over the last century (Table 2.2a, 2.2b). They operate through two different redox reactions occurring in two chambers, normally separated by a semi-permeable membrane (Fang *et al.* 2004). The first oxidation reaction produces electrons (anode) which are transferred to the second reduction reaction which accepts electrons (cathode) to create the other half of reaction of the MFC, and balanced by the migration of $H^+$ from the anode to the cathode (Rabaey & Verstraete 2005; Li *et al.* 2010). The greater the potential difference between the anode and cathode, the greater the voltage generated. The kinetics of the reactions in each chamber determines the maximum rate of electron transfer, and subsequently the current generated. In order for both the current and the voltage to be produced, an external load must be applied to the system.

There are many different factors that can adversely affect the power generation of a MFC. These include:

1. Slow kinetics of the microorganism (which can limit the amount of current)
2. Over-potential at the electrodes
3. Mass transport
4. Salt concentration of the solutions
5. Temperature
6. Electrode material
7. Electrode surface area
8. The type of microorganism used
9. The type of electron transfer
10. The amount of external load

    (Rabaey & Verstraete 2004; Wang 2006; Jadhav & Ghangrekar 2009: Liu *et al.* 2005: Oh & Logan 2006; Hubenova *et al.* 2010; Kargi & Eker 2007; Li *et al.* 2010)

With so many variables affecting the power production of MFC, it is important if possible to reduce the number of variables. As a result, the MFC used in this chapter is based on a common MFC (Allen & Bennetto 1993; Kim *et al.* 2002; Rabaey *et al.* 2003) with set variables such as salinity, cell concentration, and a buffered pH in order to enable a high level of control to give reproducible results. However, there are many variables in this MFC that have not been characterised in previous MFC studies: *A. adeninivorans* as the microorganism, TMPD as the mediator, and $KMnO_4$ as the cathode reaction in a eukaryotic MFC.

In order to characterise this microbial fuel cell, the key variable components for the MFC were tested incrementally in order to optimise the MFC. Therefore, this chapter is directed

towards optimising the external load, the anode and the cathode reactions, and characterising the MFCs behaviour with emphasis on power fluctuations and fouling of the electrodes.

## 3.3. Materials and Methods

### 3.3.1. Chemicals

Analytical grade potassium ferricyanide ($K_3[Fe(CN)_6]$) (FC) and 2,3,5,6-tetramethyl-1,4-phenylenediamine (TMPD) were purchased from Sigma Chem. Co. (St. Louis, MO, USA). Analytical grade D(+)-glucose, potassium ferrocyanide ($K_4[Fe(CN)_6]$) (FoC) and potassium di-hydrogen phosphate were purchased from BDH Chemicals Ltd (Poole, England). Potassium chloride, di-potassium hydrogen phosphate, peptone from soymeal, and potassium permanganate, were purchased from Merck (Damstadt, Germany).Yeast extract was purchased from Oxoid Ltd (Hampshire, England). Agar was purchased from Fisher Scientific (New Jersey, USA).

### 3.3.2. Strains, buffers, reagents and media

The *A. adeninivorans* strain LS3 was obtained from the yeast collection of the "Institut für Pflanzengenetik und Kulturpflanzenforschung" (IPK) Gatersleben, Germany.

Phosphate buffered saline (PBS, 0.05 M $K_2HPO_4/KH_2PO_4$, 0.1 M KCl) was used to suspend cells in the MFC and in the electrochemical cell.

The stock reagents FC/FoC 0.5 M, $KMnO_4$ 0.5 M and glucose 1 M were dissolved in PBS prior to use. TMPD 50 mM was prepared in 99.5% ethanol. Yeast extract peptone dextrose (YEPD) broth (peptone 20 g $L^{-1}$, yeast extract 10 g $L^{-1}$, glucose 20 g $L^{-1}$) was used for all cell culturing.

### 3.3.3. Yeast Microbial Fuel Cell

A polycarbonate fuel cell based on the design of Bennetto *et al.*(1985), Bennetto (1990) and Delaney *et al.* (1984) was constructed using rubber gaskets to prevent leakage. A proton exchange membrane (Naffion membrane 115, DuPont, San Diego, USA, Fang *et al.* 2004) separated the 15 mL anode and cathode compartments (Figure 2.5). The carbon fibre cloth electrodes (cross sectional surface area of 0.001018 $m^2$, 275 $gm^{-2}$, fibre diameter 6 µm), used for both anode and cathode, were cleaned by ultrasonic agitation in isopropyl alcohol, acetone and ether, each successively for 5 min followed by drying and rinsing in distilled water to remove any sizing before first use.

In the cathode compartment 0.5 M $KMnO_4$ solution in PBS was used as the cathode electrolyte. In the anode compartment pure cultures were prepared at an $OD_{600}$ = 2.5 (Novaspec II spectrophotometer) in PBS for each species. Batch cultures of *A. adeninivorans* LS3 were cultivated aerobically in indented flasks at 37$^oC$, at 180 rpm for 24 h in YEPD broth, washed twice (4,500 rcf, for 8 min) and finally re-suspended in PBS.

Four MFCs were operated simultaneously in a shaking water bath at 37°C, 180 rpm, each with a 100 ohm resistor (Figure 2.6). The potential difference across the resister was measured every 5 mins (UT20B Multimeter) and converted into power density (PD) using Equation 3.

The physical components of each MFC were fastened into place before the anode and cathode solutions were added via inlet/outlet ports. Experimental conditions could be altered using these ports during the course of the experiment via peristaltic pump (Gilson miniplus) or by pipette.

### 3.3.4. Internal resistance

A decade box is a device that is able to alter the external load on a MFC. The MFC was subjected to the following external loads: 50, 100, 150, 200, 250, 300, 350, 400, 450, 500,

550, 600, 650, 700, 750, 800, 850, 900, 950, 1000, 1500, 2000, 2500, 3000, 3500, 4000, 4500, 5000 Ω (Ohms). The voltage produce by the MFC at each external load was recorded and converted into power density.

### 3.3.5. Cyclic Voltammetry analysis

Electrochemical investigation of fouling of the cathode by $KMnO_4$ was conducted using cyclic voltammograms with a 1:1 mix of ferricyanide-ferrocyanide (50mM each) in a three electrode system comprising of a the MFC carbon cloth electrodes, a Pt auxiliary/counter and a Ag/AgCl reference electrode.

## 3.4. Results

### 3.4.1. Optimal external resistance

Varying the external load and monitoring the resulting power density is a convenient method to not only finding the optimal external resistance, but also to characterise the behaviour of the MFCs under different conditions (Jadhav & Ghangrekar 2009). In this thesis, the data is reported as external load vs. power density, but the standard procedure in the literature is to report this data as current density vs. power density (Logan 2006; Logan *et al.* 2006). The reasoning behind graphing external load vs. power density (Figures 3.1, 3.2, 3.3) is to allow for error bars, i.e. when graphing current density vs. power density if two different scans report different voltages for the same external load then the current density changes and several measurements on the same point are not possible.

The results from using either y-axis values are the same. The optimal external load can be calculated using either graph and used in future experiments by using the external load that produces the highest power density. This occurs when the internal resistance of the MFC is

the same as the external resistance if the conditions Jacobi's Law are met by MFCs (section 2.5).

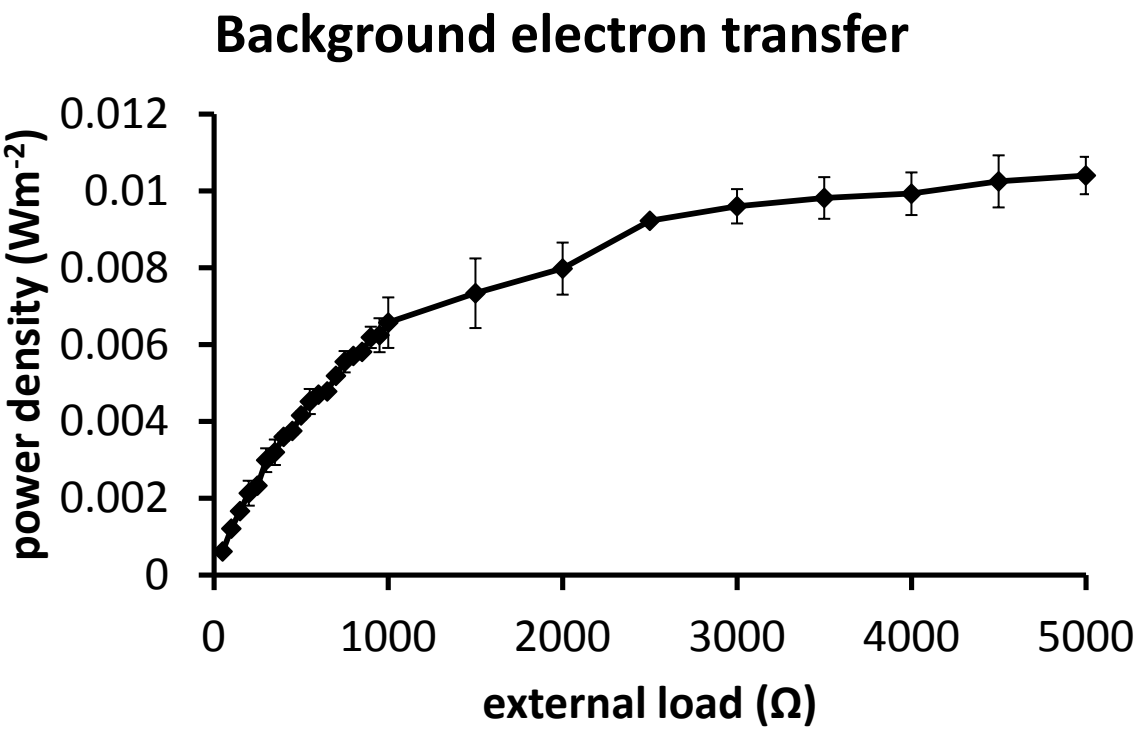


**Figure 3.1: Effect of external load on power density of acellular control.** The MFC contained 0.5 M $KMnO_4$ dissolved in PBS in the cathode, and PBS in the anode (37$^{o}$C, at 180 rpm). Error bars represent standard error of the mean (n=4)

Figure 3.1 illustrates that 0.01 $Wm^{-2}$ of power is able to be extracted from a MFC with only PBS in the anode. However, the shape of the curve demonstrates that the optimal power is generated under a high external load (above 1000 Ω). At these high external loads, fewer electrons need to be supplied to the external circuit i.e. they don't have to work as hard. This indicates that if lower external loads are used then it should be easier to distinguish the results from MFC containing cells from the background electron transfer because in the acellular controls there are no cells to perform the work required to produce electricity, i.e. at a lower external load a significant difference between acellular and cellular power density was observed (ANOVA $p<0.05$).

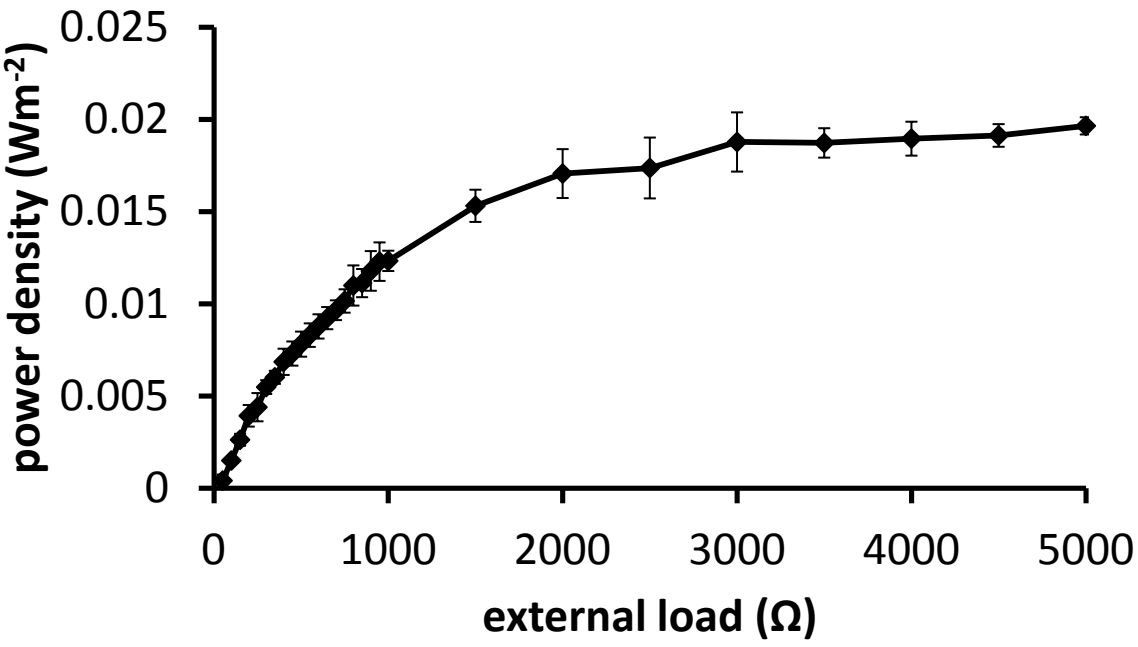


**Figure 3.2: Effect of external load on power density of mediator-less MFC.** The MFC contained 0.5 M $KMnO_4$ dissolved in PBS in the cathode, and 2.5 $OD_{600}$ *A. adeninivorans* suspended in PBS in the anode (37$^{o}$C, at 180 rpm). Error bars represent standard error of the mean (n=4)

Figure 3.2 demonstrates the same experiment conducted with $OD_{600}$ 2.5 *A. adeninivorans* in the anode. The shape of the curve is similar to that of the background control. However, the magnitude of the power density is approximately twice for the experiment containing cells vs. the acellular blank (Figure 3.1). This demonstrates that mediator-less electron transfer in the MFC from *A. adeninivorans* is possible. This also shows that either the kinetics of the mediator-less electron transfer is very slow (due to the high external load required to achieve optimal power density), or the potential difference between the mediator-less electron transfer and the cathode reaction is small (due to the low overall power density).

Figure 3.3 demonstrates the same experiment conducted with $OD_{600}$ 2.5 *A. adeninivorans* in the anode with 1.5 mM TMPD. The shape and magnitude of the curve in Figure 3.3 is

drastically different to that of Figures 3.1 and 3.2. This is likely to be due to the TMPD by-passing a kinetically slow step and/or providing electrons to the electrode at a much lower potential than is possible with mediator-less electron transfer. The highest power densities occurred with external resistances below 400 Ω, and the optimal peak power output was produced at 100 Ω. The optimal external resistance of 100 Ω will be used as the external load for all MFC work, unless otherwise stated.

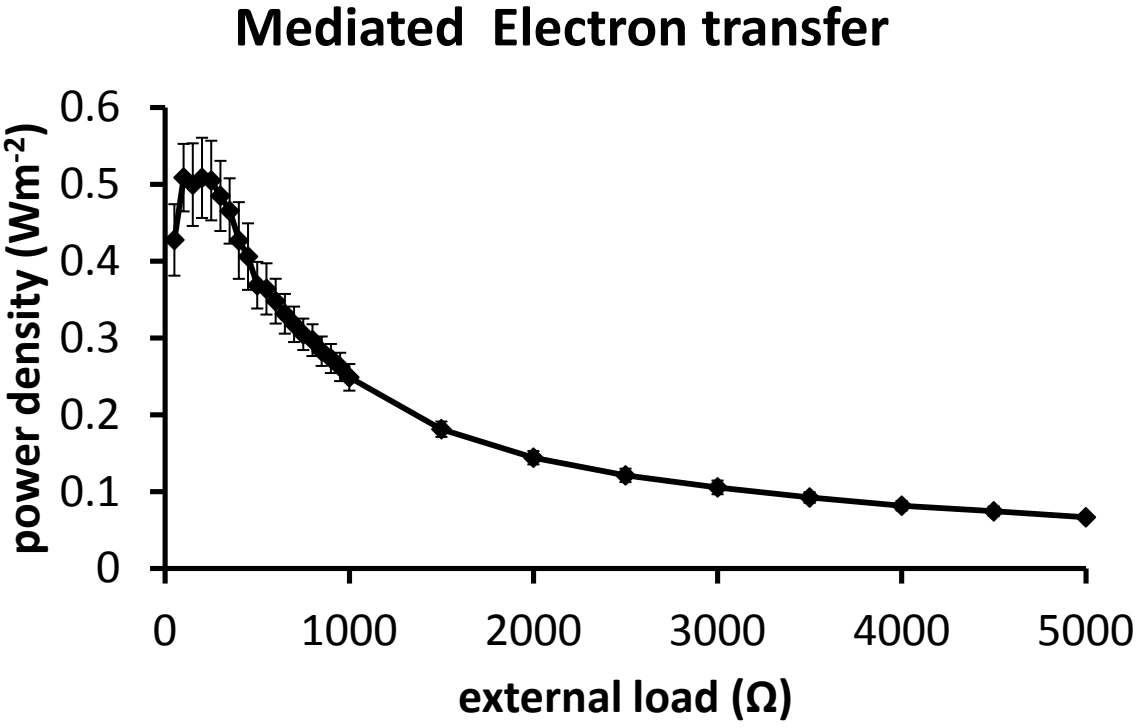


**Figure 3.3: Effect of external load on power density of mediated MFC.** The MFC contained 0.5 M $KMnO_4$ dissolved in PBS in the cathode, $OD_{600}$ 2.5 *A. adeninivorans* suspended in PBS with 1.5 mM TMPD in the anode (37$^{o}$C, at 180 rpm). Error bars represent standard error of the mean (n=4)

### 3.4.2. $KMnO_4$ concentration and fouling of components

As can be seen in Tables 2.2a and 2.2b (unabridged in Appendix 2 and 3), the most common electron acceptors used in two chambered MFC are dissolved oxygen and ferricyanide. However, as discussed in section 2.7.3, potassium permanganate has a much more positive

standard electrode potential, which should lead to much higher power densities (You *et al.* 2006; Logan 2008, Chapter 6). As demonstrated by You *et al.* (2006), the pH of the solution that the $KMnO_4$ is dissolved in has a far greater effect than the concentration on the potential held by the cathode. The possible cathode reactions (see section 2.7.3) all consume $H^+$ ions, and it is therefore hoped that by suspending the potassium permanganate in PBS buffer and using as large a PEM surface area that the cathode reaction can help produce consistent reproducible power.

Figure 3.4 demonstrates that suspending $KMnO_4$ in PBS and using a high PEM surface area produces consistent amounts of power with *A. adeninivorans* in the anode (without TMPD) and 100 Ω of external load. Figure 3.4 also demonstrates that the power generation is dependent on the presence of $KMnO_4$ even though the amount of power is independent of the concentration of the $KMnO_4$. Because the power density does not vary with the concentration of $KMnO_4$ the concentration of $KMnO_4$ used will always be in excess to ensure that concentration of $KMnO_4$ is never limiting. Since 0.5 M $KMnO_4$ does not fully dissolve in PBS, this saturated solution was therefore used as the cathode reaction for all MFC experiments, unless otherwise stated.

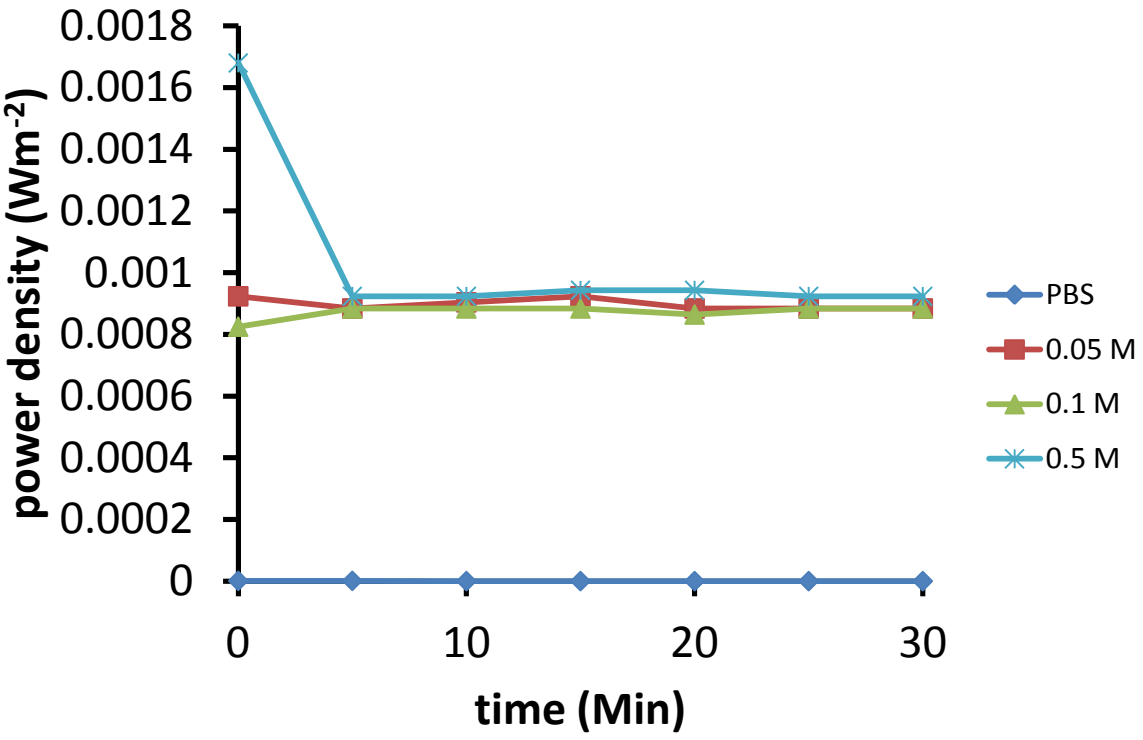


**Figure 3.4: Different concentrations of $KMnO_4$ in the cathode.** MFC anode contained $OD_{600}$ 2.5 *A. adeninivorans* suspended in PBS. External load applied (100 Ω), constant temperature (37°C) and cells kept suspended (180 rpm). Each data point represents a mean (n=4), but error bars are not shown.

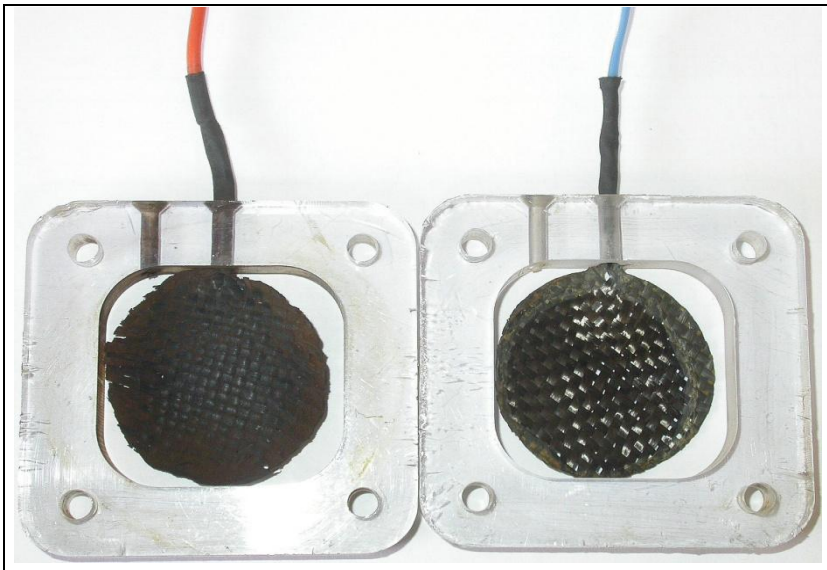

**Figure 3.5: Fouling of the cathode.** Cathode (left) and anode (right) that were used in the same MFC for a combined total of 40 h of experimental time.

After repeated use, a cathode becomes coated in a brown/black precipitate that is not able to be removed (Figure 3.5). This precipitate is believed to be $MnO_{2(s)}$ because it is brown/black and extremely un-reactive with acids, bases and insoluble in organic solvents. However, it is possible that a chemical reaction may have also occurred between the electrode and $KMnO_4$ altering electrode surface.

The power densities of cathodes that had been used for 40 h of experimental time and a new cathode were compared (Figure 3.6). Under optimal power generation conditions (with cells, glucose, and TMPD in the anode), the new cathode produced far greater power density than that produced by the old cathode. This indicates that the electrode has been altered.

Figure 3.6 also shows a steady drop of power with time with the new cathode. If this drop was solely due to $KMnO_4$ irreversibly altering the properties of the cathode, then the cathode could not be used again. The cathodes however, are able to be used repeatedly, which would suggest that this short term loss in power density is not due to an alteration of the properties of the anode. This suggests that the short term fouling of the cathode could be altering the electrode in two different ways; it could act as an inert material effectively reducing the surface area of the cathode and/or it could alter the properties of the anode making it less reactive.

A different possibility is that this short term power loss is also due to a coating/altering the PEM. Coating/altering of the PEM by $KMnO_4$ (Figure 3.7) could prevent adequate proton exchange between the anode and the cathode. This will be discussed in greater detail in section 3.4.5. No trace of $KMnO_4$ was observed in the anode.

In order to ascertain if the cathode or the anode has been chemically altered after 40 h of experimental time, cyclic voltammograms of newly made cathodes with a 1:1 mixture of ferricyanide: ferrocyanide were compared with used anodes and cathodes. The cyclic

voltammograms produced (Figure 3.8) demonstrate that fouling of both the anode and cathode had occurred. However, the fouling of the anode was far less than the cathode which had been reduced to an almost straight line. This straight line demonstrates that the cathode has been electrochemically modified, either through complete obstruction of the surface area by an inert substance or through chemical modification of the electrode material itself.

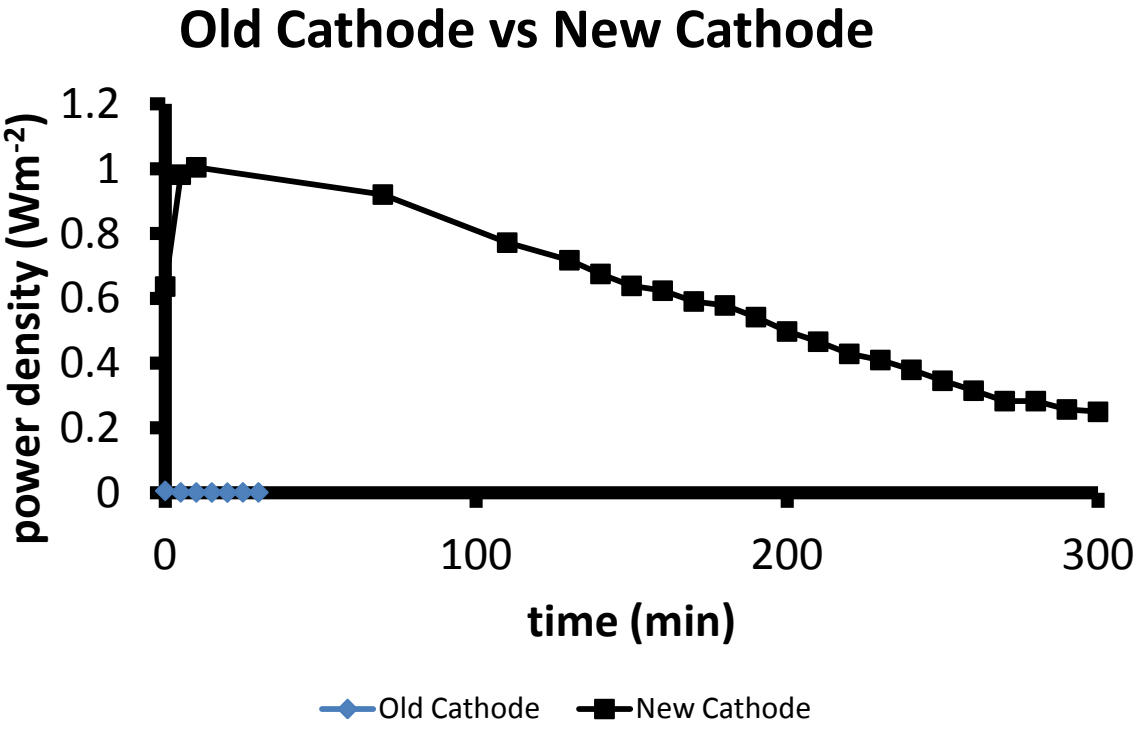


**Figure 3.6: Cathode fouling affects power density.** MFC contained 0.5 M $KMnO_4$ dissolved in PBS in the cathode, $OD_{600}$ 2.5 *A. adeninivorans* suspended in PBS with 1.5 mM TMPD and 10 mM glucose in the anode. Temperature maintained at 37°C and cells were kept suspended (180 rpm). The 'old cathode' curve is the same cathode depicted in Figure 3.5.

**Figure 3.7: Fouling of proton exchange membrane.** An unused PEM (left) is compared to a PEM (right) that has been used in a MFC for a combined total of 40 h of experimental time.

Electrochemical analysis demonstrates that the electrochemical behaviour of the cathode is altered by prolonged use (Figure 3.6). In order to combat this alteration of the cathode, regular changes of cathode were essential to maintain consistent power densities between experiments. The electrochemical experiments do not rule out other factors contributing to the short term drop of power density, but fouling of the cathode is at least partly responsible for the short term drop off of power density (Figure 3.5).

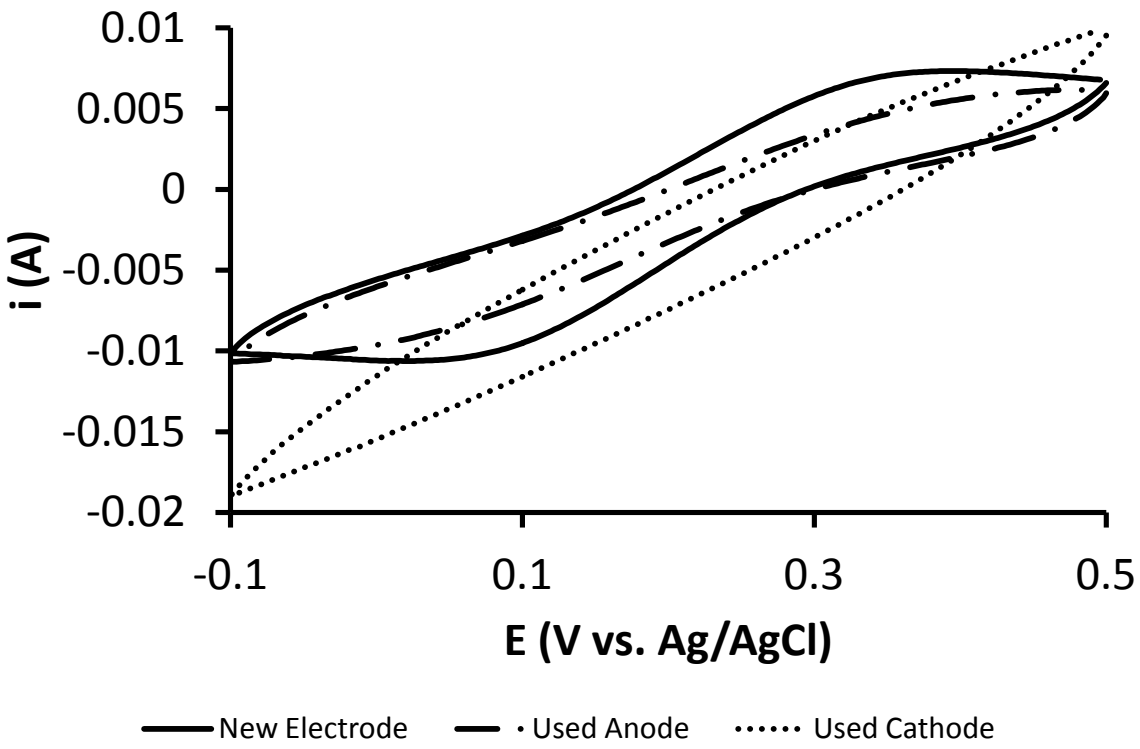


**Figure 3.8: Cyclic voltammograms of fouled electrodes.** Cyclic voltammetry was performed (from -100 mV to + 500 mV vs. Ag/AgCl at 100 $mVs^{-1}$) using the following 3 electrode set up: Working; carbon cloth MFC macro electrode, Reference; Ag/AgCl, Counter; Pt. The redox active species used was a 1:1 mixture of FC:FoC. Each cyclic voltammogram represents the mean of 3 cyclic voltammograms with for 3 different MFC electrodes for each category (i.e. n=9 for each curve).

### 3.4.3. TMPD concentration

The concentration of the mediator to be used must be optimised. In order to find out the optimal amount of TMPD to be added, two different experiments were set up. In the first, TMPD was added incrementally (Figure 3.9). In the second, TMPD was added in single doses up to the desired concentration (Figure 3.10). In both experiments, concentrations of TMPD greater than 1 mM did not increase the power density.

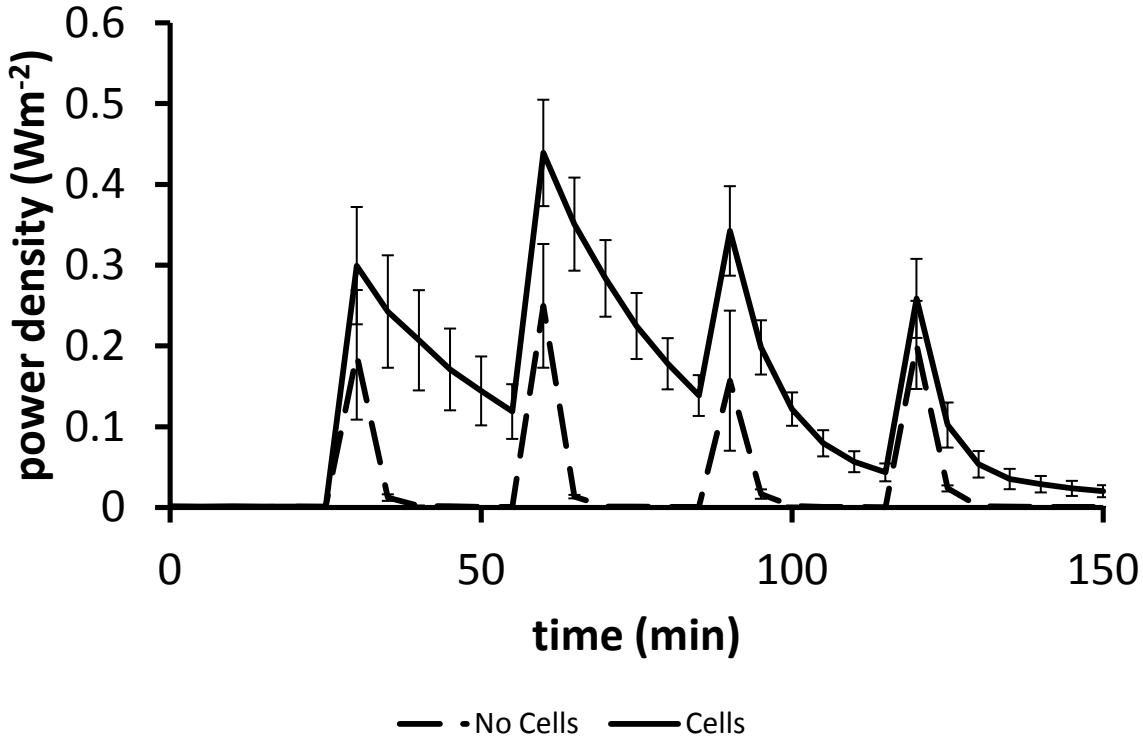


**Figure 3.9: Sequential addition of TMPD to a MFC**. TMPD was added to give a final concentration increase of 0.5 mM every 30 mins. The cathode contained 0.5 M $KMnO_4$ dissolved in PBS in the cathode and the anode contained an $OD_{600}$ 2.5 *A. adeninivorans* suspended in PBS or PBS only in the anode. Temperature was constant (37$^{o}$C) and cells were suspended (180 rpm). Error bars represent standard error of the mean (n=4).

TMPD is known to contain a small amount (4%) of the reduced species (Baronian *et al.* 2002). Therefore, the addition of TMPD resulted in a peak. As a result, acellular controls were included to demonstrate TMPD reacting with the carbon cloth electrodes, and also to demonstrate cellular dependant power densities (Figures 3.9 and 3.11). Interestingly, in Figure 3.9, the peak showed a variable power density increase when the cells were present compared to the acellular control. There are several possible reasons for this: the internal stores of electrons in *A. adeninivornas* could have been significantly depleted, the anode and/or cathode could have become fouled, and/or the cathode reaction may have changed with time due to a pH change.

In Figure 3.9, the acellular control demonstrates similar peaks from the addition of 0.5 mM TMPD (ANOVA p=0.05), but in Figure 3.11 the acellular controls demonstrate that the peak height resulting from single additions of different concentrations of TMPD at the same point in time is different (ANOVA p=0.05).

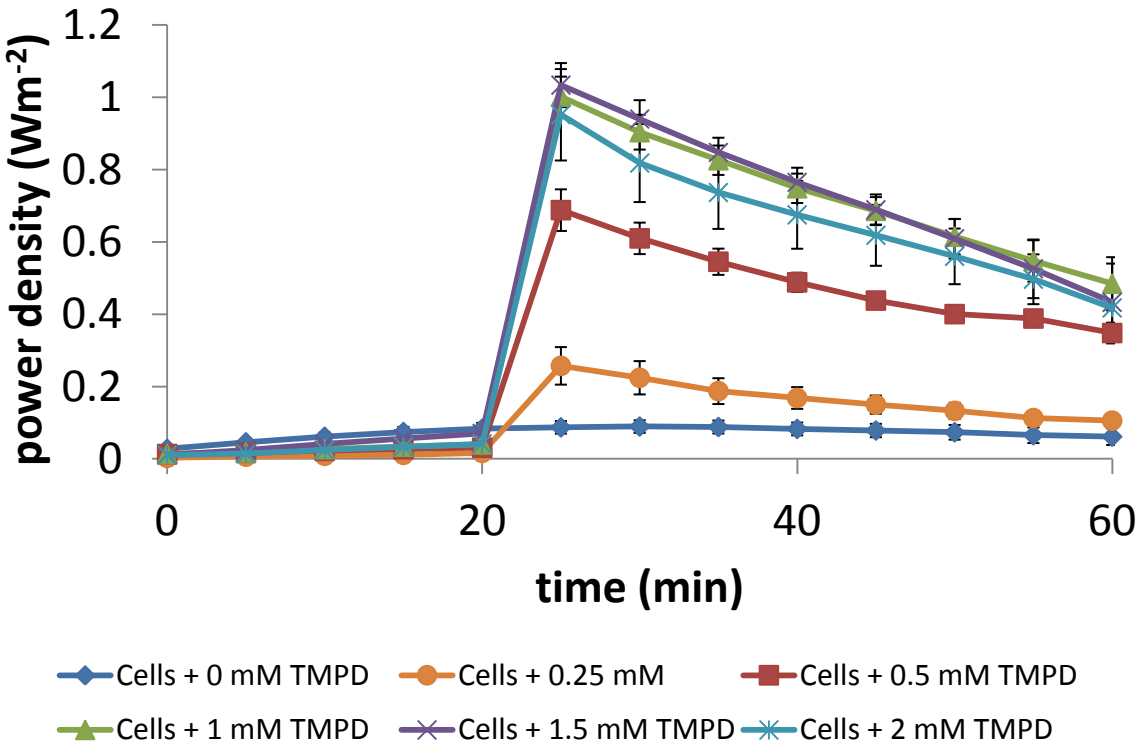


**Figure 3.10: Single additions of different TMPD concentrations.** MFC contained 0.5 M $KMnO_4$ dissolved in PBS in the cathode and $OD_{600}$ 2.5 *A. adeninivorans* suspended in PBS in the anode. Constant temperature (37°C) and cells were kept suspended (180 rpm). TMPD was added at 25 mins. Error bars represent standard error of the mean (n=4).

The raw data from the 35 minute readings of Figure 3.10 has been used to create Figure 3.12 to illustrate the power density difference in the mediator-less control and the different concentrations of mediator. The time of 35 mins was used because Figure 3.11 demonstrated that at this time there is no residual power density from the 4% reduced TMPD added to the MFC.

In Figure 3.12 there is a statistical difference between the mediator-less control and all the other concentrations of mediator (ANOVA, p=0.05). There is no statistical difference between the values of the concentrations above 1 mM (ANOVA, p=0.05). It was decided to use a 1.5 mM TMPD concentration in subsequent experiments to ensure that the mediator was in excess, to allow for experimental error.

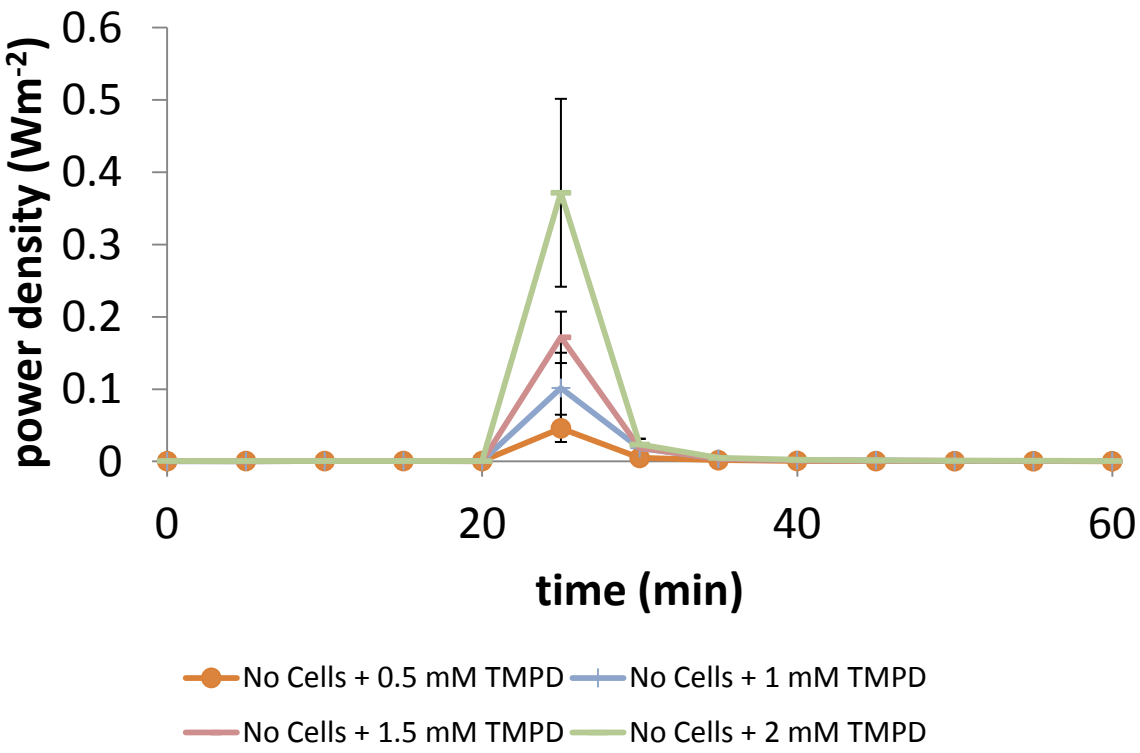


**Figure 3.11: Single addition of TMPD control**. MFC contained 0.5 M $KMnO_4$ dissolved in PBS in the cathode and PBS in the anode. Temperature was maintained at 37$^{o}$C and the solutions were agitated at 180 rpm. TMPD was added at 25 mins. Error bars represent standard error of the mean (n=4).

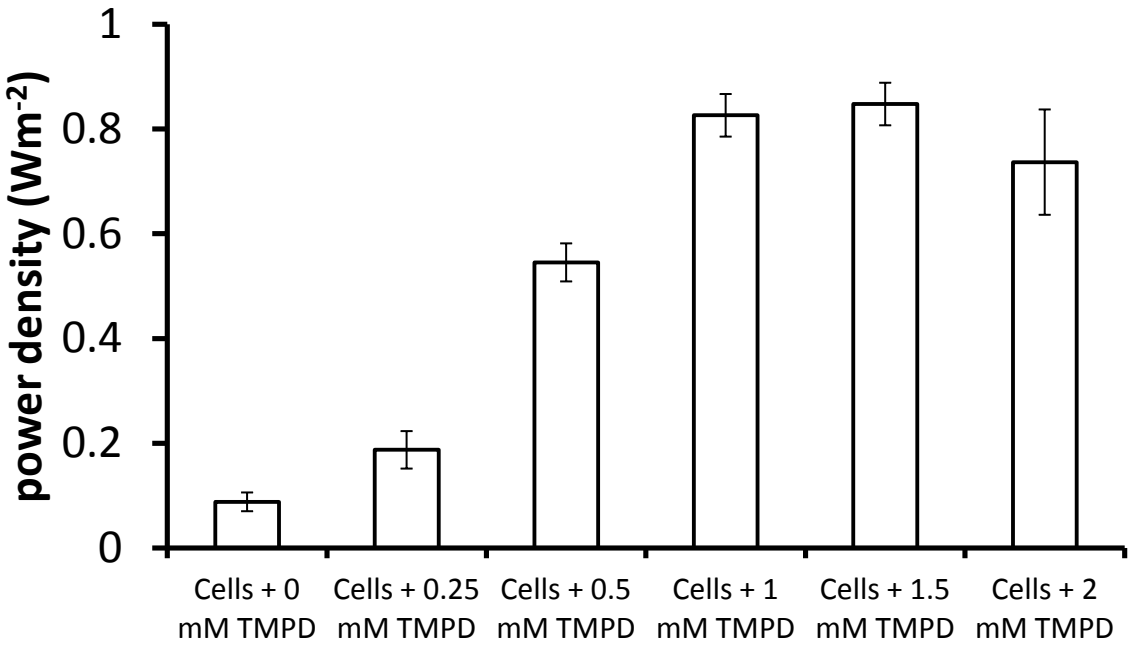


**Figure 3.12: Bar graph of TMPD single addition data.** Bar graph of power density of the above (Figure 3.10) MFC at 35 min. Error bars represent standard error of the mean (n=4).

### 3.4.4. *Arxula adeninivorans* electron transfer with and without mediator

Mediator-less electron transfer from *A. adeninivorans* was demonstrated when using both dissolved oxygen and $KMnO_4$ as the cathode reaction (Figure 3.13). Oxygen was not expected to react with the carbon cloth cathode surface because it does not contain a platinum cathode. However, a small amount of power is observed that was statistically different to the acellular control (ANOVA, p=0.05). The difference in power density between the cellular and acellular control was statistically different at all points (ANOVA, p=0.05). The difference in the power density derived from mediator-less electron transfer was not significantly different between the two different electron acceptors (ANOVA, p=0.05). However, because the difference in the power density peaks observed from the addition from $KMnO_4$ with and without cells is statistically different (ANOVA p=0.05), it suggests that a build up of charge occurs when dissolved oxygen is the electron acceptor, and when the electron acceptor is changed to $KMnO_4$, the change in potential or the change in kinetics releases these stored up electrons.

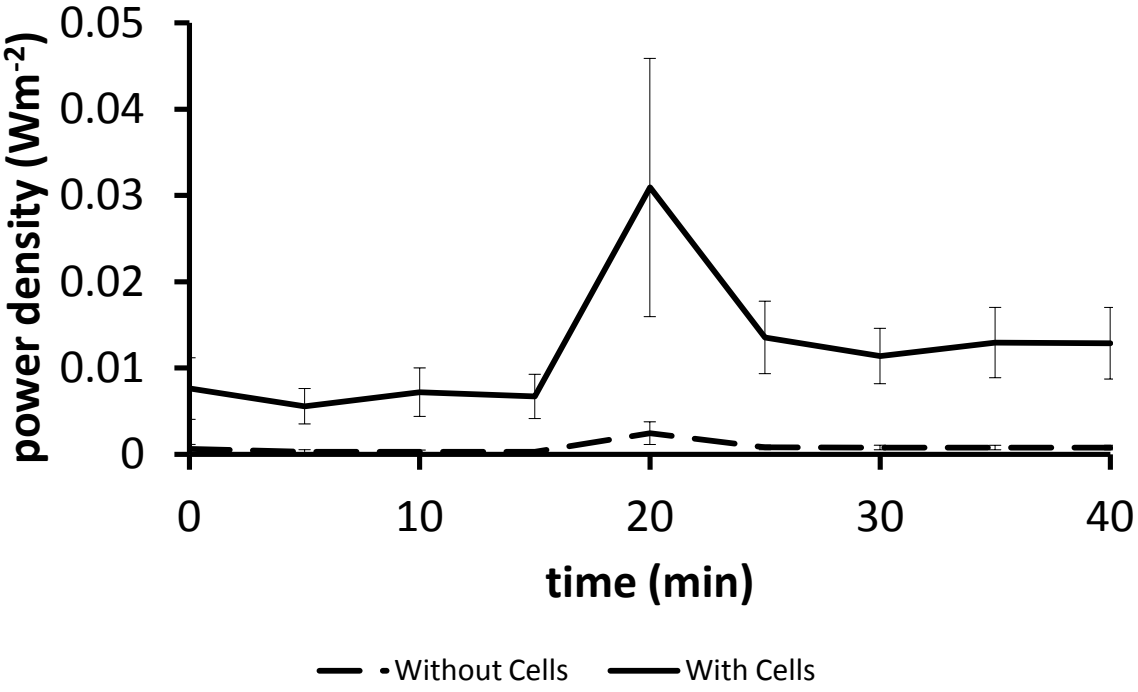


**Figure 3.13: Effect of different cathode reactions on mediator-less MFC.** MFC contained PBS in the cathode and either $OD_{600}$ 2.5 *A. adeninivorans* suspended in PBS or PBS only in the anode. Constant temperature (37$^{o}$C) and cells kept suspended (180 rpm). The PBS was removed by peristaltic pump and replaced with 0.5 M $KMnO_4$ between 15 and 20 mins. Error bars represent standard error of the mean (n=4).

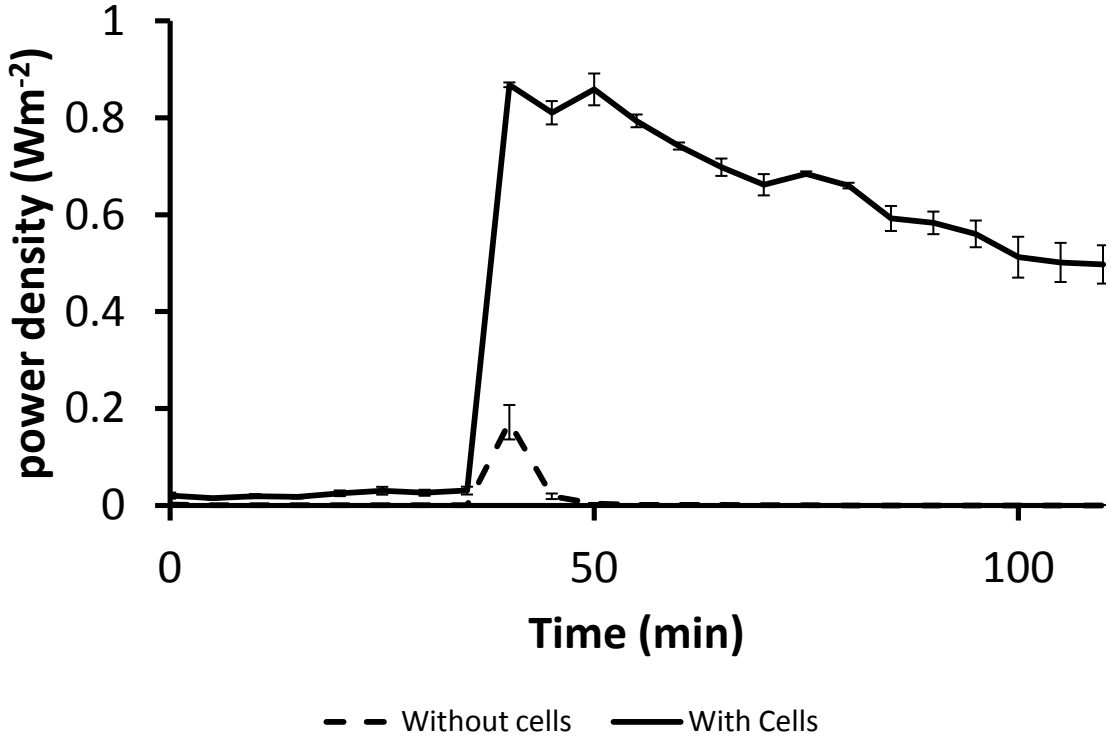


**Figure 3.14: Mediated electron transfer**. MFC contained 0.5 M $KMnO_4$ dissolved in PBS in the cathode and either $OD_{600}$ 2.5 *A. adeninivorans* suspended in PBS or PBS only in the anode. Constant temperature (37°C) and cells kept suspended (180 rpm). TMPD was added to a concentration of 1.5 mM at 40 mins. Error bars represent standard error (n<4).

Figure 3.14 demonstrates that mediator-less (before 40 mins) and mediated electron transfer (after 40 mins) produces adequate power density at 100 Ω external load to be distinguishable from the acellular control. Although many other reasons for the short term power drop have already been suggested, another possibility is that TMPD concentration may be diminishing due to the instability of the molecule. This will be investigated in later chapters.

### 3.4.5. MFC pH change, loss of power with time and glucose metabolism

Several previous figures demonstrated a steady drop off in power density with time after the addition of TMPD (Figures 3.6, 3.10 & 3.14). Fouling of the cathode has been experimentally demonstrated using both the MFC and voltammetry (Figures 3.6 & 3.7 respectively). Fouling of the anode was also demonstrated by the electrochemical study. Examination of the PEM showed a colour change resulting from exposure to $KMnO_4$. So, by preventing the exchange

of $H^+$ between chambers, the fouling of the PEM could cause a change the pH of the cathode and this would result in a change in the reaction in the cathode (see section 2.7.3). It is also possible that the drop off is due to a running out of internal stores within in *A. adeninivorans* or from TMPD instability.

With any combination of these factors responsible for the steady drop off of power density, the following experiment was conducted (Figure 3.15). Two different experiments were conducted with new anodes, cathodes and PEM, each for 5 h. The first experiment contained *A. adeninivorans*, TMPD and glucose in the anode. The second experiment did not contain glucose in the anode. The pH of the anode and cathode contents was measured before and after the experiment.

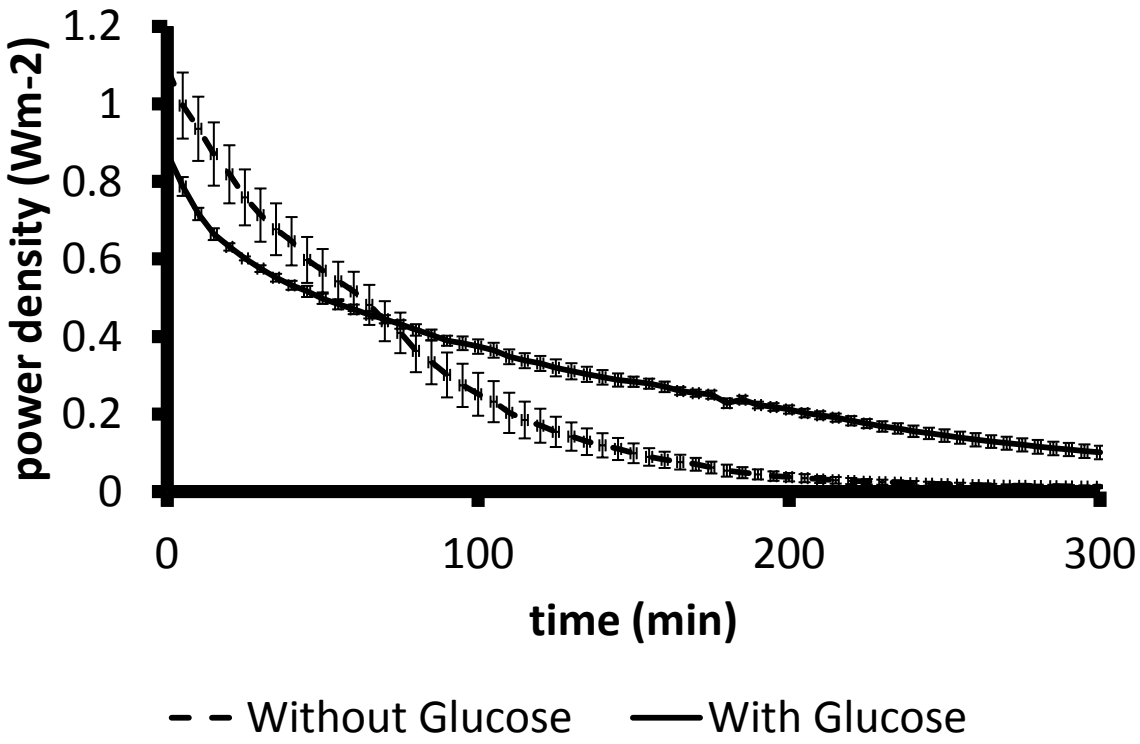


**Figure 3.15: Effect of glucose on 5 h MFC experiment**. MFC contained 0.5 M $KMnO_4$ dissolved in PBS in the cathode and $OD_{600}$ 2.5 *A. adeninivorans* suspended in PBS with 1.5 mM TMPD with or without 10 mM glucose in the anode. Constant temperature (37$^oC$) and cells kept suspended (180 rpm). Error bars represent standard error of the mean (n=4).

The MFC containing glucose produced less power density at the beginning, but maintained a higher power density over time (ANOVA p=0.05). The slope of the power density drop off was steeper when glucose was not present, which indicates that the reduction of the internal stores was partly responsible for the drop off.

The pH of the anode changed from pH 7.0 to 4.6, and the pH of the cathode changed from pH 7.0 to 9.4. This indicates that the PEM is not able to transfer $H^+$ from the anode to the cathode fast enough to meet the demands of the MFC. The inability of the PEM to meet the demand of $H^+$ transfer in the MFC is either due to the surface area not being large enough by design or from fouling from the $KMnO_4$. An increase in the pH in the cathode was demonstrated by You *et al.* (2006) to drop the maximum possible potential between the anode and cathode (open circuit potential). Therefore, the increase in cathode pH is another factor responsible for the steady drop off in power density over time.

## 3.5.Discussion

### 3.5.1. Optimisation of a MFC

As the factors that affect power density are so interconnected that it is very difficult to tease the effect of each apart. When the external load is varied, the power density is affected differently when cells are present and when a mediator is present. When fouling of the cathode and PEM is observed from the cathode reaction, the implications of their fouling and the testing methods required to confirm their contribution to this behaviour are drastically different. When the optimal concentration of TMPD is investigated, the power density drop off affected the type of experiment that can be used to investigate that.

### 3.5.2. Effect of optimal external load

The external load was shown to be optimal at 100 Ω when a mediator is present. This low external load forces the MFC into operation far away from equilibrium conditions which results in pressuring the MFC to produce a high amount of current to the external circuit in order to maintain the voltage (Ohm's Law). By creating conditions that cause a high flow of electrons from the anode to the cathode, it increases the rate of reaction in both compartments. The high current being drawn will result in potential losses due to the formation of over-potentials and concentration gradients.

By increasing the rate of reactions, the amount of acid ($H^+$) produced in the anode increased and the amount of $H^+$ used in the cathode increased. This subsequently increased the rate at which the $H^+$ ions must transfer from the anode to the cathode. However a pH change in both chambers suggests that the rate of $H^+$ transferred through the PEM is not enough to balance in long term experiments. The buffering of the anode and cathode with PBS should allow for a delay in the change of pH, and experiments should therefore be kept to less than 2 h.

It is unclear whether the fouling of the PEM by $KMnO_4$ actually decreases the rate of $H^+$ transfer or if the surface area of the PEM is too small to meet the demands of this MFC. However, in either case, initially the transfer of $H^+$ in combination with the buffer should help maintain a balanced overall MFC reaction, allowing for short term experimentation.

### 3.5.3. Effect of cathode reaction

Potassium permanganate is the chemical used in the cathode reaction in many disposable batteries currently available on the market today. It is a very strong oxidising agent and shows great potential to increase the maximum possible power obtainable from a MFC (You *et al.* 2006; Logan 2008, Chapter 6). Potassium permanganate has a far higher positive reduction potential than ferricyanide, and does not suffer the same kinetic problems as oxygen. Oxygen is ubiquitous in the atmosphere but must dissolve in order to reach the electrode and once at

the electrode a catalyst like platinum or laccase is required to overcome the high activation energy and increase the rate of reaction. In my research, the cathode did not contain platinum or any other catalyst, and therefore oxygen reduction at the cathode was expected to be very slow. This highlights the appeal of using potassium permanganate over oxygen as the cathode reaction in a MFC.

The same properties that make $KMnO_4$ appealing, such as being a strong oxidant and a high standard reaction potential, also has many drawbacks, the chief of which is fouling of both the cathode and the PEM. These drawbacks were kept to a minimum by, maintaining the pH for as long as possible by using fresh PEM, and buffering the cathode with PBS to ensure that at least short duration experiments can be conducted with $KMnO_4$.

### 3.5.4. Mediated vs. Mediator-less MFC

The ability of *A. adeninivorans* to transfer electrons to the anode with both dissolved oxygen and $KMnO_4$ has not been previously reported. Very few eukaryotic MFC have been investigated and of those, most required the use of a mediator to produce a high power output. From the literature, the likely mechanism of electron transfer from yeast include: an enzymatic reaction, such as ferricyanide reductase, or a fermented product (Prasad *et al.* 2007; Ducommun 2010). Therefore, the means by which *A. adeninivorans* is able to transfer electrons to the electrode will be investigated in later chapters.

The eukaryote electron transport chain is located within its mitochondrion. The consumption of glucose and the subsequent improvement of mediated power density indicate that the mediator penetrate the cellular membrane and access electrons released from glycolysis (cytoplasm) and also probably the electrons released from the TCA cycle (Krebs cycle, within mitochondrion) (Baronian *et al.* 2002; Heiskanen *et al.* 2009; Kotesha *et al.*2009). It is likely that due to the dramatic power density difference between mediator-less and mediated MFC,

the use of a lipophilic mediator such as TMPD enables access to the NADH that is primarily produced within the mitochondrion (Todisco *et al.* 2006; Avéret *et al.* 2002; Yang *et al.* 2007).

TMPD reacted with the electrode in the acellular controls (Figure 3.11). However, it is unclear as to whether the TMPD is able to diffuse out of the cell once reduced and transfer these electrons to the electrode outside the cell in a hydrophilic environment. The means by which mediated electron transfer of *A. adeninivorans* occurs will be investigated in later chapters.

### 3.6. Conclusion

Mediated and mediator-less MFC using *A. adeninivorans* are both possible. The mechanism of both the mediated and the mediator-less electron transfer requires further investigation. $KMnO_4$ is able to be used at a cathode reactant but there are serious problems with fouling of both the cathode and the PEM, restricting MFC experimentation to short durations. The optimal external load was identified and set as low as possible in order to promote high reaction speed in both the anode and the cathode.

# Chapter 4: Mediator-less electron transfer

## 4.1. Abstract

Mediator-less power densities were compared between MFCs containing *A. adeninivorans* and *S. cerevisiae*. Despite *S. cerevisiae* demonstrating the same rate of ferricyanide reduction, the power density from *A. adeninivorans* was significantly greater. This difference in power density is attributed to a solution species secreted by *A. adeninivorans* that appears to be absent in *S. cerevisiae* and the use of potassium permanganate in the cathode allowing the oxidation of a reduced solution species secreted by *A. adeninivorans*.

## 4.2. Introduction

In chapter 3, mediator-less electron transfer was identified and partially characterised through altering the external load and by using two different cathode reactions (dissolved $O_2$ and $KMnO_4$). The ability to transfer electrons to an electrode by eukaryotic microorganism with the assistance of a mediator has been previously reported for *S. cerevisiae* (Potter 1911; Cohen 1931; Ducummon *et al*. 2010), *Hansenula anomala* (Prasad *et al.* 2007) and *Candida melibiosica* (Hubenova *et al.* 2000). The eukaryotic electron transport chain (and the bulk of the NADH) is contained within the mitochondrion (Todisco *et al.* 2006; Avéret *et al.* 2002; Yang *et al.* 2007; Kostesha *et al.* 2009; Baronian *et al.* 2002) and therefore the means of mediator-less electron transfer in a MFC with a eukaryotic microorganism must be separate from its catabolic pathways.

Prasad *et al.* (2007) reported direct electron transfer between the yeast *H. anomala* and the anode, based on CV and MFC studies. They attributed the electron transfer contributing to the mediator-less MFC power density to direct contact between the MFC electrode and membrane bound ferricyanide reductase or lactate dehydrogenase.

The copper-dependent Fe(II) oxidase (AFRE2) has been identified in *A. adeninivorans* (Wartmann *et al.* 2002). Ferricyanide reductase was investigated for its capability as the primary cause of mediator-less electron transfer in this MFC using *A. adeninivorans* as the biological catalyst.

## 4.3. Materials and methods

### 4.3.1. Chemicals, buffer, reagents and media

All chemicals, buffers, reagents and media are the same as those reported in section 3.3.

### 4.3.2. Strains and Cell culturing

The *S. cerevisiae* NCTC 10716 was obtained from the ESR yeast collection, Porirua, New Zealand. Batch cultures of *A. adeninivorans* LS3 and *S. cerevisiae* NCTC 10716, were cultivated aerobically in indented flasks at 37$^{o}$C and 30$^{o}$C respectively, centrifuged at 180 rpm for 24 h in YEPD broth, washed twice (4,500 rcf, for 8 min) and finally re-suspended in PBS.

### 4.3.3. Cyclic Voltammetry

Two different types of electrode arrangements were used in this thesis, termed ‘hanging’ and ‘sedimentation’ (Figure 4.1). Hanging involves literally hanging all three electrodes (working, reference and counter/auxiliary) into each solution. It is the most common means of CV and has been well described (Kissinger & Heinemann 1983; Benschoten *et al.* 1983; see Section 1.8.7). Sedimentation CV involves inverting a glassy carbon working electrode and creating an electrochemical cell directly on the surface of the working electrode with the reference and counter inserted from above (Figure 4.1). In my research, sedimentation CV was conducted to find low concentration soluble molecules with a high specific density secreted by whole living yeast cells by allowing them to settle onto the surface of the electrode before experimentation.

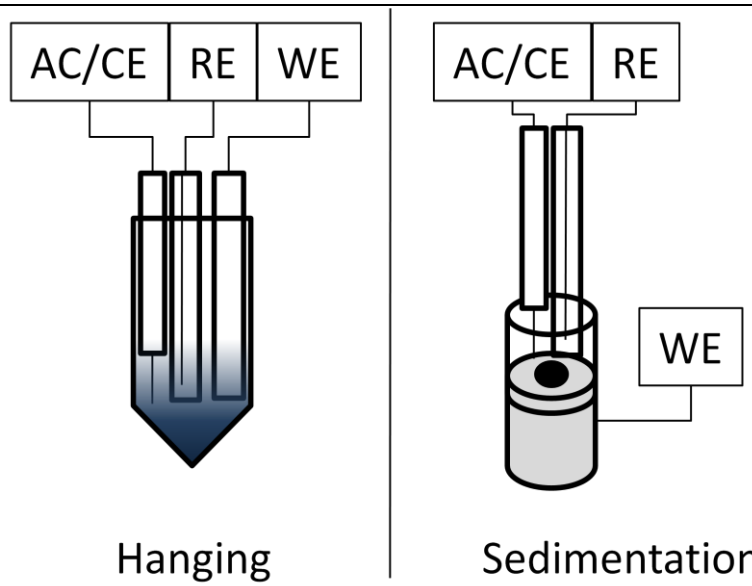


**Figure 4.1: Different cyclic voltammogram 3 electrode set ups.** WE – Working electrode, RE – reference electrode, AC/CE – auxiliary/counter electrode.

The rate of extracellular ferricyanide reduction by *A. adeninivorans* and *S. cerevisiae* was measured with the following 3 electrode set ups: platinum pseudo-micro-disk (working), Ag/AgCl (reference), platinum (auxiliary/counter). An $OD_{600}$ 2.5 of either *A. adeninivorans* or *S. cerevisiae* cells suspended in PBS and 20 mM FC (with and without glucose) were incubated in falcon tubes at 37$^{o}$C, 180 rpm. Measurements (CV) were performed at times 0, 24, 42 and 72 h, performed from 0 mV to + 400 mV vs. Ag/AgCl, 10 $mVs^{-1}$ with the point at +400 mV used to report the relative concentration of ferrocyanide to ferricyanide in the solutions.

Sedimentation CVs of concentrated yeast were obtained by harvesting the yeast species and suspending the cells in PBS (see section 4.3.2.). The harvested cells were then centrifuged again (4,500 rcf, 8 min) and as much of the supernatant as possible was removed. Concentrated supernatant could then be produced by transferring the cells to an Eppendorf tube and leaving the cells at room temperatures for at least 45 mins, and then centrifuging (12,000 rpm, 8 min) and extracting the supernatant.

### 4.3.4. Yeast Microbial Fuel Cell

MFC experiments were conducted as described in section 3.3.3. *S. cerevisiae* cells (like the *A. adeninivorans* cells reported in section 3.3.3.) were suspended in the anode at an $OD_{600}$ 2.5.

## 4.4. Results

### 4.4.1. Extracellular reduction of ferricyanide

The ability of yeast cells to reduce the hydrophilic mediator ferricyanide has been linked to direct electron transfer and other forms of mediator-less electron transfer (Prasad *et al.* 2007). Ferricyanide is extremely hydrophilic and cannot pass through the plasma-membrane of biological cells (Baronian *et al.* 2002). As a result, reduction of ferricyanide must occur either on or outside the cells' plasma membrane.

The rate of ferricyanide reduction by equal concentrations of *S. cerevisiae* and *A. adeninivorans* was measured (Figures 4.2, 4.3). The rate of ferricyanide reduction of *S. cerevisiae* was the same as *A. adeninivorans* when glucose was absent, but the rate of ferricyanide reduction was greater for *S. cerevisiae* with glucose present (ANOVA $p=0.05$). However, the rate of ferricyanide reduction did not change for *A. adeninivorans* with the addition of glucose. This suggests that in *A. adeninivorans* ferricyanide reduction is glucose independent or does not respond as rapidly to glucose as *S. cerevisiae.*

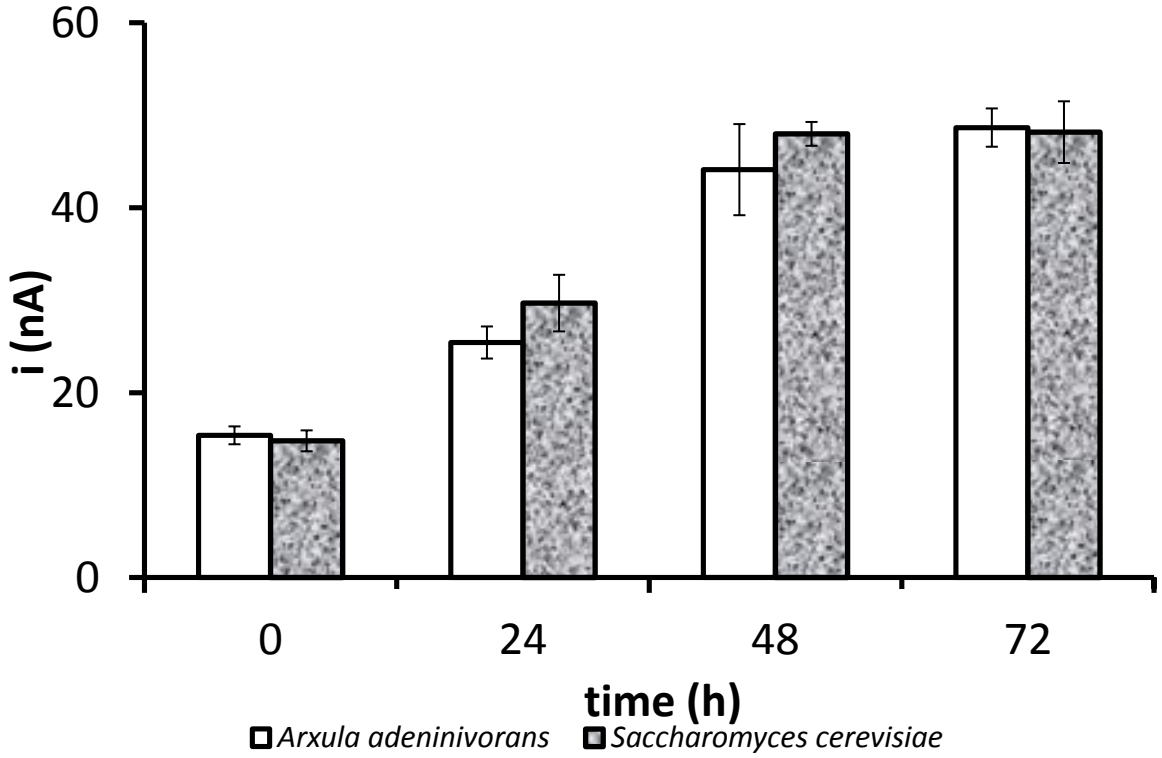


**Figure 4.2: Reduction of ferricyanide over time by *A. adeninivorans* and *S. cerevisiae*.** $OD_{600}$ 2.5 of cells suspended in PBS and 20 mM ferricyanide were incubated in falcon tubes at 37$^{o}$C, 180 rpm. Cyclic voltammetry was performed (from 0 mV to + 400 mV vs. Ag/AgCl, 10 $mVs^{-1}$) using the following 3 electrode set ups: Working; Pt microelectrode, Reference; Ag/AgCl, Counter; Pt. Error bars represent standard error of the mean (n=3).

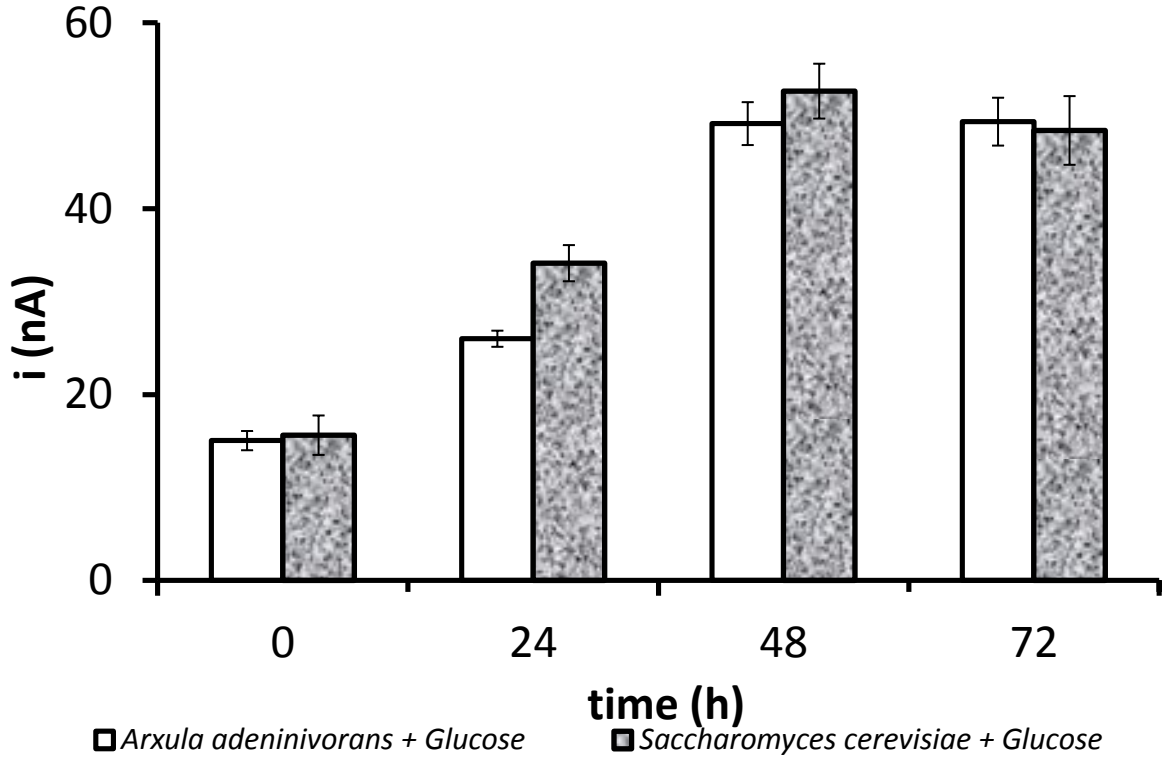


**Figure 4.3: Reduction of ferricyanide over time by *A. adeninivorans* and S. cerevisiae with glucose.** $OD_{600}$ 2.5 of cells suspended in PBS, 20 mM ferricyanide and 10 mM glucose were incubated in falcon tubes at 37$^{o}$C, 180 rpm. Cyclic voltammetry was performed (from 0 mV to + 400 mV vs. Ag/AgC, 10 $mVs^{-1}$) using the following 3 electrode set ups: Working; Pt microelectrode, Reference; Ag/AgCl, Counter; Pt. Error bars represent standard error of the mean (n=3).

### 4.4.2. Mediator-less electron transfer from *A. adeninivorans* and *S. cerevisiae* in MFC

The mediator-less electron transfer from *A. adeninivorans* and *S. cerevisiae* were examined in a MFC (Figure 4.4). The power density of *A. adeninivorans* was shown to increase with time. The power density of *S. cerevisiae* was shown to stay constant with time. The power density of both *A. adeninivorans* and *S. cerevisiae* were statistically different from the acellular control at all points (ANOVA p=0.05). The power density of both *A. adeninivorans* and *S. cerevisiae* were statistically different from each other at all points except for time zero (ANOVA p=0.05).

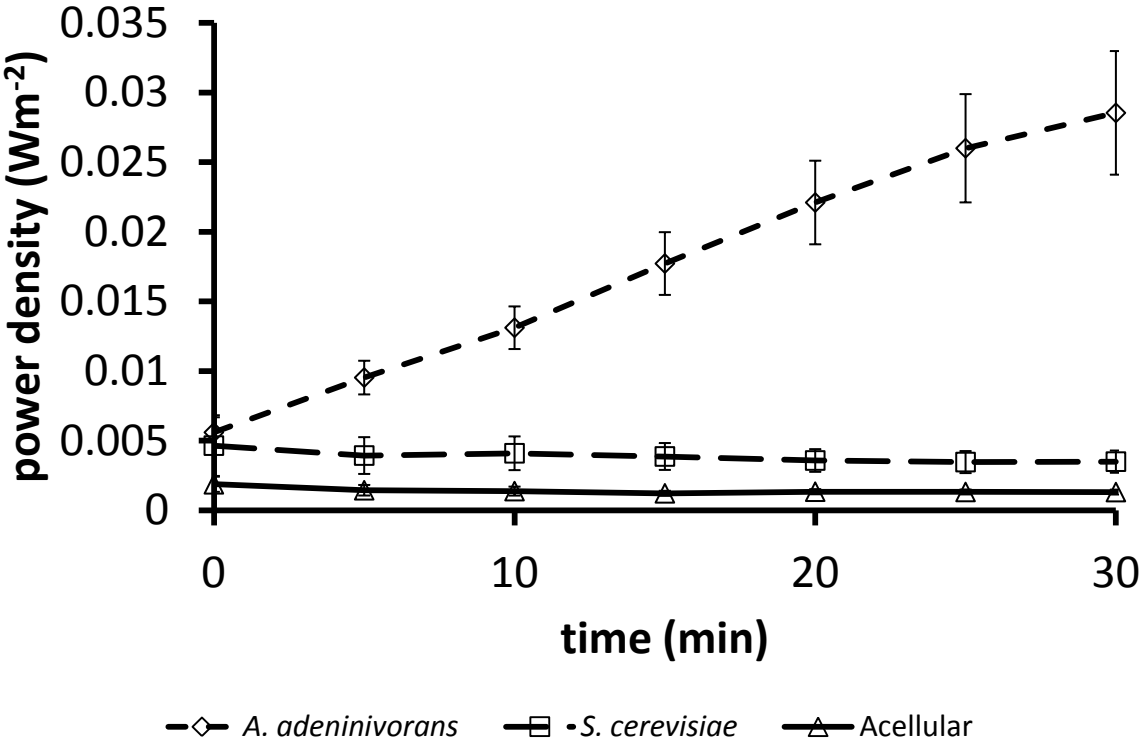


**Figure 4.4: Comparison of mediator-less electron transfer between *A. adeninivorans* and *S. cerevisiae*.** MFC contained 0.5 M $KMnO_4$ dissolved in PBS in the cathode and $OD_{600}$ 2.5 of either *A. adeninivorans* or *S. cerevisiae* suspended in PBS or PBS only in the anode. Temperature kept constant (37$^{o}$C) and cells kept suspended (180 rpm). Error bars represent standard error of the mean (*A. adeninivorans* n=33, *S. cereivisae* n=9, PBS n=7).

### 4.4.3. Sedimentation CV, Supernatant CV, Concentrated Supernatant CV

Two different experimental set ups were used to conduct the CV for the following experiments. In this thesis they have been termed 'hanging' and 'sedimentation' (See section 4.3.3 for a full description of the difference in the procedures). In brief, 'hanging' CVs have the 3 electrodes hanging in the solution of interest, and 'sedimentation' CVs have the working electrode inverted and electrochemical cell created around it, with the reference and auxiliary/counter electrodes hanging about it in the solution (Figure 4.1). The advantage of the 'sedimentation' CVs is that all the molecules (and cells) with higher relative density/specific gravity than the solution fall onto the working electrode, not away from electrode. This

enables the detection of high density molecules (and cells) to collect on the electrode surface and be detected electrochemically.

The supernatants of *A. adeninivorans* and *S. cerevisiae* suspended in PBS and were left at room temperature for 3 h. Both demonstrated an irreversible peak at +0.7 V which was not present in the PBS control (Figure 4.5) between 0.5 -1.0. This indicates that there is no electrochemically active substance produced by either yeast that can be detected using this experimental set up. The detected peak at +0.7 V was too positive to be able to reduce ferricyanide and therefore any enzyme or molecule produced that may be electrochemically active, must therefore be at a low concentration.

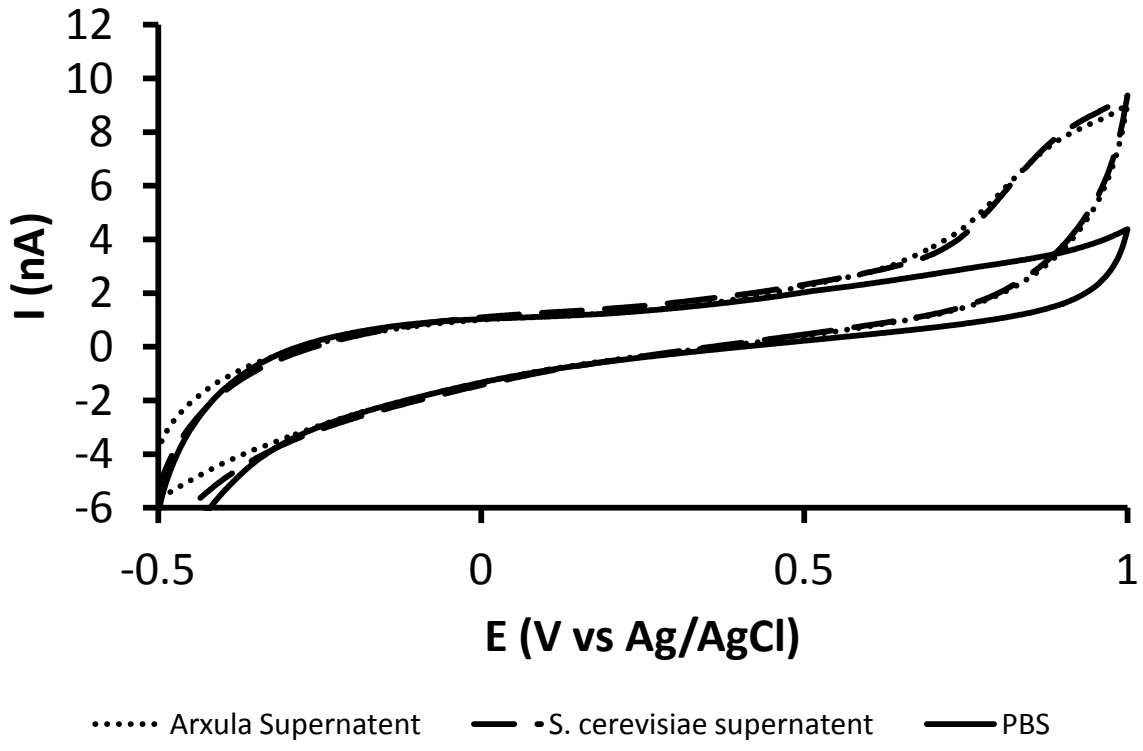


**Figure 4.5: Hanging CV of *A. adeninivorans* and *S. cerevisiae* supernatant.** Cyclic voltammetry was performed (from -1000 mV to + 1000 mV vs. Ag/AgCl at 100 $mVs^{-1}$) using the following 3 electrode set up: Working; glassy carbon macro-electrode, Reference; Ag/AgCl, Counter; Pt. All CV are a mean of 3.

Sedimentation CV of *S. cerevisiae* demonstrated no peaks below +0.7 V (Figure 4.6). The potential for ferricyanide (vs. Ag/AgCl) was +0.36 V and any enzymatic action/product that could reduce ferricyanide would have a potential below this voltage. Therefore, any enzyme responsible for ferricyanide reduction (ferricyanide reductase) or any product excreted by the cell was not detectable for *S. cerevisiae* with this method and this working electrode (glassy carbon).

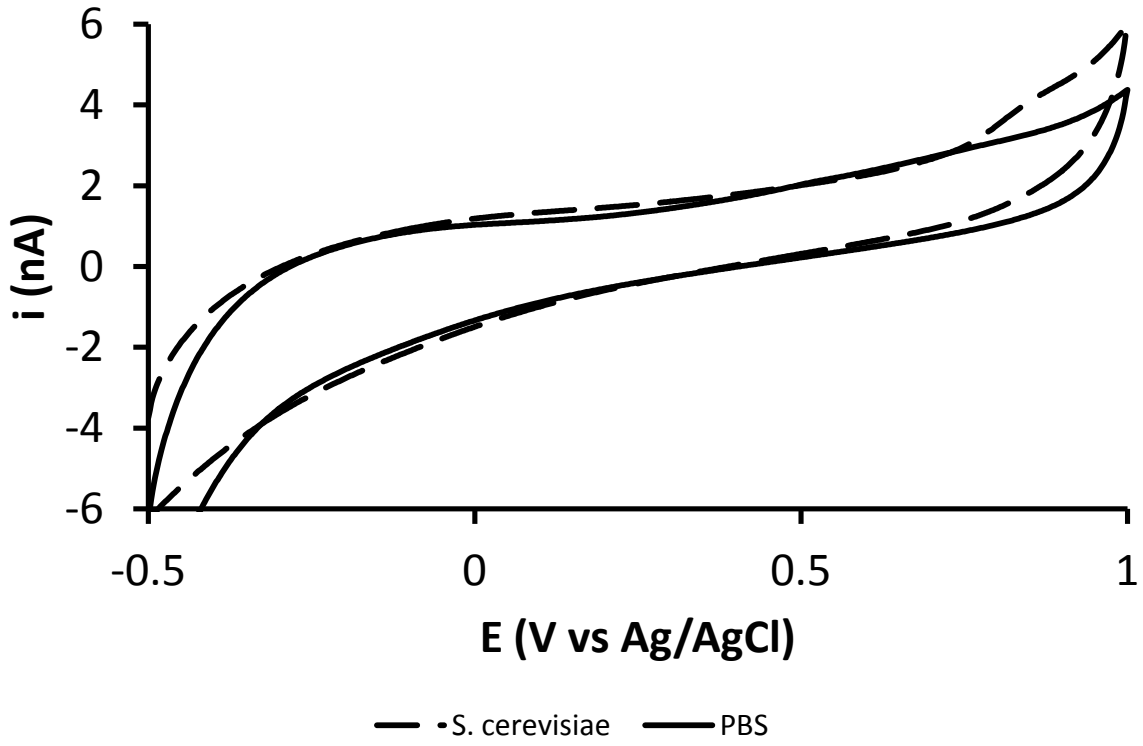


**Figure 4.6: Sedimentation CV of highly concentrated *S. cerevisiae* cells onto an inverted glassy carbon electrode.** Cyclic voltammetry was performed (from -500 mV to + 1000 mV vs. Ag/AgCl at 100 $mVs^{-1}$) using the following 3 electrode set ups: Working; glassy carbon macro-electrode, Reference; Ag/AgCl, Counter; Pt. All CV are a mean of 3.

Sedimentation CV of *A. adeninivorans* demonstrated two irreversible peaks (Figure 4.7), the first peak at +0.4 V, the second peak at +0.8 V. As with *S. cerevisiae* there was no peak below the ferricyanide reaction potential, which explains why both *A. adeninivorans* and *S. cerevisiae* have the same rate of ferricyanide reduction. However, the *A. adeninivorans*

+0.4 V peak explains the difference in the mediator-less electron transfer (Figure 4.4), if using $KMnO_4$ is able to poise the potential of the anode to a value higher than +0.4 V.

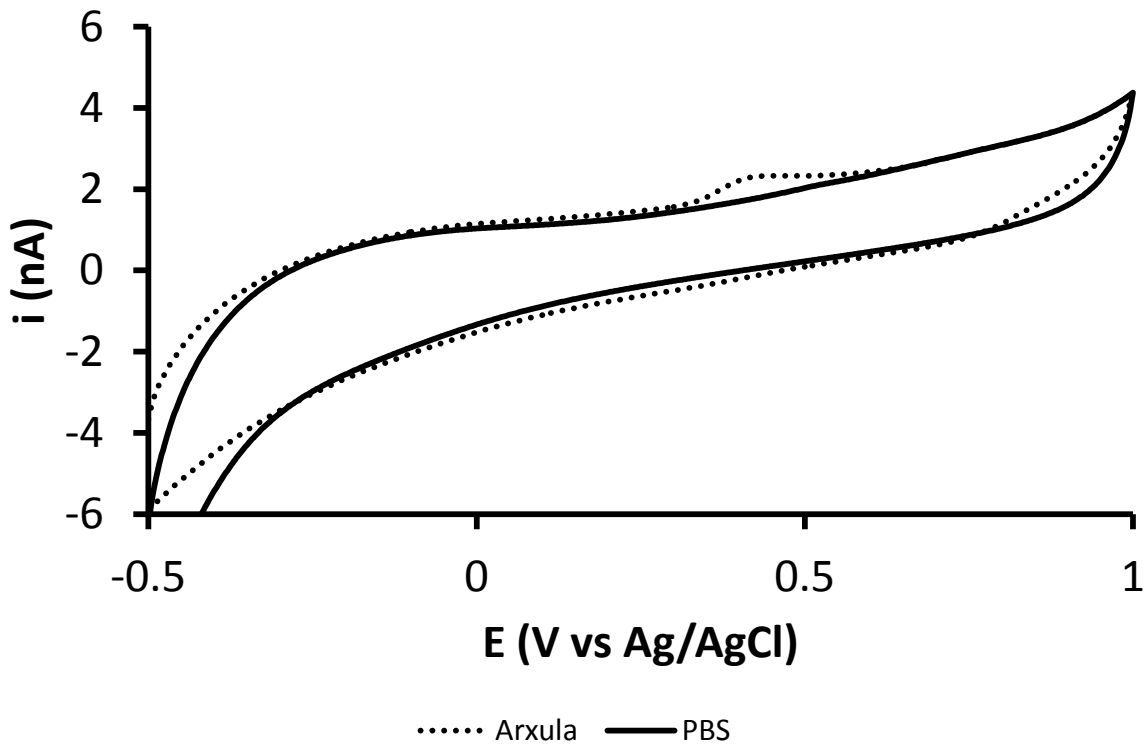


**Figure 4.7: Sedimentation CV of highly concentrated *A. adeninivorans* cells onto an inverted glassy carbon electrode.** Cyclic voltammetry was performed (from -500 mV to + 1000 mV vs. Ag/AgCl at 100 $mVs^{-1}$) using the following 3 electrode set ups: Working; glassy carbon macro-electrode, Reference; Ag/AgCl, Counter; Pt. All CV are a mean of 3.

In order to ascertain if the irreversible +0.4 V peak described above for *A. adeninivorans* is a membrane bound species or a solution species F. Barriére conducted a scan rate study (in press). He found that the peak at +0.4 V was a solution species. In order to detect this solution species, concentrated cells were left for 3 h at room temperature in PBS, the supernatant was then harvested and a sedimentation CV was conducted (Figure 4.8). This procedure revealed that both peaks observed for *A. adeninivorans* are due to solution species secreted by the yeast.

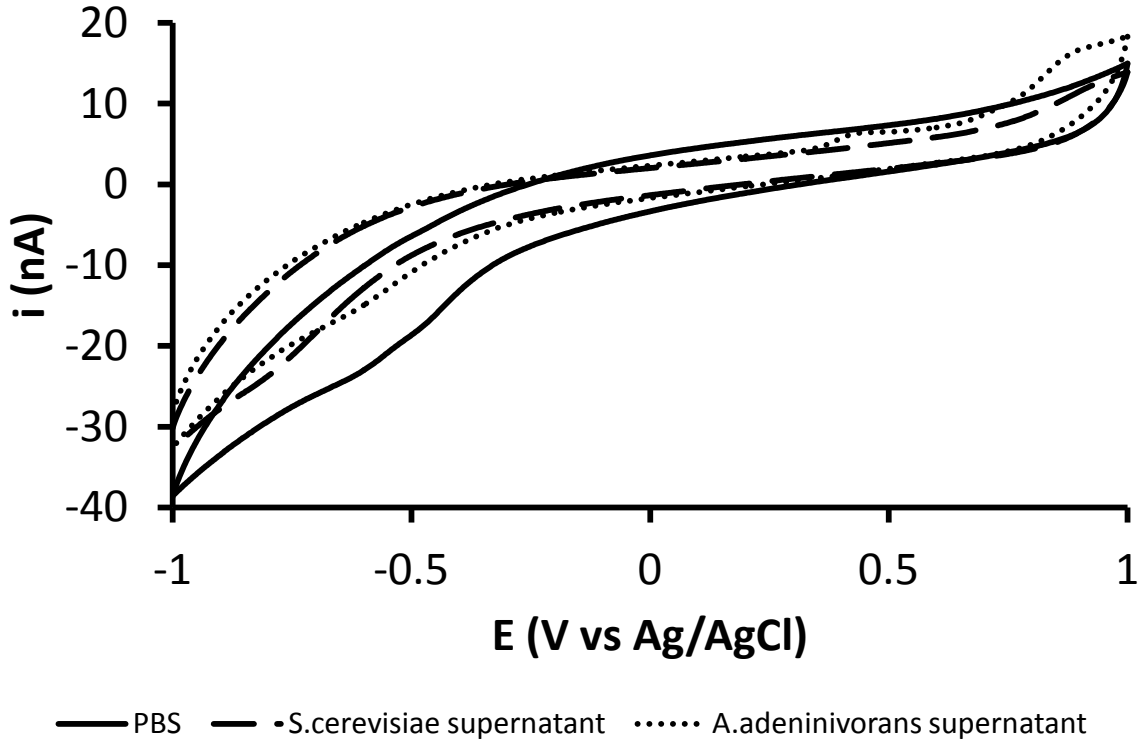


**Figure 4.8: Sedimentation CV of highly concentrated *S. cerevisiae* and *A. adeninivorans* supernatant.** Cyclic voltammetry was performed (from -1000 mV to + 1000 mV vs. Ag/AgCl at 100 $mVs^{-1}$) using the following 3 electrode set ups: Working; glassy carbon macro-electrode, Reference; Ag/AgCl, Counter; Pt. All CV are a mean of 3.

### 4.4.4. Cell concentration

A cell concentration of $OD_{600}$ 2.5 for both *A. adeninivorans* and *S. cerevisiae* equates to 1 x $10^8$ cfu (personal observation). Regardless of the mechanism for mediator-less electron transfer, the cell concentration would affect the power density achieved. Three different concentrations of *A. adeninivorans* and *S. cerevisiae* were investigated in the MFC, $OD_{600}$ 25, 2.5 & 0.25, and the peak power produced is shown in Figure 4.9. The peak mediator-less electron transfer for $OD_{600}$ 25 & 2.5 for *A. adeninivorans* was not statistically different, but was for *S. cerevisiae* (ANOVA p=0.05). The greatest mediator-less electron transfer for $OD_{600}$ 2.5 & 0.25 was statistically different for *A. adeninivorans*, but not for *S. cerevisiae* (ANOVA p=0.05). This indicates that the optimal concentration for mediator-less power

density of *A. adeninivorans* was close to 2.5 $OD_{600}$ but for *S. cerevisiae* was closer to 25 $OD_{600}$

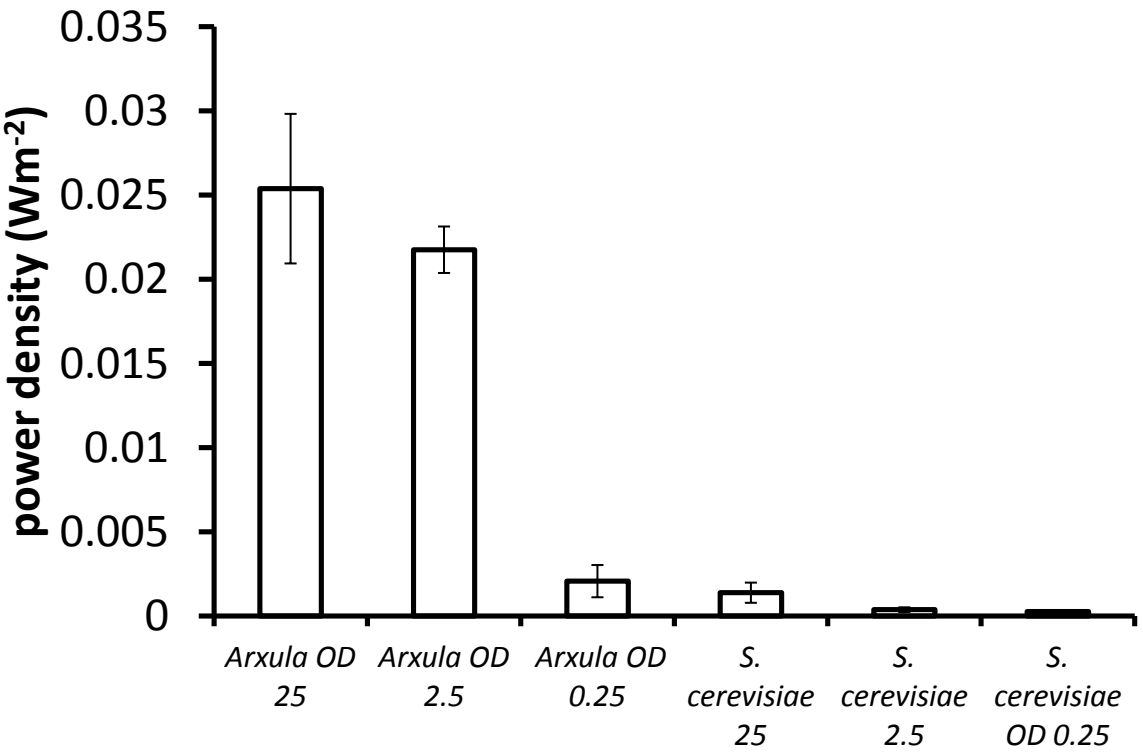


**Figure 4.9: Effect of cell concentration on mediator-less electron transfer.** MFC contained 0.5 M $KMnO_4$ dissolved in PBS in the cathode and either *A. adeninivorans* or *S. cerevisiae* suspended in PBS in the anode. Constant temperature (37$^{o}$C) and cells kept suspended (180 rpm). Fuel cells were operated under load for 2 h until steady state was achieved. Error bars represent standard error of the mean (n=4)

### 4.4.5. Different electron acceptors

The effect of $KMnO_4$ and FC used as the electron acceptors in the cathode has on mediator-less electron transfer of *A. adeninivorans* in a MFC was investigated (Figure 4.10). The results show that if FC was used, then the power density was very low compared to the power density observed when $KMnO_4$ was used. This supports the results of section 3.3 and suggests that a solution soluble species secreted from *A. adeninivorans* with a reduction potential of +0.4 V (vs. Ag/AgCl) contributes to the power density of mediator-less MFC. The difference

in redox potentials is the likely reason for this. However, the mechanism(s) involved have not been previously described.

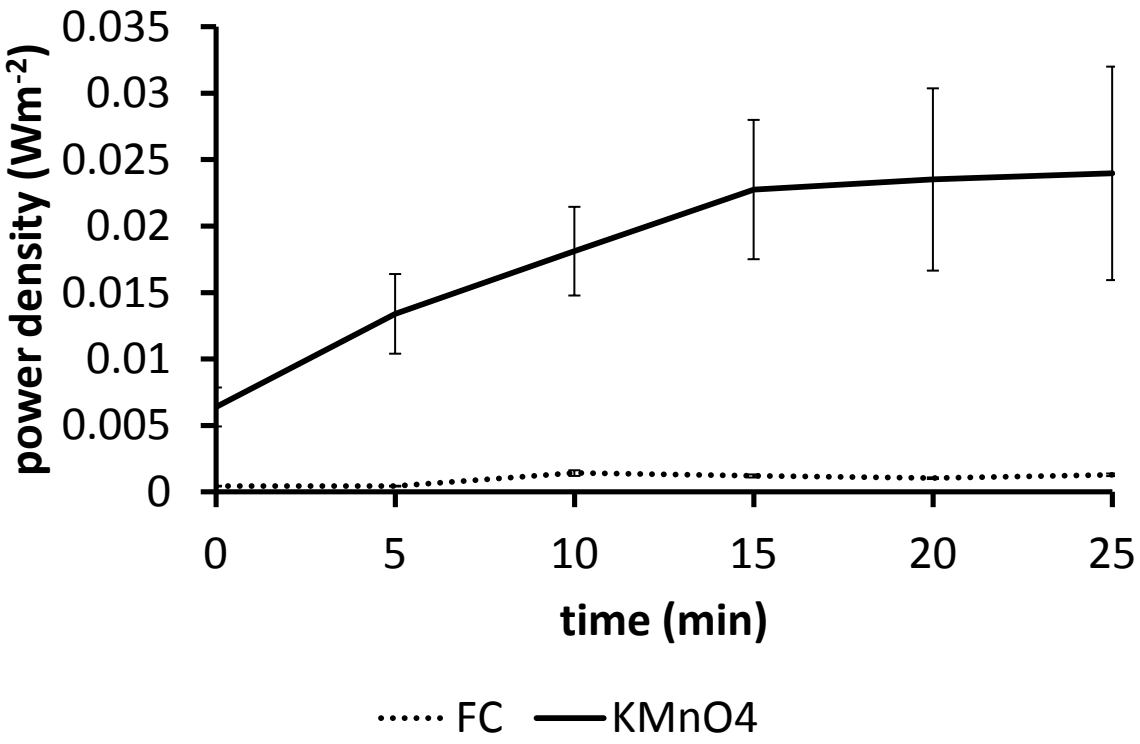


**Figure 4.10: Effect of different electron acceptors in the cathode on mediator-less MFC.** Fuel cells contained either 0.5 M $KMnO_4$, or 0.5 M FC dissolved in PBS in the cathode. An $OD_{600}$ 2.5 of *A. adeninivorans* was suspended in PBS in the anode. Constant temperature ($37^oC$) and cells kept suspended by continuous agitation (180 rpm).Error bars represent standard error of the mean (n=4).

In order to ascertain how the different reaction potentials of the electron acceptors (cathode reaction) affect the anode, first the potential of the anode, cathode, and open circuit potential was measured (Figure 4.11). The results show that different solutions give the following potentials: PBS has a variable negative potential, FC has a potential of +0.34 V and $KMnO_4$ has a potential of +0.66 V when cells are present in the anode. These results are close to the standard redox potentials for FC (+0.36) and lowest for $KMnO_4$ (+1.51, +1.76/+0.9 & +0.6; Section 2.7.3). However, the cathode potential for $KMnO_4$ was less than a potential of approximately 1V reported by You *et al.* (2006) with carbon cloth as its cathode material.

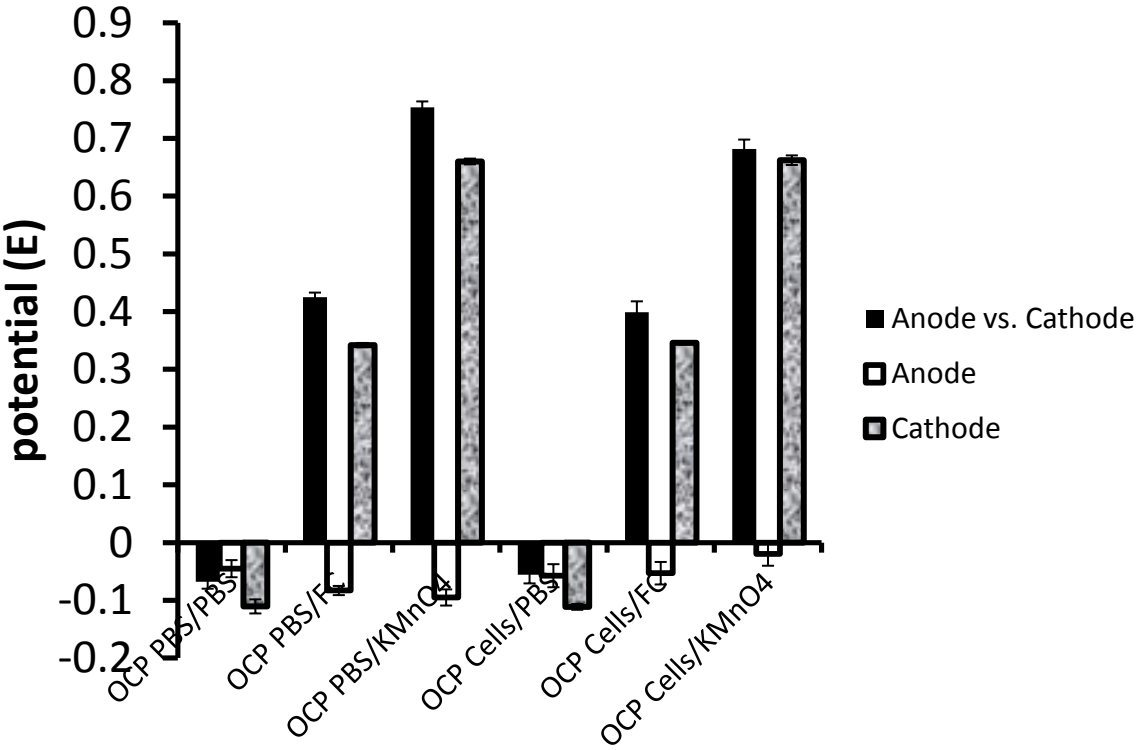


**Figure 4.11: Effect of different electron acceptors on the open circuit potential of mediator-less MFC with and without cells present.** Fuel cells contained either 0.5 M $KMnO_4$, 0.5 M FC dissolved in PBS or PBS only in the cathode. In the anode an $OD_{600}$ 2.5 of *A. adeninivorans* was suspended in PBS or PBS only. Constant temperature (37$^{o}$C) and cells kept suspended through constant agitation (180 rpm). Voltages were measured using a Ag/AgCl reference electrode and multi-meter. Error bars represent standard error of the mean (n=4).

The open circuit potential (OCP) provides infinite external resistance and no electrons are able to be transported from the anode to the cathode. As a result the OCP in Figure 4.11 is the difference between the anode and the cathode. The situation however changes when the same readings are taken when the MFC is placed under a low external load (100 Ω) which allows electrons to move from the anode to cathode at a fast rate (Figure 4.12).

In my thesis, when the MFC is under a load, it is termed the 'working potential'. The working potential when there is only PBS in the anode (dissolved $O_2$) is effectively zero whether or not cells are present. When FC and $KMnO_4$ are used in the cathode, the working potential is greater when cells are present than when they are absent (ANOVA $P = 0.05$). The working

potential is statistically greater when cells are present with $KMnO_4$ in the cathode than when FC is in the cathode (ANOVA $P = 0.05$), which matches with the difference in power density observed in the normal running of the MFC.

When the MFC is under load, it makes the anode potentials more positive when FC and $KMnO_4$ are used but not $PBS/O_2$. Potential of the anode is raised to when FC is used to just under +0.3V, compared to when $KMnO_4$ is used, the value being just under +0.65V. If the observed +0.4 V peaks observed in Figure 3.7 & 3.8 are contributing to the mediator-less electron transfer in the MFC, then this would account for the statistically significant difference in power densities in the MFC between when FC and $KMnO_4$ are used as the electron acceptors (Figure 4.10).

To my knowledge, the alteration of the anode under load by the cathode reaction has not been previously reported. However, as FC is the preferred electron acceptor in two chambered MFCs (Table 2.2a, and 2.2b unabridged in Appendix 2 and 3) then it is likely that the mediator-less electron transfer capabilities of many organisms may have been missed because the potentials of the anodes were not positive enough to allow electron transfer. If FC had been the electron acceptor of choice for the MFC, then it is unlikely that a statistical difference between *S. cerevisiae* and *A. adeninivorans* in mediator-less electron transfer (Figure 4.4) would have been observed.

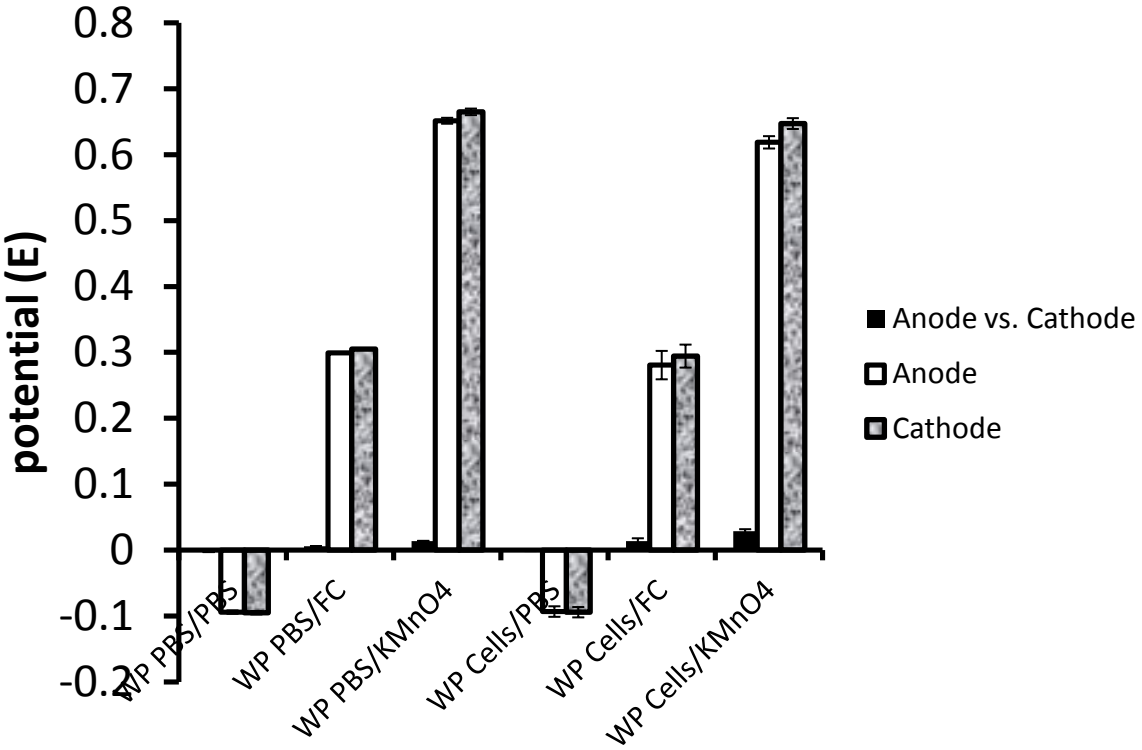


**Figure 4.12: Effect of different electron acceptors on the working potential (potential under 100 Ω external load) of mediator-less MFC with and without cells present.** Fuel cells contained either 0.5 M $KMnO_4$, 0.5 M FC dissolved in PBS or PBS only in the cathode. In the anode an $OD_{600}$ 2.5 of *A. adeninivorans* was suspended in PBS or PBS only. Constant temperature ($37^oC$) and cells kept suspended through constant agitation (180 rpm). Voltages were measured using a Ag/AgCl reference electrode and multi-meter. Error bars represent standard error of the mean (n=4).

## 4.5. Discussion

### 4.5.1. Ferricyanide reductase

Ferricyanide reductase has previously been attributed to the mediator-less electron transfer observed in previously reported yeast MFC (Prasad *et al.* 2007). Ferricyanide reduction was therefore, tested with *A. adeninivorans* and compared to *S. cerevisiae.* Without glucose, the rate of ferricyanide reduction was statistically the same between the two yeast species (Figure 4.2). However, *S. cerevisiae* demonstrated a glucose dependant increase in the rate of FC reduction, whereas with *A. adeninivorans*, ferricyanide reduction remained the same even in the presence of glucose (Figure 4.3). This suggests that the enzymatic action responsible

for FC reduction is in some way connected to the metabolism of the cell in *S. cerevisiae* but not in *A. adeninivorans* or that the internal reserves of *A. adeninivorans* are larger than those of *S. cerevisiae* and therefore does not respond to the presence of glucose in the experimental time frame.

### 4.5.2. Mediator-less MFC

In a mediator-less MFC, the power density achieved by *A. adeninivorans* was significantly different in both power density and behaviour to that of *S. cerevisiae* (Figure 4.4). These results are contrary to the results found for FC reduction between the two yeast species which found that without glucose present the rate of FC reduction was the same between species. If FC reductase is the only mechanism responsible for mediator-less electron transfer, then *S. cerevisiae* and *A. adeninivorans* should have the same power density. But the power densities of the two yeast species were different and therefore, something other than FC reductase was responsible for the mediator-less electron transfer in both yeast species.

### 4.5.3. Sedimentation cyclic voltammetry

Conducting CV of whole cells has previously shown electrochemically active molecules (Prasad *et al.* 2007). The CV's conducted in this work using the sedimentation set up revealed that *A. adeninivorans* has a peak around +0.4 V which is not present for *S. cerevisiae*, and that a peak was also present in concentrated samples of the supernatant, but not detectable in regular samples of the supernatant (Figures 4.5, 4.6, 4.7, & 4.8). The reaction potential of FC was less than +0.4 V which meant that the peak was not contributing to FC reduction. If this peak was contributing to mediator-less electron transfer, but not to FC reduction, then this would explain the discrepancy in the power density not matching the discrepancy in FC reduction.

A scan rate study of the peak by F. Barrière (Haslett *et al.* 2011) concluded that the peak was a solution species. This supports the results demonstrated above that the peak was present in concentrated samples of the supernatant. The lack of a peak in regular supernatant, suggests that the molecule was produced in very low amounts by *A. adeninivorans.*

### 4.5.4. Cell concentration affects the power density

A cell concentration study showed that the amount of power density achieved from mediator-less MFC containing *A. adeninivorans* or *S. cerevisiae* is cell concentration dependant, but that the behaviour again differed between the yeast species. For *A. adeninivorans*, the concentration of cells appears to have an upper limit, beyond which there is no significant increase in power density. This suggests that if the solution species described above was contributing to the power density, then that solution species might be regulated to a low concentration in solution or that the surface area of the anode may be insufficient.

### 4.5.5. Different cathode reactions

It appears that the use of $KMnO_4$ as the cathode reaction was a fortuitous one. If FC had been used instead, then the power density in the mediator-less MFC would have been significantly less (Figure 4.10). When $KMnO_4$ was used as the cathode reaction, the reaction potentials of the anode and cathode were significantly different without resistance ANOVA p=0.05) (Figure 4.11). When an external load was applied, the cathode potential of $KMnO_4$ did not change (+0.66 V) i.e. non-polarisable, but the anode potential was pulled up to nearly the same positive potential (Figure 3.12) i.e. polarisable. The same behaviour is true with FC, but the potential was less (+0.3 V). As a result, when $KMnO_4$ was the cathode reaction then the +0.4 V peak observed in Figures 4.7 & 4.8 was able to contribute to the power density.

## 4.6. Conclusion

The identification of the solution species in the supernatant revealed how *A. adeninivorans* participates in mediator-less MFC with $KMnO_4$ as the cathode reaction. The observation that the cathode reaction alters the anode potential when the MFC is under external load is a significant observation that warrants investigation into MFC design and modelling.

# Chapter 5: Investigation into mediated electron transfer and double mediated electron transfer

## 5.1. Abstract

TMPD increases the power density from yeast MFC by approximately 40 times. TMPD is not sequestered by the cells, and the reduced form is very stable but the oxidised form is unstable in PBS. The use of a double mediator system in a MFC was found to decrease the power density. It is proposed that TMPD is able to increase the power density by taking electrons from the intracellular redox processes such as glycolysis and respiration and by having a potential low enough to provide a useful potential difference between the anode and cathode.

## 5.2. Introduction

Table 2.2b (unabridged version in Appendix 3) describes many of the two-chambered mediated MFC reported in the literature. The mediators used are: thionin, methylene blue (MB), anthraquinone-2,6-disulfonate (AQDS), methylviolet (MV), meldola's blue (MelB), neutral red (NR), pyocyanin and 2-hydroxy-1,4-naphthoquinone (HNQ). The mediator 2, 3, 5, 6-tetramethylphenyldiamine (TMPD) is a chemically synthesized molecule. To my knowledge TMPD has not been used in a MFC before. Pyocyanin is produced by the microorganism *Pseudomonas aeruginosa* (Rabaey *et al.* 2005), and will be investigated in chapter 8. However, by first investigating the mechanism behind TMPD mediated transfer, a list of requirements for a naturally produced mediator can be made.

TMPD is a lipophilic mediator, meaning that it is able to transverse the plasma membrane of the cells and be reduced. This characteristic is necessary in order to access the electrons available within the yeast mitochondrion. In electrochemical studies, lipophilic mediators have been used effectively in conjunction with ferricyanide in a double mediator system to monitor the metabolism of *S. cerevisiae* cells (Baronian *et al.* 2002; Heiskanen *et al.* 2009; Kotesha *et al.* 2009). With the reaction potential of potassium permanganate being

significantly greater than ferricyanide (Figure 4.12), it is possible that this double mediator system could be used in the anode of a MFC.

The aims of this chapter are to asses the use of mediators within a MFC. The properties of mediators, observations on the affect on power density and the connection between cellular metabolisms were also investigated.

## 5.3. Materials and Methods

### 5.3.1. Chemicals, buffer, reagents and media

All chemicals, buffers, reagents and media are the same as those reported in section 3.3.

### 5.3.2. Cell culturing

Batch cultures of *A. adeninivorans* LS3 and *S. cerevisiae* NCTC 10716, were cultivated aerobically in indented flasks at 37$^{o}$C and 30$^{o}$C respectively, at 180 rpm for 24 h in YEPD broth, washed twice (4,500 rcf, for 8 min) and finally re-suspended in PBS. See section 4.3.2. for details.

### 5.3.3. Yeast Microbial Fuel Cell

MFC experiments were conducted as described in section 4.3.4. Two different mediators were used in this study, 1.5 mM TMPD and 20 mM ferricyanide (or ferrocyanide).

### 5.3.4. Voltammetry

Cyclic voltammetry was used to detect the presence of TMPD in solution. Falcon tubes containing $OD_{600}$ 2.5 suspensions of either *S. cerevisiae* or *A. adeninivorans* in PBS with 1.5 mM TMPD, and the acellular controls were subjected to CV (from -200 mV to + 200 mV vs. Ag/AgCl at 100 $mVs^{-1}$) using the following 3 electrode set up: Working; Pt microelectrode, Reference; Ag/AgCl, Counter; Pt. The falcon tubes were incubated for 1 h at 37$^{o}$C at 180 rpm, and cyclic voltammetry was performed again. The tubes containing either *A. adeninivorans* or

*S. cerevisiae* were centrifuged (4,500 rcf for 8 min) and the supernatants were transferred to a new tube. The pellet was re-suspended in PBS and cyclic voltammetry was performed on both the supernatants and the re-suspended pellets. The supernatants and the re-suspended pellets were then incubated for 3 h at 37$^{o}$C at 180 rpm, and cyclic voltammetry performed again.

Linear sweep voltammetry was performed to compare the rate of ferricyanide reduction between *A. adeninivorans* and *S. cerevisiae* with and without TMPD. $OD_{600}$ 2.5 of cells suspended in PBS, 20 mM ferricyanide and 10 mM glucose and/or 1.5 mM TMPD, and the acellular controls were incubated in falcon tubes at 37 $^{o}$C at 180 rpm for 1 h. Linear sweep voltammetry was performed (from +425 mV to + 100 mV vs. Ag/AgCl at 10 $mVs^{-1}$) using the following 3 electrode set up: Working; Pt microelectrode, Reference; Ag/AgCl, Counter; Pt.

A time course study was then performed of *A. adeninivorans* rate of ferricyanide reduction with and without 1.5 mM TMPD at times 0, 30 mins, 1 & 3 h. Linear sweep voltammetry was again performed from +425 mV to + 100 mV vs. Ag/AgCl at 10 $mVs^{-1}$ using a 3 electrode set up at each of the indicated times.

## 5.4. Results

### 5.4.1. Mediated MFC with *A. adeninivorans* or *S. cerevisiae*

TMPD is a lipophilic mediator that is able to dramatically increase the power density of yeast MFC (see chapter 3). The bulk of eukaryotic catabolism is carried out in the mitochondrion, which can only be accessed using lipophilic mediators capable of traversing the cell and mitochondrial membranes. Therefore, the addition of TMPD allows access to reduced molecules such as NADH within the mitochondrion that would otherwise be inaccessible.

MFCs containing either *A. adeninivorans* or *S. cerevisiae* at an $OD_{600}$ 2.5 demonstrated very similar power density curves with the addition of 1.5 mM TMPD at 30 mins. This indicated

that the catabolic rate of $OD_{600}$ 2.5, cell concentration (1 x $10^8$ cfu) for both yeast species is similar. This result enables comparative mediated studies of *A. adeninivorans* and *S. cerevisiae*.

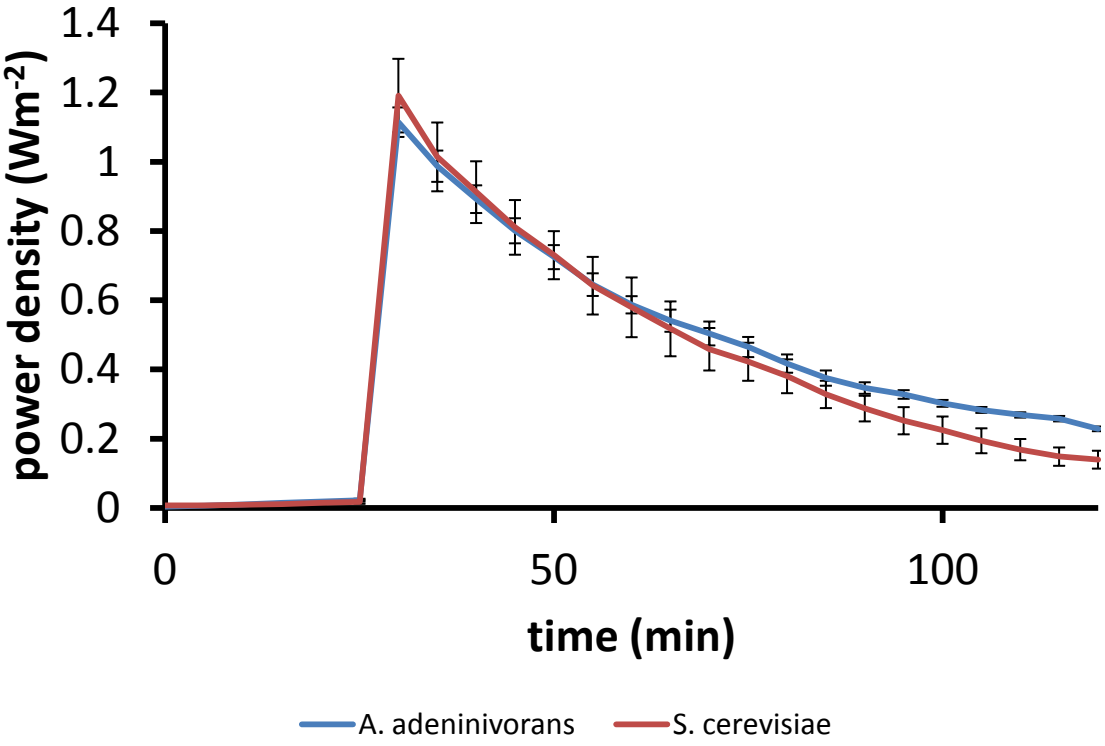


**Figure 5.1: Mediated MFC with *A. adeninivorans* or *S. cerevisiae*.** MFC contained 0.5 M $KMnO_4$ in the cathode. In the anode $OD_{600}$ 2.5 of *A. adeninivorans* or *S. cerevisiae* was suspended in PBS. Temperature was maintained constant at 37$^o$C and cells were kept suspended (180 rpm). TMPD was added at 30 mins. Error bars represent standard error (n=4).

### 5.4.2. Mediated Ferricyanide Reduction by *A. adeninivorans* and *S. cerevisiae*

A LSV study was conducted to characterise the difference between ferricyanide reduction with and without the lipophilic mediator TMPD (Figure 5.2). This double mediator system (use of a hydrophilic mediator and a lipophilic mediator together), enables monitoring of the internal reduced molecules of yeast to be conducted (Baronian *et al.* 2002; Heiskanen *et al.*2009; Kotesha *et al.*2009).

The controls show that TMPD and glucose are both capable of reducing some of the FC. This means that any difference associated with the addition of these molecules must be greater than that due to the acellular control for it to be significantly different. Accordingly, each of the acellular controls was subtracted from the appropriate cellular results in Figure 5.2 to produce Figure 5.3. The acellular controls ensure that the difference in power density is due to TMPD accessing reduced molecules within the cell and then reducing the ferricyanide.

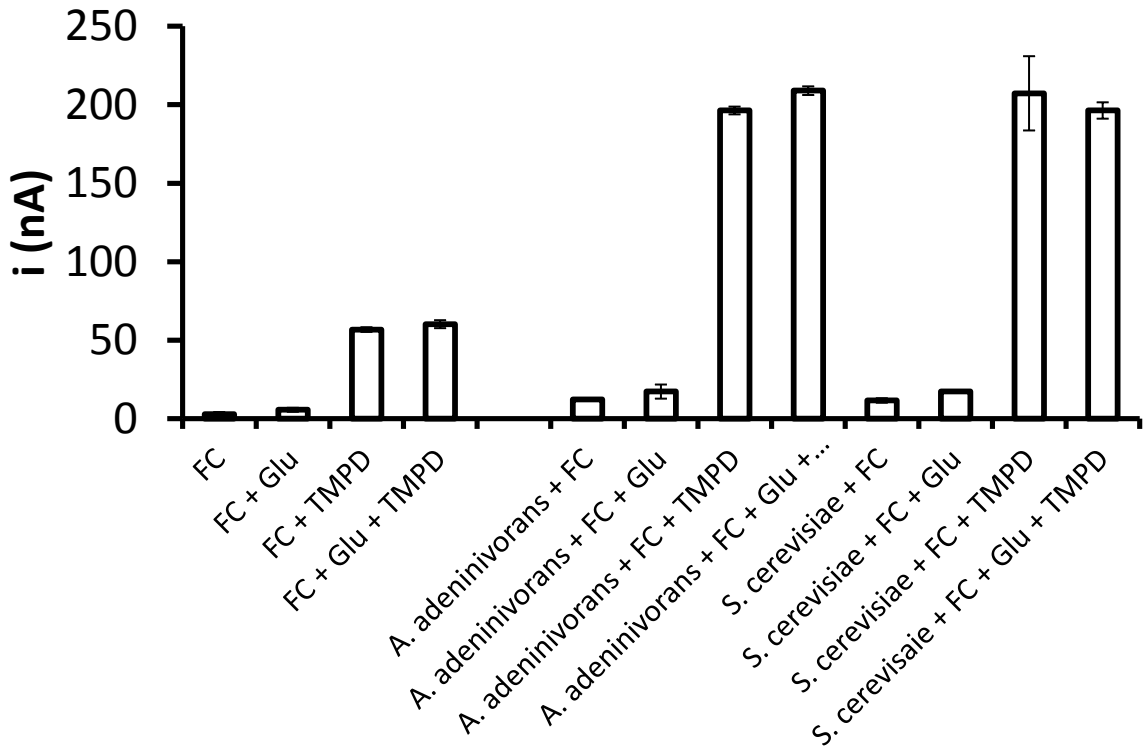


**Figure 5.2: Mediated Ferricyanide Reduction by *A. adeninivorans* and *S. cerevisiae.*** $OD_{600}$ 2.5 of cells suspended in PBS, 20 mM ferricyanide and 10 mM glucose and/or 1.5 mM TMPD were incubated in falcon tubes at 37$^{o}$C at 180 rpm for 1 h. Linear sweep voltammetry was performed (from + 425 mV to + 100 mV vs. Ag/AgCl at 10 $mVs^{-1}$) using the following 3 electrode set up: Working; Pt microelectrode, Reference; Ag/AgCl, Counter; Pt. Error bars represent standard error (n=3).

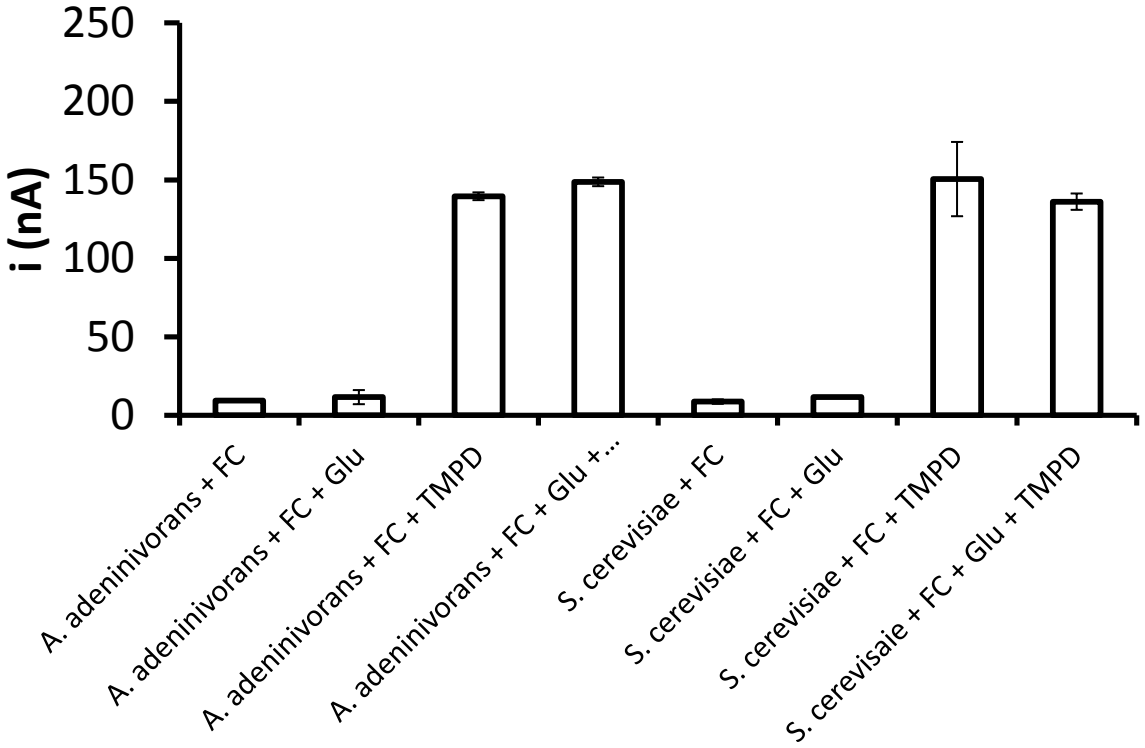


**Figure 5.3: Normalised Mediated Ferricyanide Reduction by *A. adeninivorans* and *S. cerevisiae.*** Results from Figure 5.2, with the acellular controls subtracted from the sample results. Error bars represent standard error (n=3).

### 5.4.3. Rate of FC reduction with and without TMPD

The rate of ferricyanide reduction by *A. adeninivorans* was compared with ferricyanide reduction by *A. adeninivorans* in the presence of TMPD (Figure 5.4). The presence of TMPD was found to reduce all of the ferricyanide to ferrocyanide in just over 1 h. The rate of ferricyanide reduction was much slower without TMPD present. The estimated time required to fully reduce all of the ferricyanide to ferrocyanide without TMPD was determined by extrapolating the results and was found to be approximately 40 h (working not shown). The difference between mediated and mediator-less electron transfer in Figure 5.1 is approximately 40 times for both *A. adeninivorans* and *S. cerevisiae.*

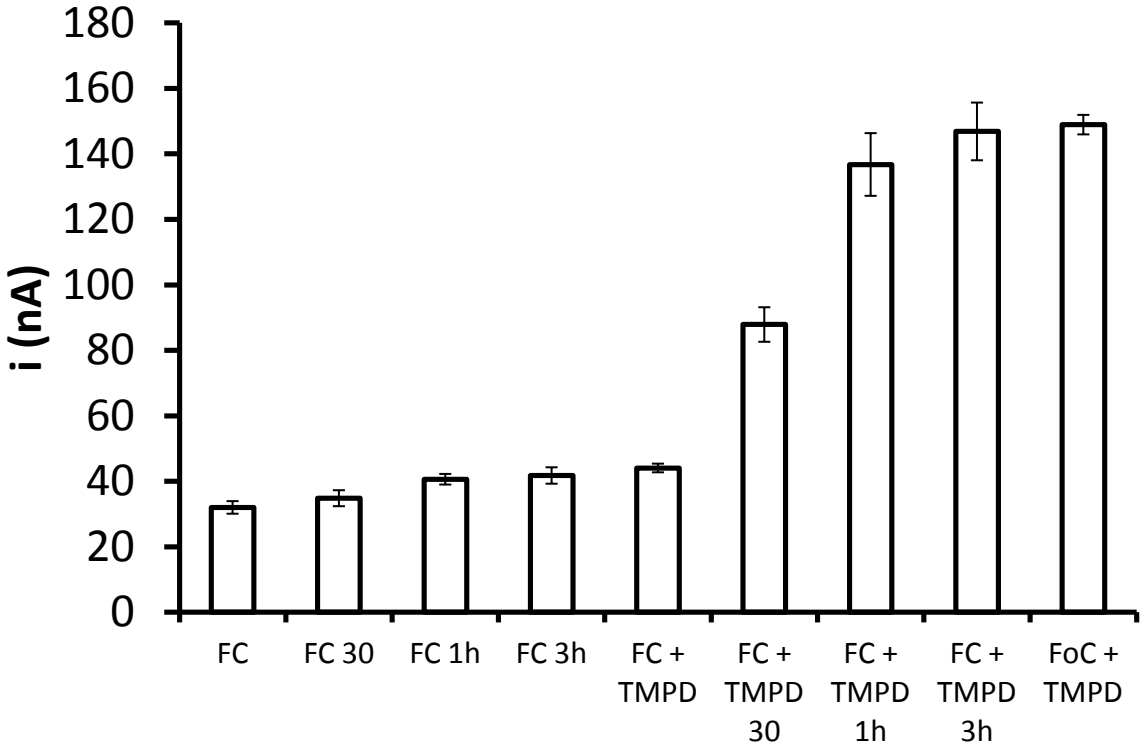


**Figure 5.4: Ferricyanide reduction over time by *A. adeninivorans*.** *A. adeninivorans* cells ($OD_{600}$ 2.5) suspended in PBS, 20 mM ferricyanide with or without 1.5 mM TMPD were incubated in falcon tubes at 37$^{o}$C at 180 rpm. Linear sweep voltammetry was performed (from +425 mV to + 100 mV vs. Ag/AgCl at 10 $mVs^{-1}$) using the following 3 electrode set up: Working; Pt microelectrode, Reference; Ag/AgCl, Counter; Pt. Error bars represent standard error (n=3).

### 5.4.4. TMPD

TMPD has been shown to be an effective mediator in this work, dramatically increasing the power density of yeast MFC. TMPD had not been used in a two chambered MFC before this work (Table 2.2b) and subsequently its behaviour is not well understood. Therefore an electrochemical study of TMPD was conducted.

Figure 5.5 demonstrates that the CV of TMPD changes after 1-h incubation with cells. TMPD has previously been shown to be able to penetrate the cell membrane, become reduced, and then pass those gained electrons onto other molecules (Figure 5.2) and the electrode

(Figure 5.1). It is therefore likely that the increase in power density observed is due to a conversion of the TMPD from an oxidised to a reduced state.

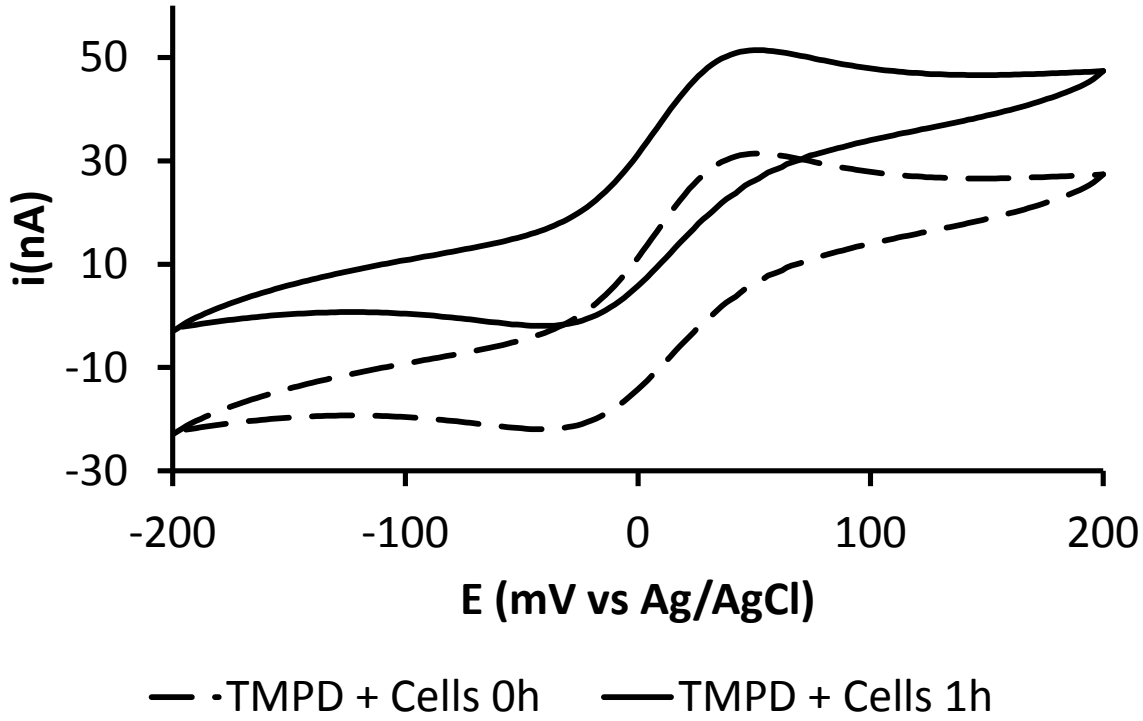


**Figure 5.5: TMPD Reduction**. *S. cerevisiae* or *A. adeninivorans* cells $OD_{600}$ 2.5 suspended in PBS with 1.5 mM TMPD and incubated in falcon tubes at 37$^{o}$C at 180 rpm for 1 h. Cyclic voltammetry was performed (from - 200 mV to + 200 mV vs. Ag/AgCl at 100 $mVs^{-1}$) using the following 3 electrode set up: Working; Pt microelectrode, Reference; Ag/AgCl, Counter; Pt.

The acellular control (Figure 5.6) demonstrates that TMPD on its own is undetectable after one h incubation in PBS. The cellular sample (Figure 5.5) was still detectable after 1 h incubation, but in a reduced form. This suggests that the oxidised form of TMPD is not as stable as the reduced form. If this is the case, then the constant cycling between the oxidised and reduced states of TMPD in a MFC could cause a drop off of TMPD concentration with time. If this occurs, then it is another possible factor that is responsible for the drop in power density with time after TMPD addition into yeast MFC (Figure 5.1).

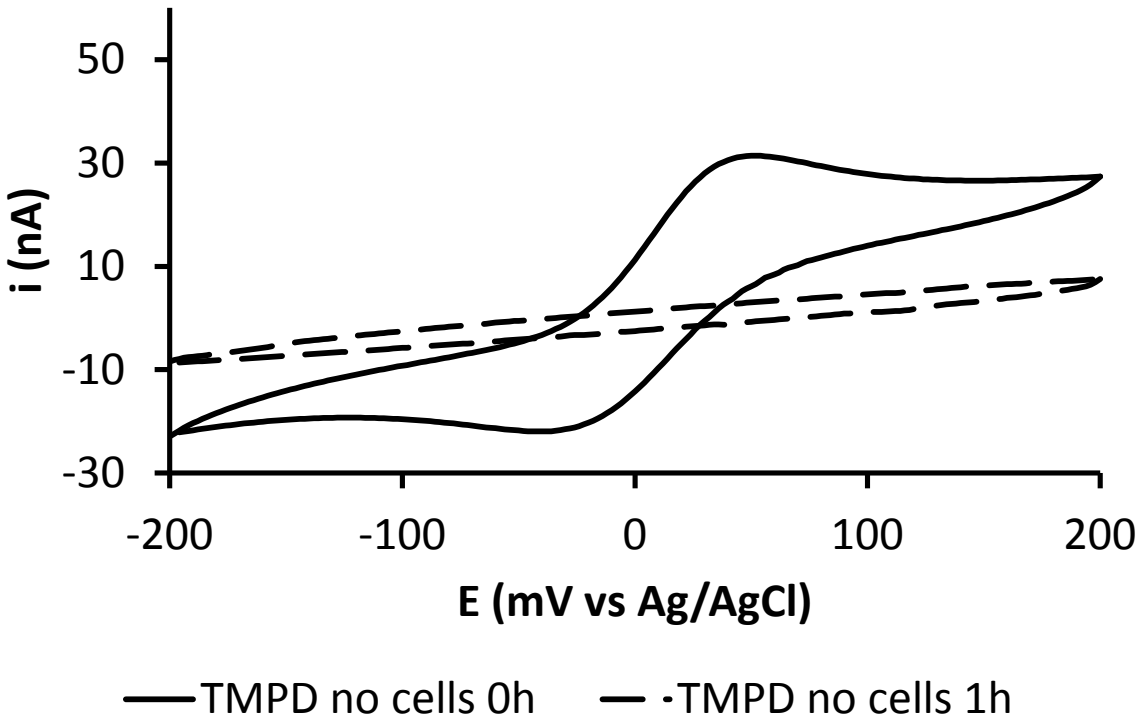


**Figure 5.6: TMPD acellular control**. A falcon tube containing 1.5 mM TMPD dissolved in PBS was incubated at 37$^{o}$C at 180 rpm for 1 h. Cyclic voltammetry was performed (from - 200 mV to + 200 mV vs. Ag/AgCl at 100 mVs$^{-1}$) using the following 3 electrode set up: Working; Pt microelectrode, Reference; Ag/AgCl, Counter; Pt.

The falcon tubes from the 3 h incubation of TMPD with cells were centrifuged and supernatants were separated from the pellet which was re-suspended in PBS. The supernatants and the re-suspended pellets were then tested to identify if TMPD is sequestered by the cells or if it freely moves between the cells and the solution. Figure 5.7 shows that TMPD was only located in the supernatants, not in the re-suspended pellets. This indicates that the bulk of TMPD is found in the solution and is not sequestered by the cells.

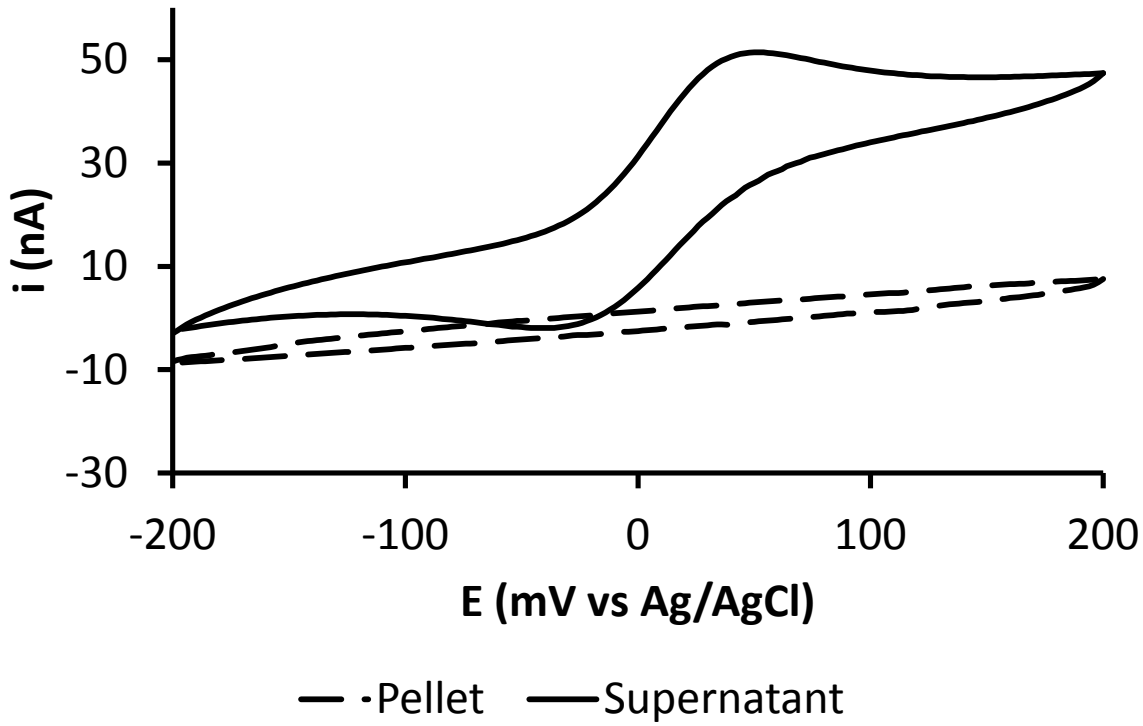


**Figure 5.7: TMPD sequestering.** The falcon tubes from Figure 5.5 containing *A. adeninivorans* and *S. cerevisiae* were centrifuged (4,500 rcf for 8 min) and the supernatants were transferred to a new tube. The pellet was re-suspended in PBS and cyclic voltammetry was performed (from -200 mV to + 200 mV vs. Ag/AgCl at 100 $mVs^{-1}$) using the following 3 electrode set up: Working; Pt microelectrode, Reference; Ag/AgCl, Counter; Pt.

In order to confirm the results of Figure 5.7, the supernatants and the re-suspended cell pellets were incubated again, and then tested (Figure 5.8). The results show that the cells did not release any TMPD with time, and the reduced TMPD did not disappear. These results in conjunction with Figure 5.5 suggest that the reduced form is more stable than the oxidised form of TMPD, and that TMPD is not sequestered by either *S. cerevisiae* or *A. adeninivorans*.

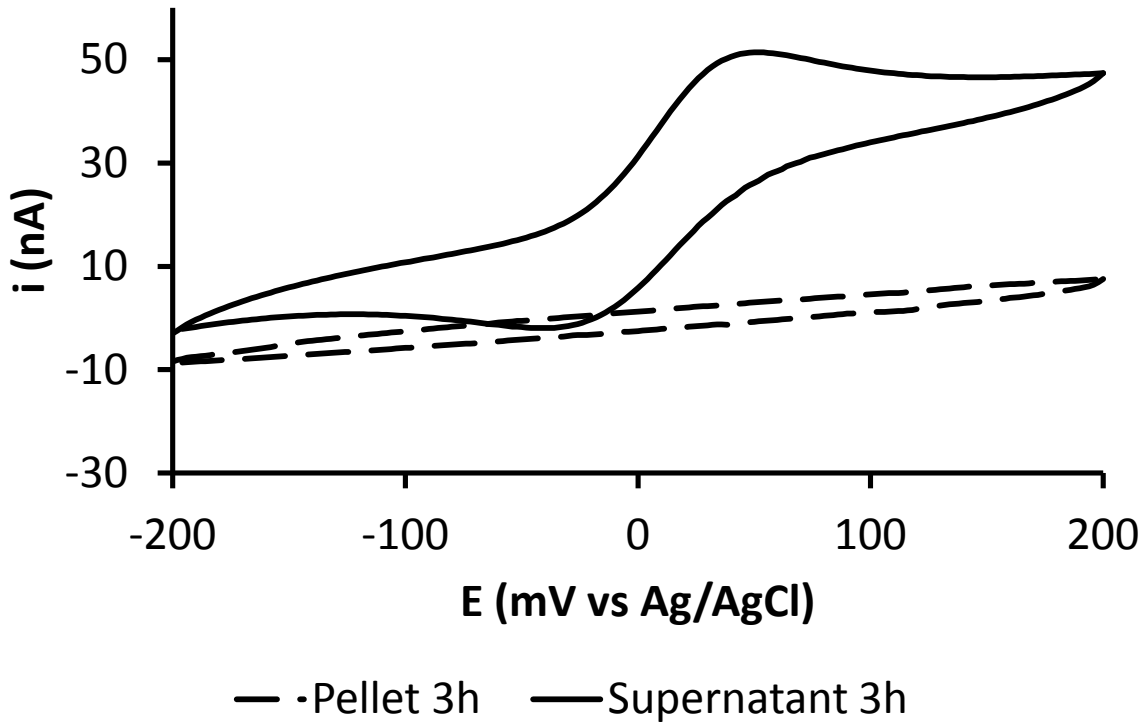


**Figure 5.8: Reduced TMPD stability**. The falcon tubes from Figure 5.2.3 were incubated at 37$^{o}$C at 180 rpm for 3 h. Cyclic voltammetry was performed (from -200 mV to + 200 mV vs. Ag/AgCl at 100 mVs$^{-1}$) using the following 3 electrode set up: Working; Pt microelectrode, Reference; Ag/AgCl, Counter; Pt.

### 5.4.5. Combining mediators

The use of $KMnO_4$ in the cathode chamber increases the reaction potential to such a high positive potential that it offers the unique opportunity to use ferricyanide in the anode chamber. To my knowledge this has not been tested before (see Table 2.2b). As described previously, ferricyanide is an extremely hydrophilic mediator, and therefore it is possible to incorporate a double mediator system into a MFC, with ferricyanide as the hydrophilic mediator and TMPD as the lipophilic mediator.

The mediators TMPD and ferricyanide were added to an *A. adeninivorans* MFC as described in Figure 5.9. The different combinations revealed that ferricyanide is capable of acting as a mediator to increase the power density of the MFC. Ferricyanide however, seems to initially compete with the electrode for the available electrons and actually decrease the power density

when added, if TMPD is already present, or if TMPD is added after FC. This phenomenon does not persist, and the power density increases again with time.

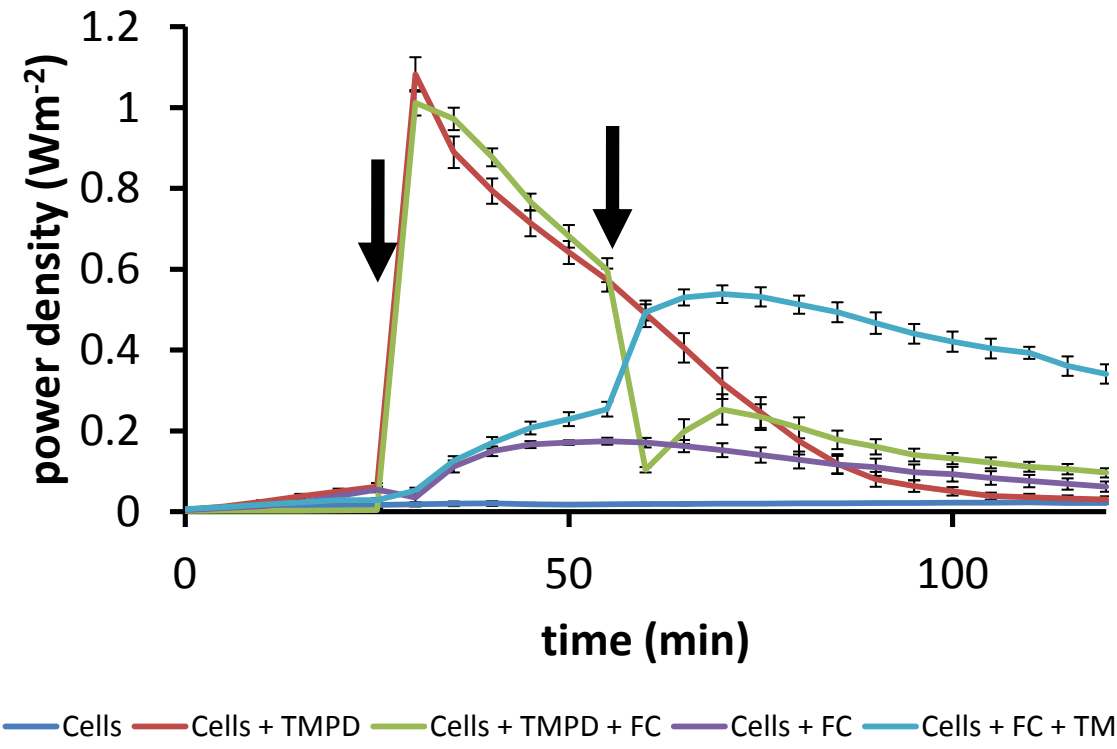


**Figure 5.9: TMPD and ferricyanide in a MFC**. MFC contained 0.5 M $KMnO_4$ in the cathode. In the anode $OD_{600}$ 2.5 of *A. adeninivorans* was suspended in PBS. Temperature was maintained at 37°C and cells kept suspended (180 rpm). The first mediator was added at 30 mins, and the second mediator at 60 mins. If only one was used, then that mediator was added at 30 mins. Error bars represent standard error (n=4).

The acellular controls demonstrate the behaviour of the mediators on their own (Figure 5.10). Ferrocyanide was used to demonstrate the maximum possible power density from ferricyanide interaction with cells. When TMPD was added first, the peak was 4 times greater than when it was added after ferricyanide or ferrocyanide. This indicates that ferricyanide, either from the initial addition or from oxidation at the electrode surface competes with the electrode to accept the electrons.

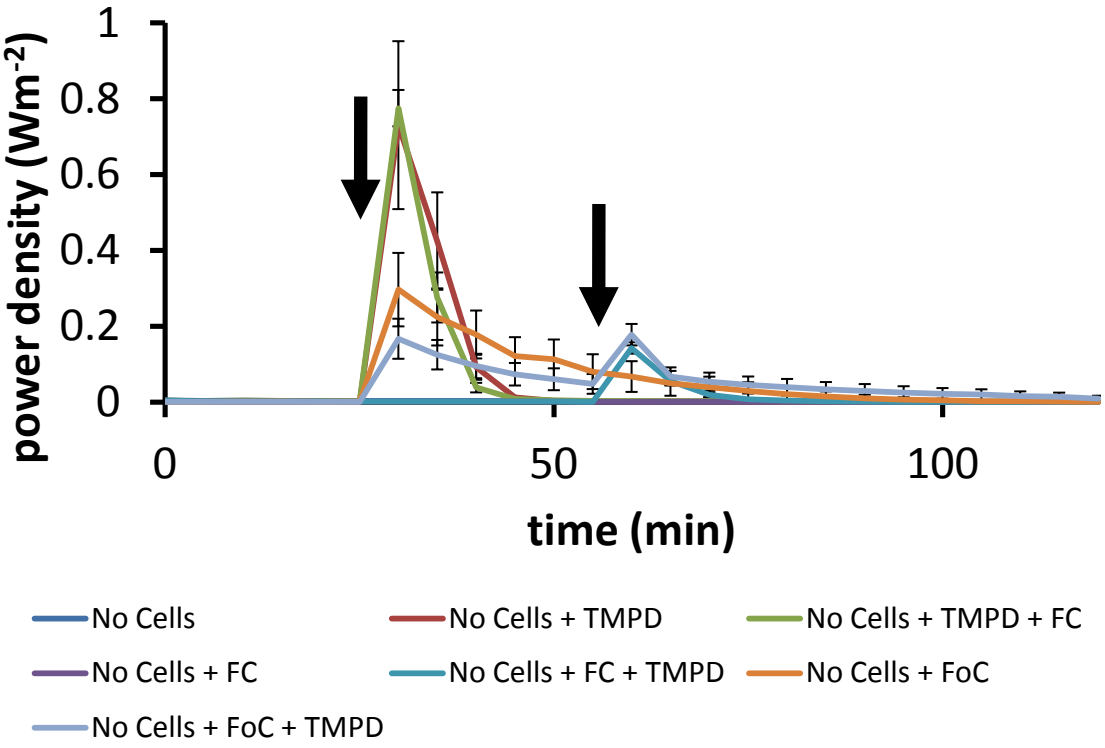


**Figure 5.10: Acellular control of TMPD and FC in MFC.** MFC contained 0.5 M $KMnO_4$ in the cathode and only PBS in the anode. Temperature was maintained at 37$^{o}$C and solutions stirred (180 rpm). The first mediator was added at 30 mins, the second mediator at 60 mins. If only one was used, then that mediator was added at 30 mins. Error bars represent standard error (n=4).

### 5.4.6. Different electron acceptors

The effect on the electrode potential from using TMPD and different cathode reactions was investigated (Figure 5.11). As identified previously, switching to the working potential (100 Ω external load) resulted in an increase of the anode potential. However, the potential of both cathode reactions dropped when the MFCs were converted from OCP to working potential.

These results suggest that the chemical action of $KMnO_4$ is working against the chemical action TMPD affecting the potential of both the cathode and the anode. This pulling of potentials by each chemical reaction can be visualised as 'tug-of-war' between the electromotive force (EMF) of each reaction. The electro chemical term for electrodes changing potential is polarisation. "Polarisation is a term that has two extremes, a perfectly

polarisable electrode is not conductive regardless of the voltage applied and a non-polarisable electrode passes current easily without having to shift from its equilibrium potential. Real electrodes fall between these boundaries" (Pasco, N. Personal Communication 2012). Therefore, in terms of EMF and the tug-of-war analogy, when a mediator is not present the EMF of the anodic reaction is too weak to significantly 'pull' against the cathode reaction and this affects the cathodic potential.

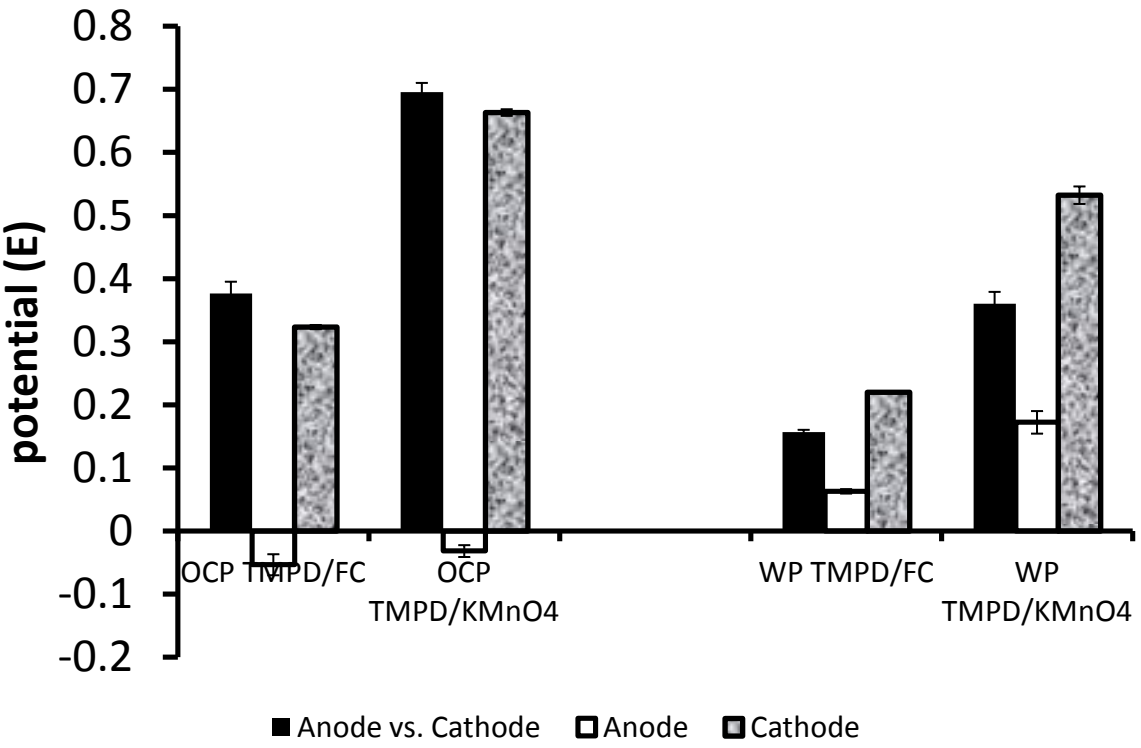


**Figure 5.11: Mediated effect on OCP and working potential.** MFC contained either 0.5 M $KMnO_4$, 0.5 M FC in PBS or PBS only in the cathode. In the anode an $OD_{600}$ 2.5 of *A. adeninivorans* was suspended in PBS. Temperature was maintained at 37$^{o}$C and cells kept suspended (180 rpm). Voltages were measured using a Ag/AgCl reference electrode and multimeter. Error bars represent standard error (n=4).

## 5.5. Discussion

### 5.5.1. Mediated MFC containing *A. adeninivorans* and *S. cerevisiae*

Both *A. adeninivorans* and *S. cerevisiae* exhibited similar power density curves in a mediated MFC (Figure 5.1). The difference in power density before and after the addition of TMPD

was approximately 40-fold for both *A. adeninivorans* and *S. cerevisiae*. This suggests that the same concentration of *A. adeninivorans* and *S. cerevisiae* have similar catabolic rates for the same concentration of cells and they both react to TMPD in the same way.

### 5.5.2. Mediated reduction of ferricyanide

Linear sweep voltammetry was conducted to investigate the difference in ferricyanide reduction with and without TMPD (Figure 5.2, 5.3 & 5.4). The rate of reduction was approximately 40-fold for both *A. adeninivorans* and *S. cerevisiae* which is similar to the difference in power density observed in the mediated MFC (Figure 5.1).

### 5.5.3. TMPD

TMPD was reduced by the cells (Figure 5.5), unstable in its oxidised form (Figure 5.6), and only found in solution (Figure 5.7 & 5.8). This indicates that when TMPD is used in a MFC, the action and TMPD must cycle between its oxidised and reduced form and that it may also decrease in concentration due to the instability of the oxidised form in PBS. If the concentration of TMPD is decreasing in the MFC, then this may be another possible reason for the short term drop in power density after mediator addition (Figure 5.1).

### 5.5.4. Double mediator system in a MFC

By using $KMnO_4$ as the cathode reaction, the possibility now exists to use both TMPD and ferricyanide in a double mediator system (Baronian *et al*. 2002). In order to characterise how each mediator works in the MFC, every combination of the two mediators was attempted (Figure 5.9). The results showed that instead of each mediator working with each other, the ferricyanide initially competed with the electrode for the electrons from TMPD. This was true irrespective of whether TMPD or ferricyanide was added first, which was confirmed with the acellular control (Figure 5.10).

It appears that using a double mediator system does not increase the power density of the MFC. All of the stored electrons seem to be easily passed from the cells to the anode by TMPD alone and the addition of ferricyanide does not facilitate this transfer any better. Subsequently, ferricyanide was removed from further experimental work in the anode with the mediated MFC.

### 5.5.5. Explanation of formal electrode potential

The effect that the addition of TMPD has on the electrode potentials of the anode and cathode in open circuit potential and working potential modes was investigated (Figure 5.11). It was found that the addition of TMPD did not alter the potential of the anode when the MFC was in OCP, but the potential of both the anode and the cathode were altered when an external load was applied (working potential – 100 Ω) when either $KMnO_4$ or ferricyanide was the cathode reaction i.e. both electrodes are non-polarisable .

This effect was not found for mediator-less MFC, where the anode potential changed from significantly different (under OCP) to almost the same (under working potential) as the cathode potential. The addition of TMPD therefore, seems to be able to maintain some of the difference between the anode and the cathode present under OCP, but only when an external load is present. These two opposing chemical forces have been termed ‘electromotive force’ and do not seem to affect the reaction potentials when the MFC is operating under OCP. It is only when an external load is applied, and therefore when electrons pass from the anode to the cathode that this effect is seen i.e. when the MFC has to do work.

## 5.6. Conclusion

TMPD can be used with both *A. adeninivorans* and *S. cerevisiae* to increase their power density from a MFC by approximately 40-fold. Neither *A. adeninivorans* nor *S. cerevisiae* sequestered TMPD. It was found that the reduced form of TMPD is very stable but the

oxidised form is unstable in PBS. The use of a double mediator system in a MFC was tested but did not increase the power density. It is proposed that TMPD is able to increase the power density by taking electrons from the reduced molecules within the cells and by providing a strong enough electrochemical force to separate the potentials of the anode and the cathode.

# Chapter 6: *Saccharomyces cerevisiae* poised potential microbial fuel cell: Replacing ferricyanide with an immobilised osmium polymer in a double mediator

## 6.1. Abstract

The osmium polymer poly(1-vinylimidazole)$_{12}$-[Os(4,4'-dimethyl-2,2'di'pyridyl)$_2$Cl$_2$]$^{2+/+}$is capable of both replacing ferricyanide in a double mediated *Saccharomyces cerevisiae* poised potential MFC and acting as a cross linker molecule helping to immobilise the microorganisms to the working electrode surface. The cross linking immobilization was stable enough to demonstrate direct electron transfer between the working electrode and the mitochondria, as well as the trans Plasma Membrane Electron Transport (tPMET) systems in yeast even after days of continuous experimentation. Several experimental procedures were used to illustrate how effective utilizing this osmium polymer in conjunction with menadione as a double mediator system is at monitoring yeast catabolism. It is anticipated that the incorporation of this osmium polymer into a *S. cerevisiae* poised potential MFC, acting as both an immobilization cross linker and as an electrochemical replacement to ferricyanide, will allow for further miniaturization and automation of poised potential MFC fabrication.

## 6.2. Introduction

As described in section 2.1.1, poised potential MFCs are effectively the same as a whole cell biosensors and as a result, the same electrochemical tests that have been conducted on whole cell biosensors have been employed on poised potential MFCs (Cho & Ellington 2007; Manohar & Mansfeld 2009). Poised potential MFCs are able to use different electrode compositions, substrates and microorganisms to produce current density – (Table 2.1) (Bond *et al.* 2002; Bond & Lovely 2003; Chaundhuri & Lovely 2003; Cho & Ellington 2007; Dumas *et al.* 2008; Niessen *et al.* 2004; Schröder *et al.* 2003; Wang *et al.* 2009; Bachman *et al.* 1998; Baronian *et al.* 2002). Chemicals that are capable of undergoing redox reactions with enzymes

in the catabolic pathway (mediators) have also been used in poised potential MFC to divert electrons to the working electrode which enables more effective electron transfer to the electrode.

Recently, it was shown that two different species of the prokaryotic genus *Pseudomonas* could be used in a whole cell biosensor with either one of two different osmium polymers facilitating direct electron transfer (DET) to the graphite working electrode (Timor *et al.* 2007). This has been termed 'wiring' as the prokaryote metabolism is effectively wired into the working electrode through the polymer interacting with the tPMETs and the electron transport chain components that span the plasma membrane, which divert electrons to the working electrode through the polymer itself. Modification of the electrode surface has proven useful in increasing the power density in a number of different MFCs (Tables 1-4). However, the behaviour of these osmium polymers is similar to that of ferricyanide, a hydrophilic mediator discussed in detail in chapter 5.

Use of an osmium polymer in a yeast poised potential MFC could prove problematic, because prokaryotes such as the two *Pseudomonas* species used in Timor *et al.* (2007) do not possess cellular organelles, whereas the bulk of metabolism in eukaryotes is located in the mitochondria, and the NADH produced in these organelles is not transported out into the cytosol (Schaetzle *et al.* 2008; Avéret*et al.* 2002; Todisco*et al.* 2006; Heiskanen *et al.* 2009; Kotesha *et al.* 2009). Eukaryotes do have tPMETs in their cellular membrane (Baronian *et al.* 2002; Schaetzle *et al.* 2008) but in order to access the entire eukaryotic metabolism and optimise the power/current density, a double mediator system is required which uses a combination of a hydrophilic and a lipophilic soluble mediators, if the lipophilic mediator cannot react with the electrode surface (Baronian *et al.* 2002; Kotesha *et al.* 2009; Heiskanen *et al.* 2009).

A two chambered double mediator MFC has, to the author's knowledge, not been attempted prior to being reported in chapter 4 of this thesis. However, there are several reported double mediator biosensors, which could be classified as double mediator poised potential MFCs (Baronian *et al.* 2002; Kotesha *et al.* 2009; Heiskanen *et al.* 2009). The lipophilic mediator penetrates the cell and the mitochondrial membranes, but the hydrophilic mediator is not capable of crossing the plasma membrane. The lipophilic mediator must therefore be capable of passing its electrons to the hydrophilic mediator, which in turn passes them to the working electrode. The two mediators must have $E^{0'}$ between $E^{0'}$ = -0.32 V(NADH) and $E^{0'}$ = +0.82 V (Standard hydrogen electrodes – SHE) of the final electron acceptor (oxygen) (Baronian *et al.* 2002; Schaetzle *et al.* 2008; Kotesha *et al.* 2009; Heiskanen *et al.* 2009). Additionally, the lipophilic mediator must also be more negative than the hydrophilic mediator. A common lipophilic/hydrophilic double mediator combinations are menadione ($E^{0'}$ = +0.13 mV vs Ag/AgCl) and ferricyanide ($E^{0'}$ = +274 mV vs Ag/AgCl) which have revealed much with regard to *S. cerevisiae* metabolism in biosensor studies (Heiskanen *et al.* 2009).

In this work, the osmium polymer will act as the hydrophilic part of a double mediator poised potential MFC where the osmium polymer facilitates the electron transfer between the lipophilic mediator and the working electrode, as well as, possibly between the cellular membrane redox enzymes (tPMETs) and the working electrode, in the same way as the hydrophilic mediator does in the double mediator systems (Timor *et al.* 2007; Baronian *et al.* 2002; Schaetzle *et al.* 2008). The osmium polymer poly(1-vinylimidazole)$_{12}$-[Os(4,4'-dimethyl-2,2'di'pyridyl)$_2$Cl$_2$]$^{2+/+}$($E^{0'}$ = +130 mV vs Ag/AgCl) (Timur *et al.* 2007) was the polymer chosen to replace ferricyanide and work in combination with menadione because it has an $E^{0'}$ similar to that of ferricyanide. Its polymeric structure should provide a matrix of external redox centres surrounding the cell which can potentially interact with both the

tPMETs and the lipophilic mediator, transferring the electrons directly to the working electrode (Figure 6.1).

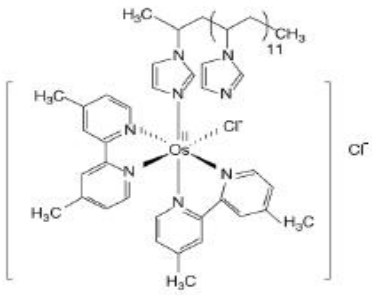


**Figure 6.1: Chemical structure of the osmium**. Structure originally published in Timur *et al.* (2007).

Osmium polymers have attracted much attention not only due to this efficient electron transfer property but also because the polymeric structure promotes the stable adsorption of enzymes to the working electrode (Degani*et al.* 1989; Heller *et al.* 1992; Katakis & Heller 1992; Wang & Hellter 1993; Ohara *et al.* 1993). However, the whole cell prokaryotic biosensors which have used osmium polymers in the past have not both covalently bound the osmium polymer to the working electrode and used it as an immobilizing agent (Timur *et al.* 2007). Instead, the prokaryotic cells and polymer have been held through adsorption onto the glassy carbon or gold electrodes surfaces. Therefore, a new immobilization procedure to attach cells and osmium polymer to the gold working electrode surface was attempted using electrostatic forces.

Thus, a double mediator poised potential MFC using an osmium polymer to act as both ferricyanide substitute and immobilising agent was attempted. The advantage of substituting the osmium polymer for ferricyanide is to eliminate the need to add a soluble mediator. This could lead to miniaturisation of MFC, enabling the highly efficient power generation required for medical applications.

## 6.3. Materials and Methods

### 6.3.1. Reagents

The osmium polymer poly(1-vinylimidazole)$_{12}$-[Os(4,4'-dimethyl-2,2'di'pyridyl)$_2$Cl$_2$]$^{2+/+}$ was generously provided as a gift from TheraSense (Alameda, CA, USA). Glucose, fructose, polyethyleneimine (PEI), cysteamine, idoacetate and ferricyanide were purchased from Sigma-Aldrich (St. Louis, MO, USA). Poly(1-vinylimidazole)$_{12}$-[Os(4,4'-dimethyl-2,2'di'pyridyl)$_2$Cl$_2$]$^{2+/+}$ was dissolved in milli-Q water. All the other chemicals were of analytical grade and dissolved in PBS (0.1 M $PO_4^-$, 0.14 M $NaCl_2$, pH 7.2) without filtration.

### 6.3.2. Biological materials

*S. cerevisiae* ENY.WA-1 (*MAT$\alpha$ura3-52 leu2-3,112 trp1-289 his3-delta1 MAL2-8c MAL3 SUC3*) and EBY44 (ENY.WA-1*Δpgi1-1Δ::Ura3*) were obtained from Prof. E. Boles (Institute of Microbiology, Frankfurt, Germany). Cells were pre-cultured in Yeast Extract Peptone Dextrose (YEPD) overnight at 30$^o$C 175 rpm, harvested by centrifugation (4000 rpm), then cultured in 50ml YEPD for 24 h under the same conditions (initial $OD_{600}$ ~ 0.14). The cells were grown to 'early stationary phase', and then the biomass was harvested at 4000 rpm and stored in PBS (0.1 M $PO_4^-$, 0.14 M NaCl, and pH 7.2).

### 6.3.3. Equipment

A microchip (Figure 6.2) was constructed by Natalie Kotesha using the Danchip facilities (DTU, Kongens Lyngby, Denmark). The microchip is illustrated and described in Figure 6.2. The casing is made from PDMS and PMMA sandwiched together with screws and is described elsewhere (Kotesha *et al.* 2007).

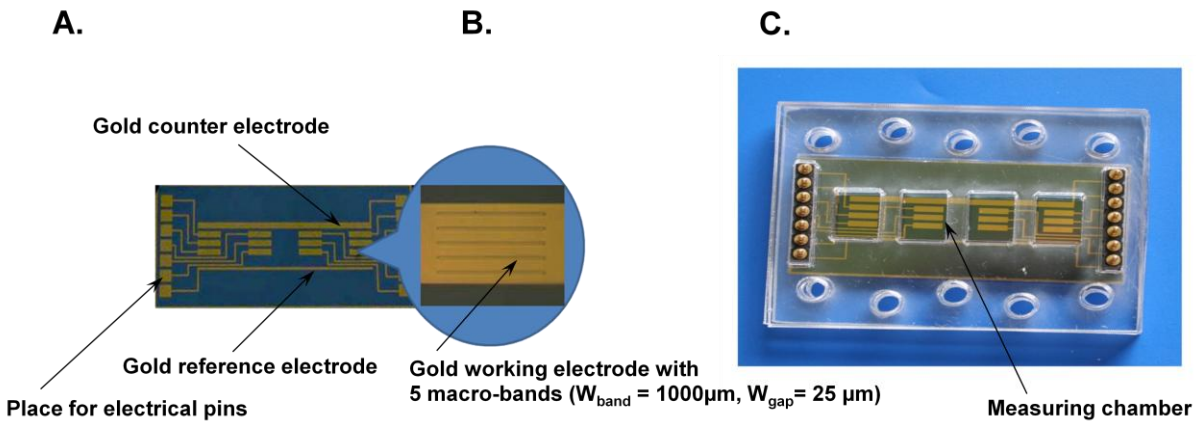


**Figure 6.2 Microelectrode set up.** (A) Silicon wafer, with titanium and then gold deposited on it in the above configuration was covered in a 5µm layer of SU-8 photo resist. The chip consists of twelve working electrodes (one of the twelve is magnified in the circle), each have 5 crevasses in the SU8 down to the gold surface, creating a total surface area for each working electrode of 125 $\mu m^2$ ([B] 5 x [25 µm x 1000 µm]). The counter electrode (thick gold band above the 12 working electrodes) and the reference electrode (thin gold band below the working electrodes) are able to hold each of the twelve electrodes at the same voltage in PBS solution. Three electrodes were connected in series increasing the working electrode surface area to 375 $\mu m^2$ but limiting the electrode to only four working electrodes which were separated by a PMMA and PDMS casing (C).

### 6.3.4. Preparation of the electrode modified with S. cerevisiae whole cells

Gold microchip electrodes (A=0.00025 $cm^2$, Natalie Kostesha) and gold disk electrodes (A=0.031 $cm^2$, BAS, West Lafayette, IN, USA) were chemically cleaned before use. The gold microchips were suspended in $H_2O_2$ and $H_2SO_4$ for 5 mins and washed with milli-Q water. The gold disk electrode was polished on microcloth (Buehler, Germany) in aqueous alumina suspension (0.1 µm, Stuers, Copenhagen, Denmark), rinsed and repeated with finer and finer grained alumina. The gold disk electrode was first sonicated for 5 mins in milli-Q water, then electrochemically cleaned by cycling in 0.1 M $H_2SO_4$ between -0.3 and + 1.6 V vs. SCE, washed thoroughly with water and immediately used for surface modification.

A self assembled monolayer (SAM) was created on the surface of both the microchip and the gold disk electrodes in order to change the charge on working electrode. This was done through immersion of the electrochemically activated gold electrode into a 100 mM solution of cysteamine in mili-Q water for 2 h. Cyclic Voltammetry and Impedance spectroscopy were used to demonstrate that a uniform layer has been formed.

### 6.3.5. Immobilization

Cells and PEI were incubated together in the refrigerator for 2 h before being mixed with osmium polymer and applied to the SAM surface of the working electrodes. The water was allowed to evaporate at room temperature for 60 mins, and then the microchip was encased in the microfluidic device and filled with PBS buffer (0.1 M phosphate buffer, pH 7.0). Equilibration occurred in PBS until a stable baseline current was achieved for 30 mins, then substrates were added to begin experimentation.

## 6.4. Results

### 6.4.1. Osmium polymer can act as a hydrophilic mediator

Wilde type *S. cerevisiae* cells (ENYWA.1) were immobilised with and without osmium polymer, and then fixed potential voltammetry (otherwise known as time based amperometry) was performed (Figure 6.3). Figure 6.3 demonstrates that the osmium polymer is capable of acting as a hydrophilic mediator in a double mediator system, transmitting the electrons from menadione to the working electrode surface. Figure 6.3 demonstrates that without the osmium polymer there was no current until menadione was added.

Figure 6.4 demonstrates a very small current when ENYWA.1 was immobilised with osmium polymer and glucose was added. This indicates that poly(1-vinylimidazole)$_{12}$-[Os(4,4'-dimethyl-2,2'di'pyridyl)$_2$Cl$_2$]$^{2+/+}$ is capable of reaching and interacting with the tPMETs in

the same way as ferricyanide (Schaetzle *et al.* 2008). Because the osmium polymer was not in solution this indicated that the osmium polymer was 'wiring' the cells to the electrode surface.

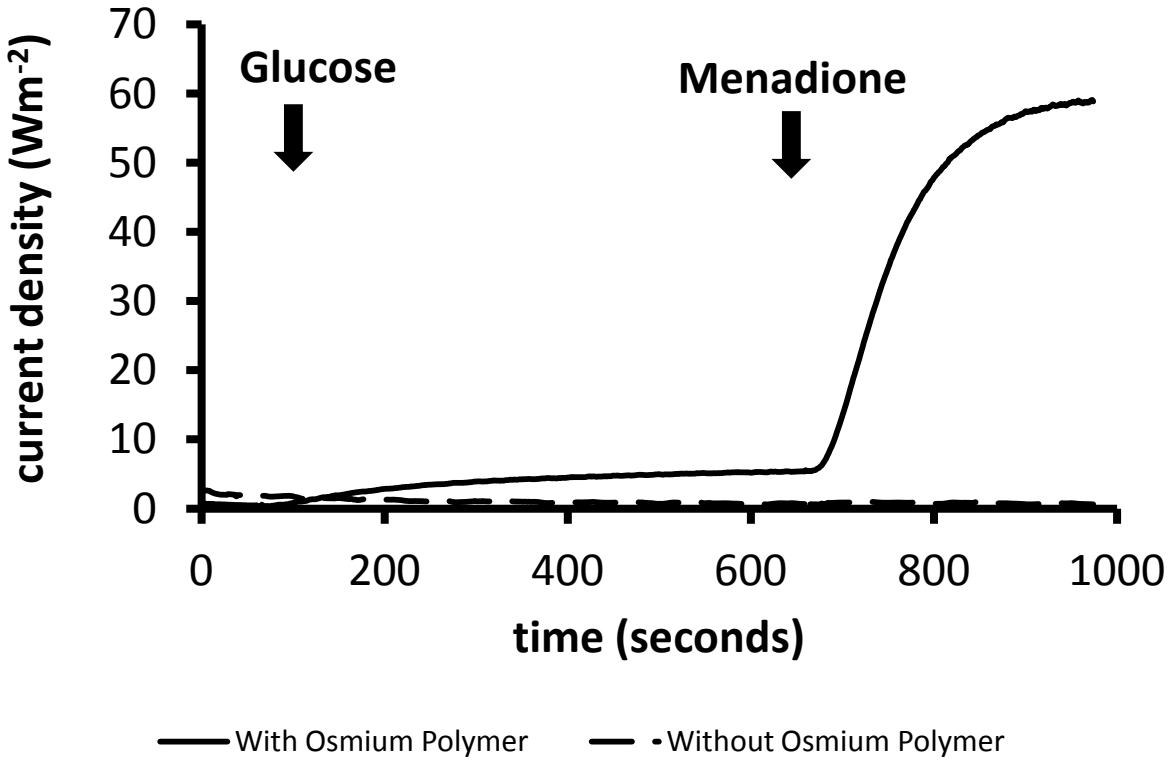


**Figure 6.3: Menadione and osmium poylmer double mediator system.** Fixed potential voltammetry (+ 300 mV vs. Ag/AgCl) was performed on the gold microelectrode chip. Baseline was achieved through 60 mins in PBS, then glucose was added (2 mM) at 100 sec, followed by menadione (100 µM) at 700 sec. Lines represent a mean of 4 recordings (error bars not shown).

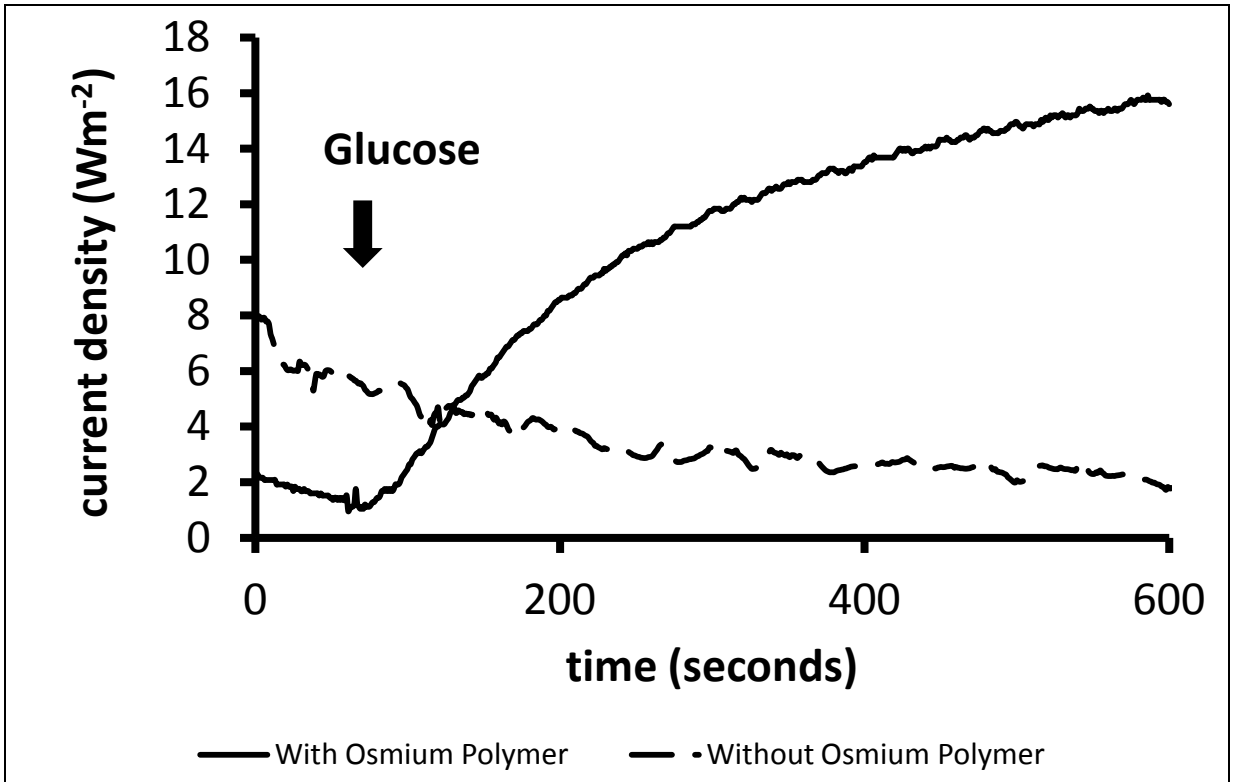


**Figure 6.4: Osmium poylmer mediated electron transfer.** Fixed potential voltammetry (+300 mV vs. Ag/AgCl) was performed on the gold microelectrode chip. Baseline was achieved through 60 mins in PBS, followed by glucose (2 mM) at 100 sec. Lines represent a mean of 4 readings (error bars not shown).

Figure 6.5 demonstrates that the current density response of osmium polymer and menadione is an order of magnitude less than ferricyanide and menadione. This indicates that either there are less redox centres in the osmium polymer compared to the concentration of ferricyanide used or that electrostatic immobilisation procedure causes steric hindrance of the osmium polymer, limiting electron transfer between the osmium polymer and the working electrode.

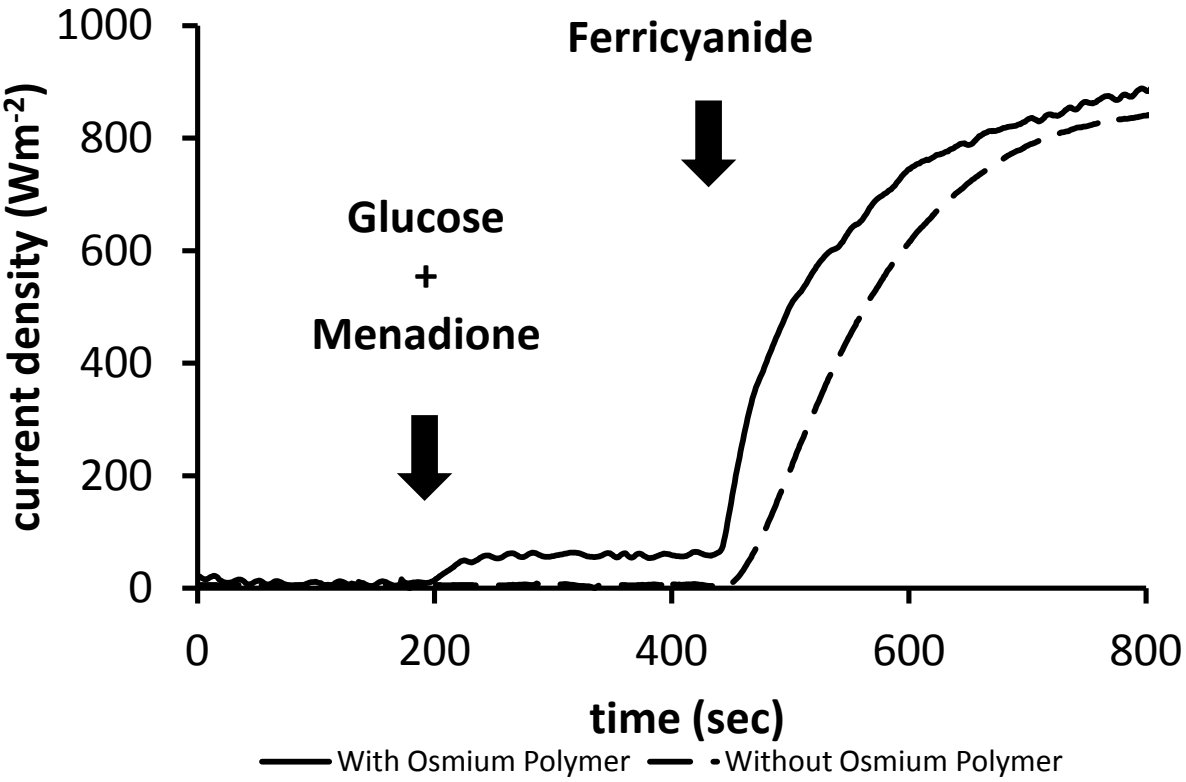


**Figure 6.5: Comparing different double mediator systems.** Fixed potential voltammetry (+300 mV vs. Ag/AgCl) was performed on the gold microelectrode chip. Baseline was achieved through 60 mins in PBS, then glucose (2 mM) followed by menadione (100 µM) at 200 sec. Ferricyanide was added (2 mM) at 450 sec. Lines represent a mean of 4 readings (error bars not shown).

### 6.4.2. Effects of immobilization procedure

Figure 6.6 shows that the immobilisation procedure uses PEI to hold the osmium polymer and the cells to the SAM layer on the surface of the gold working electrode and that the osmium polymer increases the stability of the attachment of the cells to the surface by cross-linking with the PEI to form a matrix. Figure 6.6 also demonstrates that the cells require PEI and cysteamine to be immobilised and that the use of osmium not only increases the number of cells immobilised but also increases the stability of that immobilisation.

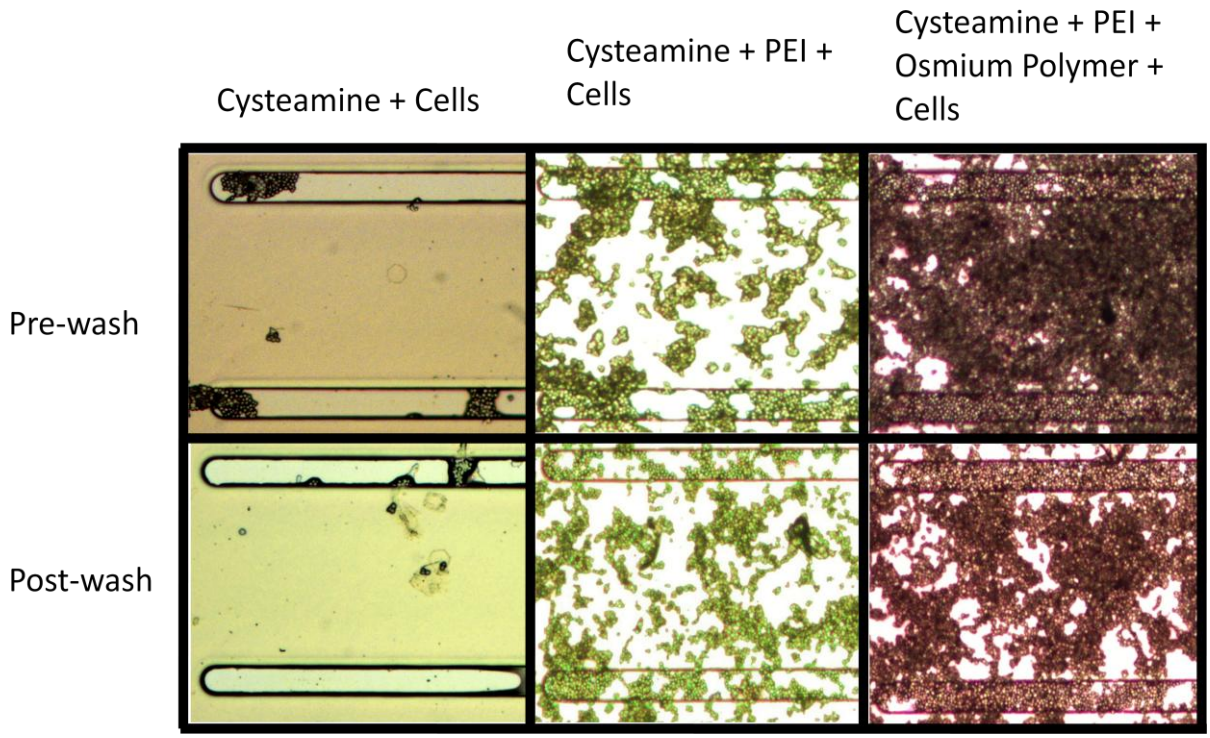


**Figure 6.6: Immobilisation.** Cells were immobilised by adsorption (Cysteamine + Cells), with PEI (Cysteamine + PEI + Cells) and with PEI and the osmium polymer (Cysteamine + PEI + Osmium Polymer + Cells). A photograph of the immobilized cells was then taken, and then the immobilisations were subjected to a shear stress of 400 µl/min for an hour. Then another photo was taken (post-wash)

Electrochemical analysis of the immobilisation by CV (Figure 6.7) revealed that the immobilised osmium polymer without cells is diffusion limited, which is similar to that reported previously for surface bound osmium polymer (Gregg & Heller 1991). The shape of the CV also indicates that by connecting three micro-electrodes together into one working

electrode, the CV has macro-electrode behaviour (see section 2.8). Introduction of cells reduces the peak height of the osmium polymer CV compared to the acellular control (Figure 6.7). The reduction in peak height indicates that the *S. cerevisiae* cells are causing steric hindrance.

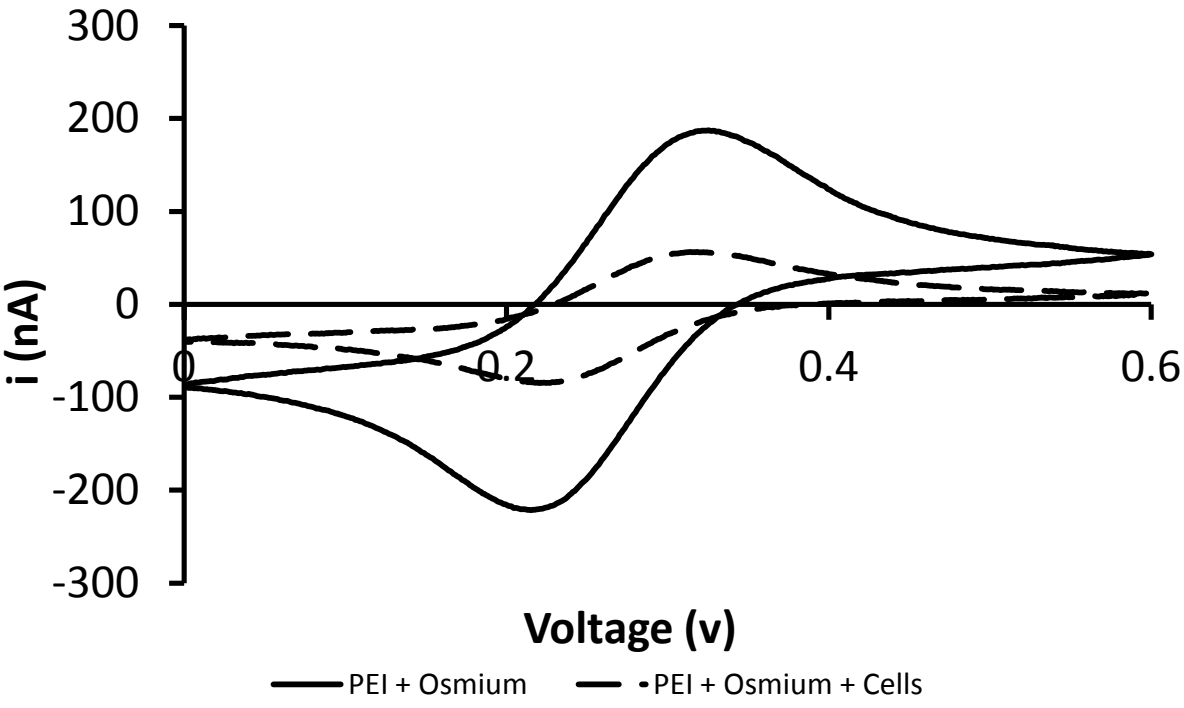


**Figure 6.7: Cyclic voltammetry of osmium polymer immobilisation.** Cyclic voltammograms of the osmium polymer poly(1-vinylimidazole)$_{12}$-[Os(4,4'-dimethyl-2,2'di'pyridyl)$_2$Cl$_2$]$^{2+/+}$ in PBS (0.1 M $PO_4^-$, 1.5 M NaCl, pH 7.2) at (25 mV/sec, from 0 mV to 600 mV vs. Ag/AgCl, with the following three electrode set up: Working; 3 gold working microelectrodes connected in series, Reference; 1 Ag/AgCl and Counter; 1 Pt electrode.).

### 6.4.3. Longevity of poised potential MFC

Over successive days, the current obtained from the same microelectrode decreased from repeated use of the microelectrode (Figure 6.8). This decrease in current could be due to cell loss from cleaning between usage and/or cell death. However, the cells do appear to be metabolically active which is consistent with previous work (Baronian *et al.* 2002) which showed that cells can be stored for weeks at 4$^o$C in PBS and are still metabolic activity. This research shows that the metabolic activity of eukaryotic cells can be repeatedly sampled for

several days. Therefore, electrostatic immobilization of cells with the osmium polymer can successfully immobilize cells in an operational poised potential MFC for several days.

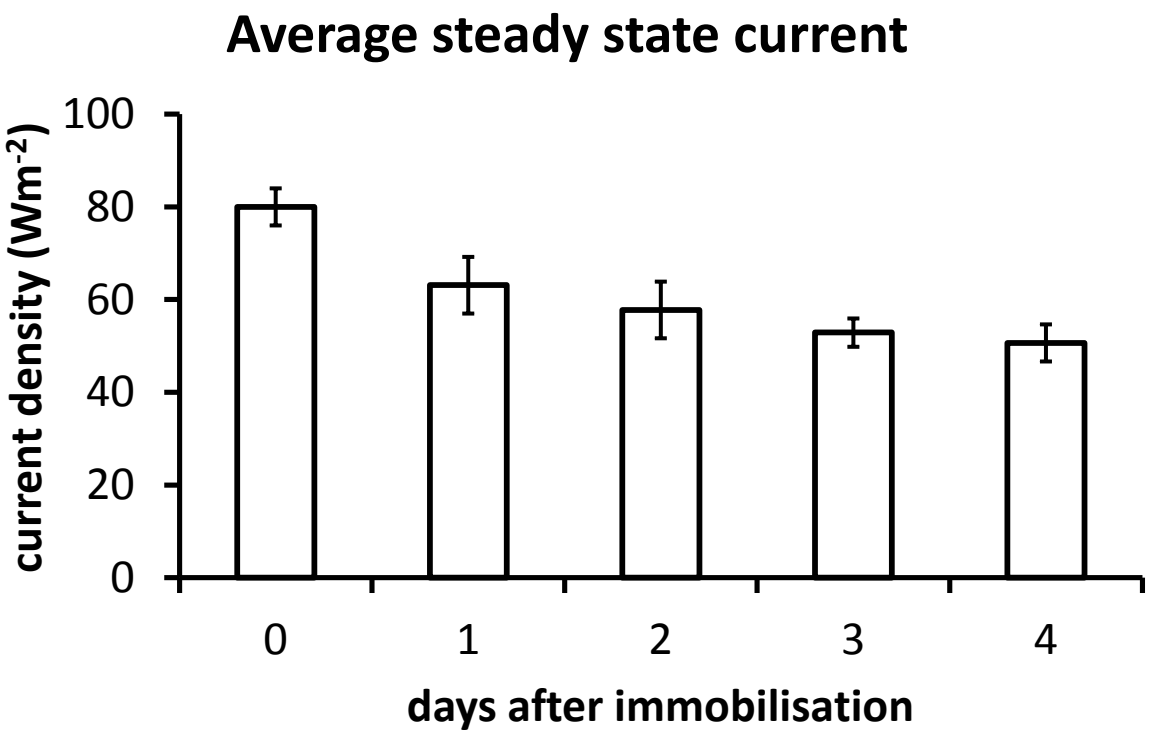


**Figure 6.8: Reliability of immobilisation.** Wild type cells were immobilised with osmium polymer. Fixed potential voltametry (+ 200 mV vs. Au) for 60 mins in PBS to achieve baseline, followed by addition of menadione and glucose (100 µM and 2 mM respectively). The increase in current was recorded and reported above. The immobilisations were tested at each time interval. Each line represents the mean current for the four electrodes from the same chip for successive days. Error bars represent standard error (n=4)

However, the nature of the current immobilization procedure resulted in each immobilization producing a different number of *S. cerevisiae* immobilized to each group of three working electrodes and therefore a different current output. Therefore, further miniaturization of the poised potential MFC to shift from using three working electrodes together, to using each of the twelve working electrodes separately (see Figure 6.2) requires greater accuracy in the addition of cells and immobilization agents in order to obtain consistent results between working electrodes. With greater accuracy and further miniaturisation of the poised potential

MFC to 12 individual electrodes, in conjunction with the use of florescence microscopy, it will be possible to ascertain the current output from an exact number of cells.

### 6.4.4. Different strains of *S. cerevisiae*

Two strains of *S. cerevisiae*, ENY.WA-1A and EBY44 were used to demonstrate the ability of the electrode to differentiate between metabolic transformants using osmium polymer in a double mediator system (Figure 6.9). ENY.WA-1A is the parental strain and EBY44 contains a deletion mutation of the phosphoglucoisomerase gene. Phosphoglucoisomerase is the second enzyme reaction in the glycolytic pathway (GP) which converts D-glucose-6-phosphate into D-fructose-6-phosphate. Fructose circumvents the phosphogulcoisomerase mutation because hexokinase (the first enzyme in GP) converts fructose into fructose-6-phosphate which is the third substrate in the GP.

The EBY44 cells incubated with glucose uses only the pentose phosphate pathway (PPP), but when incubated with only fructose, excludes it from using the PPP (Figure 6.10). The PPP involves three oxidative steps that convert glucose-6-phosphate into ribulose-5-phosphate, and 3 or 4 non-oxidative steps that convert ribulose-5-phosphate into fructose-6-phosphate or glyceraldehyde-3-phosphate respectively. It takes significantly more resources for EBY44 to grow on glucose and use only the PPP. As a result, this mutation enables comparisons between cytosolic energy (energy produced solely outside of the mitochondria) to energy produced inside and outside of the mitochondrial by comparing EBY44 incubated with glucose and EBY44 incubated with fructose.

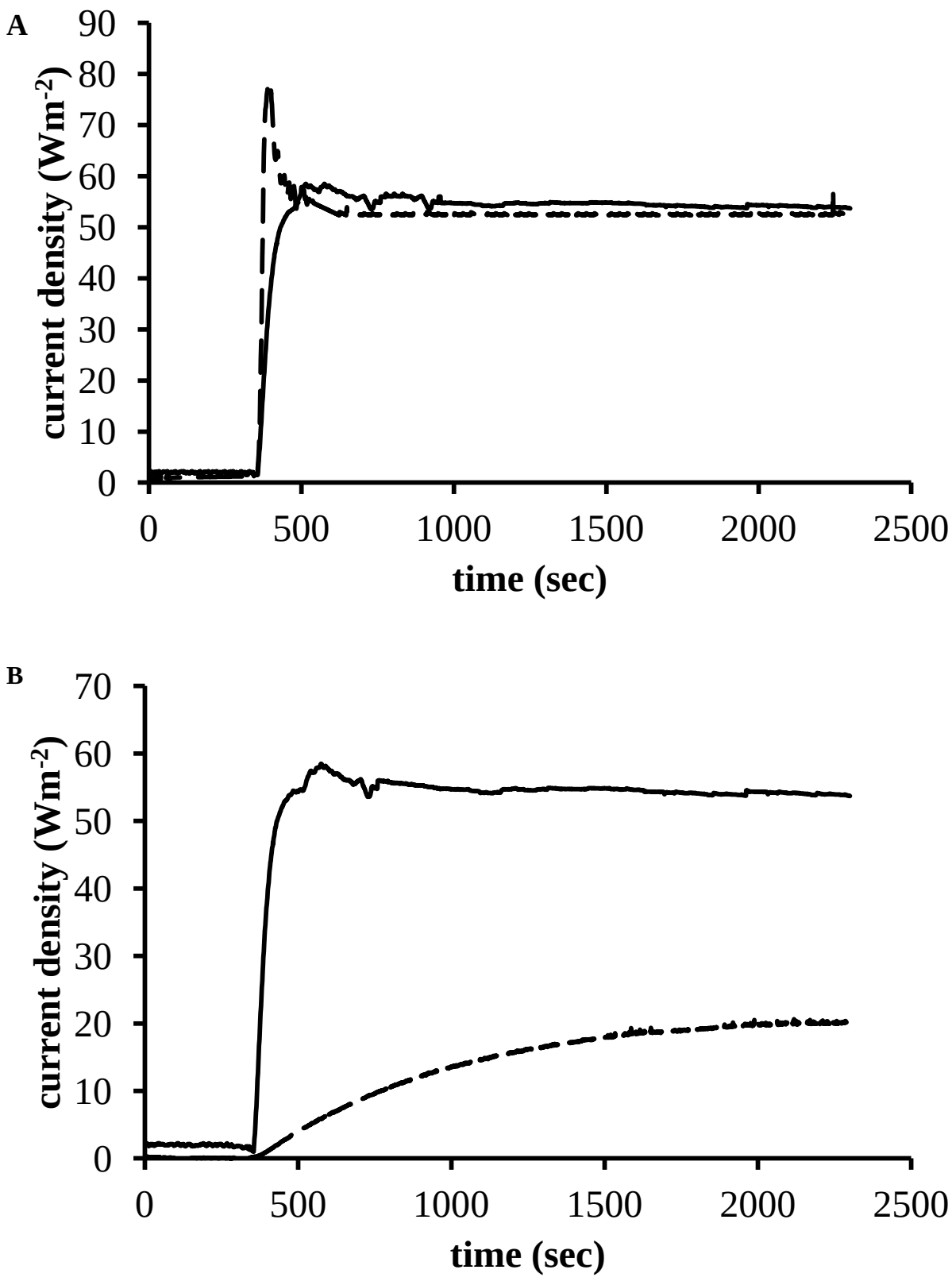


**Figure 6.9: Detection of different metabolic pathways.** (A) Mean response of 4 working electrodes with immobilised ENY WA.1 to (–) glucose and (---) fructose, (B) response of EBY44 to (–) glucose and (---) fructose.

Fixed potential voltammetry using the microelectrode microchips demonstrated that parental strain ENY.WA-1A showed the same current response to glucose and fructose (Figure 6.9 A) whereas EBY44 produced a significantly larger current when incubated with fructose compared to glucose (Figure 6.9 B). The difference between EBY44 incubated with glucose and fructose is consistent with previous work with ferricyanide (Kotesha *et al.* 2009) and demonstrates that the osmium polymer I immobilisation procedure and the microelectrodes work as effectively with menadione as does a soluble hydrophilic mediator to distinguish metabolic pathways.

### 6.4.5. Inhibition

Iodoacetate irreversibly inhibits glyceraldehyde-3-phosphate dehydrogenase (Witters & Foley 1976; Willson & Tipton 1981) which is located after the point fructose enters into the GP (Figure 6.10). This inhibition limits the cells to using only ATP and NADH produced by the PPP. The two end products of the PPP (fructose-6-phosphate and glyceraldehydes-3-phosphate) are substrates in the GP before the idoacetate inhibits the reaction. Stepwise addition of idoacetate into the biosensor (Figure 6.11) showed that iodoacetate inhibition occurs around the same concentrations as reported previously with ferricyanide and menadione (Zhao *et al.* 2005). Additionally, the current did not diminish to zero (NADPH is still produced in the PPP) and inhibition was irreversible.

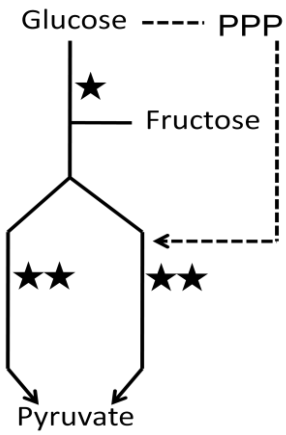


**Figure 6.10: Different metabolic pathways of *S. cerevisiae*.** The transformant EBY44 has a mutation at point (*) which forces it to use the pentose phostphate pathway (PPP) to metabolise glucose. The irreversible inhibitor idoacetate inhibits at point (**) causing a halt to the metabolism of both strains at this point.

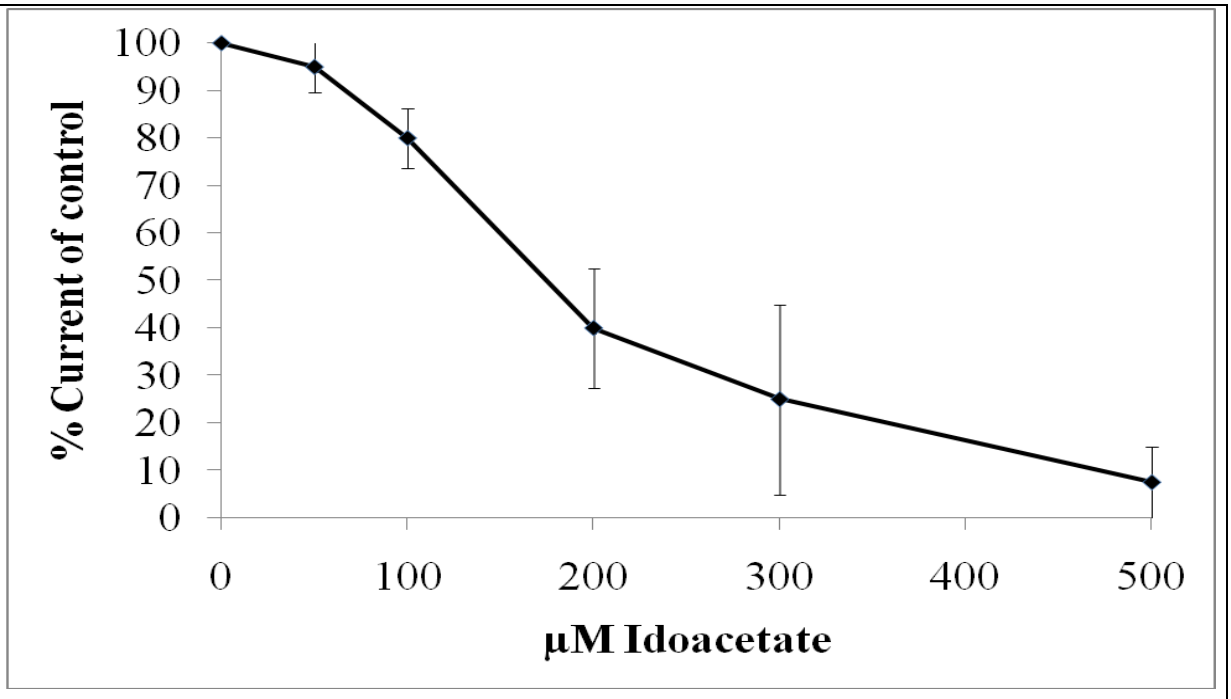


**Figure 6.11: Iodoacetate inhibition.** Dose response curve of sodium idoacetate inhibition in ENYWA.1 cells. Glucose concentration is 2 g/L.

## 6.5. Discussion

The lipophilic mediator acts as the final electron acceptor of the electron transport chain diverting the electrons away from the terminal electron actor (oxygen) and causing the electrons to flow from the working electrode into an external circuit (Baronian *et al.* 2002; Heiskanen *et al.* 2009; Kotesha *et al.* 2009). A double mediator poised potential MFC is required to tap the electron transport chain of eukaryotes located in the cristae of mitochondria within the cell. Usually a double mediator biosensor uses the hydrophobic and a lipophilic mediator combination of ferricyanide and menadione respectively. In this work, the osmium redox polymer poly(1-vinylimidazole)$_{12}$-[Os(4,4'-dimethyl-2,2'di'pyridyl)$_2$Cl$_2$]$^{2+/+}$ successfully replicated the electrical wiring previously reported in Timor *et al.*(2007) with a gold electrode using *S. cerevisiae*, replacing ferricyanide as the hydrophilic or external mediator (Figures 6.4 and 6.5), as well as, facilitated immobilisation of the microorganisms to the working electrode surface (Figure 6.6).

The results showed that osmium polymer is not as effective as 2 mM ferricyanide at facilitating electron transfer to the working electrode (Figure 6.5). However, the immobilisation was demonstrated to be stable both physically and electrochemically (Figures 6.6 and 6.8). The sensitivity of this new double mediator system was tested, and it was able to distinguish between two different cell lines, two different metabolic pathways and inhibition of those pathways (Figure 6.9 A&B and Figure 6.11).

MFCs rarely use soluble mediators due to their cost, and clean up required (Schröder *et al.* 2003). The osmium polymer and immobilisation procedure is therefore a useful alternative to a soluble mediator since it is attached to the electrode with the microorganisms, and does not require replacing. However, in order for it to be used in a single or double chambered MFC the cathode reaction must have a significantly positive reaction potential and 'electromotive force' to raise the potential of the anode above the reaction potential of the osmium polymer.

## 6.6. Conclusion

A poised potential MFC was created wiring *S. cerevisiae* cells to the working electrode using an osmium polymer. Results indicated that the osmium polymer can electrochemically replace ferricyanide in a double mediator poised potential MFC system and provided stable immobilisation of *S. cerevisiae* over several days of testing without causing noticeable detriment to the microorganisms. These results, along with the simplicity of the polymer wiring procedure should allow further miniaturization through using ink-jet like application of the materials required for immobilisation. In these miniaturization of future MFCs will enable small power devices to be used in a variety of including as medicine.

# Chapter 7: Comparing growth conditions and configurations of the MFC

## 7.1. Abstract

*A. adeninivorans* was cultivated under different growth conditions to test the effect of carbon source, morphology and growth phase have on power density. Anaerobic growth was tested. Several different modifications to the physical structure of the MFC were also tested, and small differences were identified. All growth conditions were shown to produce both mediator-less and mediated power.

## 7.2. Introduction

The choice of microorganism and configuration of a MFC has a bearing on the operating conditions, the substrates consumed and subsequently the power density. The MFC investigated in this thesis is novel in the use of *A. adeninivorans* as a biological catalyst and $KMnO_4$ as the cathode reagent.

The unconventional yeast *A. adeninivorans* was initially chosen due to its response to a wide substrate range, high temperature and osmolarity tolerances and for being a biotechnologically interesting dimorphic eukaryote (section 2.7.1. and Wartmann *et al.* 1995). Previous chapters have focussed on investigating the fundamentals behind electron transfer from yeast. This chapter will focus on investigating the substrate range and the dimorphism of *A. adeninivorans.*

The cathode reagent $KMnO_4$ has been investigated previously by You *et al.* (2006) with a prokaryote biocatalyst. In this chapter the physical composition of a eukaryotic MFC containing *A. adeninivorans* were altered and the effects on both the power density and the potentials created under open circuit and under load conditions monitored.

The goal of this investigation was to understand the conditions that promote optimal power density from both the microorganism and the MFC.

## 7.3. Materials and methods

### 7.3.1. Strains, chemicals, buffer, reagents and media

Strains, chemicals, buffers, reagents and media are the same as those reported in sections 3.3.1 and 3.3.2, except for the minimal media.

Minimal media was created by adding 12 $gL^{-1}$ yeast nitrogen base without amino acids (Difco, Bristol, UK) to distilled water and autoclaved. Carbon substrates glucose, fructose, galactose, sucrose and maltose were added to the minimal media at 20 g $L^{-1}$.

### 7.3.2. Cell culturing

*A. adeninivorans* LS3 was cultured in a number of different ways:

1) Aerobically in indented flasks at 180 rpm at 37$^{o}$C for 24 h

2) Anaerobically in indented flasks at 180 rpm at 37$^{o}$C in an anaerobic jar for 24 h

3) Filamentous in indented flasks (aerobic) at 180 rpm at 45$^{o}$C for 24 h

4) Stationary phase in indented flasks (aerobic) at 180 rpm at 37$^{o}$C for 72 h

Unless otherwise stated the media used was YPD.

### 7.3.3. Yeast Microbial fuel cell configurations

The yeast MFC configuration described in section 3.3.3 and Figure 2.5 was used exclusively in experiments described in chapters 3, 4 & 5. In this chapter, the two chambered MFC is used and is modified into different forms in order to perform different investigations. These

modifications were conducted by adding different compartments to those already present with and without extra proton exchange membrane (Figure 7.1).

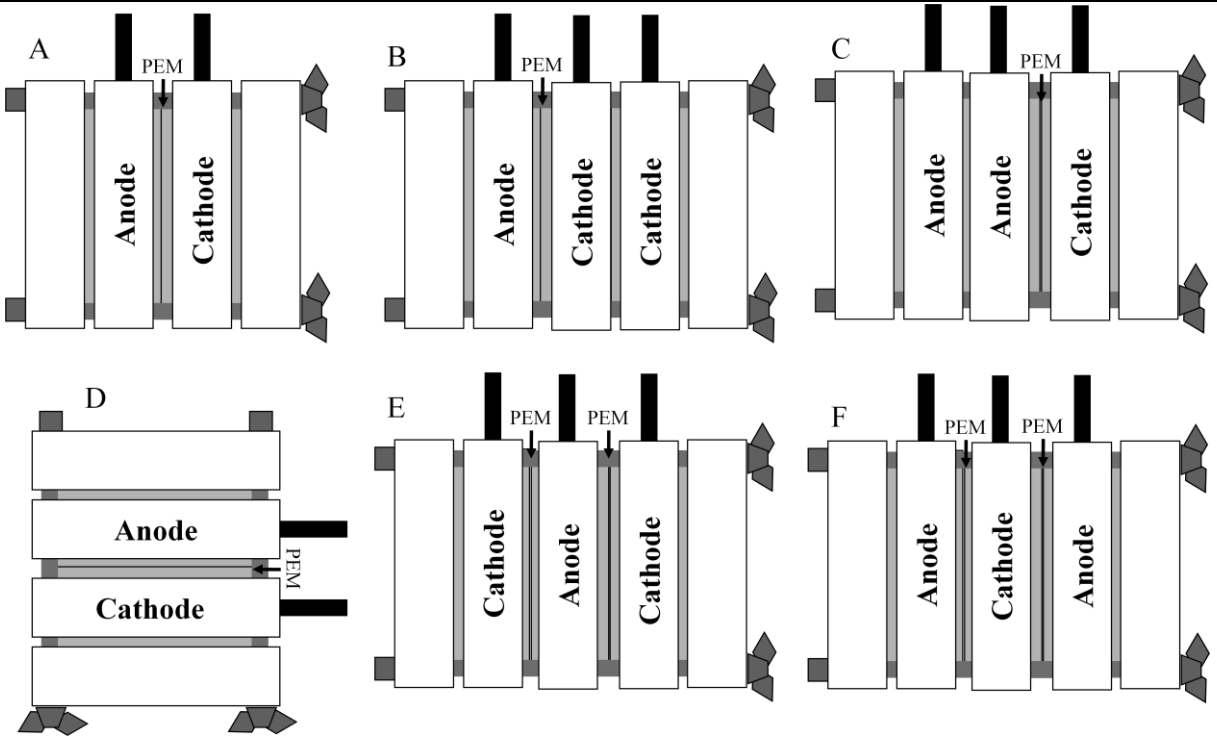


**Figure 7.1: Different configurations of yeast microbial fuel cell.** (A) Two chambers, one PEM, two electrodes, (B) two chambers, one PEM, one anode, two cathodes, double cathode volume, (C) two chambers, one PEM, two anodes, one cathode, double anode volume, (D) the same MFC as in (A) but set on its side after each chamber was completely filled an sealed, (E) three chambers, two PEM, one anode, two cathodes, (F) three chambers, two PEM, two anodes, one cathode.

## 7.4. Results

### 7.4.1. Different carbon sources

The ability of *A. adeninivorans* to generate power density in a MFC from different substrates was investigated using two different methods. The first method grew cells up in a single batch and suspended them in PBS. The cells were then aliquoted and given a specific carbon source and incubated at 37$^{o}$C for 3 h, then immediately placed into the MFC (Figure 7.2). The second method grew cells in separate flasks of minimal media plus respective carbon source

(37°C, 180 rpm, 24 h), then harvested them and re-suspended them in PBS before use in MFC (Figure 7.3).

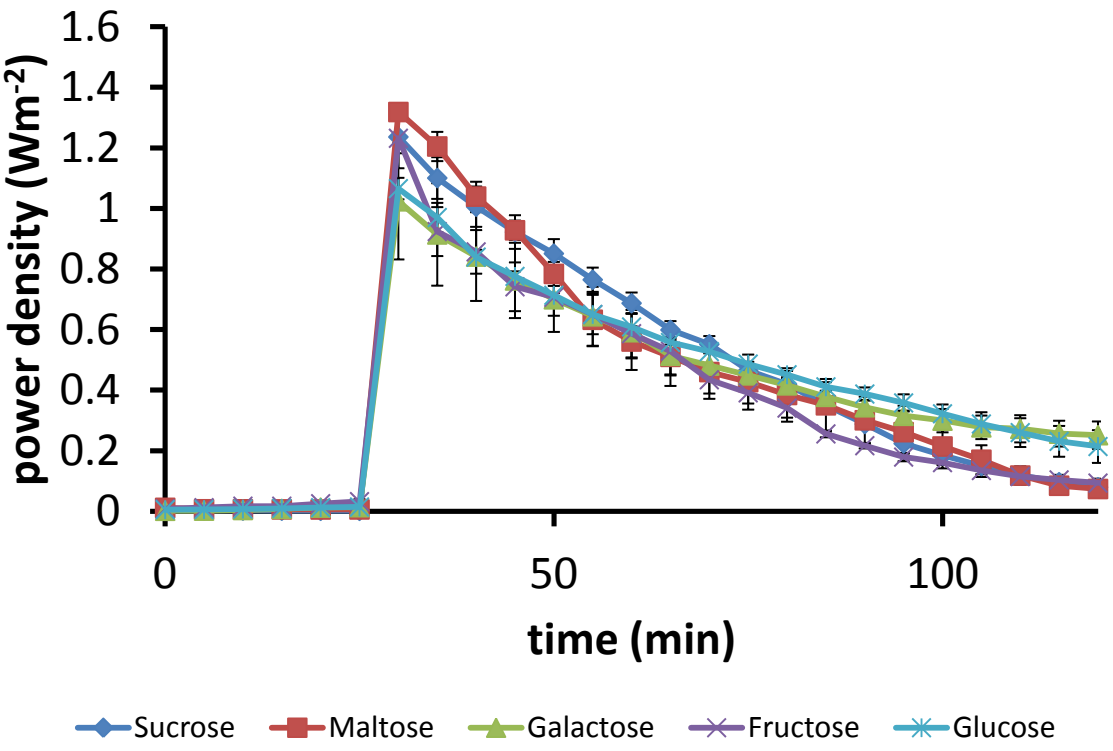


**Figure 7.2: Power density generated by *A. adeninivorans* grown on YPD then incubated on different carbon sources.** *A. adeninivorans* were grown overnight in YPD, harvested (4,500 rcf for 8 min), washed twice and re-suspended in PBS. Cells were then incubated for 3 h in 10 mM of each of the carbon sources, at $OD_{600}$ 2.5, at 37°C at 180 rpm. The MFC contained 0.5 M $KMnO_4$ in PBS in the cathode and 10 mL of 3 h incubated cells in the anode. Temperature kept constant (37°C), cells kept suspended (180 rpm) and 1.5 mM TMPD was added at 25 min. Error bars represent standard error (n=4).

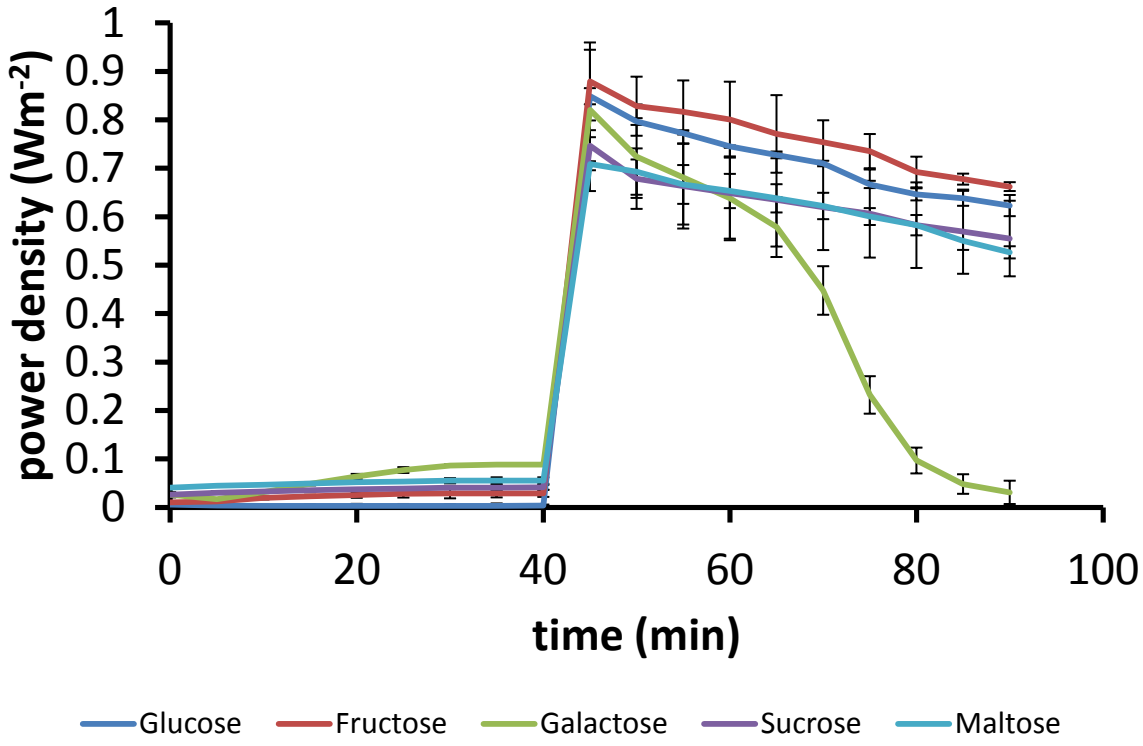


**Figure 7.3: Power density generated by *A. adeninivorans* grown on minimal media substituted with different carbon sources.** *A. adeninivorans* were grown overnight in minimal media (with glucose substituted with the different carbon sources reported), harvested (4,500 rcf for 8 min), washed twice and re-suspended in PBS. MFC contained 0.5 M $KMnO_4$ in PBS in the cathode and $OD_{600}$ 2.5 of cells in the anode. Temperature kept constant (37$^{o}$C), cells kept suspended through constant agitation (180 rpm) and 1.5 mM TMPD added at 40 min. Error bars represent standard error (n=4).

Figure 7.2 demonstrates no difference in mediator-less or mediated electron transfer between any of the substrates. This indicates that the *A. adenivorans* is not inducing any genes in response to incubation with any of the substrates. It is likely that the internal stores within *A. adeninivorans* from growth in YPD are responsible for the similar power densities shown by this experiment.

Figure 7.3 demonstrates a clear difference between galactose and the other carbon sources tested. This experiment shows that galactose is not used by *A. adeninivorans* a dietary carbohydrate, which involves intricate biochemical pathways in order to be metabolised (Campbell *et al.* 1990).

### 7.4.2. Yeast vs. Filamentous

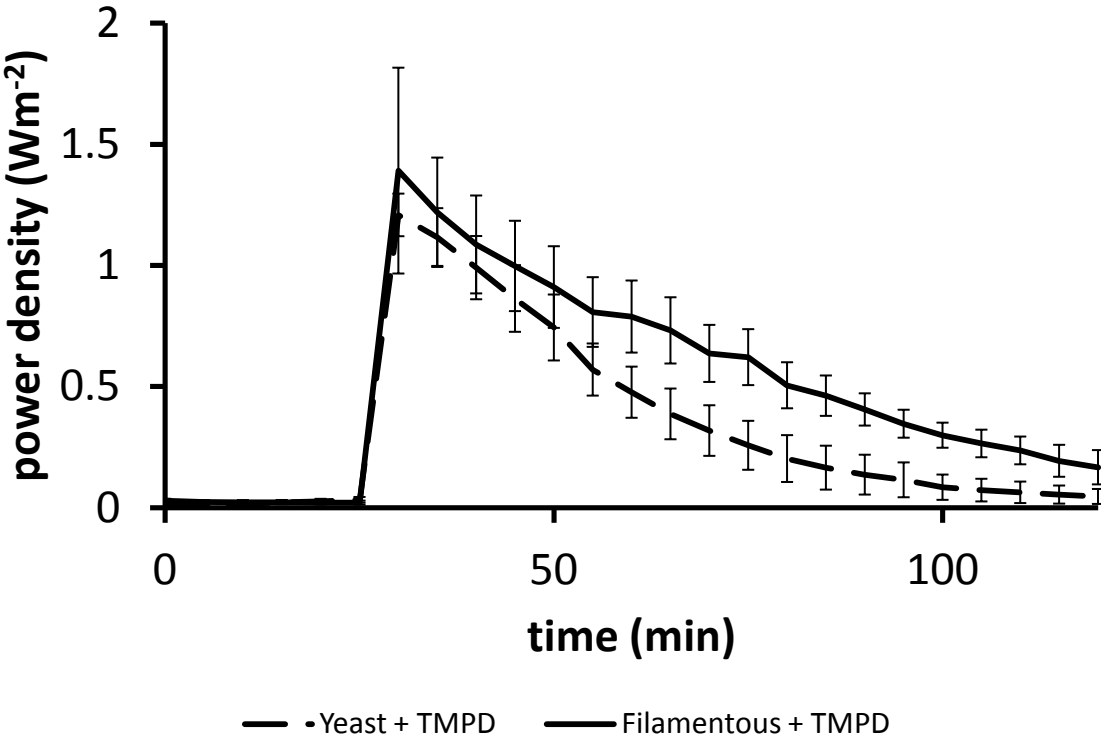


**Figure 7.4: Power density generated by mediated electron transfer between yeast and filamentous forms.** Harvested *A. adeninivorans* cells at $OD_{600}$ 2.5 in PBS with 10 mM glucose were incubated for 2 h at 37$^{o}$C (Yeast) or 42$^{o}$C (Filamentous) to induce morphic change. MFC contained 0.5 M $KMnO_4$ in PBS in the cathode and 10 mL of either yeast or filamentous cell incubations in the anode. Temperature kept constant (37$^{o}$C Yeast, 45$^{o}$C Filamentous), cells kept suspended (180 rpm) and 1.5 mM TMPD added at 40 min. Error bars represent standard error (n=4).

*A. adeninivorans* is an unconventional dimorphic yeast (Wartmann *et al.* 1995). The temperature dependant dimorphism has been linked to different biochemical behaviours and was tested in the MFC. The mediated MFC showed a slightly greater power density from filamentous cells (Figure 7.4). However, this slight difference could easily be due to the difference in temperature of operation of the two different MFC. Mediator-less MFC using yeast and filamentous *A. adeninivorans* showed no significant difference between the two forms (Figure 7.5). In order to observe the effect of temperature, another set of MFC was

inoculated with filamentous *A. adeninivorans* but the MFC was exposed to 37°C and it was found that the power density of yeast and filamentous *A. adeninivorans* were the same.

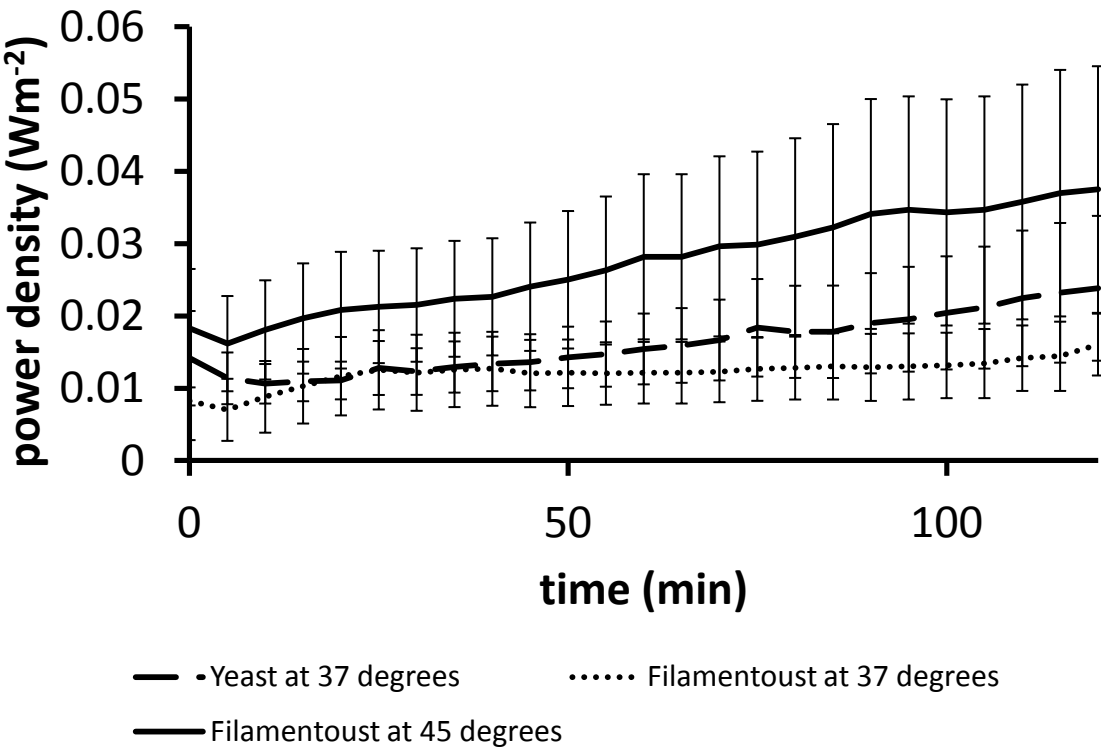


**Figure 7.5: Power density from mediator-less electron transfer of yeast and filamentous forms.** Harvested *A. adeninivorans* cells were incubated for 2 h at 37°C (Yeast) or 45°C (Filamentous) at $OD_{600}$ 2.5 in PBS with 10 mM glucose. MFC contained 0.5 M $KMnO_4$ in PBS in the cathode and 10 mL of either yeast or filamentous cell incubations in the anode. Temperature kept constant at either 37°C or 45°C, cells kept suspended (180 rpm). Error bars represent standard error (n=4).

### 7.4.3. Aerobic vs. Anaerobic

*A. adeninivorans* is capable of both anaerobic and aerobic growth. The mediated power densities of cells grown aerobically and anaerobically were compared in a MFC with and without glucose (Figure 7.6). The two power density curves for cells without glucose present were higher. This difference was greater for anaerobic cells than for aerobic cells.

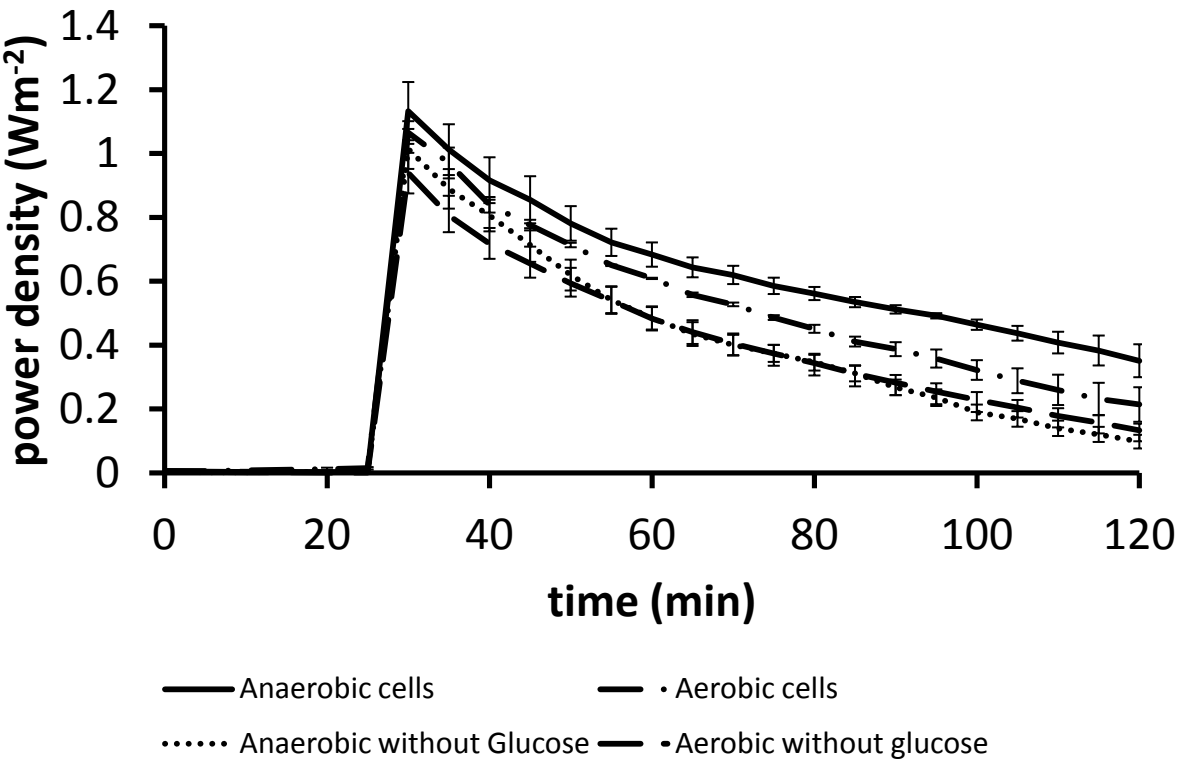


**Figure 7.6: Power density from mediated electron transfer of *A. adeninivorans* grown aerobically and anaerobically.** *A. adeninivorans* cells were grown overnight in 50 mL YPD at 37$^{o}$C at 180 rpm either aerobically or anaerobically (in an anaerobic jar). Cells were harvested (4500 rcf, 8 min) and washed twice in PBS, then concentrated to $OD_{600}$ 25. Fuel cells contained 0.5 M $KMnO_4$ dissolved in PBS in the cathode and $OD_{600}$ 2.5 cells with and without 10 mM glucose in the anode. Temperature of the MFC was kept constant at 37$^{o}$C, cells kept suspended (180 rpm) and 1.5 mM TMPD added at 30 min. Error bars represent standard error (n=4).

The mediator-less electron transfer observed from the cells demonstrated that the anaerobic cells without glucose present also exhibited greater power density without mediator present (Figure 7.7). The reduction of power density due to the presence of glucose indicates that there is repression associated with glucose.

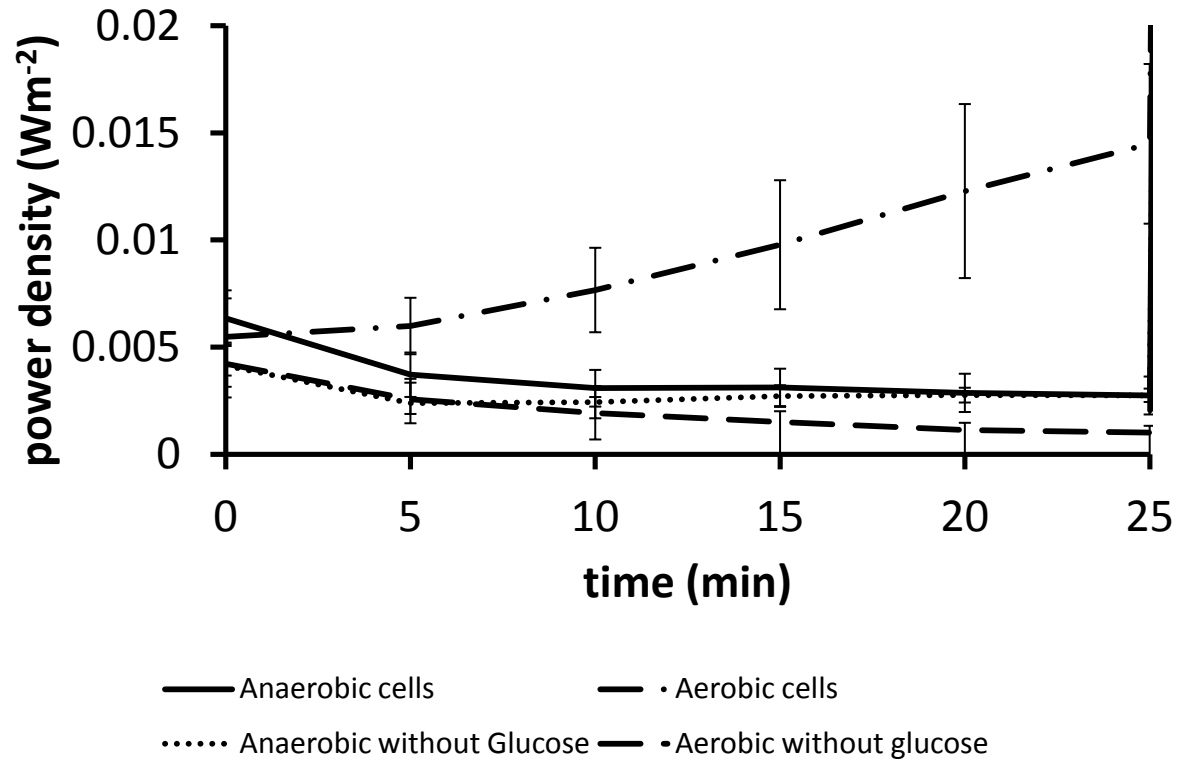


**Figure 7.7: Power density from mediator-less electron transfer of *A. adeninivorans* grown aerobically and anaerobically.** *A. adeninivorans* cells were grown overnight in 50 mL YPD at 37$^{o}$C at 180 rpm either aerobically or anaerobically (in an anaerobic jar). Cells were harvested (4500 rcf, 8 min) and washed twice in PBS, then concentrated to $OD_{600}$ 25. Fuel cells contained 0.5 M $KMnO_4$ in PBS in the cathode and $OD_{600}$ 2.5 cells with 10 mM glucose in the anode. Temperature of the MFC was kept constant at 37$^{o}$C, cells kept suspended (180 rpm). Error bars represent standard error (n=4).

### 7.4.4. Growth phase

Different gene products are produced from microorganisms depending on the growth phase of the cells (Campbell *et al.* 1999). The power density of cells harvested at different stages of the growth curve (Figure 7.8) was investigated in a MFC (Figure 7.9). Exponential phase cells demonstrated a greater mediated power density over stationary phase cells. However, stationary phase cells demonstrated a greater mediator-less power density over exponential phase cells (Figure 7.10).

Stationary phase cells exist in an environment where the carbon source and other nutrients have become limiting and scavenging for these nutrients become necessary. The genes expressed in this growth phase to scavenge for these molecules is therefore the most likely cause for the increase in power density.

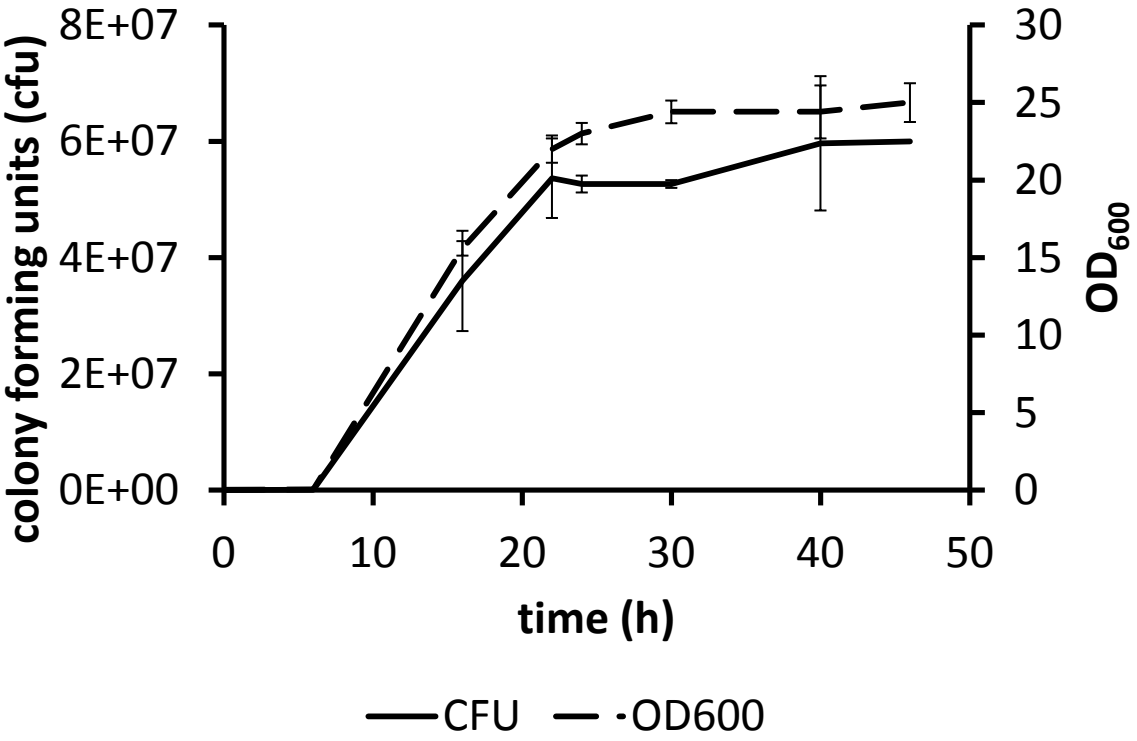


**Figure 7.8: Growth curve of *A. adeninivorans.*** Cells grown in YPD at 37$^{o}$C at 180 rpm. Error bars represent standard error (n=3).

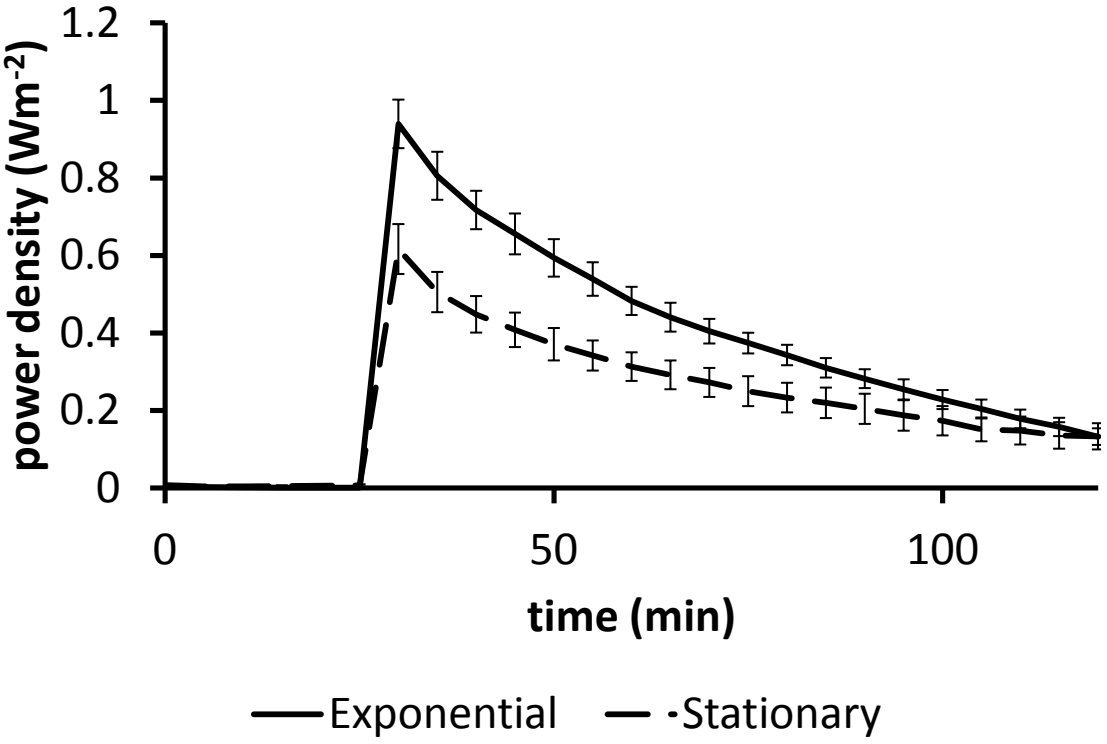


**Figure 7.9: Power density from mediated electron transfer of exponential and stationary phase *A. adeninivorans.*** Exponential phase (16 h) and stationary phase (40 h) *A. adeninivorans* cells were grown in 50 mL YPD at 37$^{o}$C at 180, cells were then harvested (4500 rcf, 8 min) and washed twice in PBS, then concentrated to $OD_{600}$ 25. MFC contained 0.5 M $KMnO_4$ in PBS in the cathode and $OD_{600}$ 2.5 cells with 10 mM glucose in the anode. Temperature of the MFC was kept constant at 37$^{o}$C, cells kept suspended (180 rpm) and 1.5 mM TMPD added at 30 min. Error bars represent standard error (n=4).

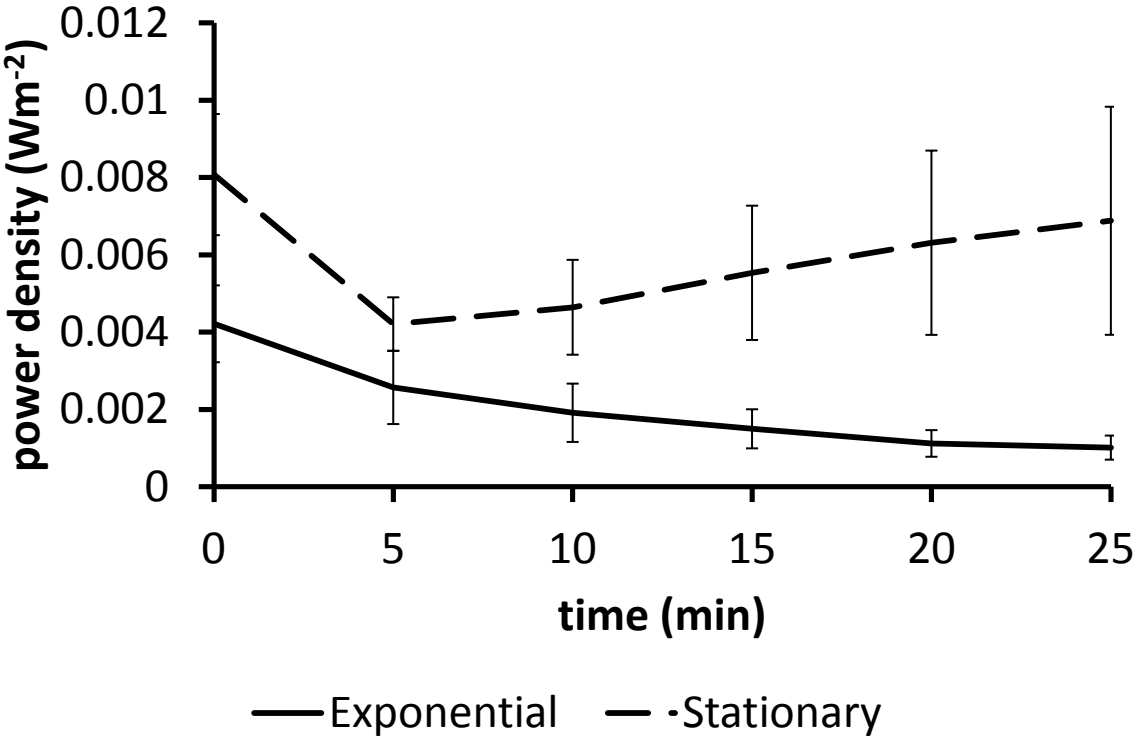


**Figure 7.10: Power density from mediator-less electron transfer of exponential phase and stationary phase *A. adeninivorans.*** Exponential phase (16 h) and stationary phase (40 h) *A. adeninivorans* cells were grown in 50 mL YPD at 37$^{o}$C at 180, cells were then harvested (4500 rcf, 8 min) and washed twice in PBS, then concentrated to $OD_{600}$ 25. MFC contained 0.5 M $KMnO_4$ in PBS in the cathode and $OD_{600}$ 2.5 cells with 10 mM glucose in the anode. Temperature of the MFC was kept constant at 37$^{o}$C, cells kept suspended (180 rpm). Error bars represent standard error (n=4).

### 7.4.5. Electrochemical analysis

Cyclic voltammetry was used to detect redox molecules in the supernatant and on the surface of the *A. adeninivorans*, using both 'hanging' and 'adsorption' CV (see section 4.3.3). The supernatant of anaerobic and stationary phase cells were compared to aerobically grown exponential phase cells using hanging CV (Figure 7.11). Adsorption CV were conducted of anaerobic cell and stationary cell pellets, then left for 30 mins and then CV was conducted again to identify any redox molecules secreted (Figures 7.12 and 7.13). Both anaerobic and stationary phase cells demonstrated the same peaks observed for exponential phase aerobic cells (Figure 3.7).

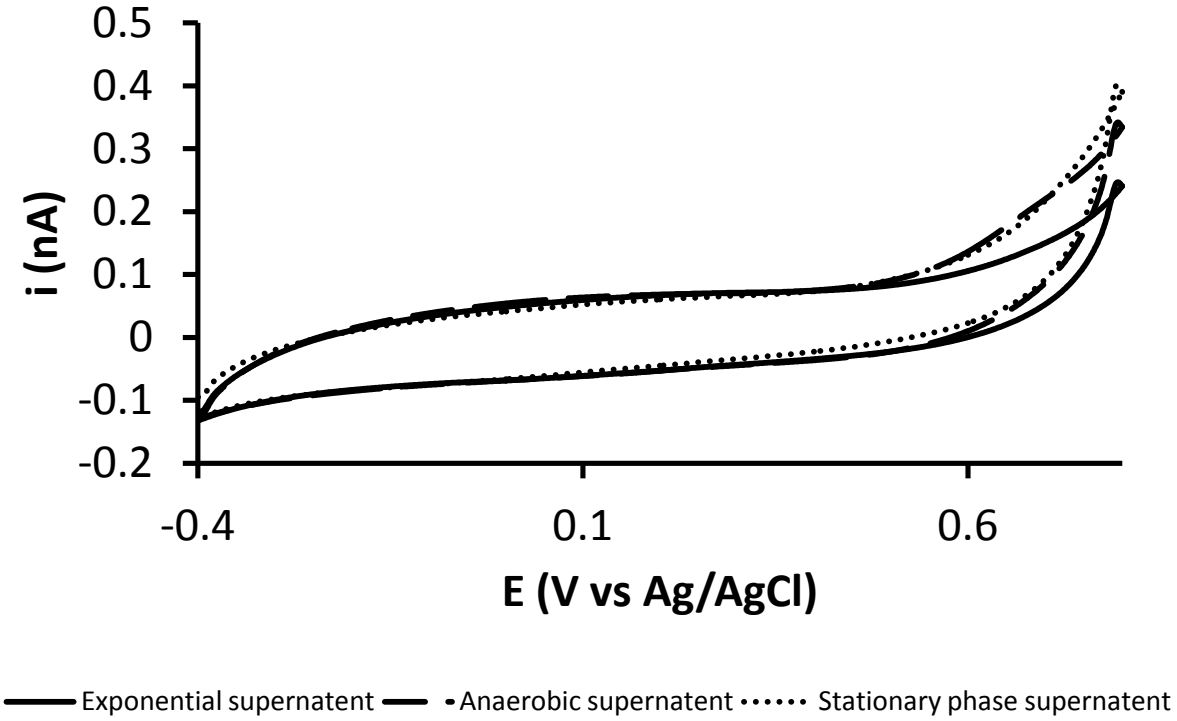


**Figure 7.11: Cyclic voltammetry scans of supernatants from different growth phases and conditions.** Cyclic voltammetry was performed (from -400 mV to + 800 mV vs. Ag/AgCl at 100 $mVs^{-1}$) using the following 3 electrode set up: Working; glassy carbon macro-electrode, Reference; Ag/AgCl, Counter; Pt. traces represent a mean of 3 cyclic voltammograms. Lines represent mean of 3.

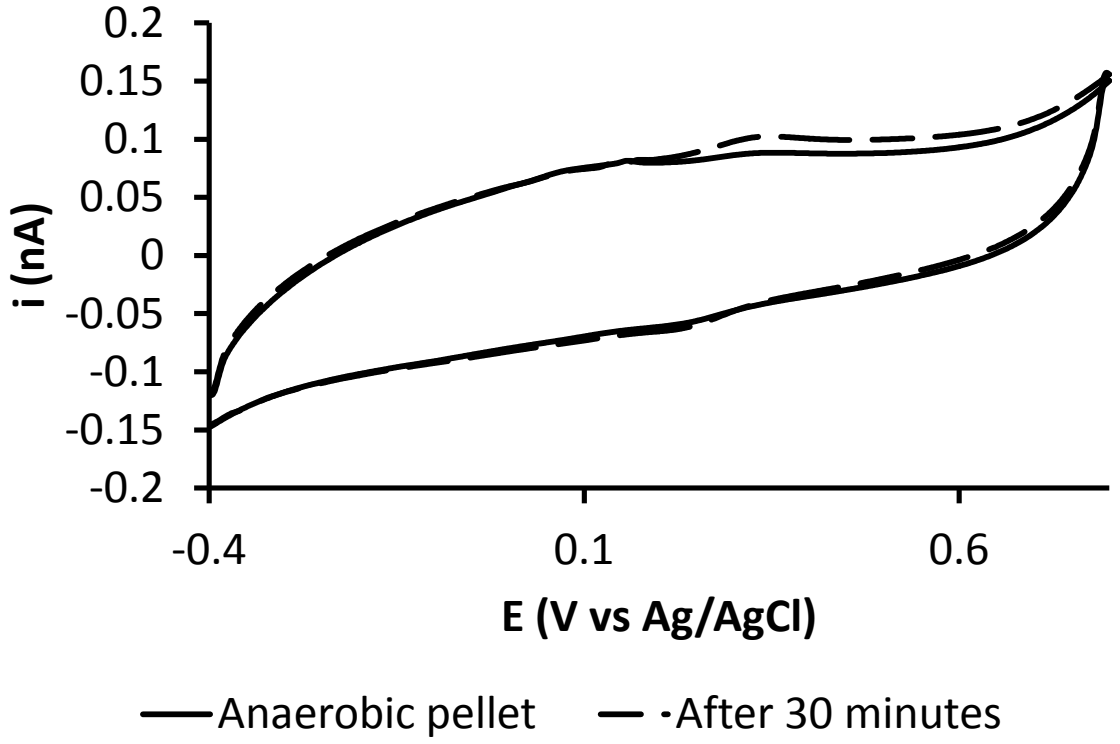


**Figure 7.12: Adsorption cyclic voltammetry scans of anaerobic cell pellets.** Cyclic Voltammetry was performed (from -400 mV to + 800 mV vs. Ag/AgCl at 100 $mVs^{-1}$) using the following 3 electrode set up: Working; glassy carbon macro-electrode, Reference; Ag/AgCl, Counter; Pt. Lines represent a mean of 3 CV.

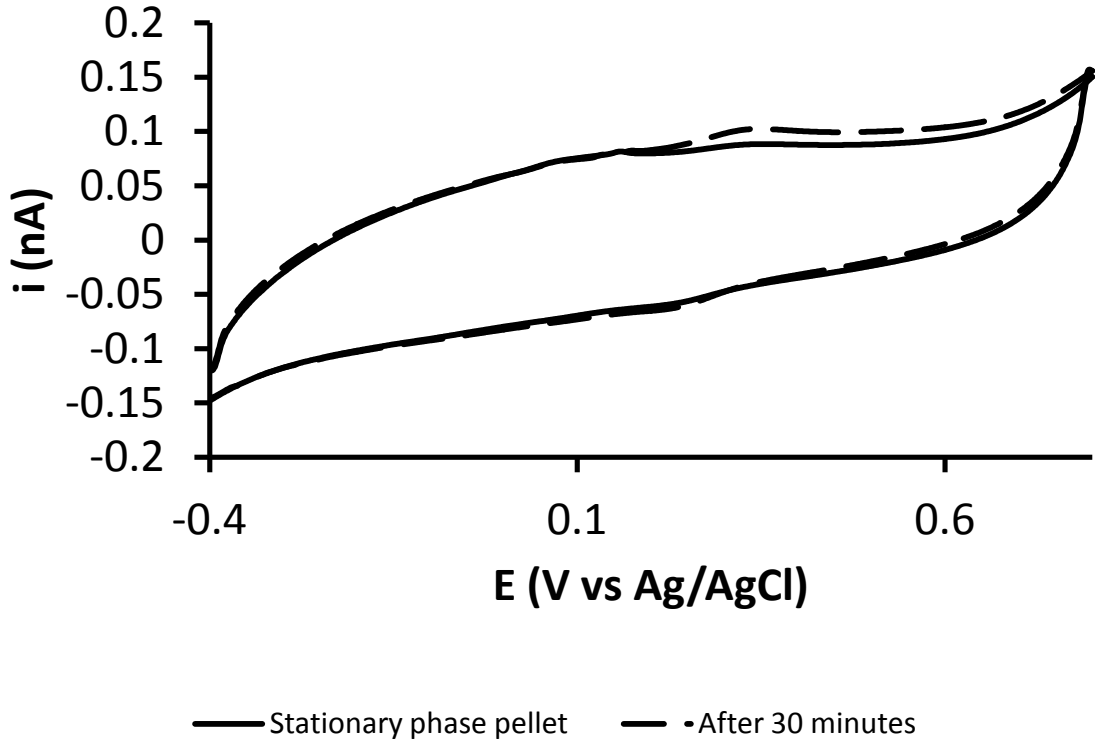


**Figure 7.13: Adsorption cyclic voltammetry scans of stationary phase cell pellets.** Cyclic voltammetry was performed (from -400 mV to + 800 mV vs. Ag/AgCl at 100 $mVs^{-1}$) using the following 3 electrode set up: Working; glassy carbon macro-electrode, Reference; Ag/AgCl, Counter; Pt. Lines represent a mean of 3 CV.

### 7.4.6. Different configurations of microbial fuel cell

Several different configurations (Figure 7.1) of the MFC were tested to observe the effect of each modification has on the power density from mediated (Figure 7.14) and mediator-less conditions (Figure 7.15).

Figure 7.14 demonstrates that the presence of two cathodes initially produces a greater power density, but that having two anodes allows for longer sustained power. If the anode is the rate limiting compartment the presence of a second cathode should not alter the power density. A point of note is that because the power density is calculated by dividing the power of the MFC by the surface area of the anode (equations 1&3), by using two anodes the surface area doubles and therefore the power in order to maintain the same power density.

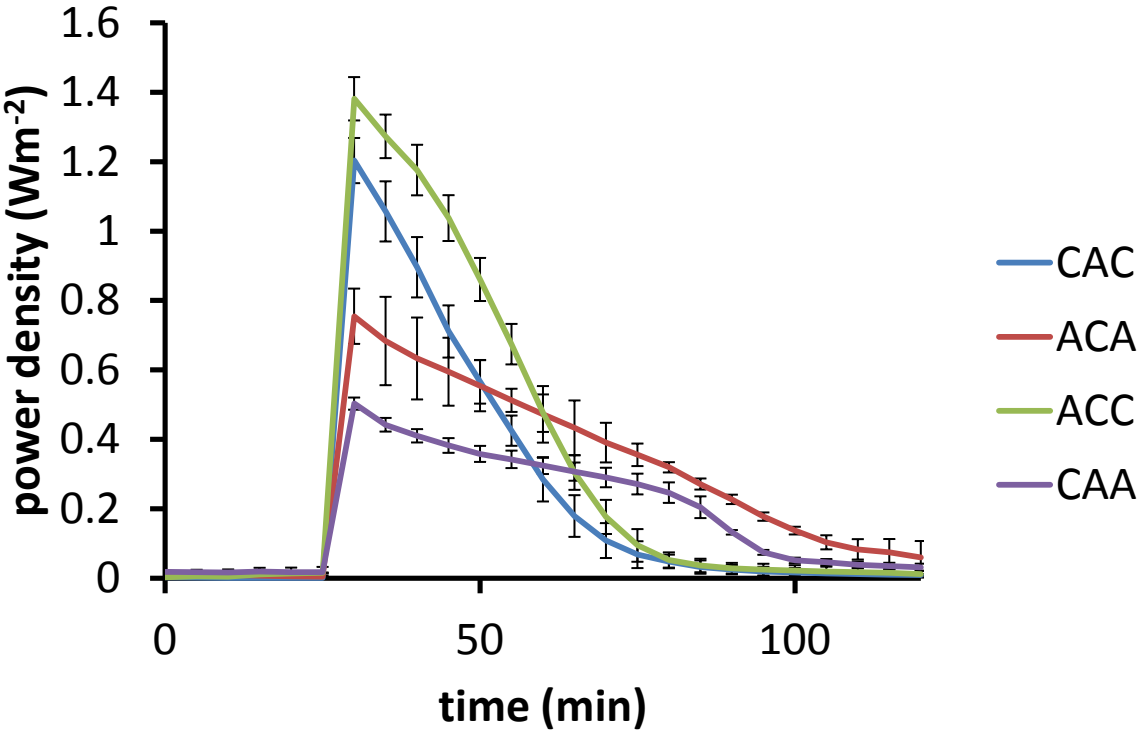


**Figure 7.14: Mediated electron transfer in different configurations of the microbial fuel cell.** The different configurations were: CAC – two cathode compartments sandwiching an anode compartment, ACA – two anode compartments sandwiching a cathode compartment, ACC – One anode compartment separated from one cathode compartment which is twice the to normal and has two electrodes, CAA – One cathode compartment separated from one anode compartment which is twice the size to normal and has two electrodes. *A. adeninivorans* cells were grown overnight in 50 mL YPD at 37$^{o}$C at 180, cells were then harvested (4500 rcf, 8 min) and washed twice in PBS, then concentrated to $OD_{600}$ 25. MFC contained 0.5 M $KMnO_4$ in PBS in the cathode and $OD_{600}$ 2.5 cells in the anodes. Temperature of the MFC was kept constant at 37$^{o}$C, cells kept suspended (180 rpm) and 1.5 mM TMPD was added to each anode compartment at 25 mins. Error bars represent standard error (n=4).

NB: The surface area of the anode has doubled for ACA and CAA so the power density shown is a result of dividing by the new surface area.

The introduction of a second proton exchange membrane (PEM) increased the power density with two anodes but decreased the power density with two cathodes. A possible explanation for the second PEM increasing the power density with two anodes sandwiching a cathode, is

that the increased surface area increases the amount of $H^+$ able to pass from the anodes to the cathode and the resulting difference in pH allows for a lower pH to be maintained for a longer period of time. A possible explanation for the second PEM decreasing the power density when two cathodes sandwich an anode, is that the second PEM increases the internal resistance of the MFC. Figure 7.15 shows that mediator-less electron transfer from two cathode MFC start off lower than two anode MFC. Over time, the MFC containing two PEM produced less power density than those with only one. It is possible that the second PEM is increased the internal resistance of both MFC.

In order to investigate if the second PEM increases the internal resistance, a power density verses external load graph was generated for both mediator-less (Figure 7.16) and mediated (Figure 7.17) MFC of all configurations. The shape of the power density verses external load curve for the mediator-less MFCs is different for these configurations than it was for the simple two chambered MFC (Figure 2.2), and shows optimal power density at 100 Ω for all configurations.

The mediated MFCs show an optimal power density at 100 Ω for all configurations except for cathode-anode-cathode (Figure 7.17). The optimal power density for the cathode-anode-cathode configuration is 300 Ω, indicating that the internal resistance of this configuration has increased. This increase in internal resistance could account for the drop in power density between the two, double-cathode configurations.

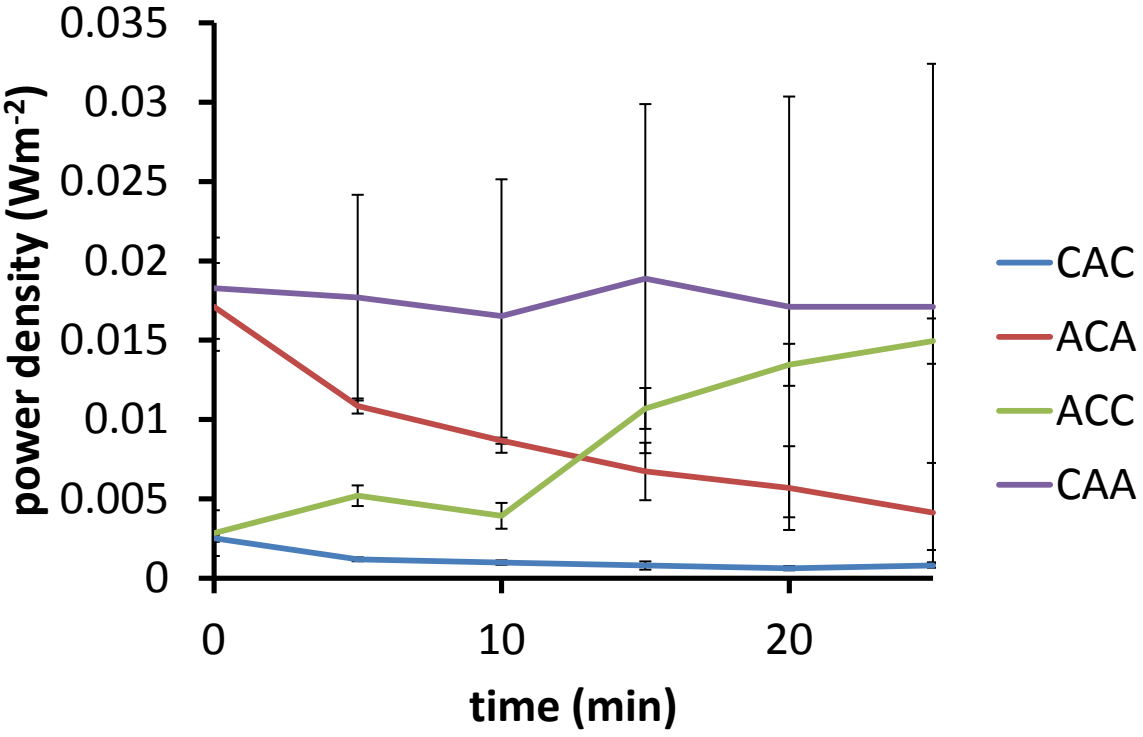


**Figure 7.15: Power density from mediator-less electron transfer in different configurations of the microbial fuel cell.** The different configurations were: CAC – two cathode compartments sandwiching an anode compartment, ACA – two anode compartments sandwiching a cathode compartment, ACC – One anode compartment separated from one cathode compartment which is twice the size to normal and has two electrodes, CAA – One cathode compartment separated from one anode compartment which is twice the size to normal and has two electrodes. *A. adeninivorans* cells were grown overnight in 50 mL YPD at 37$^{o}$C at 180, cells were then harvested (4500 rcf, 8 min) and washed twice in PBS, then concentrated to $OD_{600}$ 25. MFC contained 0.5 M $KMnO_4$ in PBS in the cathode and $OD_{600}$ 2.5 cells in the anodes. Temperature of the MFC was kept constant at 37$^{o}$C, cells kept suspended (180 rpm). Error bars represent standard error (n=4).

NB: The surface area of the anode has doubled for ACA and CAA so the power density shown is a result of dividing by the new surface area.

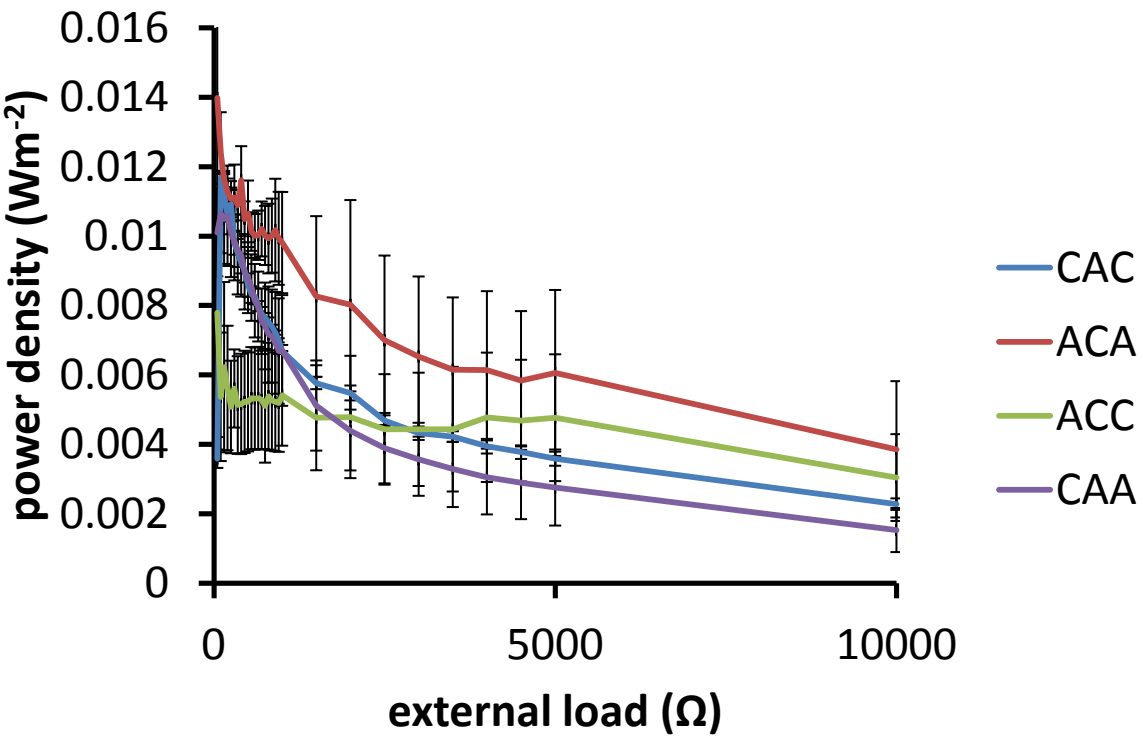


**Figure 7.16: Power density of changes to different mediator-less MFC configurations due to stepwise changes to the external resistance.** The different configurations were: CAC – two cathode compartments sandwiching an anode compartment, ACA – two anode compartments sandwiching a cathode compartment, ACC – One anode compartment separated from one cathode compartment which is twice the size to normal and has two electrodes, CAA – One cathode compartment separated from one anode compartment which is twice the size to normal and has two electrodes. *A. adeninivorans* cells were grown overnight in 50 mL YPD at 37$^{o}$C at 180, cells were then harvested (4500 rcf, 8 min) and washed twice in PBS, then concentrated to $OD_{600}$ 25. MFC contained 0.5 M $KMnO_4$ in PBS in the cathode and $OD_{600}$ 2.5 cells in the anodes. Temperature of the MFC was kept constant at 37$^{o}$C, cells kept suspended (180 rpm). Error bars represent standard error (n=4).

NB: The surface area of the anode has doubled for ACA and CAA so the power density shown is a result of dividing by the new surface area.

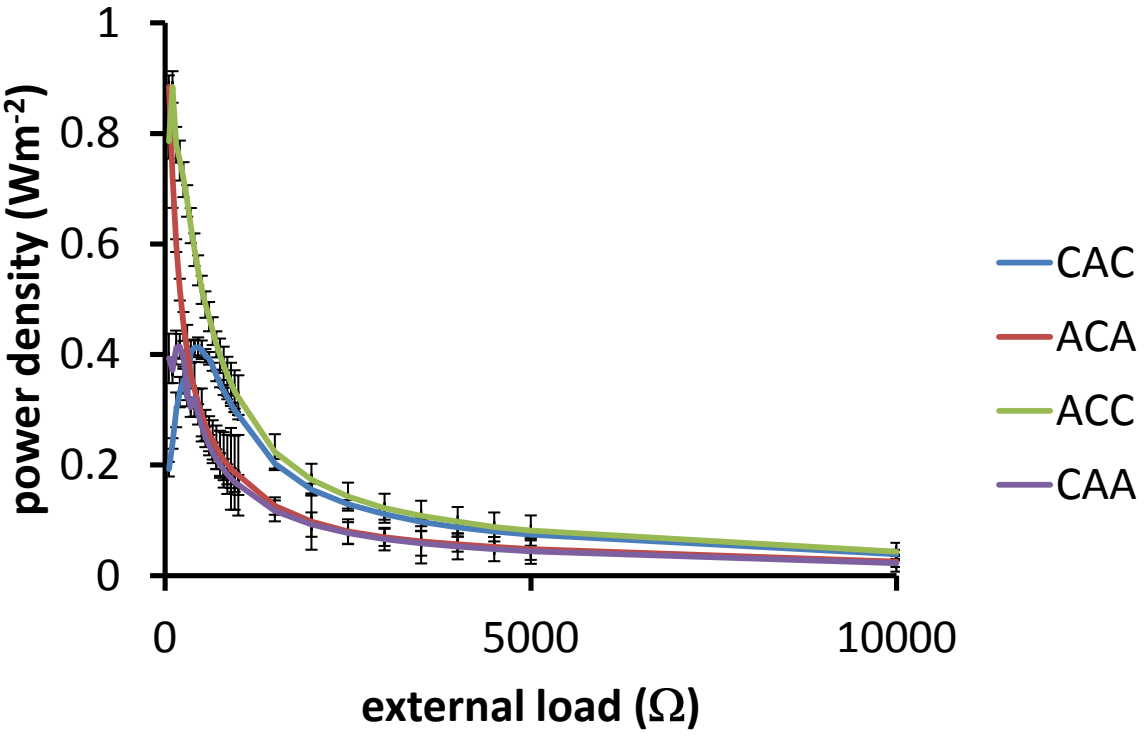


**Figure 7.17: Power density of changes to different mediated MFC configurations due to stepwise changes to the external resistance.** The different configurations were: CAC – two cathode compartments sandwiching an anode compartment, ACA – two anode compartments sandwiching a cathode compartment, ACC – One anode compartment separated from one cathode compartment which is twice the size to normal and has two electrodes, CAA – One cathode compartment separated from one anode compartment which is twice the size to normal and has two electrodes. *A. adeninivorans* cells were grown overnight in 50 mL YPD at 37$^{o}$C at 180, cells were then harvested (4500 rcf, 8 min) and washed twice in PBS, then concentrated to $OD_{600}$ 25. MFC contained 0.5 M $KMnO_4$ dissolved in PBS in the cathode and $OD_{600}$ 2.5 cells in the anodes with 1.5 mM TMPD. Temperature of the MFC was kept constant at 37$^{o}$C, cells kept suspended (180 rpm). Error bars represent standard error (n=4).

NB: The surface area of the anode has doubled for ACA and CAA so the power density shown is a result of dividing by the new surface area.

The potentials of the anode(s) and cathode(s) in an OCP configuration were measured for all mediator-less MFC configurations (Figure 7.18). The cathode potential for each configuration

was the same except for anode-cathode-anode which demonstrated a significantly greater positive potential. This statistically significant increase (ANOVA p=0.05) could be a result of the increase in PEM surface area allowing a greater transfer of $H^+$ from the anode to the cathode, dropping the cathode pH. The cathode potentials increased and the anode potentials dropped to the same level with the introduction of TMPD into the anode (Figure 7.19) except for the cathode-anode-cathode configuration.

Applying an external load causes a dramatic increase in the anode potential for all configurations under mediator-less conditions (Figure 7.20). This is consistent with previous results with the simple two-chambered MFC (Figure 4.12). The introduction of a mediator drops the potential of the anode(s) and the cathode(s) which is also consistent with previous results (Figure 5.12). It appears the drop in potential of the anode(s) and cathode(s) is greater when two anodes are present.

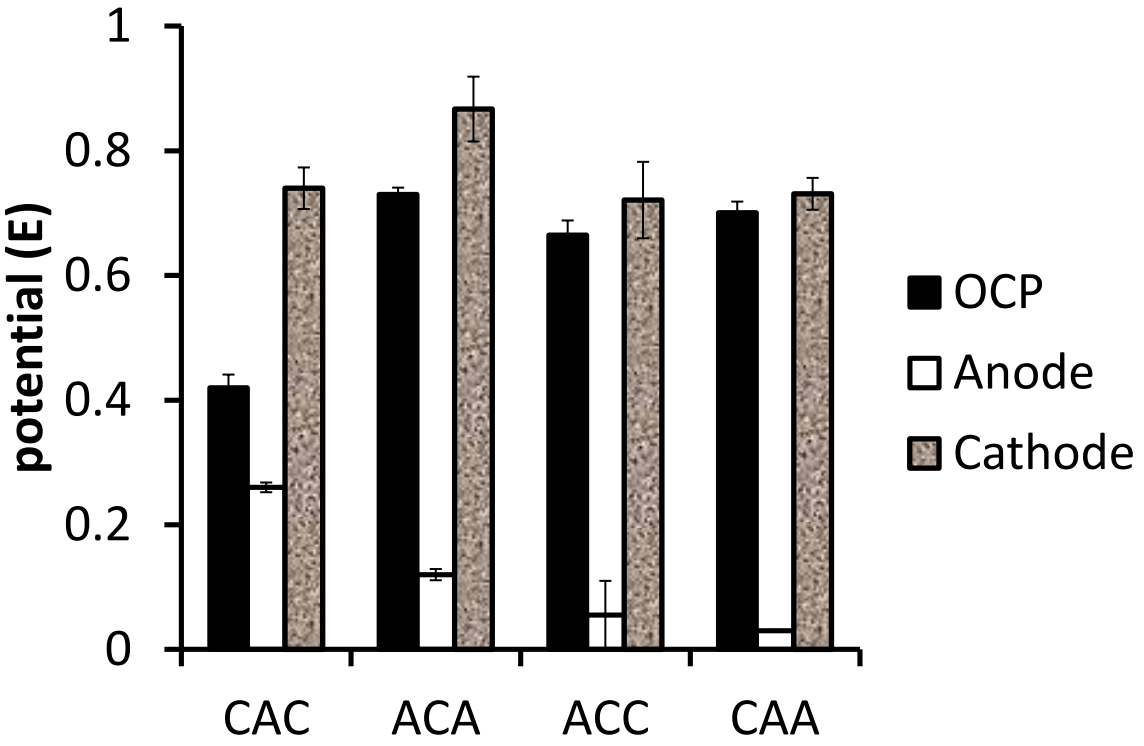


**Figure 7.18: Open circuit potential and potentials of the anode and the cathode of the different configurations of the MFC without TMPD present.** The different configurations were: CAC – two cathode compartments sandwiching an anode compartment, ACA – two anode compartments sandwiching a cathode compartment, ACC – One anode compartment separated from one cathode compartment which is twice the size to normal and has two electrodes, CAA – One cathode compartment separated from one anode compartment which is twice the volume to normal and has two electrodes. *A. adeninivorans* cells were grown overnight in 50 mL YPD at 37$^{o}$C at 180, cells were then harvested (4500 rcf, 8 min) and washed twice in PBS, then concentrated to $OD_{600}$ 25. MFC contained 0.5 M $KMnO_4$ in PBS in the cathode(s) and $OD_{600}$ 2.5 cells in the anode(s). Temperature of the MFC was kept constant at 37$^{o}$C, cells kept suspended (180 rpm). Error bars represent standard error (n=4).

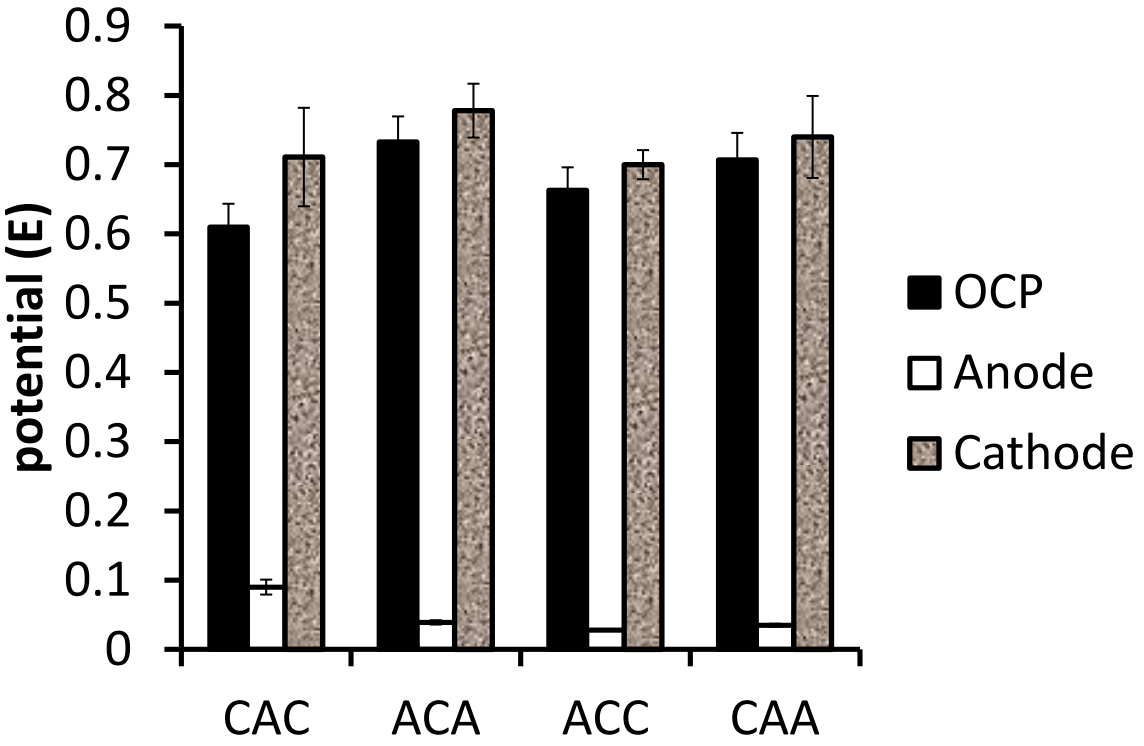


**Figure 7.19: Open circuit potential and the potentials to the anode(s) and the cathode(s) of the different configurations of the MFC with TMPD present.** The different configurations were: CAC – two cathode compartments sandwiching an anode compartment, ACA – two anode compartments sandwiching a cathode compartment, ACC – One anode compartment separated from one cathode compartment which is twice the volume to standard configuration and has two electrodes, CAA – One cathode compartment separated from one anode compartment which is twice the size to normal and has two electrodes.
*A. adeninivorans* cells were grown overnight in 50 mL YPD at 37$^{o}$C at 180, cells were then harvested (4500 rcf, 8 min) and washed twice in PBS, then concentrated to $OD_{600}$ 25. MFC contained 0.5 M $KMnO_4$ in PBS in the cathode(s) and $OD_{600}$ 2.5 cells in the anode(s) with 1.5 mM TMPD. Temperature of the MFC was kept constant at 37$^{o}$C, cells kept suspended (180 rpm). Error bars represent standard error (n=4).

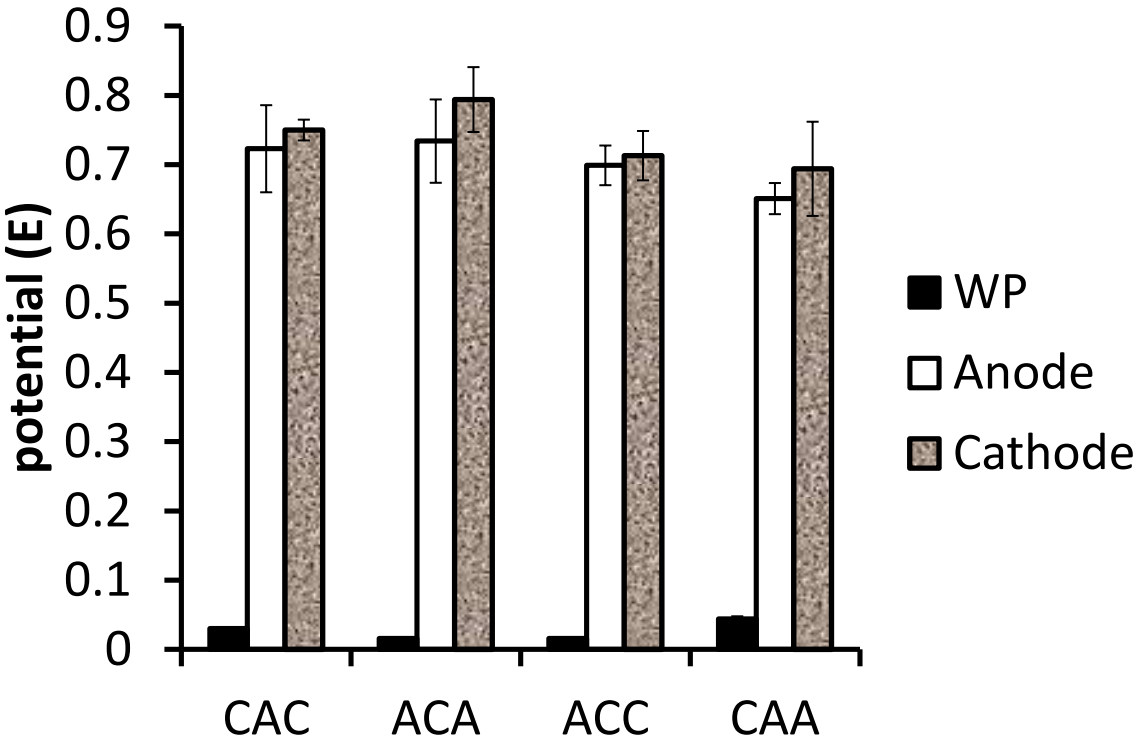


**Figure 7.20: Working potential (100 Ω load) and the potentials of the anode(s) and the cathode(s) of the different configurations of the MFC without TMPD present.** The different configurations were: CAC – two cathode compartments sandwiching an anode compartment, ACA – two anode compartments sandwiching a cathode compartment, ACC – One anode compartment separated from one cathode compartment which is twice the size to normal and has two electrodes, CAA – One cathode compartment separated from one anode compartment which is twice the size to normal and has two electrodes. *A. adeninivorans* cells were grown overnight in 50 mL YPD at 37 $^{o}$C at 180, cells were then harvested (4500 rcf, 8 min) and washed twice in PBS, then concentrated to $OD_{600}$ 25. MFC contained 0.5 M $KMnO_4$ in PBS in the cathode(s) and $OD_{600}$ 2.5 cells in the anode(s). Temperature of the MFC was kept constant at 37$^{o}$C, cells kept suspended (180 rpm). Error bars represent standard error (n=4).

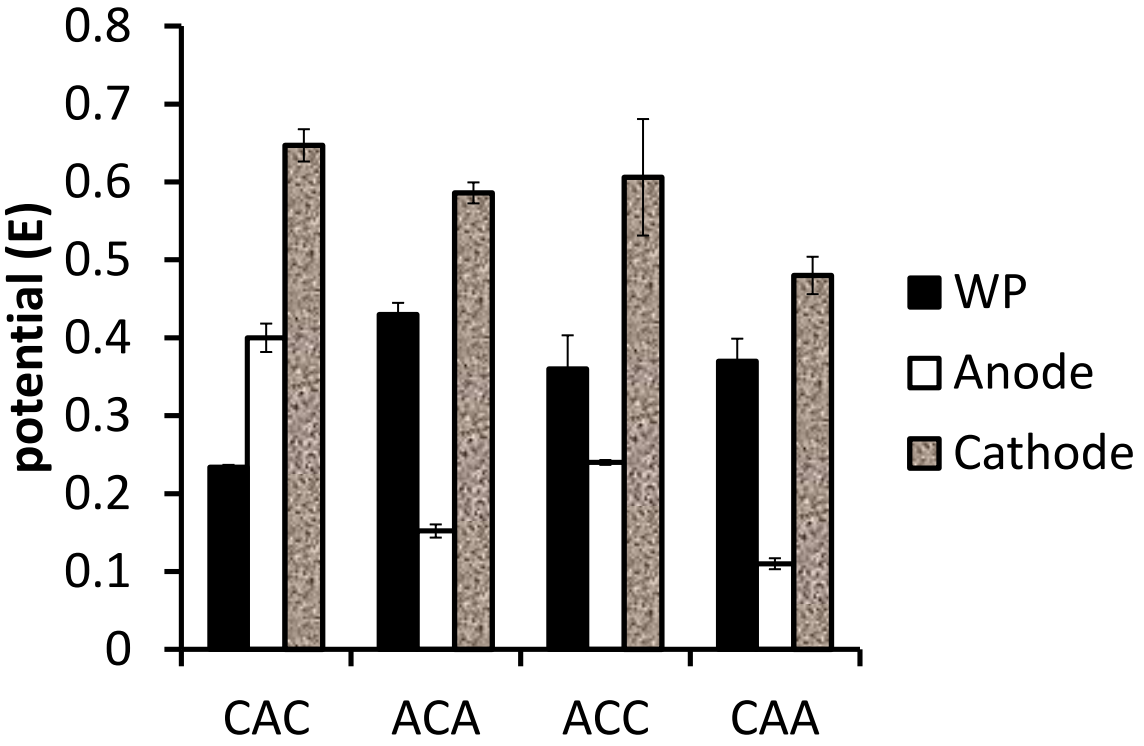


**Figure 7.21: Working potential (100 Ω load) to the potentials of the anode(s) and the cathode(s) of the different configurations of the MFC with TMPD present.** The different configurations were: CAC – two cathode compartments sandwiching an anode compartment, ACA – two anode compartments sandwiching a cathode compartment, ACC – One anode compartment separated from one cathode compartment which is twice the size to normal and has two electrodes, CAA – One cathode compartment separated from one anode compartment which is twice the size to normal and has two electrodes. *A. adeninivorans* cells were grown overnight in 50 mL YPD at 37$^{o}$C at 180, cells were then harvested (4500 rcf, 8 min) and washed twice in PBS, then concentrated to $OD_{600}$ 25. MFC contained 0.5 M $KMnO_4$ in PBS in the cathode(s) and $OD_{600}$ 2.5 cells in the anode(s) with 1.5 mM TMPD. Temperature of the MFC was kept constant at 37$^{o}$C, cells kept suspended (180 rpm). Error bars represent standard error (n=4).

The simple two chambered MFC was modified in order to be used flipped 90$^{o}$ (Figure 7.1). In order to accomplish this, the inlet ports and gaps around the electrodes were sealed with glue and insulation tape after the contents of the anode and cathode chamber were added. In order for the PEM to allow the passage of $H^+$ from the anode to the cathode, the solutions of the two chambers must both contact the membrane. This required both chambers to be filled to

capacity before sealing (the MFCs normally have a total of 10 mL of solutions in them at any one time).

Once filled and sealed the MFC was laid on its side in the water bath and monitoring of the power density began. The object of this experiment was to observe if this modification will increase the mediator-less power density, by allowing greater contact between the anode and the cells by using gravity. Figure 7.22 demonstrates that this modification to the MFC does not increase the power density of mediator-less MFC.

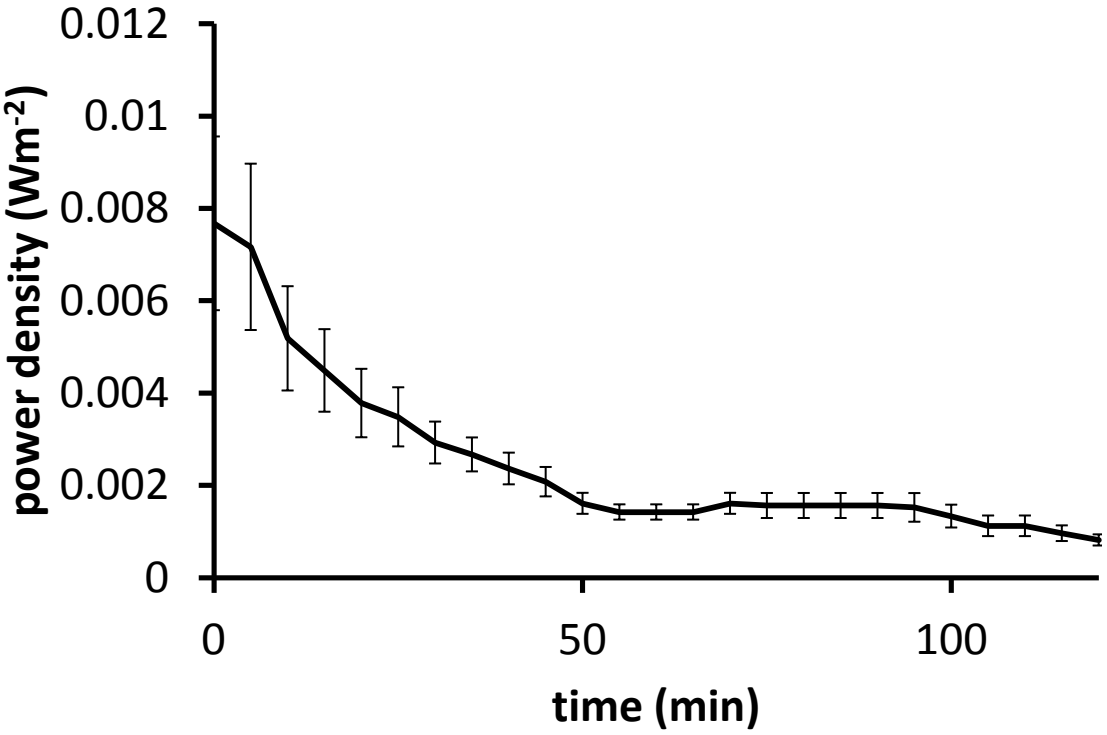


**Figure 7.22: Power density from mediator-less electron transfer in a MFC set up horizontally.** *A. adeninivorans* cells were grown overnight in 50 mL YPD at 37$^{o}$C at 180, cells were then harvested (4500 rcf, 8 min) and washed twice in PBS, then concentrated to $OD_{600}$ 25. Fuel cells contained 0.5 M $KMnO_4$ dissolved in PBS in the cathode and $OD_{600}$ 2.5 cells in the anode. The anode and cathode were filled to capacity then the openings were seals before the experiment began. Temperature of the MFC was kept constant at 37$^{o}$C, cells kept suspended (180 rpm). Error bars represent standard error (n=4).

## 7.5. Discussion

### 7.5.1. *A. adeninivorans* growth conditions

The biological catalyst in a MFC is a vitally important component and as such all aspects of the microorganism should be investigated with regard to power density. *A. adeninivorans* was shown to be able to grown on and produce mediator-less and mediated power density with several carbohydrates (Figures 7.2 & 7.3). The difference in the power density produced from yeast and filamentous forms of *A. adeninivorans* was attributed to the temperature the MFC was held at (Figure 7.5). *A. adeninivorans* generated mediated and mediator-less power density from anaerobic and aerobic growth as well as from exponential and stationary phase (Figures 7.6, 7.7, 7.9 & 7.10).

These results are promising for the incorporation of *A. adeninivorans* MFC into real world application. With a wide range of substrates usable and power density achievable independent of growth phase or type of growth, the versatility of *A. adeninivorans* makes it a promising biological catalyst for MFC. However, the power density achieved from mediator-less MFC is still low and a means of increasing this is vital.

### 7.5.1. Microbial fuel cell configurations

There are a few cases of use of multiple anodes and/or cathodes reported elsewhere (Rabaey *et al.* 2003; Aelterman *et al.* 2006). The modifications made did not produce greater power density from the simpler original MFC (Figure 7.14 and Figure 2.10). There was a power increase observed from adding a second anode (with or without a second PEM), but it was not enough to maintain the power density once divided by the increased anode surface area (Figure 7.14 and equation 3).

The internal resistance of the modified mediator-less MFC was demonstrated to be drastically different from the simpler two chambered version, with all MFC demonstrating optimal

power density at an external load of 100 Ω. The introduction of TMPD demonstrated that the internal resistance of the cathode-anode-cathode configuration with TMPD present increase from 100 Ω to 300 Ω. It is unclear why adding a second PEM would increase the internal resistance for two cathodes but not for two anodes, unless the internal resistance could be affected by the transport of $H^+$ from the anode(s) to the cathode(s) in which case there are more $H^+$ ions available in the anode-cathode-anode configuration.

The potential of the anode(s) and cathode(s) of all the MFC configurations, mediator-less and mediated, under external load and in open circuit configurations were measured. The mediator-less MFCs all behaved similar to the simpler original, except for the anode-cathode-anode which demonstrated a higher potential for the cathode. As mentioned previously, this configuration could allow a more rapid transport of $H^+$ from the anode(s) to the cathode(s) in which case there are more $H^+$ ions available, which reduced the pH, increasing the potential (You *et al.* 2006). The mediated MFCs all behaved similarly to the simpler original version, except that the configurations with an extra anode, and therefore the extra TMPD, dropped both the anode and cathode potentials greater than the configurations with one anode.

Lastly, a 'horizontal' configuration was tested to determine if having the anode on the bottom of the MFC and the *A. adeninivorans* settling down onto it would increase the mediator-less electron transfer. This configuration was shown not to increase the power density.

### 7.6. Conclusion

A wide range of characteristic of *A. adeninivorans* growth was tested to study the effects they have on power density. It was shown that the temperature the MFC is maintained at affects the power density of the MFC, more than the growth phase, or the morphology the cells. The same solution species secreted by anaerobic and stationary phase cells is secreted by aerobically grown exponential phase cells.

Modifications to the MFC demonstrated that while the addition of another anode does increase the power of a MFC, it does not increase the power significantly to increase the power density (due to the increased anode surface area). In some cases the addition of a PEM membrane can increase the internal resistance of the MFC, but the reasoning behind this is unclear. The potential of the anode(s) and cathode(s) were tested and both mediator-less and mediated MFCs demonstrated similar behaviour to that observed for the simpler two chambered MFC.

# Chapter 8: Mixed cultures in a MFC

## 8.1. Abstract

The mediator pyocyanin was produced by *Pseudomonas aeruginosa* at a concentration of approximately 40 µM in an overnight culture. Pyocyanin was ineffective at mediating *A. adeninivorans* electron transfer and generating current densities. Pyocyanin was produced in mixed cultures. However, the concentrations of pyocyanin required to generate optimal power density as a mediator in a MFC was far greater than the concentration produced by the cells in solutions.

## 8.2. Introduction

Adding mediators to MFC is undesirable because they are expensive and need to be replenished with each batch if the MFC is of batch configuration or added constantly if the MFC is a flow through operation (Bullen *et al.* 2006). One possible alternative has come from an observation made by Rabaey *et al.* (2004) that the MFC environment selected for microbial consortia containing microorganisms that produced their own mediators, termed exoelectrogens (Logan 2008). Such microorganisms are able to produce molecules capable of increasing power density by facilitating the transfer of electrons from the microorganism to the electrode (Rabaey *et al.* 2005). The microorganism *P. aeruginosa* was identified by Rabaey *et al.* (2006) to produce a molecule called pyocyanin. Rabaey *et al.* (2005) demonstrated that purified pyocyanin was capable of increasing the power density of a MFC containing *P. aeruginosa* cells that had been genetically modified to halt their own production of pyocyanin.

In Chapter 7 it was demonstrated that *A. adeninivorans* is capable of producing power density from a wide range of carbon sources and in a wide variety of growth conditions. If pyocyanin produced from *P. aeruginosa* could act as a mediator increasing the power density of a MFC containing *A. adeninivorans* in the same way as with TMPD, then many of the negative connotations of mediated electron transfer are negated and a versatile mixed culture MFC is

possible. pyocyanin can be dissolved in ethanol and is sparingly soluble in aqueous buffers (Caymen chemical - Pyocyanin – Product Information 2007), suggesting that pyocyanin is lipophilic in nature like TMPD.

The goal of this chapter was to investigate if the growth versatility of *A. adeninivorans* can be explored in conjunction with an exoelectrogen microorganism. If these two microorganisms can be used together to produce greater power density and versatility than either on their own, this would be a significant breakthrough in MFC technology.

## 8.3. Materials and Methods

### 8.3.1. Chemicals

Chemicals are the same as section 3.3.1. Pyocyanin was brought from Sigma Chem. Co. (St. Louis, MO, USA).

### 8.3.2. Strains, buffers, reagents and media

Strains, buffers, reagents and media were the same as sections 3.3.2 and 4.3.2. *P. aeruginosa* strain UMRL 1203 was obtained from the ESR yeast collection, Porirua, New Zealand. *Pseudomonas* medium (20 g/L peptone, 1.4 g/L magnesium chloride, 10 g/L potassium sulfate and 20 mL/L glycerol) was used as growth medium as well as YEPD. Pyocyanin was dissolved in 99.5% ethanol.

### 8.3.3. Cell culturing

*A. adeninivorans*, *P. aeruginosa* and *S. cerevisiae* were all grown in either YEPD or *Pseudomonas* medium overnight, 37$^{o}$C, 210 rpm, in indented flasks. Monocultures and mixed cultures were grown and harvested (4,500 rcf, 8 min), washed twice and suspended in PBS.

## 8.4. Results

### 8.4.1. Establishing Pyocyanin production in mono and mixed cultures

Pyocyanin production by *P. aeruginosa* is easily recognisable by a blue/green colour change to the growth medium (Figure 8.1). *P. aeruginosa* produces pyocyanin in both YEPD and *Pseudomonas* Medium. The colour change was found to be most prominent after overnight growth, at 37$^{o}$C, at 210 rpm in *Pseudomonas* medium. Both *A. adeninivorans* and *S. cerevisiae* were found to grow well in both of these mediums under these conditions and both produced a pale yellow medium under the same growth conditions (Figure 8.1).

Mixed cultures were created by placing 1 x $10^{6}$ cells into the each indented flask with 25 mL of medium (Table 8.1). The indented flasks were then grown overnight at 210 rpm, at 37$^{o}$C. Blue/green colour changes are reported in Table 8.1.

There was no colour change when *P. aeruginosa* was grown in mixed culture. However cyclic voltammetry was performed and the presence of peaks at the correct positions (oxidation peak at approximately -0.18 V and reduction peak at approximately -0.25 V) indicated that pyocyanin is present in each solution (see Table 8.1).

**Figure 8.1: Pyocyanin production by *P. aeruginosa*.** The left culture is an overnight culture of *A. adeninivorans* and on the right *P. aeruginosa* both grown in *P. aeruginosa* specific medium at 37 $^{o}$C at 210 rpm. The blue/green colour is characteristic of pyocyanin.

**Table 8.1 Pyocyanin production of mixed culture growth**

| | **YEPD Colour change** | **YEPD CV Results** | ***Pseudomonas Media* Colour change** | ***Pseudomonas Media* CV Results** |
|---|---|---|---|---|
| ***P. aeruginosa*** | **Blue** | **Pyocyanin** | **Blue/green** | **Pyocyanin** |
| ***S. cerevisiae*** | **Pale Yellow** | **No Peak** | **Pale Yellow** | **No Peak** |
| ***A. adeninivorans*** | **Pale Yellow** | **No Peak** | **Pale Yellow** | **No Peak** |
| ***P. aeruginosa* + *S. cerevisiae*** | **Pale Yellow** | **Pyocyanin** | **Pale Yellow** | **Pyocyanin** |
| ***P. aeruginosa* + *A. adeninivorans*** | **Pale Yellow** | **Pyocyanin** | **Pale Yellow** | **Pyocyanin** |
| ***S. cerevisiae* + *A. adeninivorans*** | **Pale Yellow** | **No Peak** | **Pale Yellow** | **No Peak** |
| ***P. aeruginosa* + *S. cerevisiae* + *A. adeninivorans*** | **Pale Yellow** | **Pyocyanin** | **Pale Yellow** | **Pyocyanin** |

### 8.4.2. Electrochemical characterisation of pyocyanin

Cyclic voltammograms of pyocyanin, TMPD and PBS were conducted with the MFC (Figure 8.2) and the glassy carbon working electrodes (Figure 8.3) to ensure that these electrodes are capable of reacting with it. Both electrodes were found to react with the two mediators and produce reversible peaks. The peak separation for both mediators is greater when using the MFC electrode than when using the glassy carbon electrode, indicating that the reaction is not as efficient with this electrode.

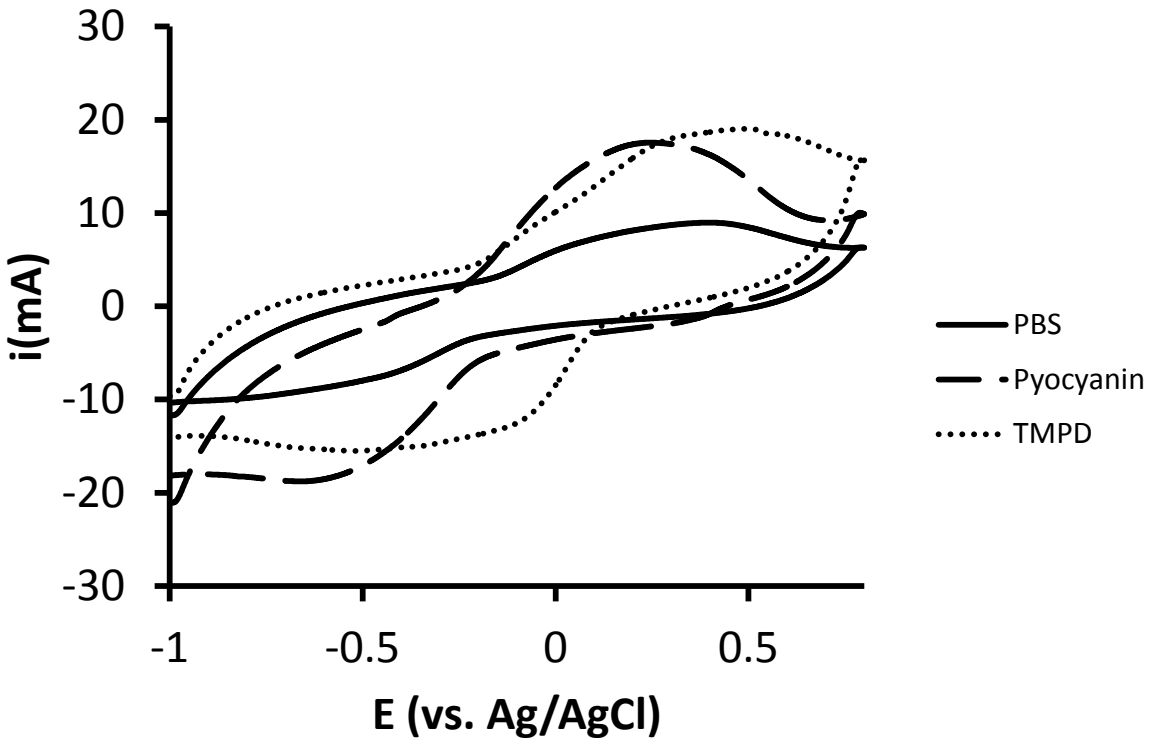


**Figure 8.2: Cyclic voltammograms of TMPD and pyocyanin in PBS using the MFC electrode**. Cyclic voltammetry was performed (from -1000 mV to + 800 mV vs. Ag/AgCl at 100 $mVs^{-1}$) using a 3 electrode set up: Working; Microbial fuel cell electrode, Reference; Ag/AgCl, Counter; Pt. Each line represents a mean of 3 CVs.

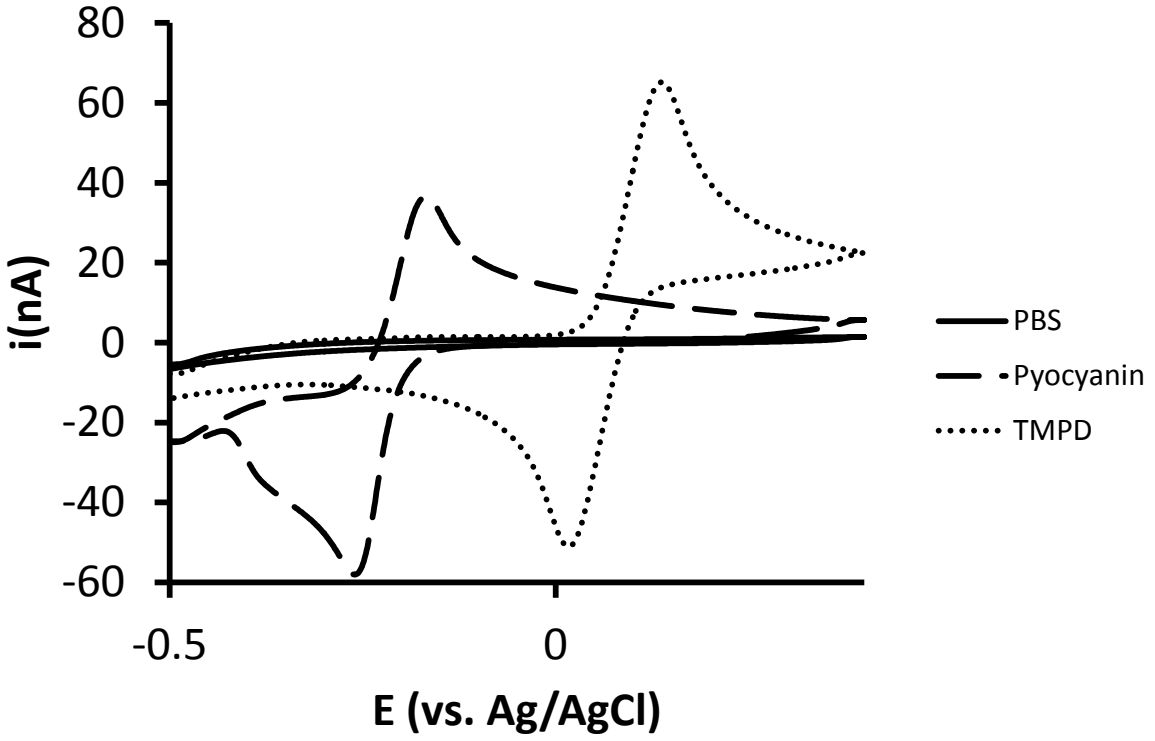


**Figure 8.3: Cyclic voltammogram of TMPD and pyocyanin dissolved in PBS using glassy carbon macro electrodes.** The concentration of mediators was 50 mM. Cyclic voltammetry was performed (from -500 mV to +400 mV vs. Ag/AgCl at 100 $mVs^{-1}$) using the following 3 electrode set up: Working; glassy carbon macro electrode, Reference; Ag/AgCl, Counter; Pt. Each line represents a mean of 3 CVs.

### 8.4.3. Establish pyocyanin production and concentration

Pyocyanin was produced by *P. aeruginosa* when it is grown in *Pseudomonas* media at 37$^{o}$C at 210 rpm (Table 8.1). This pyocyanin produced by *P. aeruginosa* is detectable by cyclic voltammetry with both the glassy carbon (Figure 8.4) and the MFC electrodes (Figure 8.5). This indicates that pyocyanin is being produced in adequate amounts to act as a mediator with this electrode material.

The exact concentration of the pyocyanin produced by *P. aeruginosa* in a 16 h cultivation at 37$^{o}$C was calculated by conducting a CV of the medium, then adding specific amounts of pyocyanin to the medium, measuring the peak height of the oxidation peak, creating a trend-

line and then extrapolating that line back to the x-axis, otherwise known as the method of additions (Figure 8.6). The calculated concentration was approximately 40 µM using this method, and this was checked by creating a concentration curve using the peak height of the oxidation peak and different concentrations of pyocyanin in a cellular *Pseudomonas* media (Figure 8.7). The trend line for the calibration curve and the sample were almost identical, and therefore, the concentration was determined to be approximately 40 µM.

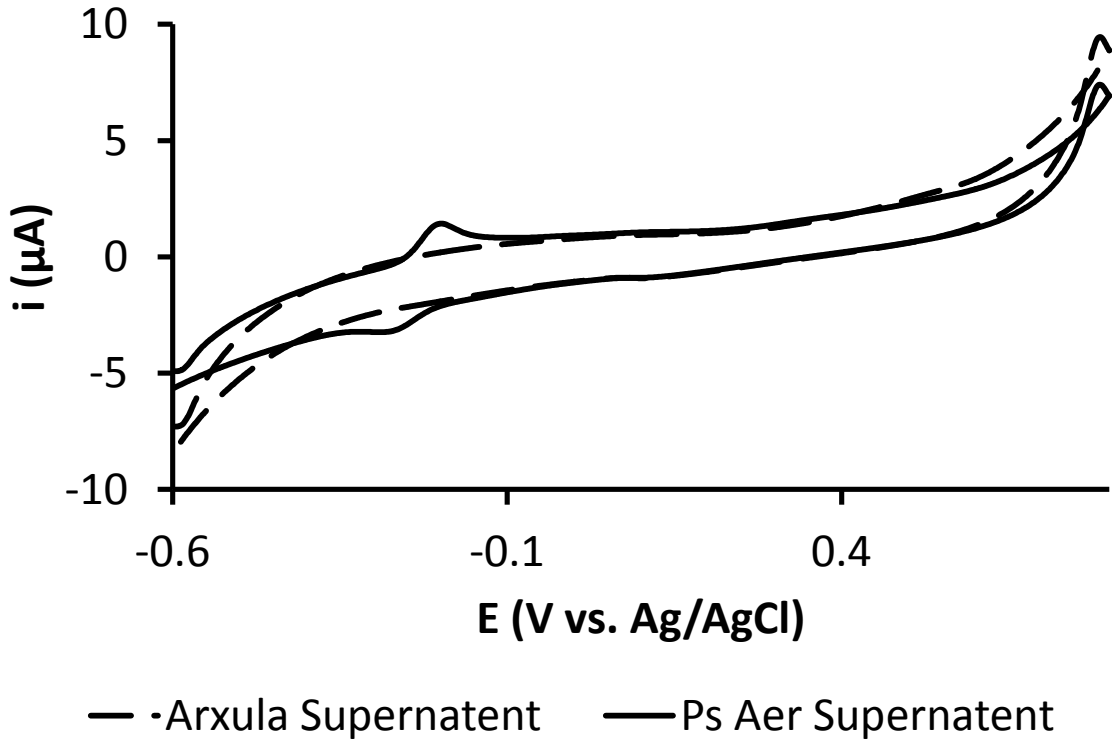


**Figure 8.4: Cyclic voltammogram of *A. adeninivorans* and *P. Aeruginosa* supernatant with glassy carbon electrode.** Cyclic voltammetry was performed (from -600 mV to +800 mV vs. Ag/AgCl at 100 $mVs^{-1}$) using the following 3 electrode set up: Working; glassy carbon macro electrode, Reference; Ag/AgCl, Counter; Pt. Each line represents a mean of 3 CV.

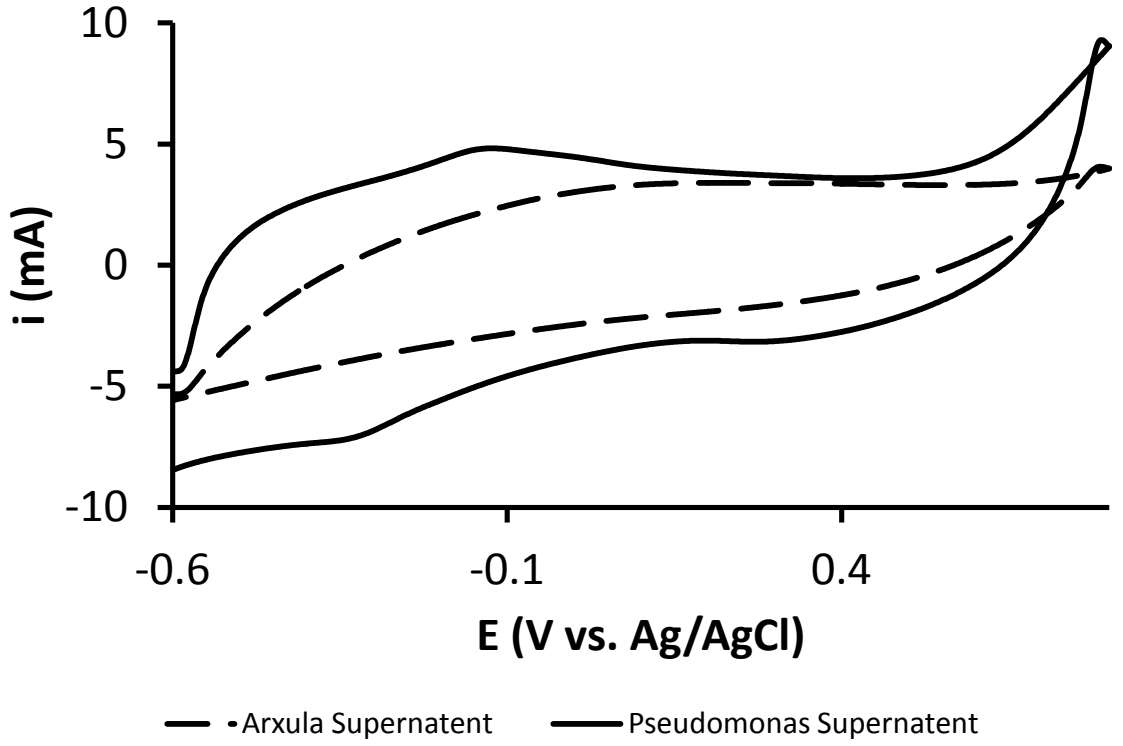


**Figure 8.5: Cyclic voltammogram of *A. adeninivorans* and *P. Aeruginosa* supernatant with MFC electrode.** Cyclic voltammetry was performed (from -600 mV to +800 mV vs. Ag/AgCl at 100 $mVs^{-1}$) using the following 3 electrode set up: Working; MFC electrode, Reference; Ag/AgCl, Counter; Pt. Each line represents a mean of 3 CV.

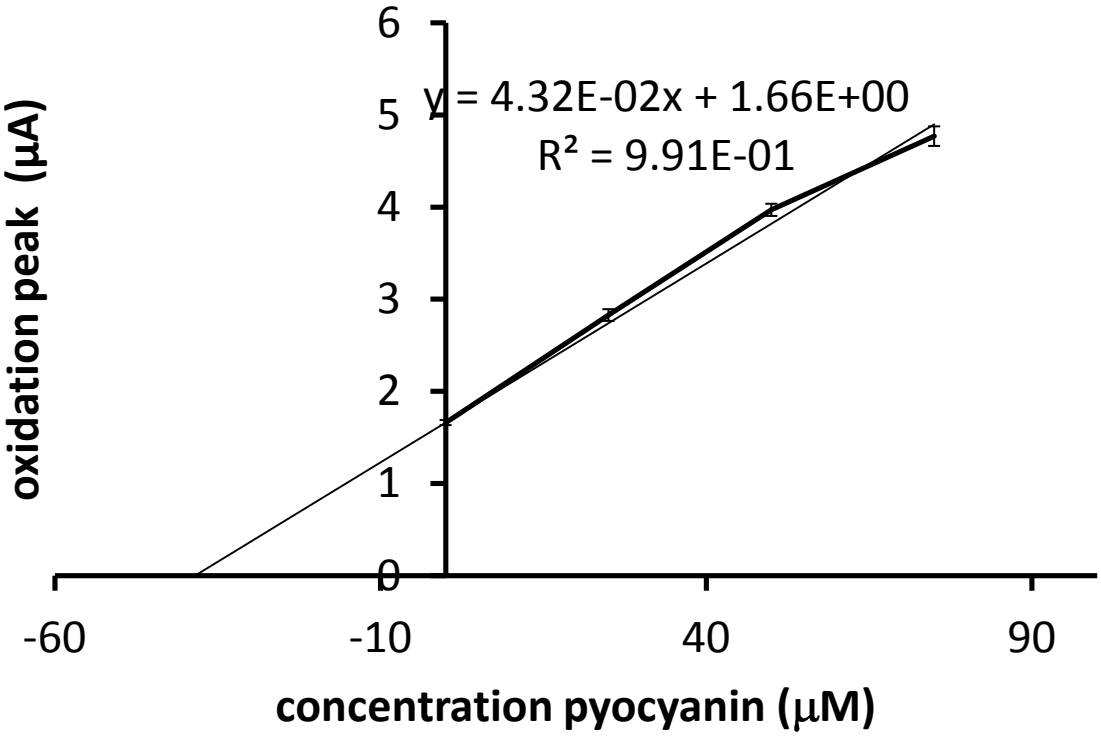


**Figure 8.6: Calibration graph of the Oxidation peak heights of supernatant, and supernatant with 25 µM, 50 µM and 75 µM pyocyanin additions.** A trend line was calculated and extrapolated in order to calculate the concentration of pyocyanin in the supernatant. The trend line cuts the x-axis at 38 µM. Each data point is the mean of 3 samples on which 3 cyclic voltammograms (from - 500 mV to + 0 mV vs. Ag/AgCl at 100 $mVs^{-1}$) were conducted on each of them (i.e. n=9)

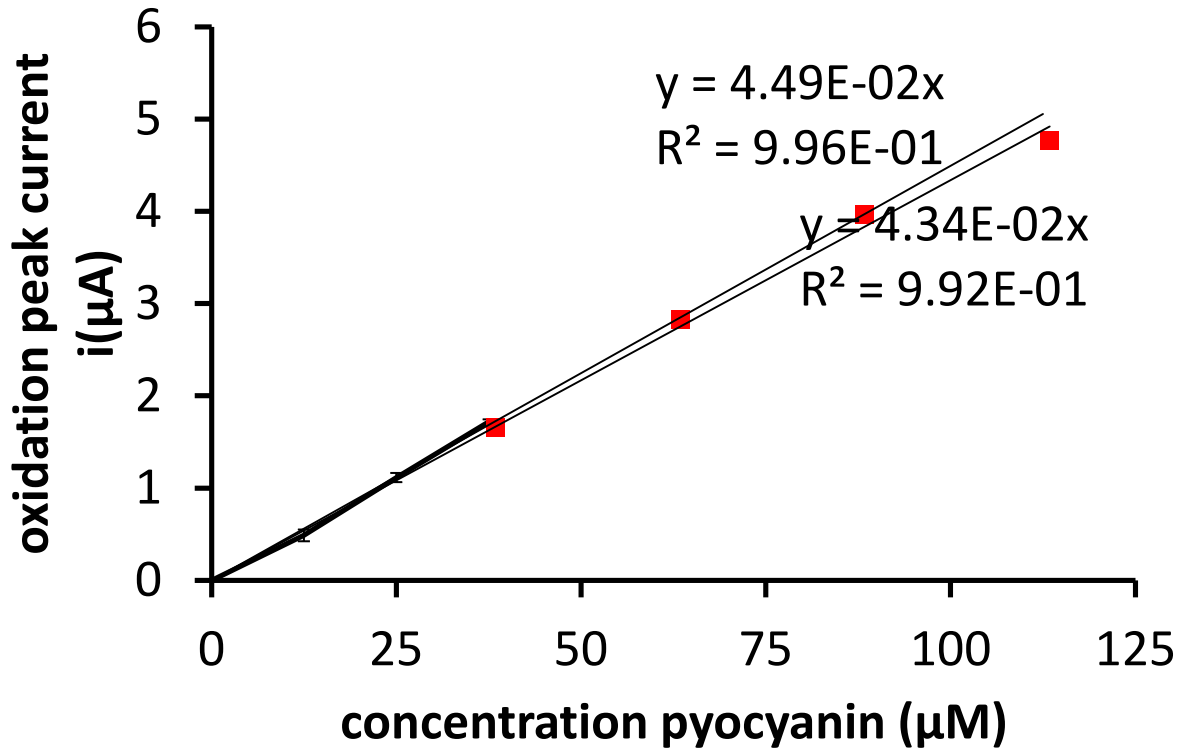


**Figure 8.7: Oxidation current peak heights of cyclic voltammograms of *P. aeruginosa* media, media + 12.5 µM, + 25 µM and + 37.5 µM pyocyanin.** A trend line was calculated and extrapolated in order to compare it to the trend line used to calculate concentration of pyocyanin in the supernatant represented by red squares (Figure 8.6). Each data point is the mean of 3 samples which have had 3 cyclic voltammograms (from -500 mV to 0 mV vs. Ag/AgCl at 100 $mVs^{-1}$) were conducted on each of them (i.e. n=9)

### 8.4.4. Mediated MFC using pyocyanin and *A. adeninivorans.*

The concentration of pyocyanin produced by *P. aeruginosa* in an overnight culture was found to be 40 µM. When 50 µM pyocyanin was added to MFC containing *A. adeninivorans* which demonstrated an increase in power density (Figure 8.8). The optimal concentration of pyocyanin to produce power density was found to be 2 mM (Figure 8.9). There is a great difference between the optimal concentration and that observed in an overnight concentration of growth. In order to meet this concentration demand, pyocyanin would have to be produced separately and concentrated before addition to the MFC with the substrate into the anode or *P. aeruginosa* could be genetically modified to produce more pyocyanin.

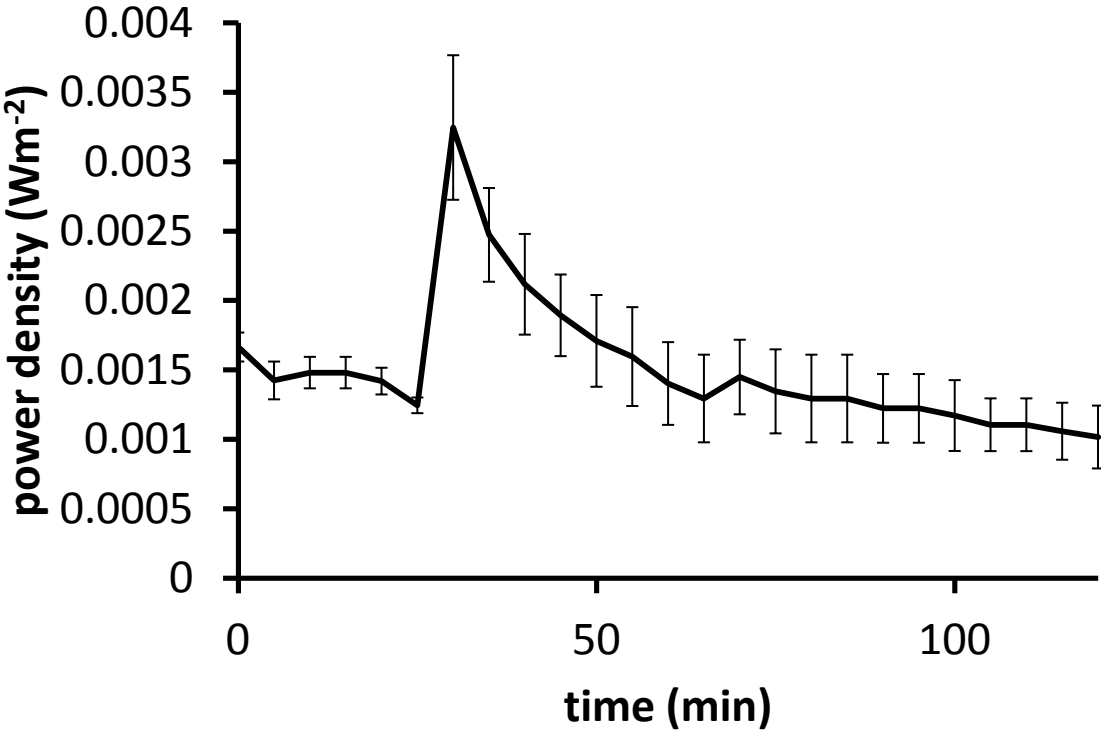


**Figure 8.8: Addition of 50 µM Pyocyanin to *A. adeninivorans* fuel cell.** Fuel cells contained 0.5 M $KMnO_4$ dissolved in PBS in the cathode and $OD_{600}$ 2.5 cells in the anode. Temperature kept constant (37$^{o}$C), cells kept suspended through constant agitation (180 rpm) and 50 µM pyocyanin added at 25 min. Error bars represent standard error (n=4).

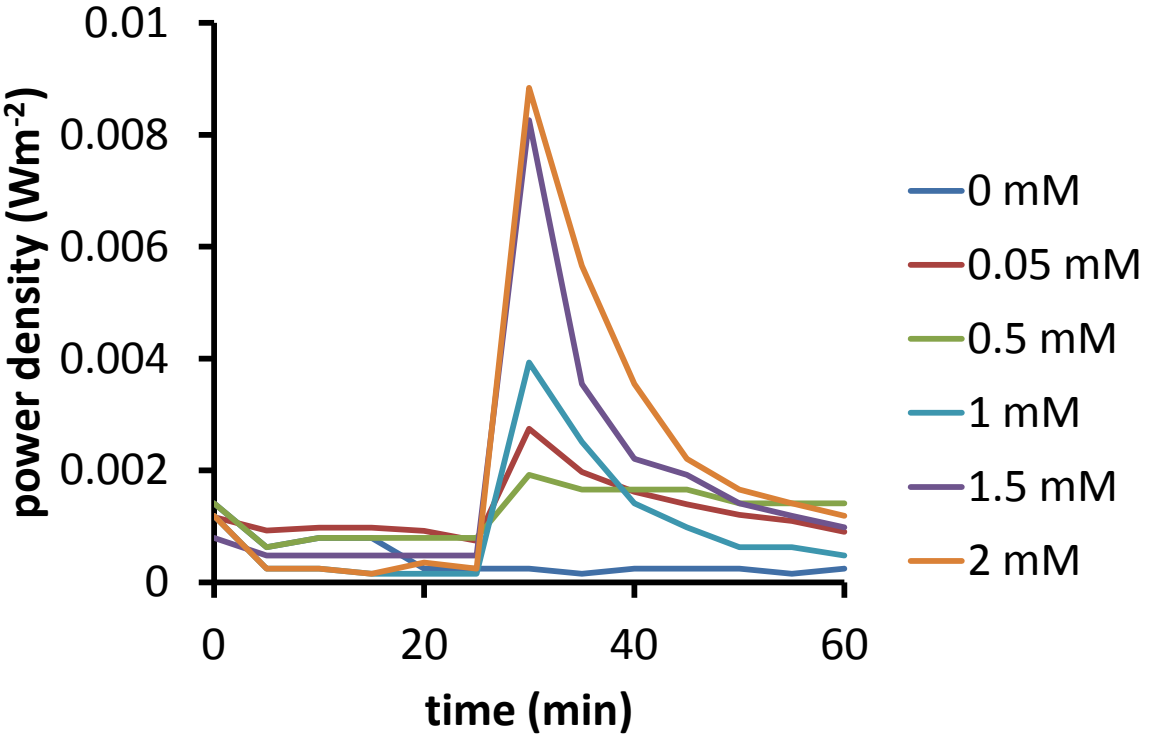


**Figure 8.9: Single addition of different pyocyanin concentrations to *A. adeninivorans* MFC.** Fuel cells contained 0.5 M $KMnO_4$ dissolved in PBS in the cathode and $OD_{600}$ 2.5 cells in the anode. Temperature kept constant (37$^{o}$C), cells kept suspended through constant agitation (180 rpm) and pyocyanin added at 25 min. Error bars represent standard error (n=4).

### 8.4.5. Pyocyanin reaction with NADH

Pyocyanin was reduced by *A. adeninivorans* after 3 h of incubation at 37$^{o}$C, 210 rpm (Figure 8.10). Because pyocyanin is still present, and is reduced this suggests that either pyocyanin cannot enter the cells or it is consumed by the cells.

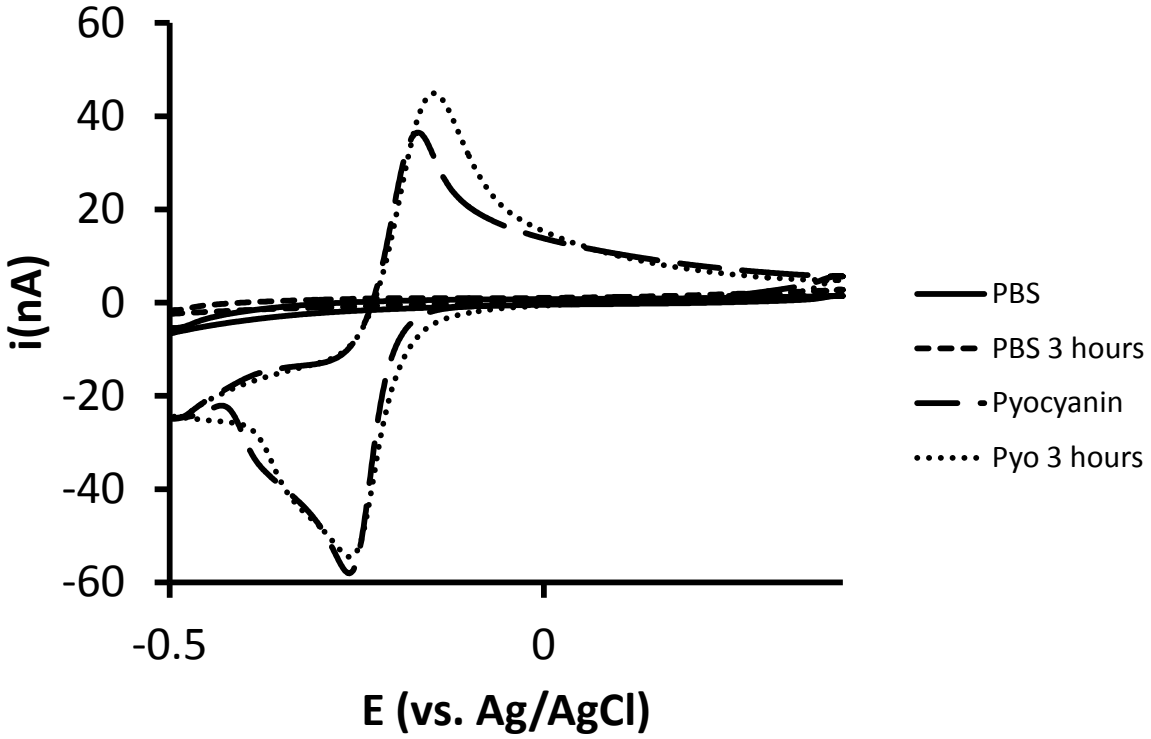


**Figure 8.10: Cellular reduction of pyocyanin.** Cyclic voltammograms were conducted in falcon tubes containing 1.5 mM pyocyanin in PBS, then 2.5 $OD_{600}$ *A. adeninivorans* was added and the flask was incubated for 3 h at 37$^{o}$C at 210 rpm. Cyclic voltammograms were then conducted again. Cyclic voltammograms were conducted from -0.5 to 0.4 V (vs. Ag/AgCl, with the following electrode set up: Glassy carbon (working), Platinum (counter/auxiliary) and Ag/AgCl (reference). Each line represents a mean of 3 CVs.

Falcon tubes containing TMPD, pyocyanin or PBS only were analysed with CV. Then NADH was added and the flasks an analysed again with CV after 1 h incubation at 37$^{o}$C, 210 rpm. The peak heights were then conducted and compared (Figure 8.11). TMPD and Pyocyanin were shown to both react with NADH becoming reduced (Figure 8.11).

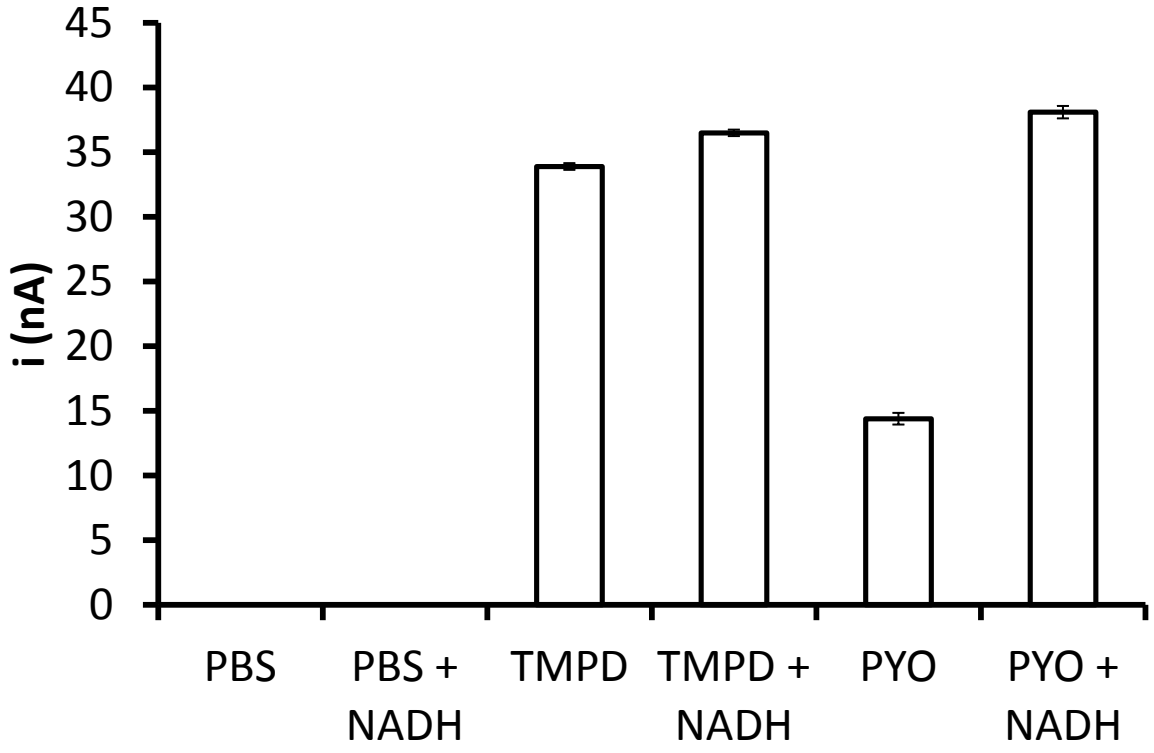


**Figure 8.11: Changes in oxidation peak height due to NADH addition.** Falcon tubes containing 0.1 mM TMPD, 0.1 mM pyocyanin or PBS only were analysed with cyclic voltammetry: -0.5 to +0.4 V (vs. Ag/AgCl, with the following electrode set up: Glassy carbon (working), Platinum (counter/auxiliary) and Ag/AgCl (reference). Then 0.1 mM NADH was added and the flasks and analysed again with cyclic voltammetry after 1 h incubation at 37$^{o}$C 210 rpm. The peak heights were then conducted and compared. Error bars represent standard error (n=4).

### 8.5. Discussion

Pyocyanin was found to be produced in concentrations high enough to change the colour of the solution only in pure cultures of *P. aeruginosa*. However, pyocyanin was still produced at electrochemically detectable concentrations in mixed cultures (Table 8.1). Electrochemical redox activity of pyocyanin was shown with both glassy carbon and MFC carbon cloth electrodes (Figures 8.2 & 8.3). The concentration of pyocyanin produced by an overnight culture was detectable with both glassy carbon and carbon cloth electrodes (Figure 8.4 & 8.5). Because different concentrations of pyocyanin can be detected using the MFC electrode and

pyocyanin can be produced and detected in a mixed culture it suggests that a mixed culture MFC using pyocyanin as a mediator and the current MFC set up is possible.

The exact concentration of pyocyanin produced in overnight cultures was calculated through the construction of a calibration curve and additions of pyocyanin to the overnight culture (Figures 8.6 & 8.7). That concentration was then used in a MFC containing *A. adeninivorans*, which demonstrated a small, short lived peak in power density with the addition of 50 μM pyocyanin (Figure 8.8).

The optimal concentration of pyocyanin in an *A. adeninivorans* MFC was found to be 1.5 mM (Figure 8.9). However, because the peak heights are short lived it appears that pyocyanin is not lipophilic like TMPD. The optimal concentration required to produce optimal power density in the MFC was found to be far greater than that produced by *P. aeruginosa* cell cultures. One possible solution to this is to separately grow the *P. aeruginosa* cells up and then concentrate the pyocyanin before using it in the MFC. Another possibility is to investigate other electrode materials which are more electrochemically active, which will enable a lower concentration of mediator to be used.

In order to determine if pyocyanin is lipophilic CV of *A. adeninivorans* solutions containing pyocyanin were compared before and after 3 h of incubation at 37$^{o}$C, 210 rpm (Figure 8.10). This suggests that pyocyanin is capable of acting as a hydrophilic mediator and not capable of acting as a lipophilic mediator in the same way as TMPD. To test if both mediators can be reduced by NADH cyclic voltammograms of each mediator were compared before and after incubation for 1 h with NADH (Figure 8.11). Pyocyanin was shown to be reduced by NADH. Both Figures 8.10 and 8.11 strongly suggest that pyocyanin is hydrophilic in nature and because it cannot behave as a lipophilic mediator it is suitable for use as a mediator with eukaryotes in a MFC.

## 8.6. Conclusion

Pyocyanin is not as effective as TMPD at mediating *A. adeninivorans* and producing current densities. The results suggest that the reason for this is because pyocyanin cannot behave as a lipophilic mediator, which is consistent with product information provided by the company (Pyocyanin 2007). Therefore, pyocyanin is not suitable for use with eukaryotes that require lipophilic mediators, such as *A. adeninivorans*.

# Chapter 9: Ferri-reductase overexpression in *A. adeninivorans* affect on mediator-less electron transfer

## 9.1. Abstract

*A. adeninivorans* was transformed with a plasmid containing the AFRE2 gene. Several transformant cell lines were investigated for increase reduction and power density. The transformants of *A. adeninivorans* demonstrated an increased rate of ferricyanide reduction but not an increase in mediator-less power density.

## 9.2. Introduction

In chapter 3 the production of mediator-less MFC using *A. adeninivorans* and *S. cerevisiae* was investigated. A peak was produced by *A. adeninivorans* at approximately +0.4 volts on an adsorption CV and that was attributed to an increase in mediator-less power density of *A. adeninivorans* over *S. cerevisiae*. In this chapter *A. adeninivorans* that have been genetically modified through transformation with a plasmid containing AFRE2 were investigated to determine if this iron reductase encoding gene is responsible for the observed mediator-less power density. This is the first time to this authors knowledge that an amplification of a gene has been attempted for a MFC application. Previous genetic manipulations in a MFC have been knockout mutations (Rabaey *et al.* 2005).

## 9.3. Materials and methods

### 9.3.1. Strains

The *Arxula adeninivorans* strains AYNI1 – 1, 3, 7, 14, 18 (G1212/YRC102-AYNI1-AFRE2) and TEF1 – 1, 8, 18 (G1212/YRC102-TEF1-AFRE2) were obtained from the yeast collection of the “Institut für Pflanzengenetik und Kulturpflanzenforschung” (IPK) Gatersleben, Germany. All strains were transformants containing the AFRE2 gene, the AYNI1 strains use a nitrite-reductase gene promoter and the TEF1 strains use a TEF1 promoter.

## 9.4. Results

### 9.4.1. Comparison between Transformant and wild type in MFC

All of the transformants, *A. adeninivorans* LS3 and *S. cerevisiae* were all tested without mediator in the MFC (Figure 9.1). None of the transformants was found to increase the power density over that of LS3.

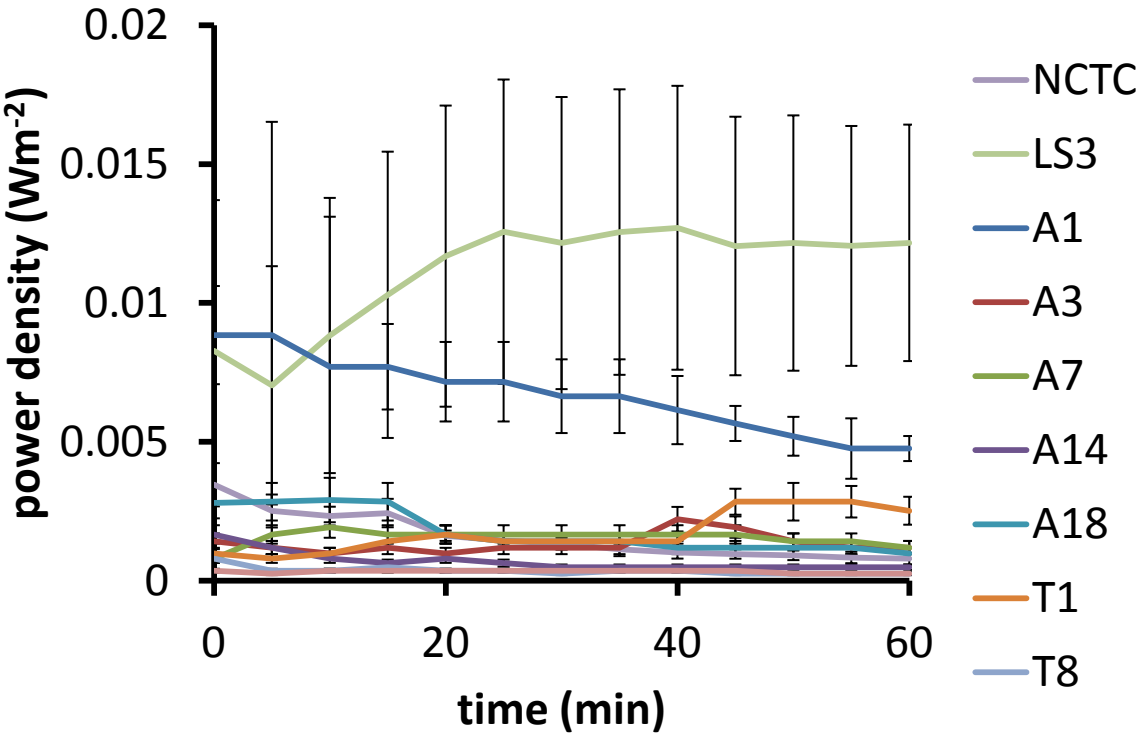


**Figure 9.1: Transformants in mediator-less MFC.** MFC contained 0.5 M $KMnO_4$ in PBS in the cathode and cells of *A. adeninivorans*, *A. adeninivorans* transformants or *S. cerevisiae* suspended in PBS at $OD_{600}$ 2.5. Temperature was 37°C and cells were suspended 180 rpm. Error bars represent standard error (n=4).

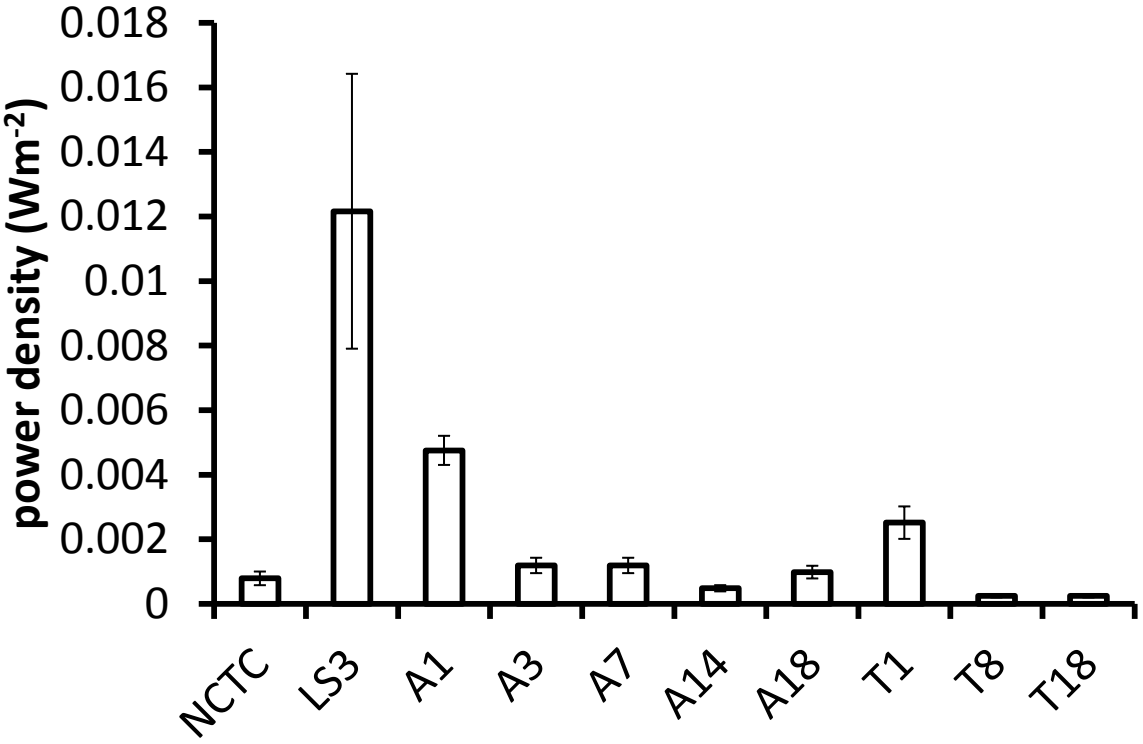


**Figure 9.2: Transformants in mediator-less MFC at 60 mins.** MFC contained 0.5 M $KMnO_4$ in PBS in the cathode and $OD_{600}$ 2.5 of *A. adeninivorans*, *A. adeninivorans* transformants or *S. cerevisiae* suspended in PBS. As Figure 9.1 above the temperature is kept constant ($37^oC$) and cells kept suspended (180 rpm). Error bars represent standard error (n=4). Note: NCTC – *S. cerevisiae*

### 9.4.2. Comparison between Transformant and wild type with CV (Adsorption)

Adsorption CVs were conducted for each of the transformants (Figure 9.3 - 9.12) and it was found that compared to the wild type LS3 control, the transformants produced a larger oxidation peak at +0.4 V and a new previously unidentified reduction peak at +0.1 V.

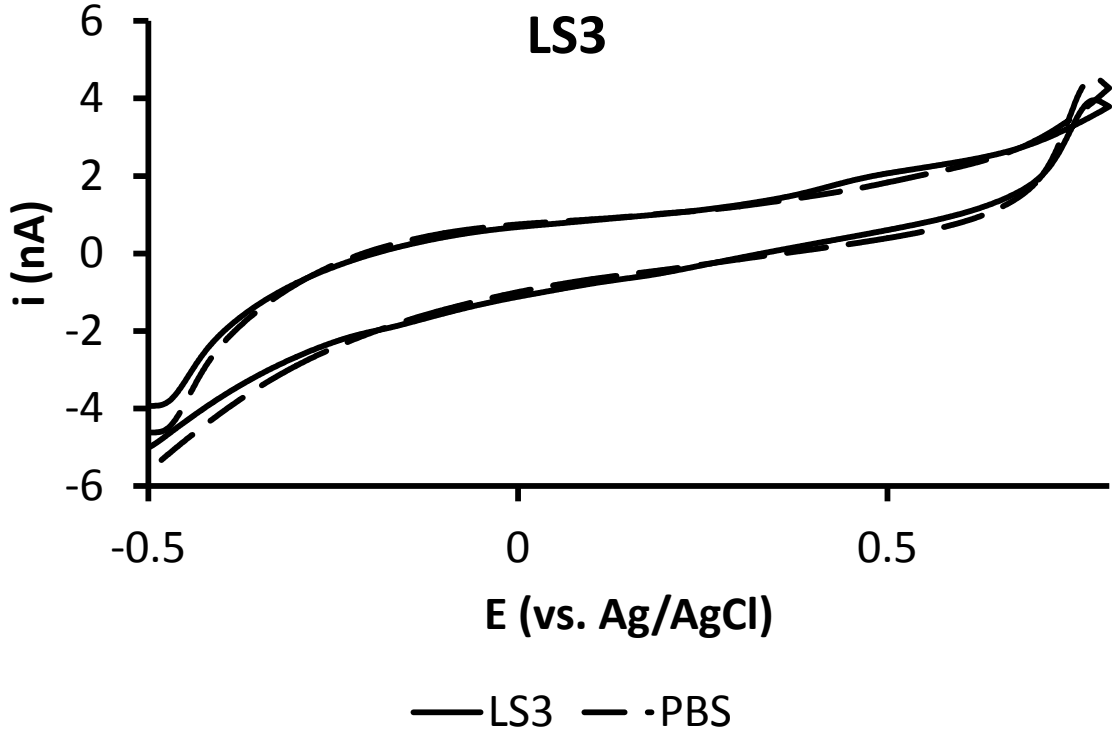


**Figure 9.3: Adsorption CV of highly concentrated *A. adeninivorans* LS3 cells onto an inverted glassy carbon electrode.** Cyclic voltammetry was performed (from -500 mV to + 800 mV vs. Ag/AgCl at 100 $mVs^{-1}$) using the following 3 electrode set up: Working; glassy carbon macro-electrode, Reference; Ag/AgCl, Counter; Pt. All scans are a mean of 3.

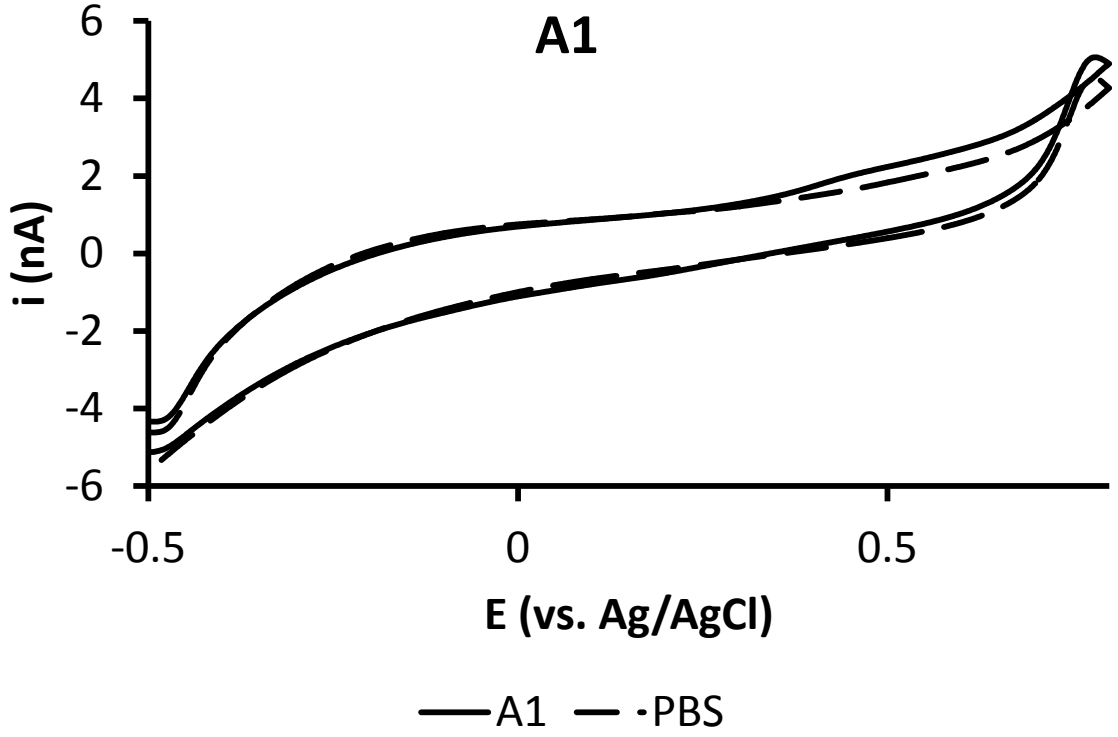


**Figure 9.4: Adsorption CV of highly concentrated *A. adeninivorans* A1 cells onto an inverted glassy carbon electrode.** Cyclic voltammetry was performed (from -500 mV to + 800 mV vs. Ag/AgCl at 100 $mVs^{-1}$) using the following 3 electrode set up: Working; glassy carbon macro-electrode, Reference; Ag/AgCl, Counter; Pt. All CV are a mean of 3.

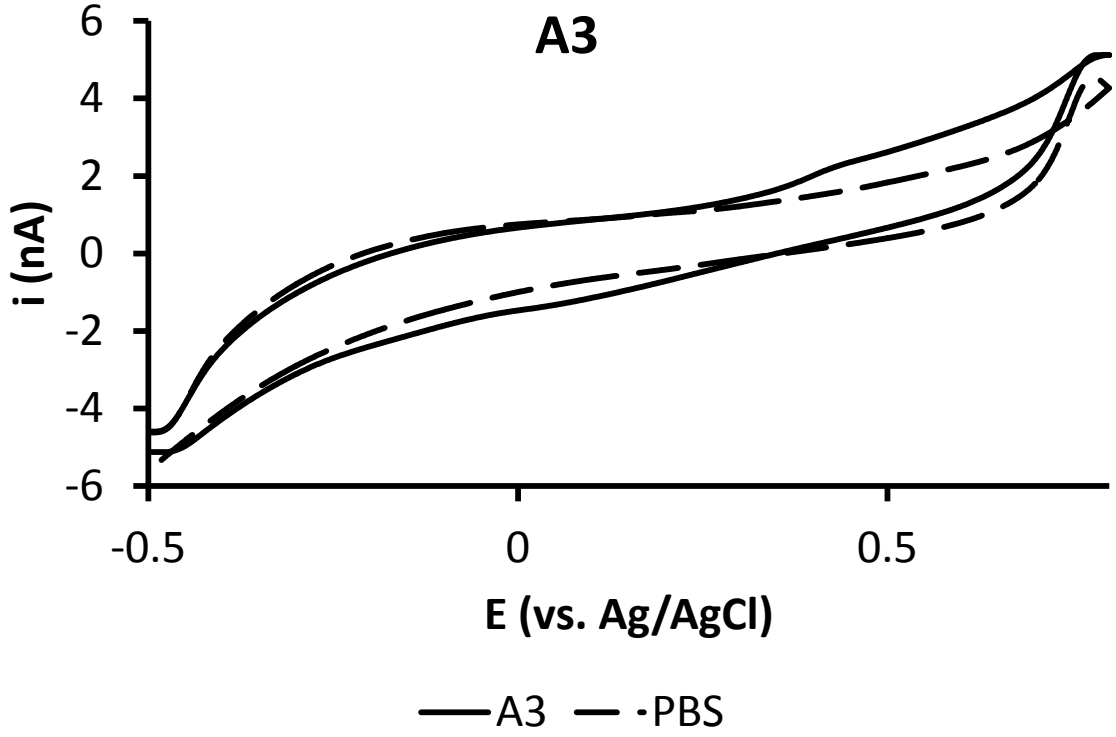


**Figure 9.5: Adsorption CV of highly concentrated *A. adeninivorans* A3 cells onto an inverted glassy carbon electrode.** Cyclic voltammetry was performed (from -500 mV to + 800 mV vs. Ag/AgCl at 100 $mVs^{-1}$) using the following 3 electrode set up: Working; glassy carbon macro-electrode, Reference; Ag/AgCl, Counter; Pt. All CV are a mean of 3.

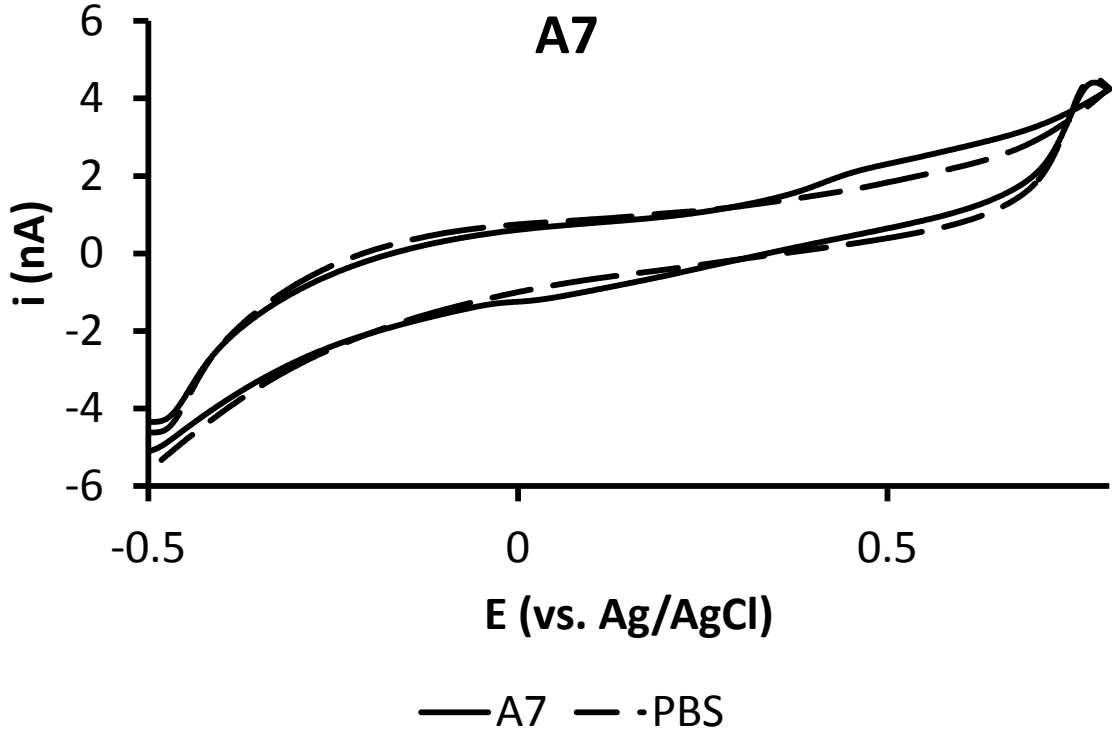


**Figure 9.6: Adsorption CV of highly concentrated *A. adeninivorans* A7 cells onto an inverted glassy carbon electrode.** Cyclic voltammetry was performed (from -500 mV to + 800 mV vs. Ag/AgCl at 100 $mVs^{-1}$) using the following 3 electrode set up: Working; glassy carbon macro-electrode, Reference; Ag/AgCl, Counter; Pt. All CV are a mean of 3.

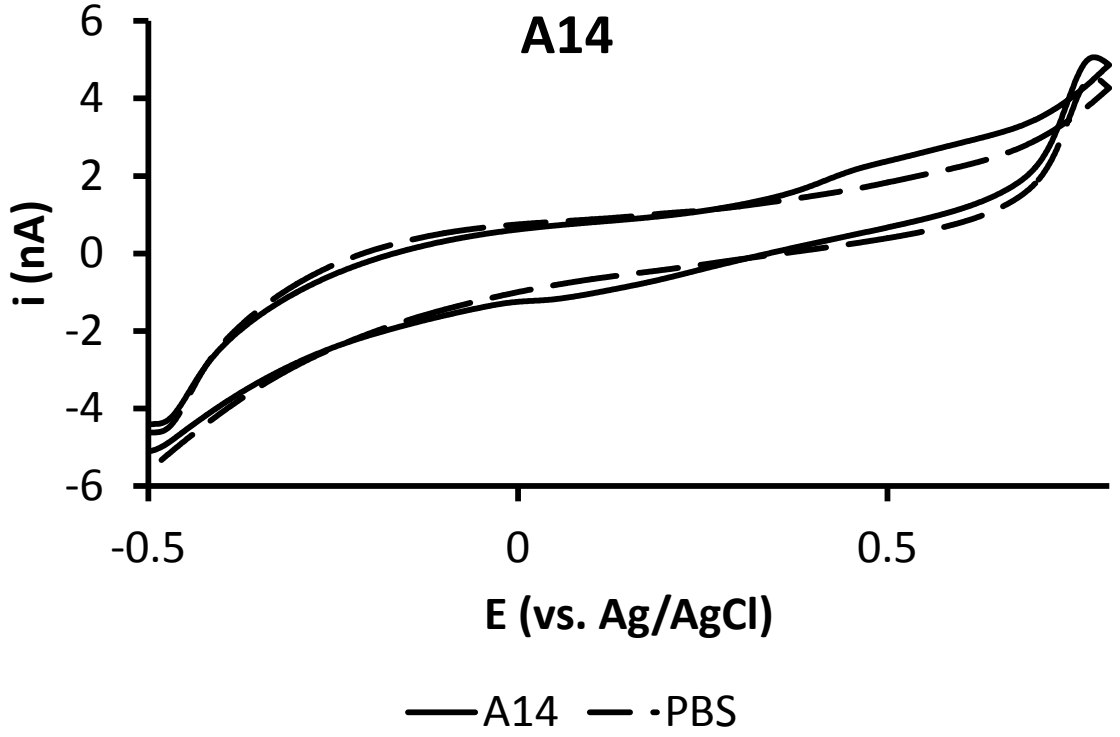


**Figure 9.7: Adsorption CV of highly concentrated *A. adeninivorans* A14 cells onto an inverted glassy carbon electrode.** Cyclic voltammetry was performed (from -500 mV to + 800 mV vs. Ag/AgCl at 100 $mVs^{-1}$) using the following 3 electrode set up: Working; glassy carbon macro-electrode, Reference; Ag/AgCl, Counter; Pt. All CV are a mean of 3.

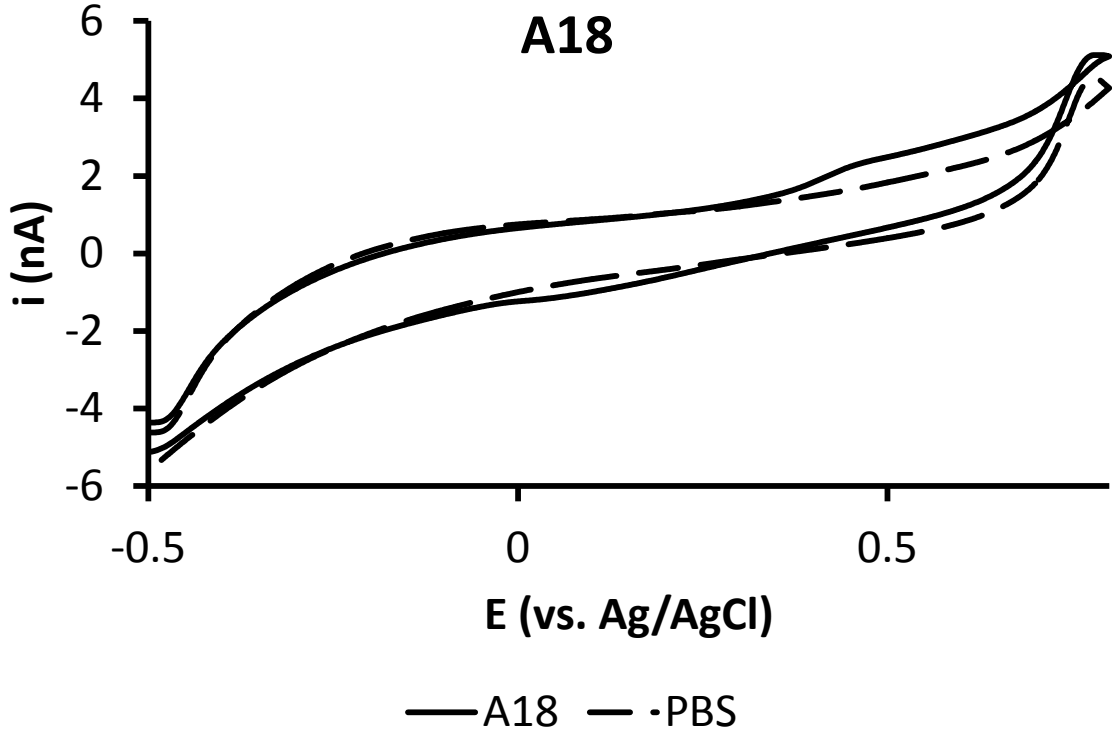


**Figure 9.8: Adsorption CV of highly concentrated *A. adeninivorans* A18 cells onto an inverted glassy carbon electrode.** Cyclic voltammetry was performed (from -500 mV to + 800 mV vs. Ag/AgCl at 100 $mVs^{-1}$) using the following 3 electrode set up: Working; glassy carbon macro-electrode, Reference; Ag/AgCl, Counter; Pt. All CV are a mean of 3.

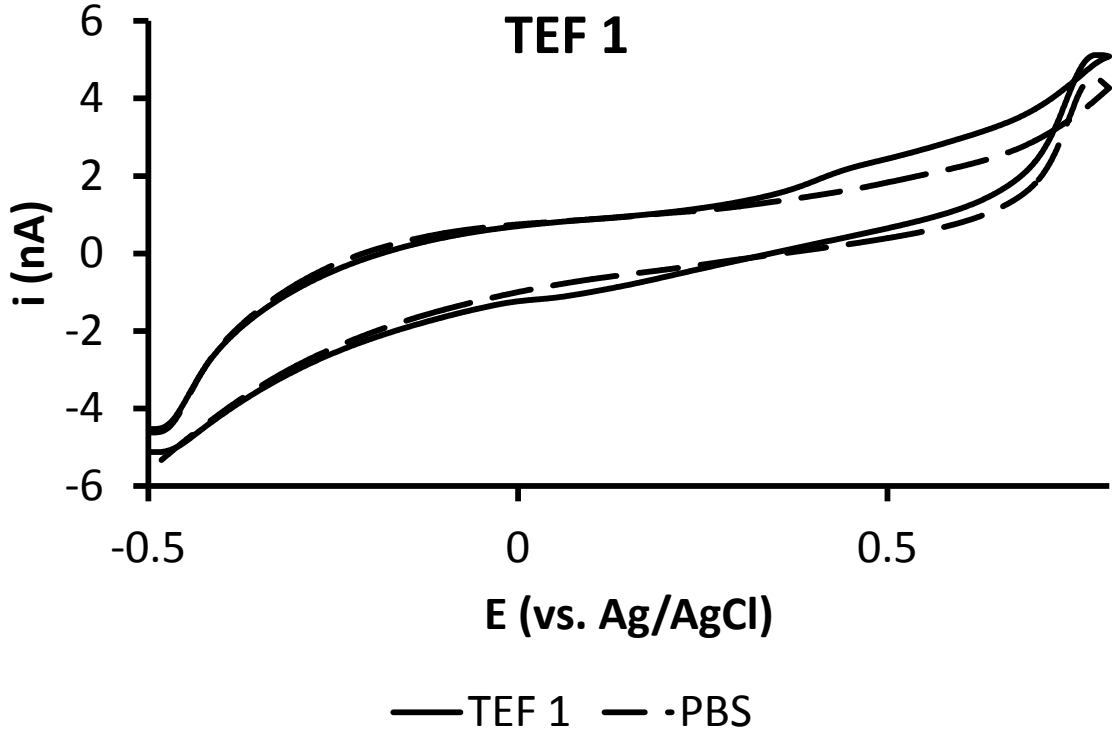


**Figure 9.9: Adsorption CV of highly concentrated *A. adeninivorans* TEF1 cells onto an inverted glassy carbon electrode.** Cyclic voltammetry was performed (from -500 mV to + 800 mV vs. Ag/AgCl at 100 $mVs^{-1}$) using the following 3 electrode set up: Working; glassy carbon macro-electrode, Reference; Ag/AgCl, Counter; Pt. All CV are a mean of 3.

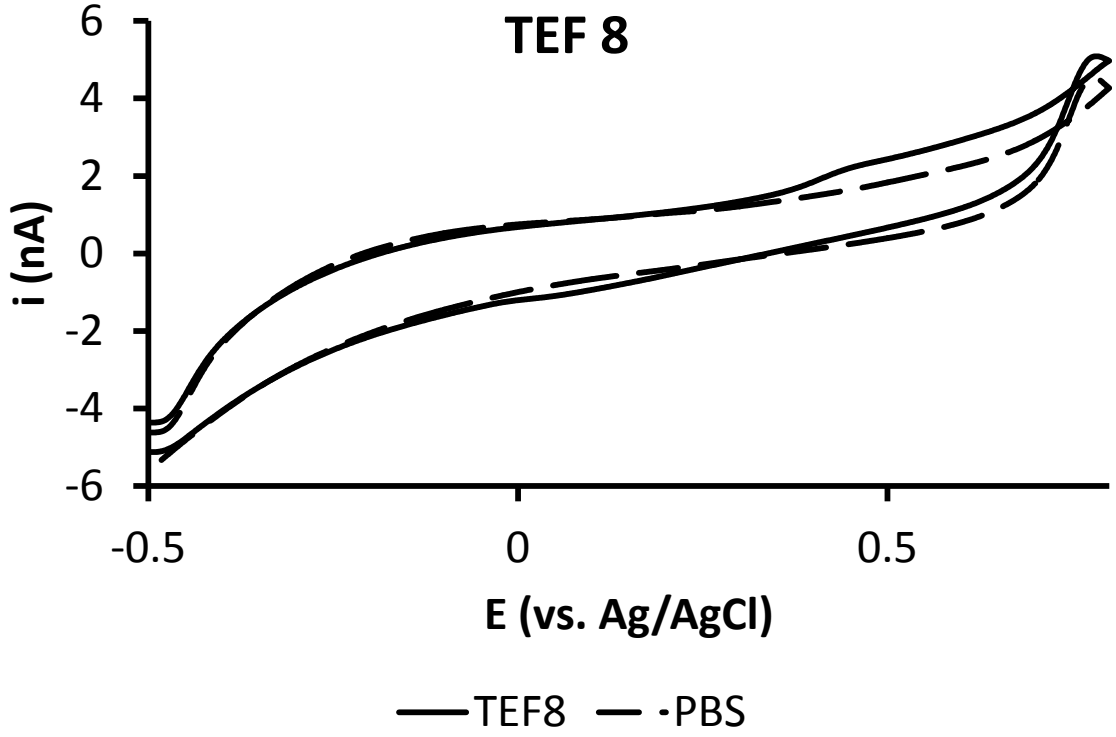


**Figure 9.10: Adsorption CV of highly concentrated *A. adeninivorans* TEF8 cells onto an inverted glassy carbon electrode.** Cyclic voltammetry was performed (from -500 mV to + 800 mV vs. Ag/AgCl at 100 $mVs^{-1}$) using the following 3 electrode set up: Working; glassy carbon macro-electrode, Reference; Ag/AgCl, Counter; Pt. All CV are a mean of 3.

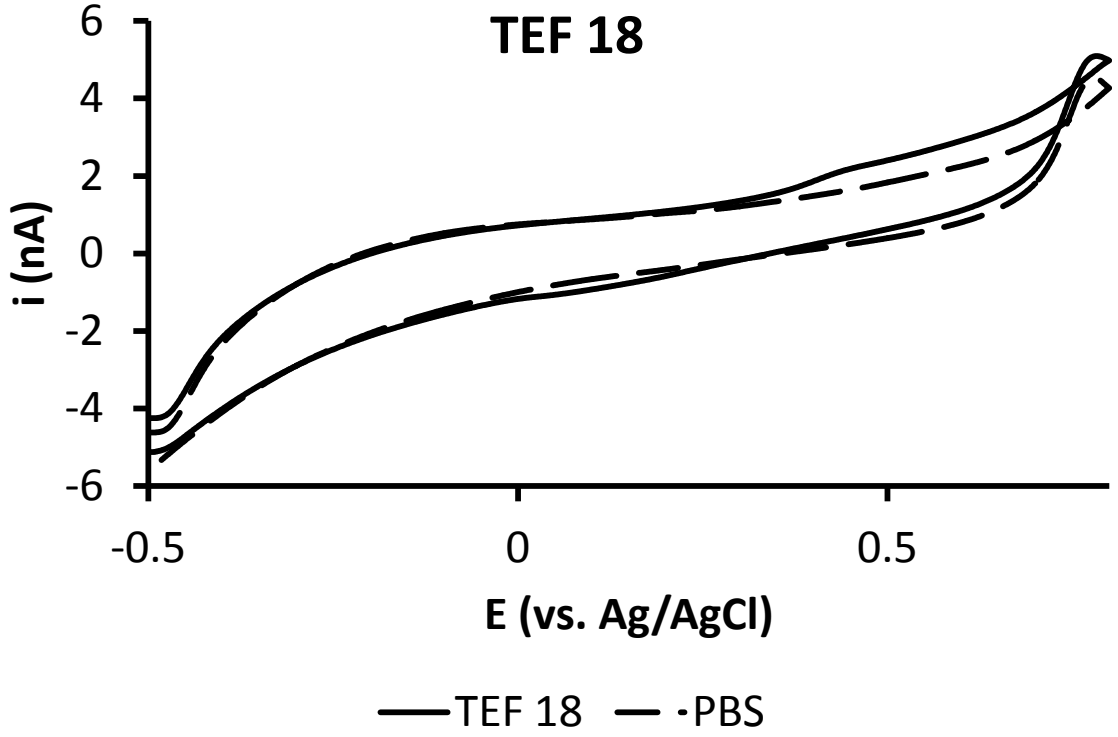


**Figure 9.11: Adsorption CV of highly concentrated *A. adeninivorans* T18 cells onto an inverted glassy carbon electrode.** Cyclic voltammetry was performed (from -500 mV to + 800 mV vs. Ag/AgCl at 100 $mVs^{-1}$) using the following 3 electrode set up: Working; glassy carbon macro-electrode, Reference; Ag/AgCl, Counter; Pt. All CV are a mean of 3.

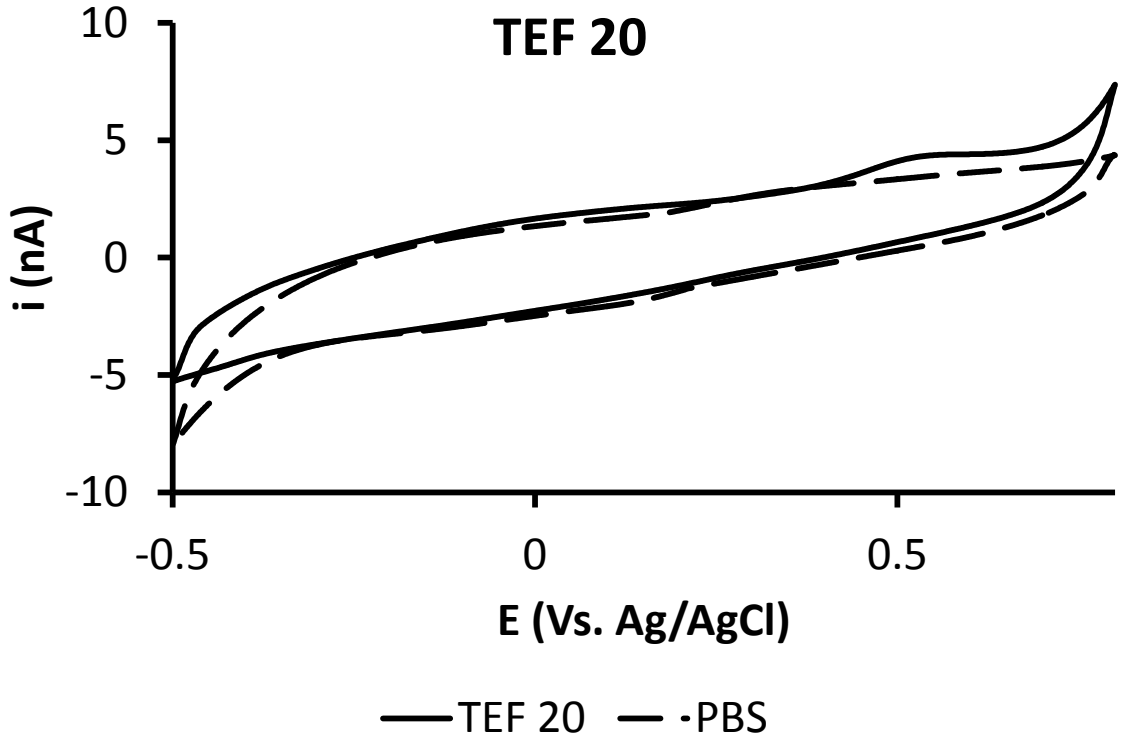


**Figure 9.12: Adsorption CV of highly concentrated *A. adeninivorans* T18 cells onto an inverted glassy carbon electrode.** Cyclic voltammetry was performed (from -500 mV to + 800 mV vs. Ag/AgCl at 100 $mVs^{-1}$) using the following 3 electrode set up: Working; glassy carbon macro-electrode, Reference; Ag/AgCl, Counter; Pt. All CV are a mean of 3.

### 9.4.3. Ferricyanide reduction of transformants

The rate of ferricyanide reduction between the transformants, the wild type and *S. cerevisiae* were compared in the same method used in section 4.4.1 (Figure 9.13). All of the transformants were capable of reducing ferricyanide at a greater rate than the wild type (ANOVA p=0.05).

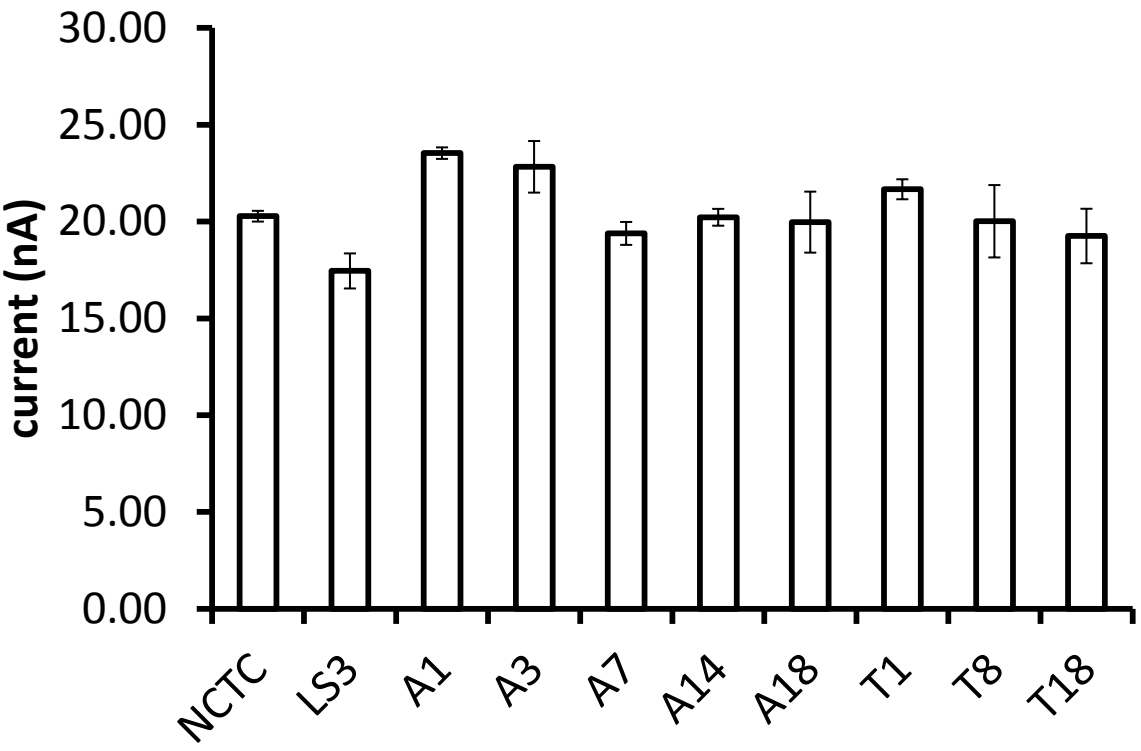


**Figure 9.13: Transformant rate of ferricyanide reduction.** $OD_{600}$ 2.5 of cells suspended in PBS, 2 mM ferricyanide and 10 mM glucose were incubated in falcon tubes at 37$^{o}$C and sparged with nitrogen. Linear sweep voltammetry was performed (from +425 mV to + 0 mV vs. Ag/AgCl, 10 $mVs^{-1}$) using the following 3 electrode set up: Working; Pt microelectrode, Reference; Ag/AgCl, Counter; Pt. Error bars represent standard error (n=3). Note: NTCC – *S. cerevisiae.*

### 9.5. Discussion

Transformants of *A. adeninivorans* demonstrated an increased rate of ferricyanide reduction (Figure 9.13) but not an increase in mediator-less power density over LS3 (Figure 9.1). As demonstrated in Chapter 4 the reduction of ferricyanide requires a lower reaction potential than the soluble mediator secreted by *A. adeninivorans.* This indicates that the plasmid insertion into the *LS3* resulted in a reductive change that is unrelated to the soluble mediator which was attributed to the mediator-less power density.

The inability of *A. adeninivorans* transformed with a plasmid containing the AFRE2 gene to produce greater mediator-less power density, suggests that this gene is not responsible for the mediator-less power density. However, the introduction does appear to increase the size of this +0.4 V peak (Figure 8.2 – 8.12) but creates a previously unobserved reduction peak at +0.1 V. This new peak should be investigated in order to ascertain the characteristics of the electro-active molecule. An attempt should also be made to isolate the electro-active molecule responsible for the +0.4 V peak and study it's characteristics.

The AFRE2 or another gene on the plasmid is responsible for the +0.1 V reduction peak which has not been previously reported. The +0.4 V oxidation peak may or may not be the result of a completely different gene, and only further investigation will be able to confirm this.

Future work should concentrate on more stable transformants which have been recently constructed (Gotthard Kunze personal communication). The investigations conducted using those transformants should be conducted comparing the responses of the transformants in the presence and absence of nitrite to determine the difference that occurs when the AFRE2 gene is turned on. A control should also be run with the wild type to establish any effect due to nitrite presence.

### 9.6. Conclusion

Transformants of *A. adeninivorans* demonstrated an increased rate of ferricyanide reduction but not an increase in mediator-less power density. This is likely due to side effects from the introduction of the plasmid into LS3, which has also resulted in a previously unidentified reduction peak at +0.1 V.

# Chapter 10: General Discussion

## 10.1. Chapter Summaries

In chapter 3, a two chambered MFC was investigated using *A. adeninivorans* as the anode biological catalyst and $KMnO_4$ as the cathode reagent (electron acceptor). Power density was monitored from both mediator-less and mediated mechanisms, with an increase in power density and a decrease in internal resistance attributed to the introduction of the mediator TMPD. The optimal concentration of TMPD and the optimal external load were determined to obtain maximum power density.

In chapter 4, the mediator-less MFC was investigated in order to understand the mechanism behind yeast electron transfer. Mediator-less MFC containing *A. adeninivorans* created significantly greater power density to those containing *S. cerevisiae*. However, when ferricyanide was used as a reporter molecule both *A. adeninivorans* and *S. cerevisiae* showed similar rates of ferricyanide reduction. A solution species secreted by *A. adeninivorans* which can transfer electrons to an MFC anode through the action of the $KMnO_4$ cathode reagent was deduced to be responsible for this behaviour.

In chapter 5, the mediated MFC was investigated in order to understand the mechanism of TMPD interactions with *A. adeninivorans* and the anode. TMPD was equally effective with *A. adeninivorans* and *S. cerevisiae*, and the rate of ferricyanide reduction was approximately 40 fold with TMPD present, which is approximately the same amount the TMPD increased the power density in a MFC. TMPD was unstable and not sequestered by the cells. When used with ferricyanide in a MFC, the two mediators initially competed with each other for electrons, causing an initial drop in power density. However, once the competition for electrons was over, the power density returned to its previous level. If the drop in power density was only over a short period of time (within 30 seconds), then it could be attributed to

addition of the mediator bringing about a change to the double-layer at the electrode surface and the system re-adjusting to this change. However, as this power density decline takes nearly 20 mins to correct, it is likely that there are other factors that also contribute. Using the tug-of-war analogy, the addition of TMPD was found to pull against the cathode reaction when the MFC was operated under an external load making the observed potential of both the anode and the cathode more negative i.e. compare Figure 4.12 with 5.11. Electrochemically, it can be viewed that the addition of TMPD provided a greater supply of electrons converting the anode to a non-polarisable electrode (Pasco N, personal communication 2012) i.e. an electrode whose potential does not change. However, because the potential of both of the anode and the cathode change the terms 'polarisable' and 'non-polarisable' should be used with caution.

In Chapter 6, an osmium polymer was used as a replacement for ferricyanide in a double mediated single celled poised potential MFC. The osmium polymer was found to be able to replace the low concentrations of ferricyanide acting as a hydrophilic mediator in a double mediator system. The osmium polymer was shown to have the secondary property of assisting with immobilisation of the microorganisms to the electrode.

In chapter 7, a wide variety of growth conditions and MFC configurations were investigated. *A. adeninivorans* was shown to be capable of growing and producing power with a wide range of carbon sources. Growth conditions such as carbon source, temperature, anaerobic growth, and growth phase were investigated. Different MFC configurations were shown to affect the MFC in different ways. Doubling the anode required a modification of the power density equation, and while an increase in power was observed, the power density for these configurations was ultimately lower. Doubling the surface area of the PEM increased the internal resistance in one configuration, but not in another.

In chapter 8, the properties of pyocyanin produced by *Pseudomonas aeruginosa* were investigated as a mediator in a MFC. Pyocyanin was produced by *P. aeruginosa* under a variety of growth conditions, but not in the presence of either *S. cerevisiae* or *A. adeninivorans*. The optimal concentration of pyocyanin produced by *P. aeruginosa* to be functional in a MFC was calculated. The increase in power density was very small in all cases and therefore, further investigation into this line of inquiry was not pursued.

In chapter 9, *A. adeninivorans* transformants containing the AFRE 2 gene were investigated in mediator-less MFC. The transformants did not produce a higher power density than the LS3 wild-type, but differences in ferricyanide reduction were observed with additional peaks recorded on the adsorption CV.

### 10.2. Chemical forces affecting power density

The use of potassium permanganate as the cathode reactant has been used effectively in short run MFCs to study the fundamental mechanisms associated with mediator-less and mediated MFCs. By using potassium permanganate and comparing the results to ferricyanide in the cathode with and without an external load, a new behaviour was identified. With a low external load, both potassium permanganate and ferricyanide increased the potential of the anode depending on the anode contents and the addition of mediators to the anode decreased the potential of both the anode and cathode.

It is well established that the MFCs are not able to reach the maximum power output because of the surface area of the anode in addition to inefficiencies such as the internal resistance and over-potentials (Rabaey 2008; Logan 2009; Logan 2008). In chapter 4, the change in power density observed when the catholyte was switched from ferricyanide to potassium permanganate was different for the mediator-less power densities of *A. adeninivorans* compared to *S. cerevisiae*. The potential of the anode had become positive enough to allow

for a previously unobserved solution species secreted by *A. adeninivorans* to contribute to the power density of the MFC. The solution species secreted by *A. adeninivorans* has a reduction potential greater than that of ferricyanide and as a result is not able to provide electrons to a MFC containing ferricyanide as the catholyte. However, potassium permanganate is able to be accessed, since it has  more positive reaction potential and pull which raises the potential of the anode above the external load (Figure 10.1).

In chapter 5, it was demonstrated that the mediator in the anode pulled against the cathode potential when the MFC was under load, decreasing both the anode and the cathode potentials. The physical response is a lowering of the internal resistance of the MFC due to the presence of the mediator. TMPD allows greater access to electrodes within the cells (NADH/NADPH) increasing the power density and lowering of internal resistance of the system. However, TMPD achieves this at a price, with hydrophobicity, chemical reversibility, and proton exchange being just a few of the many contributing factors which are not yet fully understood. It is the increased availability of electrons in combination with these factors that cause the change in both the anode and cathode potentials and subsequently the power density.

Also in chapter 5, with a double mediator system it was found that ferricyanide competed with the electrode for the electrons available from TMPD. This indicates the concentration of ferricyanide was too high for the anodic conditions and some needed to be converted into ferrocyanide before the power density could become stable again. Effectively by adding a new element to the MFC system, all parts of the system must adjust to try and achieve a new equilibrium. This indicates that it is not that the presence of a mediator will generate a greater power output, but a case of what the supply and demands are from the system.

Redox molecules follow the Nernst equation when under extremely high external load and the competition observed must be the ratios of the oxidised and reduced forms for each species altering the potentials of each electrode.

When a low external load is introduced, then electrons must flow (ohms law) and all the equations in the system try to achieve equilibrium with each other. This highlights how large and complex an equation would have to become to incorporate all of the different factors in a MFC and explains why the initial attempts at modelling a MFC were extremely complex (Chang & Halme 1995; Halme & Chang 1995).

### 10.3. Basis for new model of MFC

Ultimately the power density of a MFC is derived from the potential difference between the anode and the cathode. The theoretical limit is the potential difference between NADH and the reaction in the cathode if microorganisms are to remain as a biological catalyst (Rabaey & Verstraete 2005; Logan 2009). Therefore, in order to produce a greater power density in a MFC, the potentials of the anode and the cathode need to be as close as possible to the reaction potentials of NADH and the final electron acceptor. There has been very little work conducted to create models of how a eukaryotic MFC behaves (Chang & Halme 1995; Halme & Chang 1995). It is hoped that there is enough data reported on the variables known to affect the power density in a MFC in this thesis to sketch out the basis on which a model could be constructed. .

Increasing the difference in the reaction potentials of NADH and the cathode reaction by changing the cathode reaction does not directly correspond to a greater power density i.e. ohmic loss. When the reduction of ferricyanide occurs in the cathode reaction, the potential of the anode is raised but not above the solution species (see Figures 4.10, 4.11 and 4.12). As a result, the power density is lower for a mediator-less MFC containing ferricyanide as the

cathode reaction compared to potassium permanganate. That is, potassium permanganate raises the potential well above that of the solution species, making those electrons available to the external circuit (Figure 10.1).

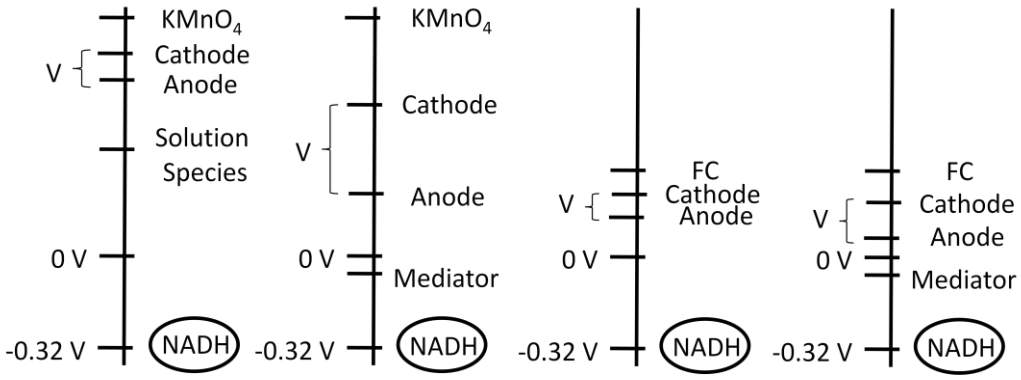


**Figure 10.1: Potentials of different components in microbial fuel cells.** Information taken from Figures 4.12, 5.5 and 5.11

In the literature (Bullen *et al.*2006; Logan 2009; Logan 2008; Chang & Halme 199; Rabaey & Verstraete 2004; Wang 2006; Jadhav & Ghangrekar 2009; Liu *et al.* 2005; Oh & Logan 2006; Hubenova *et al.* 2010; Kargi & Eker 2007; Li *et al.* 2010) several different factors have been shown to affect the power density of a MFC, namely:

1) Electrode material
2) Distance between electrodes
3) Proton/cation exchange membranes
4) Surface area of electrodes
5) External load
6) Cathode reaction
7) Mediator
8) Microorganism
9) Substrate

10) Over potential at the electrodes

11) Mass transport

12) Temperature

13) The type of electron transfer

All these factors shift and move the potentials depicted as lines on the vertical potential axis of Figure 10.1. For instance, when a mediator such as TMPD is added, it does not alter the potential of NADH or $KMnO_4$/FC, but changes the potential of the substance reacting with the anode (anolyte). TMPD presence changes the potentials of both the anode(s) and the cathode(s), as the access to electrons within the microorganisms is increased. It does this by creating a shorter pathway for the electrons to reach the anode from NADH at a lower potential and at a greater concentration than is available for mediator-less power density. By changing the potential of the species providing the electrons to the anode, the concentration of electrons to the anode at a given potential is changed. Any increase in electron availability will change the potential of the anode potential and the cathode when an MFC is under load.

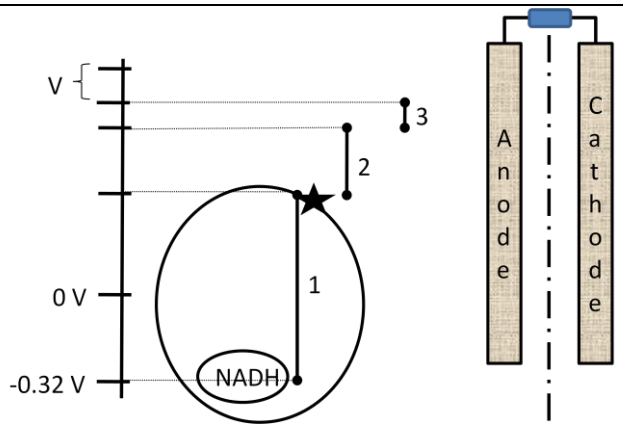


**Figure 10.2: Diagrammatic representation of the potential loss in a mediator-less MFC containing *A. adeninivorans* in the anode and $KMnO_4$ in the cathode.** The potential losses shown above are: 1) the loss from the inaccessibility of NADH, 2) the loss from transferring the electrons from the cell to the electrode, 3) the losses from the MFC set up. V is the potential difference between the anode and the cathode. The star indicates the solution species secreted by *A. adeninivorans.*

In the anode of a TMPD mediated MFC containing *A. adeninivorans* and $KMnO_4$ in the cathode, the potentials (see Figure 5.11) can be visualised in Figure 10.3. The first barrier here is the activation energy between TMPD and NADH which is affected by the lipophilicity of TMPD, the reaction potential between the two molecules, and the concentration of both TMPD and NADH (i.e. the supply of electrons available for the circuit). The second barrier is a combination of TMPD concentration, hydrophobicity of TMPD, conductivity of the solution, the reactivity of the electrodes, the activation energy of the reaction, the surface area of the anode, the kinetics of the reaction, temperature of system and the reversibility of the reaction. The third barrier is internal resistance, external resistance, distance between electrodes and surface area of the PEM. In this case it is unclear which of the three barriers provides the greatest potential loss to the system.

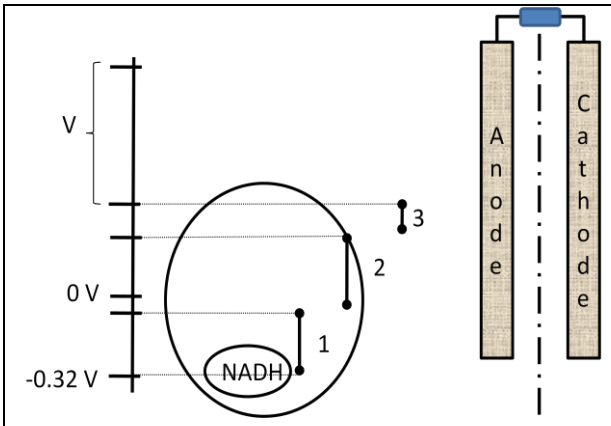


**Figure 10.3 Diagrammatic representation of the potential loss in a mediated MFC containing TMPD + *A. adeninivorans* in the anode and $KMnO_4$ in the cathode.** The potential losses shown above are: 1) the loss from TMPD accessing NADH, 2) the loss from transferring the electrons to the electrode, 3) the losses from the MFC configuration. V is the potential difference between the anode and the cathode.

By using Figures 10.2 and 10.3, it is easy to visualise the cause and effect a mediator can have in a eukaryotic MFC with the same cathode reaction. However, when the cathode reaction changes from $KMnO_4$ to one with a lower reaction potential such as ferricyanide (Figure 4.11 and 4.12), then the inability to reduce the solution species becomes clear (Figure 10.4). The

cathode reaction must absorb as many electrons as possible, as fast as possible to promote an unbalance anode requiring the optimal amount of electrons to be provided to the external circuit. The potential difference between the anode and cathode would then increase as the lines on the potential axis move.

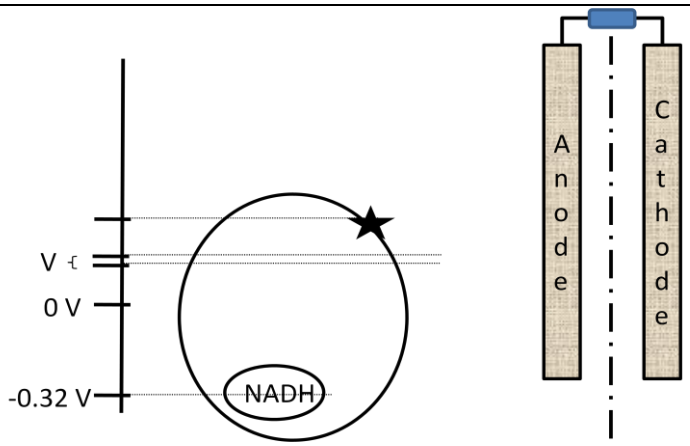


**Figure 10.4: Diagrammatic representation of the mediator-less MFC containing *A. adeninivorans* in the anode and ferricyanide in the cathode.** The potential of the cathode reaction is lower than the reaction of the solution species (star) resulting in a very small potential difference between the anode and the cathode.

Then when TMPD is added to the anode and the potential of the MFC increases when ferricyanide is used as the cathode reaction (Figure 5.11), which is due to the reaction potential of the anode being dragged downwards (Figure 10.5). Just as in Figure 10.3 shown above, the potential losses are grouped into three separate groups. However, due to the constraints of the potential differences of the anode and cathode reactions, the potential increase is less in this case than with $KMnO_4$.

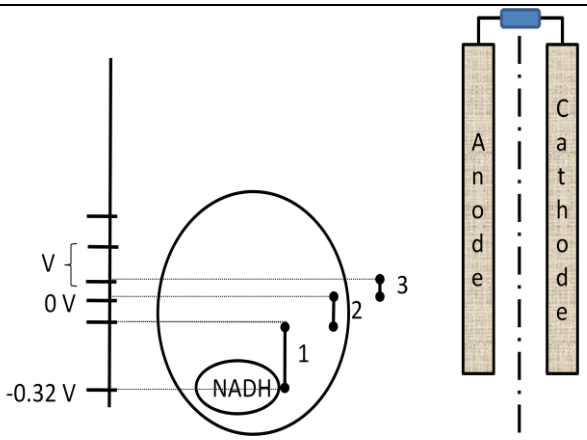


**Figure 10.5: Diagrammatic representation of the mediated MFC containing TMPD + *A. adeninivorans* in the anode and ferricyanide in the cathode.** The potential losses grouped above are: 1) the loss from TMPD accessing NADH, 2) the loss from transferring the electrons to the electrode, 3) the losses from the MFC set up. V is the potential difference between the anode and the cathode.

When comparing the results of the different potentials of $KMnO_4$ and ferricyanide cathode reactions in a mediated MFC (Figures 5.11, 10.1, 10.3 & 10.5), it is clear that the potential difference between the mediators' reaction potential and the anode is less with ferricyanide than with $KMnO_4$. This effectively reduces the potential losses from barriers 2 and 3 between the mediator and the electrode, i.e. comparing Figures 10.3 and 10.5 in order to visualise the reduction in potentials of barriers 2 and 3 for the different MFCs. The initial composition within the anode is the same for both fuel cells. However, because of the choice of cathode reaction, the demand for electrons from the anode is higher when $KMnO_4$ is used (Chapter 5).

Several different carbon sources, different growth phases, different mediators, mixed cultures, MFC configurations, and external resistances have been tested in this thesis. Each had different affects on the overall power density. However, where and how they affected the chain of electron flow from NADH to the final electron acceptor in the cathode reaction is in most cases unclear. A systematic breakdown of each reaction, testing as many variables as possible along the way would enable to reach a clearer picture of the system of MFC. The

number of permutations is large but not insurmountable. A model could be constructed which would enable this technology to be used effectively in the future.

### 10.4. Future work

As has been repeatedly pointed out, the reaction potential for $KMnO_4$ is far greater than for ferricyanide and this seem to in turn exert a greater strain on the anode to supply electrons to the external circuit. This has proven beneficial in enabling the detection of secreted electroactive species that would otherwise not have been detected (Chapter 3, chapter 9, Haslett *et al.* 2011). The introduction of the lipophilic mediator TMPD was able to provide a shorter pathway between NADH and the electrode to increase the power density. However, TMPD is not the optimal mediator, and future research should focus on finding other mediators better suited for a eukaryotic MFC.

In chapter 5, ferricyanide was also used as a mediator in the MFC and it did increase the power density. A lipophilic mediator and a hydrophilic mediator could be used together. However, that would limit the anode potential to the reaction potential of the hydrophilic mediator. That chapter demonstrated that when using eukaryotes, a lipophilic mediator that could also react with the anode was necessary in order to achieve a higher power density in eukaryotic MFC.

The same fact was highlighted in chapter 6, where an osmium polymer was able to wire *S. cerevisiae* to a gold electrode. The osmium polymer was hydrophilic and able to react with the gold electrode, whereas the lipophilic mediator was only able to react with NADH and the osmium polymer. In order for that system to be further optimised, a polymer that has a lipophilic tail that could penetrate into the cell and react with the NADH, as well as react with the gold electrode would be advantageous. However, mediators would not be necessary if cells could secrete electrochemical molecules. Genetic engineering of *A. adeninivorans* to

encourage the secretion of electrochemical products could provide a means of circumventing the need to use any mediators at all. The inability of *A. adeninivorans* transformed with a plasmid containing the AFRE2 gene to produce a higher mediator-less power density, and to increase the size of this +0.4 V peak and create a new reduction peak at +0.1 V suggests that this gene is probably not responsible for the mediator-less power density. The gene AFRE2 is more likely responsible for the +0.1 V reduction peak, but the +0.4 V oxidation peak may be the result of a completely different gene.

Since the completion of Chapter 9, several more transformant strains have produced and this line of inquiry should continue to be pursued. When all the chapters in this thesis are viewed together, it is clear that some aspects of MFC are well known, but that the chain of reactions from NADH to the final electron acceptor in the cathode chamber subjected to barriers are not well understood. This work has shown that the introduction of a lipophilic mediator circumvents several physical barriers which are present in a mediator-less MFC which lowers the potential the system holds the anode at. This is a previously unobserved phenomenon and should assist the systematic dissemination of each reaction barrier in a MFC.

Many factors have been found to affect the overall power density of a MFC (see section 9.3). Each one of these factors should be analysed within a single MFC in order to build up a model of how a MFC behaves. By attempting to fully analyse the MFC system and the reaction barriers within it greater power density could be achieved and more versatile devices constructed.

## 10.5. Conclusion

The microbial fuel cell systems discussed in this thesis covers a wide range of configurations and factors. This work has given an overview of the field which points to a systematic way to move forward and develop a model. The transfer of NADH to the final electron acceptor can

be used to generate electricity, and the theoretical upper limit of the possible power generated is generally well understood by the work outlined in Chapter 2. What is unclear is the how each of the barriers in the chain of reactions affects the whole system. This will be the key to effectively miniaturising as well as the production of large scale MFC.

# References:

Aelterman, P., Rabaey, K., Pham, H. T., Boon, N., & Verstraete, W. (2006) Continuous Electricit Generation at High Voltages and Currents Using Stacked Microbial Fuel Cells. *Environmental Science Technology, 40*(10), 3388-3394

Aldrovandi, A., Marsili, E., Stante, L., Paganin, P., Tabacchioni, S., & Giordano, A. (2009) Sustainable power production in a membrane-less and mediator-less synthetic wastewater microbial fuel cell. *Bioresource Technology, 100,* 3252-2260

Allen, R. M., & Bennetto, H. P. (1993) Microbial fuel-cells - Electricity production from carbohydrates. *Applied Biochemistry and Biotechnology, 39*(1), 27-40

Avéret, N., Aguilaniu, H., Bunoust, O., Gustafsson, L., & Rigoulet, M. (2002) NADH Is Specifically Channeled Through the Mitochondrial Porin Channel in *Saccharomyces cerevisiae. 34*(6), 499-506

Bachman, T. T., Bilitewski, U., & Schmit, R. T., (1998) A microbial sensor based on *Pseudomonas putida* for phenol, benzoic acid and their monochlorinated derivatives which can be used in water and *n*-hexane. Analitical Letters *31*, 2361-2373

Baronian, K. H. R., Downard, A. J., Lowen, R. K., & Pasco, N. (2002) Detection of two distinct substrate-dependent catabolic responses in yeast cells using a mediated electrochemical method. *Applied Microbiology and Biotechnology.* **60**, 108-113

Behera, M., & Ghangrekar, M. M. (2009) Performance of microbial fuel cell in response to change in sludge loading rate at different anodic feed pH, *Bioresource Technology. 100,* 5114-5121

Benneto, H. P. (1990) Electricity generation by microorganisms. *Biotechnology Education, 1*(4), 163–168

Bennetto, H. P., Delaney, G. M., Mason, J. R., Roller, S. D., Stirling, J. L., & Thurston, C. F. (1985) The Sucrose Fuel Cell: Efficient Biomass Conversion Using A Microbial Catalyst. *Biotechnology Letters, 7*(10), 699-704

Bergel, A., Féron, D., & Mollica, A. (2005) Catalysis of oxygen reduction in PEM fuel cell by seawater biofilm. *Electrochemistry communications, 7*, 900-904

Biffinger, J. C., Pietron, J., Ray, R., Little, B., & Ringeisen, B. R. (2007) A biofilm enhanced miniature microbial fuel cell using *Shewanella oneidensis* DSP10 and oxygen reduction cathodes. *Biosensors and Bioelectronics, 22*, 1672-1679

Bond, D. R., Holmes, D. E., Tender, L. M., & Lovely, D. R. (2002) Electrode-Reducing Microorganisms That Harvest Energy from marine Sediments. *Science, 295*, 483-485

Bond, D. R., & Lovley, D. R. (2003) Electricity Production by *Geobacter sulfurreducens* Attached to Electrodes. *Applied and Environmental Microbiology, 69*(3), 1548-1555

Bond, D. R., & Lovley, D. R. (2005) Evidence for Involvement of an Electron Shuttle in Electricity Generation by *Geothrix fermentans*. *Applied and Environmental Microbiology, 71*(4), 2186-2189

Bullen, R. A., Arnot, T. C., Lakeman, J. B., & Walsh, F. C. (2006) Biofuel cells and their development. *Biosensors and Bioelectronics, 21*. 2015-2045

Campbell, N. A., Reece, J. B. & Mitchell, L. G. (1999) Biology. 5th Edition. *Addison-Wesley.* Addison Wesley Longman, New York, New York.

Cartwright, K. V. (2009) Non-Calculus Derivation of the Maximum Power Transfer Theorem. *The Technology Interface/Spring. 8*(2), 1-19

Catal, T., Li, K., Bermek, H., & Liu, H. (2008a) Electricity production from twelve monosaccharides using microbial fuel cells. *Journal of Power Sources, 175,* 196–200.

Catal, T., Xu, S., Li, K., Bermek, H., & Liu, H. (2008b) Electricity generation from polyalcohols in single-chamber microbial fuel cells. *Biosensors and Bioelectronics, 24,* 849-854

Chiao, M., Lam, K. B., Lin L. 2006. Micromachined microbial and photosynthetic fuel cells. *Journal Micromechanical Microengineering, 16***,** 2547

Chaundhuri, S. K., & Lovely, D. R. (2003) Electricity generation by direct oxidation of glucose in mediatorless microbial fuel cells. *Nature biotechnology, 21*(10), 1229-1232

Cheng, S., Dempsey, B., & Logan, B. E. (2007) Electricity Generation from Synthetic Acid-Mine Drainage (AMD) Water using Fuel Cell Technologies. *Environmental Science Technology*, *41*, 8148-8153

Cho, E. J., & Ellington, A. D. (2007) Optimization of the biological component of a bioelectrochemical cell. *Bioelectrochemistry. 70*(1), 165-172

Choi, Y., Jung, E., Kim, S., & Jung, S. (2003) Membrane fluidity sensoring microbial fuel cell. *Bioelectrochemistry, 59,* 121-127

Cohen, B. (1931). The Bacterial Culture as an Electrical Half-Cell, *Journal of Bacteriology, 21,* 18–19

Davis, J. B., & Yarbrough, H. F. (1962) Preliminary Experiments on a Microbial Fuel Cell. *Science, 137,* 615-616

Davis, F., & Higson, S. P. J. (2007) Biofuel cells – Recent advances and applications. *Biosensors and Bioelectronics, 22,* 1224-1235

Delaney, G. M., Bennetto, H. P., Mason, J. R., Roller, H. D., Stirling, J. L. & Thurston, C. F. (1984) Electron-transfer coupling in microbial fuel cells: 2. Performance of fuel cells containing selected microorganism-mediator-substrate combinations. *Journal of Chemical Technology and Biotechnology. 34B,* 13-27

Degani, Y., & Heller, A. (1989) Electrical communication between redox centers of glucose-oxidase and electrodes via electrostatically and covalently bound redox polymers. Journal of the American Chemical Society. *111*, 2357-2358

Ducommun, R., Favre, M. F., Carrard, D., & Fischer, F. (2010) Outward electron transfer by *Saccharomyces cerevisiae* monitored with a bi-cathodic microbial fuel cell-type activity sensor. *Yeast, 27*, 139–148

Dumas, C., Basseguy, R., & Bergel, A. (2008) Microbial electrocatalysis with *Geobacter sulfurreducens* biofilm on stainless steel cathodes. *Electrochimica Acta, 53*, 2494–2500

Fang, C., Wu, B., & Zhou, X. (2004) Nafion membrane electrophoresis with direct and simplified end-column pulse electrochemical detection of amino acids. *Electrophoresis, 25*, 375–380

Feng, Y., Wang, X., Logan, B. E., & Lee, H. (2008) Brewery wastewater treatment using air-cathode microbial fuel cells. *Applied Microbiology and Biotechnology, 78*, 873–880

Forster, R. J. (1994) Microelectrodes: new dimensions in electrochemistry. *Chemical Society Reviews*, **4**, 289-297.

Ganguli, R., & Dunn, B. S. (2008) Kinetics of Anode Reactions for a Yeast-Catalysed

Microbial Fuel Cell. *Fuel Cells*, 9(1), 44-52

Greenman, J., Gálvez, A., Giusti, L., & Ieropoulos, I. (2009) Electricity from landfill leachate using microbial fuel cells: Comparison with a biological aerated filter. *Enzyme and Microbial Technology, 44*, 111-119

Gregg, B., & Heller, A. (1991) Redox polymer films containing enzymes. 1. A redox-containing epoxy cement: synthesis, characterization and electrocatalytic oxidation of hydroquinone. *Journal of Physical Chemistry, 95*, 5970-5975

Gunawardena, A., Fernando, S., & To, F. (2008) Performance of a Yeast-mediated Biological Fuel Cell. *International Journal of Molecular Science, 9*, 1893-1907

Ha, P. T., Tae, B., & Chang, I. S. (2008) Performance and Bacterial Consortium of Microbial Fuel Cell Fed with Formate. *Energy and Fuels, 22*, 164-168

Halme, A. & Zhang, X. C. (1995) Biofuel cell utilizing *Saccharomyces cerevisiae* – a modelling of the process. Reprints of the 6th International Conference on Computer Applications in Biotechnology, ISSN: 0080423779, 165-170

Han, Y., Yu, C., & Liu, H. (2010) A microbial fuel cell as power supply for implantable medical devices. *Biosensors and Bioelectronics, 25*, 2156-2160

Haslett, N.D., Rawson, F.J., Barrière, F., Hunze, G., Pasco, N., Gooneratne, R. and Baronian, K.H.R. (2011) Characterisation of yeast microbial fuel cell with the yeast Arxula adeninivorans as the biocatalyst. *Biosensors and Bioelectronics, 26*, 3742-3747.

He, Z., Shao, H., & Angenent, L. (2007) Increased power production from a sediment microbial fuel cell with a rotating cathode. *Biosensors and Bioelectronics, 22*, 3252-3255

He, Z., Minteer, S. D., & Angenet, L. T. (2005) Electricity Generation from Artificial Wastewater Using an Upflow Microbial Fuel Cell. *Environmental Science and Technology, 39*(14), 5262-5267

Heijne, A. T., Hamelers, H. V. M., De Wilde, V., Rozendal, R. A., & Buisman, C. J. N. (2006) A Bipolar Membrane combined with Ferric iron Reduction as an Efficient Cathode System in microbial Fuel Cells. *Environmental Science and Technology, 40*(17), 5200-5205

Heilmann, J., & Logan, B. E. (2006) Production of Electricity from Proteins Using a Microbial Fuel Cell. *Water Environment Research, 78*(5), 531-537

Heiskanen, A., Spégel, C., Kostesha, N., Lindahl, S., Ruzgas, T., & Emnéus, J. (2009) Mediator-assisted simultaneous probing of cytosolic and mitochondrial redox activity in living cells. *Analytical Biochemistry, 384*, 11-19

Heller, A. (1992) Electrical connection of enzyme redox centers to electrodes. Journal of Physical Chemistry. *96*, 3579-3587

Hu Z. (2008) Electricity generation by a baffle-chamber membraneless microbial fuel cell. *Journal of power sources, 179*, 27-33

Huang L., & Angelidaki I. (2008) Effect of Humic Acids on Electricity Generation Integrated With Xylose Degradation in Microbial Fuel Cells. *Biotechnology and Bioengineering, 100*(3), 413-422

Huang, L., Zeng, R. J., & Angelidaki, I. (2008) Electricity production from xylose using a mediator-less microbial fuel cell. *Bioresource Technology, 100*(3), 413-422

Huang, L. P., & Logan, B. E. (2008) Electricity generation and treatment of paper recycling wastewater using a microbial fuel cell. *Applied Microbiology and Biotechnology, 80,* 349-355

Hubenova, Y. V., Rashkov, R. S., Buchvarov, V. D., Arnaudova, M. H., Babanova, S. M., & Mitov M. Y. (2010) Improvement of Yeast-Biofuel Cell Output by Electrode Modifications. *Industrial & Engineering Chemistry Research*, Publication Date (Web): June 15, 2010

Ieropoulos, I. A., Greenman, J., Melhuish, & C., Hart, J. (2005) Comparative study of three types of microbial fuel cell. *Enzyme and Microbial Technology, 37,* 238-245

Jadhav, G. S., & Ghangrekar, M. M. (2009) Performance of a microbial fuel cell subjected to variation in pH, temperature, external load and substrate concentration. *Bioresource Technology, 100,* 717-723

Jang, J. K., Pham, T. H., Chang, I. S., Kang, K. H., Moon, H., Cho, K. S., & Kim, B. H. (2004) Construction and operation of a novel mediator- and membrane-less microbial fuel cell. *Process Biochemistry, 39,* 1007-1012

Kargi, F., & Eker, S. (2007) Electricity generation with simultaneous wastewater treatment by a microbial fuel cell (MFC) with Cu and Cu-Au electrodes. *Journal of Chemical Technology and Biotechnology, 82,* 658-662

Katakis, I., & Heller, A. (1992) L-α-glycerophosphate and L-lactate electrodes based on the electrochemical "wiring" of oxides. *Analytical Chemistry, 64,* 1008-1013

Kim, N., Choi, Y., Jung, S., & Kim, S. (2000) Development of microbial fuel cells using *Proteus vulgaris*. *Bulletin of the Korean Chemical Society*, ***21*****(**1), 44–48

Kim, N., Choi, Y., Jung, S., & Kim, S. (2000) Effect of initial carbon sources on the performance of microbial fuel cells containing *Proteus vulgaris*. *Biotechnology and Bioengineering (Communications to the editor),* 70(1), 109–114

Kim, J. R., Jung, S. H., Regan, J. M., & Logan, B. E. (2007) Electricity generation and microbial community analysis of alcohol powered microbial fuel cells. *Bioresource Technology*, *98*, 2568-2577

Kim, H. J., Park, H. S., Hyun, M. S., Chang, I. S., Kim, M., & Kim, B. H. (2002) A mediator-less microbial fuel cell using a metal reducing bacterium *Shawanella putrefaciens. Journal of Applied Microbial Technology, 30*, 145-152

Kim, J. R., Jung, S. H., Regan, J. M., & Logan, B. E. (2007) Electricity generation and microbial community analysis of alcohol powered microbial fuel cells. *Bioresource Technology*, *98*, 2568-2577

Kissinger, P. T., & Heineman W. R. (1983) Cyclic Voltammetry. *Journal of Chemical Education.* **60,** 9, 702-706

Kotesha, N., Heiskanen, A., Spégel, C., Hahn-Hägerdal, B., Gorwa-Grauslund, M., & Emnéus, J. (2009) Real-time detection of cofactor availability in genetically modified living *Saccharomyces cerevisiae* cells – Simultaneous probing of different geno- and phenotypes. *Bioelectrochemistry, 76*, 180-188

Li, F., Sharma, Y., Lei, Y., Li, B., & Zhou, Q. (2010) Microbial fuel Cells: The Effects of Configurations, electrolyte solutions and Electrode Materials on Power generation. *Applied Biochemistry and Biotechnology, 160*, 168-181

Liu, H., & Logan, B. E. (2004) Electricity Generation Using an Air-Cathode Single chamber microbial fuel Cell in the Presence and Absence of a Proton Exchange Membrane. *Environmental Science and Technology, 38*(14), 4040-4046

Liu, H., Ramnarayanan, R. & Logan, B. E. (2004) Production of electricity during Wastewater Treatment Using a single chamber Microbial Fuel Cell. *Environmental Science and Technology*, *38*(7), 2281-2285

Liu, H., Cheng, S. & Logan, B. E. (2005) Power Generation in Fe-Batch Microbial Fuel Cells as a Function of Ionic Strength, Temperature and Reactor Configuration. *Environmental Science and Technology*, *39*(14), 5488–5493

Liu, H., Cheng, S. & Logan, B. E. (2005) Production of electricity from acetate or butyrate using a single-chamber microbial fuel cell. *Environmental Science and Technology, 39*, 658-662

Liu, Z., Liu, J., Zhang, S., & Su, Z. (2009) Study of operational performance and electrical response on mediator-less microbial fuel cells fed with carbon- and protein-rich substrates. *Biochemical Engineering Journal*, *45***,** 185-191

Logan, B. E. (2005) Simultaneous wastewater treatment and biological electricity generation. *Water Science and Technology*, *25*(1), 31-37

Logan, B. E. (2008) Microbial Fuel Cells, *1st Edition, John Wiley & Sons,* Hoboken, New Jersey

Logan, B. E., Cheng, S., Watson, V., & Estadt, G. (2007) Graphite fiber brush anodes for increased power production in air-cathode microbial fuel cells. *Environmental Science and Technology*, *41*, 3341-3346

Logan, B. E., Hamelers, B., Rozendal, R., Schröder, U., Keller, J., Freguia, S., Aelterman, P., Verstraete, W., & Rabaey, K. (2006) Microbial Fuel Cells: Methodology and Technology. *Environmental Science and Technology, 40*(17), 5181-5192

Logan, B. E., Murano, C., Scott, K., Gray, N. D., & Head, I. M. (2005) Electricity generation from cysteine in a microbial fuel cell. *Water Research, 39*, 942-952

Lowy, D. A., Tender, L. M., Zeikus, J. G., Park, D. H., & Lovely, D. R. (2006) Harvesting from the marine sediment-water interface II Kinetic activity of anode materials. *Biosensors and Bioelectronics, 21*, 2058-2063

Lu, N., Zhou, S., Zhuang, L., Zhang, J., & Ni, J. (2009) Electricity generation from starch processing wastewater using microbial fuel cell technology. *Biochemical Engineering Journal, 43*, 246-251

Luo, Y., Liu, G., Zhang, R., & Zhang, C. (2009) Phenol degradation in microbial fuel cells. *Chemical Engineering Journal, 147*, 259-264

Luo, Y., Liu, G., Zhang, R., & Zhang, C. (2010) Power generation from furfural using microbial fuel cell. *Journal of Power Sources, 195*, 190-194

MacKay, D., J., C., (2009) Sustainable Energy – without the hot air. *First edition. UIT Cambridge Ltd.* Cambridge. England.

Menicucci, J., Beyenal, H., Marsili, E., Veluchamy, R. A., Memir, G., & Lewandowski, Z. (2006) Procedure for Determining maximum Sustainable Power Generated by Microbial fuel Cells. *Environmental Science and Technology, 40*(3), 1062–1068

Min, B., & Angelidaki, I. (2008) Innovative microbial fuel cell for electricity production from anaerobic reactors. *Journal of Power Sources, 180***,** 641–647

Min, B., Kim, J., Oh, S., Regan, J. M., & Logan, B. E. (2005) Electricity generation from swine wastewater using microbial fuel cells. *Water Research, 39*, 4961-4968

Min, B., & Logan, B. E. (2004) Continuous electricity Generation from Domestic Wastewater and Organic Substrates in a Flat Plate Microbial Fuel Cell, *Environmental Science and Technology*. *38*(21), 5809-5814

Mohan, Y., Kumar, S. M. M., & Das, D. (2008) Electricity generation using microbial fuel cells. *International Journal of Hydrogen Energy, 33*, 423-426

Monohar, A. K., & Mansfeld, F. (2009) The internal resistance of a microbial fuel cell and its dependence on cell design and operating conditions. *Electrochimica Acta, 54,* 1664-1670

Niessen, J., Schröder, U., & Scholz, F. (2004) Exploiting complex carbohydrates for microbial electricity generation – a bacterial fuel cell operating on starch. *Electrochemistry Communications, 6*, 955-958

Oh, S., Min, B., & Logan, B. E. (2004) Cathode Performance as a Factor in electricity Generation in Microbial Fuel Cells. *Environmental Sciences and Technology, 38*(18), 4900-4904

Oh, S., & Logan, B. E. (2005) Hydrogen and electricity production from a food processing wastewater using fermentation and microbial fuel cell technologies. *Water Research, 39*, 4673-4682

Oh, S., & Logan, B. E. (2006) Proton exchange membrane and electrode surface areas as factors that affect power generation in microbial fuel cells. *Applied Microbiology and Biotechnology, 70*, 162-169

Ohara, T. J., & Rajagopalan, R. (1993) A Heller, Glucose electrodes based on crosslinked [Os $(bpy)_2Cl]^{+/2+}$ complexed poly(1-vinylimidazole) films. *Analytical Chemistry, 65,* 3512-3517

Pant, D., Bogaert, G. V., Diels, L., & Vanbroekhoven, K. (2010) A review of the substrates used in a microbial fuel cells (MFCs) for sustainable energy production. *Bioresource Technology, 101,* 1533-1543

Park, D. H., Kim, S. K., Shin, I. H., & Jeong, Y. J. (2000) Electricity production in biofuel cell using modified graphite electrode with Neutral Red. *Biotechnology Letters, 22,* 1301-1304

Park, D. H., & Zeikus, J. G. (2000) Electricity Generation in Microbial Fuel Cells Using Neutral Red as an Electronophore. *Applied and Environmental Microbiology, 66*(4), 1292-1297

Park, D. H., & Zeikus, J. G. (2003) Improved fuel cell and electrode Designs for Producing electricity from Microbial Degradation. *Biotechnology and Bioengineering, 81*(3), 348-355

Park, D. H., & Zeikus, J. G. (2002) Impact of electrode composition on electricity generation in a single-compartment fuel cell using *Shewanella putrefaciens. Applied Microbiology and Biotechnology, 59,* 58-61

Patil, S. A., Surakasi, V. P., Koul, S., Ijmulwar, S., Vivek, A., Shouche, Y. S., & Kapadnis, B. P. (2009) Electricity generation using chocolate industry wastewater and its treatment in activated sludge based microbial fuel cell and analysis of developed microbial community in the anode chamber. *Bioresource Technology, 100,* 5132-5139

Pham, H., Boon, N., Marzorati, M., & Verstraete, W. (2009) Enhanced removal of 1,2-dichloroethane by anodophilic microbial consortia. *Water Research, 43,* 2936-2946

Potter, M. C. (1911) Electrical Effects accompanying the Decomposition of Organic Compounds. *Royal Society (Formerly Proceedings of the Royal Society) B, 84,* 260-276

Prasad, D., Arun, S., Murugesan, M., Padmanaban, S., Satyanarayanan, R. S., Berchmans, S., & Yegnaraman, V. (2007) Direct electron transfer with yeast cells and construction of a mediatorless microbial fuel cell. *Biosensors and Bioelectronics, 11,* 2604-2610

Pyocyanin (2007) Retrieved November 14, 2010, from the Caman Chemicals website: http://www.caymanchem.com/pdfs/10009594.pdf

Rabaey, K., & Verstraete, W. (2005) Microbial fuel cells: Novel biotechnology for energy generation. *Trends in Biotechnology, 23*(8), 291-298

Rabaey, K., Boon, N., Höfte, M., & Verstraete, W. (2005) Microbial Phenazine Production Enhances Electron Transfer in Biofuel Cells. *Environmental Science and Technology, 38*(9), 3401-3408

Rabaey, K., Lissens, G., Siciliano, S. D., & Verstraete, W. (2003) A microbial fuel cell capable of converting glucose to electricity at high rate and efficiency. *Biotechnology Letters, 25*, 1531-1535

Rabaey, K., Boon, N., Siciliano, S. D., Verhaege, M., & Verstraete, W. (2004) Biofuel Cells Select for Microbial Consortia That Self-Mediate Electron Transfer. *Applied and Environmental Microbiology, 70*(9), 5373-5382

Rabaey, K., Clauwaert, P., Aelterman, P., & Verstraete, W. (2005) Tubular Microbial Fuel Cells for Efficient Electricity Generation. *Environmental Science Technology, 39,* 8077-8082

Rawson, F. J. (2008) The Design, Development and Application of a Novel Electrochemical Biosensor/Sensor System for the Real-Time Monitoring of In-Vitro Cell Toxicity. *Ph.D. thesis. Personal Communication.* University of the West of England

Reguera, G., McCarthy, K. D., Mehta, T., Nicoll, J. S., Tuominen, M. T., & Lovley, D. R. (2005) Extracellular electron transfer via microbial nanowires. *Nature, 435,* 1098-1101

Reimers, C. E., Tender, L. M., Fertig, S., & Wang, W. (2001) Harvesting energy from the Marine Sediment-Water Interface. *Environmental Science Technology, 35,* 192-195

Rezaei, F., Xing, D., Wagner, R., Regan, J. M., Richard, T. L., & Logan, B. E. (2009) Simultaneous cellulose degradation and electricity production by *Enterobacter cloacae* in a microbial fuel cell. *Applied Environmental Microbiology, 75*(11), 3673-3678

Rhoads, A., Beyenal, H., & Lewandowski, Z. (2005) Microbial Fuel Cell using Anaerobic Respiration as an Anodic Reaction and Biomineralized Manganese as a Cathodic Reactant. *Environmental Science and Technology, 39*(12), 4666-4671

Rismani-Yazdi, H., Christy, A. D., Dehority, B. A., Morrison, M., Yu, Z., & Tuovinen, O. H. (2007) Electricity Generation From Cellulose by Rumen Microorganisms in Microbial Fuel Cells. Biotechnology and Bioengineering, *97*(6), 1398-1407

Rodrigo, M. A., Canizares, P., Lobato, J., Paz, R., Saez, C., & Linares, J. J. (2007) Production of electricity from the treatment of urban waste water using a microbial fuel cell. *Journal of Power Sources, 169,* 198-204

Schaetzle, O., Barriére, F., & Baronian, K. H. R. (2008) Bacteria and yeasts as catalysts in microbial fuel cells: electron transfer from micro-organisms to electrodes for green electricity. *Energy Environmental Science,* 607-620

Schröder, U., Nieβen, J., & Scholz, F. (2003) A Generation of Microbial Fuel Cells with Current Output Boosted by more Than One Order of Magnitude. *Angewandte Chemie International Edition, 42,* 2880-2883

Scott, K., & Murano, C. (2007) A study of a microbial fuel cell battery using manure sludge waste. *Journal of chemical technology and biotechnology, 82,* 809-817

Sharma, Y., & Li, B. (2010) The variation of power generation with organic substrates in single-chamber microbial fuel cells (SCMFCs). *Bioresource Technology. 101*, 1844-1850

Shukla, A. K., Suresh, P., Berchmans, S., & Rajendran, A. (2004) Biological fuel cells and their applications. *Current Science, 87*(4), 455-468

Sun, J., Hu, Y., Bi, Z., & Cao, Y. (2009) Simultaneous decolorization of azo dye and bioelectricity generation using a microfiltration membrane air-cathode single-chamber microbial fuel cell. *Bioresource Technology, 100,* 3195-3192

Tender, L. M., Reimers, C. E., Stecher III, H. A., Holmes, D. E., Bond, D. R., Lowy, D. A., Pilobello, K., Fertig, S. J., & Lovley, D. R. (2002) Harnessing microbially generated power on the seafloor. *Nature Biotechnology, 20,* 821-825

Terentiev, Y., Gellissen, G., and Kunze, G. (2003) *Arxula adeninivorans* – A non-conventional dimorphic yeast of great biotechnological potential. *Recent research developments in applied microbiology and biotechnology, 1,* 135-145

Thurston, C. F., Bennetto, H. P., Delaney, G. M., Mason, J. R., Roller, S. D., & Stirling, J. L. (1985) Glucose Metabolism in a Microbial Fuel Cell. Stoichiometry of Product Formation in a Thionine-mediated *Proteus vulgaris* Fuel Cell and its Relation to Coulombic Yields. *Journal of General Microbiology*, *131*, 1393-1401

Timur, S., Haghighi, B., Tkac, J., Pazarlioğu, N., Telefoncu, A., & Gorton, L. (2007) Electrical wiring of *Pseudomonas putida* and *Pseudomonas fluorescens* with osmium redox polymers. Bioelectrochemistry, 71, 38-45

Todisco, S., Agrimi, G., Castegna, A., & Palmieri, F. (2006) Identification of the Mitochondrial $NAD^+$ Transporter in *Saccharomyces cerevisiae*. *Journal of Biological Chemistry, 281*(3), 1524-1531

Tsujimura, S., Fujita, M., Tatsumi, H., Kano, K., & Ikeda, T. (2001) Bioelectrocatalysis-based digydrogen/dioxygen fuel cell operating at physiological pH. *Physical Chemistry Chemical Physics*, *3*, 1331-1335

Van Denschoten, J. J., Lewis, J. Y., Heineman, W. R., Roston, D. A., & Kissinger, P. T. (1983) Cyclic Voltammetry Experiment. *Journal of Chemical Education.* **60**, 9, 772-776

Velasquez-Orta, S. B., Curtis, T. P., & Logan, B. E. (2009) Energy From Algae Using Microbial Fuel Cells. *Biotechnology and Bioengineering*, *103*(6), 1068-1076

Venkata Mohan, S., Mohanakrishna, G., Purushotham Reddy, B., Saravanan, R., & Sarma, P. N. (2008) Bioelectricity generation from chemical wastewater treatment in mediatorless (anode) microbial fuel cell (MFC) using selectively enriched hydrogen producing mixed culture under acidophilic microenvironment. *Biochemical Engineering Journal*, *39*, 121-130

Walker, A. L. & Walker, C. W. (2006) Biological fuel cell and an application as a reserve power source. *J. Power Sources, 160,* 123–129

Wang, X., Feng, Y., Ren, N., Wang, H., Lee, H., Li, N., & Zhao, Q. (2009) Accelerated start-up of two-chambered microbial fuel cells: Effect of anodic positive poised potential. *Electrochemica Acta, 1109-1114*

Wang, J. (2006) Analytical Electrochemistry, 3rd Edition. *Wiley-VCH*. John Wiley & Sons, Inc., Hoboken, New Jersey

Wang, D. L., & Heller, A. (1993) Miniaturized flexible amperometric lactate probe, *Analytical Chemistry, 65,* 1069-1073

Wartmann, T., Krüger, A., Adler, K., Duc, B. M., Kunze, I., & Kunze, G. (1995) Temperature-dependent dimorphism of the yeast *Arxula adeninivorans* LS3. *Antonie van Leeuwenhoek. 68.* 215-223

Wen, Q., Wu Y., Cao D., Zhao L., & Sun Q. (2010) Electricity generation and modelling of microbial fuel cell from continuous beer brewery wastewater. *Bioresouce Technology, 100,* 4171-4175

Wilkinson, S., (2000) *"Gastrobots*"—Benefits and Challenges of Microbial Fuel Cells in Food Powered Robot Applications. *Autonomous Robots, 9,* 99-111

Willson, V. J. C. & Tipton, K. F. (1981) The Effect of Ligands on the Irreversible Inhibition of the NADi-Dependent Isocitrate Dehydrogenase from Ox Brain. *European Journal of Biochemistry, 117,* 65-68

Witters, W. L., & Foley, C. W. (1976) Effect of selected inhibitors and methylene-blue on a possible phosphogluconate pathway in washed boar sperm. *Journal of Animal Science, 43(1),* 159-163.

Yang, H., Yang, T., Baur, J. A., Perez, E., Matsui, T., Carmona, J. J., Lamming, D. W., Souza-Pinto, N. C., Bohr, V. A., Rosenzqeig, A., de Cabo, R., Sauve, A. A., & Sinclair,

D. A. (2007) Nutrient-Sensitive Mitochondrial $NAD^+$ Levels Dictate Cell Survival. *Cell*, *130*, 1095-1107

You, S., Zhao, Q., Zhang, J., Jiang, J., & Zhao, S. (2006) A microbial fuel cell using permanganate as the cathodic electron acceptor. *Journal of Power Sources, 162*, 1409-1415

Zhao, F., Slade, R. C. T. And Varcoe, J. R. (2009) Techniques for the study and development of microbial fuel cells: an electrochemical perspective. *Chemical Society Reviews*, *38*, 1926-1939

Zhao, J., Wang, M., Yang, z., Wang, Z., Wang, H., & Yang, Z. (2007) The different behaviours of three oxidative mediators in probing the redox activities of the yeast *Saccharomyces cerevisiae*. *Analytica chimica Acta*, *597*, 67-74

Zhao, J., Yang, Z., Gong, Q., Lu, Y., Yang, Z., & Wang, M. (2005) Electrochemical insights into the Glucose metabolism pathways within *Saccharomyces cerevisiae.* Analytical Letters, *38*, 89-98

Zou, T., Pisciotta, J., Billmyre, R. B., & Baskakov, I. V. (2009) Photosynthetic Microbial Fuel Cells with Positive Light Response. *Biotechnology and Bioengineering*, *104*(5), 939-946

# Appendix 1

**Poised Potential Microbial Fuel Cells**

| Anode composition and Surface Area (SA) | Anode Contents | Poised Potential (V) | Mediators | Current Density ($Am^{-2}$) | Reference |
|---|---|---|---|---|---|
| Graphite electrode SA=0.0100 $m^2$ | *Desulfuromonas acetoxidans* + Acetate | 1.2 V (vs. Ag/AgCl) | N/A | 0.45 | Bond *et al.* (2002) |
| Graphite electrode SA=0.0100 $m^2$ | *Geobacter metallireducens* + benzoate | 1.2 V (vs. Ag/AgCl) | N/A | 0.675 | Bond *et al.* (2002) |
| Graphite Rod SA=0.00612 $m^2$ | *Geobacter sulfurreducens* + Acetate | 0.2 V (vs. Ag/AgCl) | N/A | 1.143 | Bond & Lovley (2003) |
| Graphite Rod SA=0.0065 $m^2$ | *Rhodoferax ferrireducens* + Glucose | 0.2 V (vs. Ag/AgCl) | N/A | 0.1 | Chaundhuri & Lovely (2003) |
| Graphite Plate SA=0.007 $m^2$ | *Shewanella oneidensis MR-1* + Lactate | 0.5 V (vs. Ag/AgCl) | N/A | 0.228 | Cho & Ellington (2007) |
| Graphite SA=0.00125 $m^2$ | *Geobacter sulfurreducens* | -0.6 V (vs. Ag/AgCl) | fumarate | 0.75 | Dumas *et al.* (2008) |
| Stainless Steel SA=0.00025 $m^2$ | *Geobacter sulfurreducens* | -0.6 V (vs. Ag/AgCl) | fumarate | 20.5 | Dumas *et al.* (2008) |
| Pt+ Polytetrafluoroaniline SA=0.0015 $m^2$ | *Clostridium butyricum* + Starch (Fermented) | 0.2 V (vs. Ag/AgCl) | N/A | 0.0011 $Am^{-2}$ | Niessen *et al.*(2004) |
| Pt+ Polytetrafluoroaniline SA=0.0015 $m^2$ | *Clostridium butyricum* + Molasses (Fermented) | 0.2 V (vs. Ag/AgCl) | N/A | 0.0011 $Am^{-2}$ | Niessen *et al.*(2004) |
| Pt+ Polytetrafluoroaniline SA=0.0015 $m^2$ | *Clostridium beijerinckii* + glucose (Fermented) | 0.2 V (vs. Ag/AgCl) | N/A | 0.0011 $Am^{-2}$ | Niessen *et al.*(2004) |
| Pt+ Polytetrafluoroaniline SA=0.0015 $m^2$ | *Clostridium beijerinckii* + lactate (Fermented) | 0.2 V (vs. Ag/AgCl) | N/A | 0.0011 $Am^{-2}$ | Niessen *et al.*(2004) |

| | | | | | |
|---|---|---|---|---|---|
| Pt+ Polytetrafluoroaniline SA=0.0015 $m^2$ | *Clostridium beijerinckii* + Starch (Fermented) | 0.2 V (vs. Ag/AgCl) | N/A | 0.0011 $Am^{-2}$ | Niessen *et al.*(2004) |
| Pt + Polyaniline SA=0.0001 $m^2$ | *Escherichia coli* + glucose (Fermented) | 0.2 V (vs. Ag/AgCl) | N/A | 12 | Schröder *et al.* (2003) |
| Plain Graphite SA=0.005 $m^2$ | Domestic wastewater + Anaerobic Sludge | 0.2 V (vs. Ag/AgCl) | N/A | 0.6 | Wang *et al.* (2009) |

# Appendix 2

**Two Chambered Mediator-less Microbial Fuel cells**

| Anode composition and Surface Area (SA) | Anode Contents | Cathode | Cathode Contents | Power Density $Wm^{-2}$ | External Load Ω | Reference |
|---|---|---|---|---|---|---|
| Stainless steel mesh SA=0.021329 $m^2$ | Anaerobic Sludge + Synthetic Wastewater (PBS pH 6.0) | Stainless steel mesh SA=0.017645 $m^2$ | Aerated Water ($O_2$) | 0.02722 | 60 Ω | Behera & Ghangrekar (2009) |
| Stainless steel mesh SA=0.021329 $m^2$ | Anaerobic Sludge + Synthetic Wastewater (PBS pH 8.0) | Stainless steel mesh SA=0.017645 $m^2$ | Aerated Water ($O_2$) | 0.12004 | 40 Ω | Behera & Ghangrekar (2009) |
| Stainless steel mesh SA=0.021329 $m^2$ | Biofilm + Synthetic Wastewater (PBS pH 6.0) | Stainless steel mesh SA=0.017645 $m^2$ | Aerated Water ($O_2$) | 0.02334 | 90 Ω | Behera & Ghangrekar (2009) |
| Stainless steel mesh SA=0.021329 $m^2$ | Biofilm + Synthetic Wastewater (PBS pH 8.0) | Stainless steel mesh SA=0.017645 $m^2$ | Aerated Water ($O_2$) | 0.06467 | 70 Ω | Behera & Ghangrekar (2009) |
| Stainless steel mesh SA=0.021329 $m^2$ | Anaerobic + Synthetic Wastewater (PBS pH 6.0) | Stainless steel mesh SA=0.017645 $m^2$ | $KMnO_4$ | 0.14962 | 60 Ω | Behera & Ghangrekar (2009) |
| Stainless steel mesh SA=0.021329 $m^2$ | Anaerobic + Synthetic Wastewater (PBS pH 8.0) | Stainless steel mesh SA=0.017645 $m^2$ | $KMnO_4$ | 0.54454 | 10 Ω | Behera & Ghangrekar (2009) |
| Platinum mesh SA=0.0196 $m^2$ | Sea water and $NaOH/H_2$ | Stainless Steel SA=0.00018 $m^2$ | Seawater biofilm | 0.325 | 10 Ω | Bergel *et al.* (2005) |
| Graphite Felt SA=0.061 $m^2$ (0.0033) m2 | *Shewanella oneidensis* (Suspended cells) | Graphite Felt 0.061 $m^2$ | Ferricyanide | 0.00023 (0.07) | 820 Ω | Biffinger *et al.* (2007) |
| Graphite Felt SA=0.061 $m^2$ (0.0033) m2 | *Shewanella oneidensis* (Suspended cells) | Graphite Felt 0.061 $m^2$ | PBS ($O_2$) | 0.0025 (0.75) | 820 Ω | Biffinger *et al.* (2007) |

| | | | | | | |
|---|---|---|---|---|---|---|
| Graphite Felt SA=0.061 $m^2$ (0.0033) m2 | *Shewanella oneidensis* (Suspended cells) | Graphite Felt 0.061 $m^2$ (+Pt) | PBS ($O_2$) | 0.0085 (2.5) | 820 Ω | Biffinger *et al.* (2007) |
| Graphite Felt SA=0.061 $m^2$ (0.0033) m2 | *Shewanella oneidensis* (Biofilm) | Graphite Felt 0.061 $m^2$ | Ferricyanide | 0.00052 (0.16) | 820 Ω | Biffinger *et al.* (2007) |
| Graphite Felt SA=0.061 $m^2$ (0.0033) m2 | *Shewanella oneidensis* (Biofilm) | Graphite Felt 0.061 $m^2$ (+Pt) | PBS ($O_2$) | 0.0049 (1.5) | 470 Ω | Biffinger *et al.* (2007) |
| Graphite electrode SA=0.0100 $m^2$ | *Desulfuromonas acetoxidans* + *Acetate* | Graphite electrode SA=0.0100 $m^2$ | Seawater | 0.014 | 500 Ω | Bond *et al.* (2002) |
| Graphite Rod SA=0.00612 $m^2$ | *Geobacter sulfurreducens* + *Acetate* | Graphite Rod SA=0.00612 $m^2$ | Tris buffer ($O_{2)}$ | 0.0165 | 500 Ω | Bond & Lovley (2003) |
| Graphite Rod SA=0.0062 $m^3$ | *Geothrix fermentans* + *Acetate* | Graphite Rod SA=0.0062 $m^3$ | Tris buffer ($O_{2)}$ | 0.00052 | 500 Ω | Bond & Lovley (2005) |
| Graphite Rod SA=0.0062 $m^3$ | *Geothrix fermentans* + *Propionate* | Graphite Rod SA=0.0062 $m^3$ | Tris buffer ($O_{2)}$ | 0.00775 | 500 Ω | Bond & Lovley (2005) |
| Graphite Rod SA=0.0062 $m^3$ | *Geothrix fermentans* + *Lactate* | Graphite Rod SA=0.0062 $m^3$ | Tris buffer ($O_{2)}$ | 0.00545 | 500Ω | Bond & Lovley (2005) |
| Graphite Rod SA=0.0062 $m^3$ | *Geothrix fermentans* + *Malate* | Graphite Rod SA=0.0062 $m^3$ | Tris buffer ($O_{2)}$ | 0.00098 | 500 Ω | Bond & Lovley (2005) |
| Graphite Rod SA=0.0062 $m^3$ | Geothrix fermentans + Succinate | Graphite Rod SA=0.0062 $m^3$ | Tris buffer ($O_{2)}$ | 0.00181 | 500 Ω | Bond & Lovley (2005) |
| Graphite Rod SA=0.0062 $m^3$ | Geothrix fermentans + Peptone | Graphite Rod SA=0.0062 $m^3$ | Tris buffer ($O_{2)}$ | 0.00013 | 500 Ω | Bond & Lovley (2005) |
| Graphite Rod SA=0.0062 $m^3$ | Geothrix fermentans + Yeast Extract | Graphite Rod SA=0.0062 $m^3$ | Tris buffer ($O_{2)}$ | 0.00007 | 500 Ω | Bond & Lovley (2005) |
| Graphite Rod SA=0.0065 $m^2$ | *Rhodoferax ferrireducens* | Graphite Rod SA=0.0065 $m^2$ | Tris buffer ($O_2$) | 0.00171 | 1000 Ω | Chaundhuri & Lovely (2003) |
| Graphite Felt SA=0.02 $m^2$ | *Rhodoferax ferrireducens* | Graphite Felt SA=0.02 $m^2$ | Tris buffer ($O_2$) | 0.01262 | 1000 Ω | Chaundhuri & Lovely (2003) |

| | | | | | | |
|---|---|---|---|---|---|---|
| Graphite Foam SA=0.0061 $m^2$ | *Rhodoferax ferrireducens* | Graphite Foam SA=0.0061 $m^2$ | Tris buffer ($O_2$) | 0.00147 | 1000 Ω | Chaundhuri & Lovely (2003) |
| Carbon cloth SA=0.0007 $m^2$ | *Acid mine drainage* | Carbon cloth SA=0.0007 $m^2$ (+Pt) | NaCl + $NaHCO_3$ ($O_2$) | 0.293 | 1000 Ω | Cheng *et al.* (2007) |
| Platinum SA=0.019 $m^2$ | *Escherichia coli* + *glucose* | Platinum SA=0.019 $m^2$ | Ferricyanide | 0.135 | 1000 Ω | Davis & Yarbrough (1962) |
| Platinum SA=0.019 $m^2$ | *Escherichia coli* + *glucose* | Platinum SA=0.019 $m^2$ | PBS + Glucose ($O_2$) | 0.1 V | 1000 Ω | Davis & Yarbrough (1962) |
| woven graphite SA=0.0026 $m^2$ | *Saccharomyces cerevisiae* + *Yeast Extract* | woven graphite SA=0.00152 $m^2$ | Ferricyanide | 0.01 | 16 KΩ | Ducommun *et al.* (2010) |
| Carbon veil SA=0.036 $m^2$ | Landfill leachate | Carbon veil SA=0.036 $m^2$ | PBS + Ferricyanide | 0.00138 | 500 Ω | Greenman *et al.* (2009) |
| Graphite Felt SA=0.00045 $m^2$ | Anaerobic digested + Formate | Graphite Felt SA=0.00045 $m^2$ | Water ($O_2$) | 0.022 | 10 Ω | Ha *et al.* (2008) |
| RVC SA=0.0097 $m^2$ | anaerobic sludge blanket | RVC SA=0.0194 $m^2$ | Ferricyanide | 0.17 | 66 Ω | He *et al.* (2005) |
| Graphite Felt SA=0.029 $m^2$ | Effulent from acetate fuel cell | Graphite Felt SA=0.029 $m^2$ | *Acidithiobacillus ferrooxidans* $Fe(III)_2(SO_4)_3$ | 0.86 | 1.5 Ω | Heijne *et al.* (2006) |
| Carbon paper SA=0.003825 $m^2$ | Anaerobic sludge + Humic Acids + Xylose | Carbon paper SA=0.003825 $m^2$ | Phosphate buffer + Ferricyanide | 0.069 | 180 Ω | Huang & Angelidaki (2008) |
| Carbon paper SA=0.003825 $m^2$ | Anaerobic sludge + Humic Acids + Glucose | Carbon paper SA=0.003825 $m^2$ | Phosphate buffer + Ferricyanide | 0.097 | 180 Ω | Huang & Angelidaki (2008) |
| Carbon paper SA=0.003825 $m^2$ | Digested manure wastewater + Xylose | Carbon paper SA=0.003825 $m^2$ | Phosphate buffer + Ferricyanide | 0.057 | 180 Ω | Huang & Angelidaki (2008) |
| Carbon Paper SA=0.00176$m^2$ | *Wastewater + PBS + Xylose* | Carbon Paper SA=0.00176 $m^2$ | Ferricyanide | 0.006 | 1000 Ω | Huang *et al.* (2008) |
| Carbon Paper SA=0.00176$m^2$ | *Wastewater + PBS + Xylose + Stiring* | Carbon Paper SA=0.00176 $m^2$ | Ferricyanide | 0.0084 | 1000 Ω | Huang *et al.* (2008) |

| | | | | | | |
|---|---|---|---|---|---|---|
| Carbon Felt SA=0.0004 $m^2$ | *Candida melibiosica* | Carbon Felt SA=0.0004 $m^2$ | Ferricyanide | 0.036 | 1250 Ω | Hubenova *et al.* (2010) |
| Carbon Felt (+Ni) SA=0.0004 $m^2$ | *Candida melibiosica* | Carbon Felt SA=0.0004 $m^2$ | Ferricyanide | 0.72 | 530 Ω | Hubenova *et al.* (2010) |
| Carbon fibre veil SA=0.018 $m^2$ | *Desulfovibro desulfuricans* + *Sucrose* | Carbon fibre veil SA=0.018 $m^2$ | Ferricyanide | 0.00253 | 10 KΩ | Ieropoulos *et al.* (2005) |
| Carbon fibre veil SA=0.018 $m^2$ | *Geobacter sulfurreducens* + *Acetate* | Carbon fibre veil SA=0.018 $m^2$ | Ferricyanide | 0.00118 | 1000 Ω | Ieropoulos *et al.* (2005) |
| Stainless steel SA=0.017 $m^2$ | Anarobic consortia + Synthetic wastewater | Three Graphite Rods SA=0.015 $m^2$ | $O_2$ | 0.00576 | 50 Ω | Jadhav & Ghangrekar (2009) |
| 8 Copper wires SA=0.00201 $m^2$ | Anaerobic consortium + Synthetic wastewater | 8 Gold covered Copper wires SA=0.00201 $m^2$ | Synthetic wastewater ($O_2$) | 0.0055 | 100 Ω | Kargi & Eker (2007) |
| Carbon Paper SA=0.001125 m2 | Anaerobic Sludge + Ethanol | Carbon Paper SA=0.001125 m2 (+ Pt) | Ethanol + PBS ($O_2$) | 0.08 | 1000 Ω | Kim *et al.* (2007) |
| Graphite Felt SA=0.000025 $m^2$ | *Shewanella putrefaciens* + Lactate | Graphite Felt SA=0.000025 $m^2$ | PBS ($O_2$) | 0.064 | 1000 Ω | Kim *et al.* (2002) |
| Carbon Cloth SA= 0.0006 m2 | Municipal Wastewater | Carbon Cloth SA= 0.0006 m2 | $NO_3^-$ | 0.069 | 1000 Ω | Li *et al.* (2010) |
| Carbon Cloth SA= 0.0006 m2 | Anaerobic treated Wastewater | Carbon Cloth SA= 0.0006 m2 | $NO_3^-$ | 1.292 | 1000 Ω | Li *et al.* (2010) |
| Carbon paper SA=0.0007 m2 | Wastewater | Carbon paper SA=0.0007 m2 (+ Pt) | Wastewater ($O_2$) | 0.262 | 218 Ω | Liu *et al.* (2004) |
| Graphite Rod SA=0.0065 $m^2$ | Synthetic Wastewater (Protein Rich) | Graphite Rod SA=0.0065 $m^2$ | PBS ($O_2$) | 0.00615 | 500 Ω | Liu *et al.* (2009) |
| Graphite Rod SA=0.0065 $m^2$ | Synthetic Wastewater (Acetate Rich) | Graphite Rod SA=0.0065 $m^2$ | PBS ($O_2$) | 0.0154 | 200 Ω | Liu *et al.* (2009) |
| Carbon Paper SA=0.0023 $m^2$ | Wastewater enriched consortia | Carbon cloth (+Pt) SA=0.00049 $m^2$ | ($O_2$) | 0.6 | 65 Ω | Logan *et al.* (2007) |

| | | | | | | |
|---|---|---|---|---|---|---|
| Graphite Fibre Brush SA=1.06 $m^2$ | Wastewater enriched consortia | Carbon cloth (+Pt) SA=0.00049 $m^2$ | ($O_2$) | 1.43 | 50 Ω | Logan *et al.* (2007) |
| Graphite Fibre Brush SA=0.22 $m^2$ | Wastewater enriched consortia | Carbon cloth (+Pt) SA=0.0007 $m^2$ | ($O_2$) | 2.4 | 50 Ω | Logan *et al.* (2007) |
| Carbon paper SA=0.001125 $m^2$ | Sediment + MSM + methane | Carbon paper SA=0.001125 $m^2$ (+ Pt) | MSM + Air ($O_2$) | 0.018 | 493 Ω | Logan *et al.* (2005) |
| Carbon paper SA=0.0025 $m^2$ | 1:1 Aerobic and Anarobic Sludge + Phenol | Carbon paper SA=0.0025 $m^2$ (+Pt) | ($O_2$) | 0.006 | 1000 Ω | Luo *et al.* (2009) |
| Carbon cloth SA=0.0028 $m^2$ | 1:1 Aerobic and Anarobic Sludge + Glucose + Phenol | Carbon cloth SA=0.0028 $m^2$ | PBS + Ferricyanide | 0.342 | 500 Ω | Luo *et al.* (2009) |
| Carbon fiber Brush SA=0.079 $m^2$ | Anaerobic and aerobic sludge + furfural | Carbon fiber Brush SA=0.079 $m^2$ | Ferricyanide | 0.64 | 1000 Ω | Luo *et al.* (2010) |
| Carbon fiber Brush SA=0.079 $m^2$ | Anaerobic and aerobic sludge + furfural | Carbon fiber Brush SA=0.079 $m^2$ | Ferricyanide | 0.72 | 1000 Ω | Luo *et al.* (2010) |
| Carbon cloth SA=0.0007 $m^2$ | Anaerobic and aerobic sludge + glucose | Carbon cloth SA=0.0007 $m^2$ (+Pt) | $O_2$ | 0.298 | 400 Ω | Luo *et al.* (2010) |
| Carbon cloth SA=0.0007 $m^2$ | Anaerobic and aerobic sludge + furfural | Carbon cloth SA=0.0007 $m^2$ (+Pt) | $O_2$ | 0.361 | 200 Ω | Luo *et al.* (2010) |
| Graphite rod with RVC SA=0.4 $m^2$ | *Klebsiella pneumoniae* | Active carbon with Ni mesh SA=0.0079 $m^2$ | PBS ($O_2$) | 0.0003 | 1000 Ω | Menicucci *et al.* (2006) |
| Carbon paper SA=0.0016 $m^2$ | Domestic wastewater | Carbon paper SA=0.0016 $m^2$ (+Pt) | $O_2$ | 0.218 | 180 Ω | Min & Angelidaki (2008) |
| Carbon paper SA=0.001125 $m^2$ | Swine Wastewater | Carbon paper SA=0.001125 $m^2$ (+Pt) | $O_2$ | 0.045 | 1000 Ω | Min *et al.* (2005) |
| Carbon paper SA=0.0001 $m^2$ | Domestic Wastewater + Acetate | Carbon Cloth SA= 0.0006 $m^2$ | Wastewater ($O_2$) | 0.309 | 33 Ω | Min & Logan (2004) |

| | | | | | | |
|---|---|---|---|---|---|---|
| Carbon paper SA=0.001125 $m^2$ | anaerobic sludge blanket + Acetate | Carbon paper SA=0.001125 $m^2$ (+Pt) | ($O_2$) | 0.16 | 1125 Ω | Oh *et al.*(2004) |
| Carbon paper SA=0.001125 $m^2$ | anaerobic sludge blanket + Acetate | Carbon paper SA=0.001125 $m^2$ (+Pt) | Ferricyanide | 0.0862 | 1077Ω | Oh *et al.*(2004) |
| Carbon paper SA=0.001125 $m^2$ | Anaerobic sludge + Cereal Wastewater | Carbon paper SA=0.001125 $m^2$ (+Pt) | Nutrient Mineral Buffer ($O_2$) | 0.081 | 500 Ω | Oh & Logan (2005) |
| Carbon paper SA=0.001125 $m^2$ | anaerobic sludge blanket + Acetate | Carbon paper SA=0.001125 $m^2$ (+Pt) | ($O_2$) | .39/Sa | 178 Ω | Oh & Logan (2006) |
| Carbon paper SA=0.001125 $m^2$ | anaerobic sludge blanket + Acetate | Carbon paper SA=0.001125 $m^2$ (+Pt) | Ferricyanide | .79/SA | 178Ω | Oh & Logan (2006) |
| Neutral red Graphite SA=0.042 $m^2$ | *Escherichia coli* | Graphite plate SA=0.042 $m^1$ | ($O_2$) | 0.004 | 1000 Ω | Park *et al.* (2000) |
| Graphite Rod SA=0.0016 cm2 | Activated Sludge and Chocolate Wastewater | Graphite Rod SA=0.0016 cm2 | Phosphate buffer ($O_2$) | 0.58 | 100 Ω | Patil *et al.* (2009) |
| Graphite Rod SA=0.0016 cm2 | Activated Sludge and Chocolate Wastewater | Graphite Rod SA=0.0016 cm2 | Chocolate Wastewater | 1.02 | 100 Ω | Patil *et al.* (2009) |
| Graphite Rod SA=0.0016 cm2 | Activated Sludge and Chocolate Wastewater | Graphite Rod SA=0.0016 cm2 | Ferricyanide | 1.5 | 100 Ω | Patil *et al.* (2009) |
| Graphite plate SA=0.002 $m^2$ | Microbial consortia (Acetate) | Graphite Granuals (diameters 1.5 - 5 mm) | Ferricyanide | 462 | 20 Ω | Pham *et al.*(2009) |
| Rod Anode SA=0.005 $m^2$ | *Pseudomonas Aerugenosa* | Graphite SA=0.005 $m^2$ | Ferricyanide | 0.00121 | 20 Ω | Rabaey *et al.* (2005) |
| Rod Anode SA=0.005 $m^2$ | *Escherichia coli* | Graphite SA=0.005 $m^2$ | Ferricyanide | 0.00085 | 20 Ω | Rabaey *et al.* (2005) |
| Rod Anode SA=0.005 $m^2$ | *Lactobacillus amylovorus* | Graphite SA=0.005 $m^2$ | Ferricyanide | 0.00027 | 20 Ω | Rabaey *et al.* (2005) |
| Rod Anode SA=0.005 $m^2$ | *Alcaligenes faecalis* | Graphite SA=0.005 $m^2$ | Ferricyanide | 0.00044 | 20 Ω | Rabaey *et al.* (2005) |
| Rod Anode SA=0.005 $m^2$ | *Enterococcus faecium* | Graphite SA=0.005 $m^2$ | Ferricyanide | 0.00029 | 20 Ω | Rabaey *et al.* (2005) |
| Graphite SA=0.005 $m^2$ | Enriched sludge | Graphite SA=0.005 $m^2$ | Ferricyanide | 3.6 | 20 Ω | Rabaey *et al.* (2003) |

| | | | | | | |
|---|---|---|---|---|---|---|
| Graphite SA=0.005 $m^2$ | Enriched sludge (suspended cells) | Graphite SA=0.005 $m^2$ | Ferricyanide | 4.31 | 100 Ω | Rabaey *et al.* (2004) |
| Graphite SA=0.005 $m^2$ | Enriched sludge (Biofilm) | Graphite SA=0.005 $m^2$ | Ferricyanide | 3.63 | 100 Ω | Rabaey *et al.* (2004) |
| Granualar Graphite SA=0.147-0.4896 $m^2$ | Enriched sludge cells + Synthetic Influent | Woven Graphite | Ferricyanide | Between 0.13-0.039 | 20 Ω | Rabaey *et al.* (2005) |
| Ammonia treated Carbon Cloth SA=0.000113 $m^2$ | *Enterobacter cloacae* ATCC 13047$^T$ + Growth medium + Plant Cellulose | Five tow strands of 15-cm-long carbon fiber | Ferricyanide | 0.0054 | 5000 Ω | Rezaei*et al.* (2009) |
| Ammonia treated Carbon Cloth SA=0.000113 $m^2$ | *Enterobacter cloacae FR* + Growth medium + Plant Cellulose | Five tow strands of 15-cm-long carbon fiber | Ferricyanide | 0.0049 | 5000 Ω | Rezaei*et al.* (2009) |
| Ammonia treated Carbon Cloth SA=0.000113 $m^2$ | *Enterobacter cloacae (Both)* + Growth medium + Plant Cellulose | Five tow strands of 15-cm-long carbon fiber | Ferricyanide | 0.018 | 5000 Ω | Rezaei*et al.* (2009) |
| Ammonia treated Carbon Cloth SA=0.000113 $m^2$ | *Enterobacter cloacae* ATCC 13047$^T$ + Growth medium + Sucrose | Five tow strands of 15-cm-long carbon fiber | Ferricyanide | 0.027 | 1000 Ω | Rezaei*et al.* (2009) |
| Ammonia treated Carbon Cloth SA=0.000113 $m^2$ | *Enterobacter cloacae* ATCC 13047$^T$ + Growth medium + Glycerol | Five tow strands of 15-cm-long carbon fiber | Ferricyanide | 0.0267 | 1000 Ω | Rezaei*et al.* (2009) |
| Ammonia treated Carbon Cloth SA=0.000113 $m^2$ | *Enterobacter cloacae* ATCC 13047$^T$ + Growth medium + Glucose | Five tow strands of 15-cm-long carbon fiber | Ferricyanide | 0.0122 | 1000 Ω | Rezaei*et al.* (2009) |
| Ammonia treated Carbon Cloth SA=0.000113 $m^2$ | *Enterobacter cloacae* ATCC 13047$^T$ + Growth medium + Glucosamine | Five tow strands of 15-cm-long carbon fiber | Ferricyanide | 0.0107 | 1000 Ω | Rezaei*et al.* (2009) |

| | | | | | | |
|---|---|---|---|---|---|---|
| Ammonia treated Carbon Cloth SA=0.000113 $m^2$ | *Enterobacter cloacae* ATCC $13047^T$ + Growth medium + Lactate | Five tow strands of 15-cm-long carbon fiber | Ferricyanide | 0.0004 | 1000 Ω | Rezaei*et al.* (2009) |
| Ammonia treated Carbon Cloth SA=0.000113 $m^2$ | *Enterobacter cloacae* ATCC $13047^T$ + Growth medium + Acetate | Five tow strands of 15-cm-long carbon fiber | Ferricyanide | 0 | 1000 Ω | Rezaei*et al.* (2009) |
| Graphite plate SA=0.00348 $m^2$ | rumen microorganisms + Cellulose | Graphite plate SA=0.00348 $m^2$ | Ferricyanide | 0.132 | 211 Ω | Rismani-Yazdi *et al.* (2007) |
| Graphite cylinder SA=0.002 $m^2$ | Domestic wastewater | Graphite bar SA=0.002 $m^2$ | ($O_2$) | 0.005 | 125 Ω | Rodrigo *et al.* (2007) |
| Graphite cylinder SA=0.002 $m^2$ | Domestic wastewater | Graphite bar SA=0.002 $m^2$ | ($O_2$) | 0.025 | 10 Ω | Rodrigo *et al.* (2007) |
| Carbon Felt SA=0.00025 $m^2$ | *Desulfovibrio vulgaris* ($H_2$) | Carbon Felt SA=0.00025 $m^2$ | BOD + $ABTS^{2-}$ ($O_2$) | 3.6 | 1100 Ω | Tsujimura *et al.* (2001) |
| Perferated Graphite SA=0.0025 $m^2$ | Enriched anaerobic consortia + Chemical Wastewater | Plain Graphite SA=0.0025 $m^2$ | Ferricyanide | 0.44 | 100 Ω | Venkata Mohan *et al.* (2008) |
| Plain Graphite SA=0.005 $m^2$ | Domestic wastewater + Anaerobic Sludge | Plain Graphite SA=0.005 $m^2$ | Ferricyanide | 0.08 | 1000 Ω | Wang *et al.* (2009) |
| Carbon felt + graphite rods SA=0.0199 $m^2$ | *Brewery Wastewater* | Carbon Felt SA=0.0036 $m^2$ | Biofilm ($O_2$) | 0.0075 | 300 Ω | Wen *et al.* (2010) |
| Carbon paper SA=0.001 $m^2$ | Anaerobic sludge | Carbon cloth SA=0.001 $m^2$ | $KMnO_4$ | 0.1156 | 4000 Ω | You *et al.* (2006) |
| Carbon paper SA=0.001 $m^2$ | Anaerobic sludge | Carbon cloth SA=0.001 $m^2$ | Ferricyanide | 0.0256 | 4000 Ω | You *et al.* (2006) |
| Carbon paper SA=0.001 $m^2$ | Anaerobic sludge | Carbon cloth SA=0.001 $m^2$ | $O_2$ | 0.0102 | 11 KΩ | You *et al.* (2006) |
| Carbon paper SA=0.001 $m^2$ | Anaerobic sludge | Carbon cloth SA=0.001 $m^2$ (+Pt) | $O_2$ | 0.0034 | 8500 Ω | You *et al.* (2006) |
| Carbon paper SA=0.001 $m^2$ | Anaerobic sludge | Carbon cloth SA=0.004 $m^2$ | $KMnO_4$ | 3.986 | 110 Ω | You *et al.* (2006) |

| | | | | | | |
|---|---|---|---|---|---|---|
| Carbon paper SA=0.001 $m^2$ | Anaerobic sludge | Carbon cloth SA=0.004 $m^2$ | Ferricyanide | 1.231 | 110 Ω | You *et al.* (2006) |
| Carbon SA=0.005 $m^2$ | Synechocystis PCC-6803 biofilm (Light) | Carbon (+Pt) SA=0.00096 $m^2$ | Water ($O_2$) | 0.35 | 1000 Ω | Zou *et al.* (2009) |
| Carbon (Poly A) SA=0.005 $m^2$ | Synechocystis PCC-6803 biofilm (Light) | Carbon (+Pt) SA=0.00096 $m^2$ | Water ($O_2$) | 0.95 | 1000 Ω | Zou *et al.* (2009) |
| Carbon (Poly P) SA=0.005 $m^2$ | Synechocystis PCC-6803 biofilm (Light) | Carbon (+Pt) SA=0.00096 $m^2$ | Water ($O_2$) | 1.3 | 1000 Ω | Zou *et al.* (2009) |

# Appendix 3

**Two Chambered Meditated Microbial Fuel cells**

| Anode composition and Surface Area (SA) | Anode Contents | Mediator | Cathode | Cathode Contents | Power Density $Wm^{-2}$ | External Load Ω | Reference |
|---|---|---|---|---|---|---|---|
| Graphite Felt SA=0.00495 $m^2$ | *Proteus vulgaris* | HNQ | PCP SA=0.002025 $m^2$ | Ferricyanide in Phosphate Buffer | 0.032 | 1000 Ω | Allen & Bennetto (1993) |
| RVC SA=0.08 m2 | *Proteus vulgaris + Sucrose* | Thionin | Platinum Foil SA=0.0004 $m^2$ | Ferricyanide | 0.015 | 100 Ω | Bennetto *et al.* (1985) |
| Graphite electrode SA=0.0100 $m^2$ | *Desulfuromonas acetoxidans + Acetate* | *AQDS* | Graphite electrode SA=0.0100 $m^2$ | Seawater | 0.0174 | 500 Ω | Bond *et al.* (2002) |
| RVC SA=0.0009 $m^2$ | *Proteus vulgaris + glucose in PBS* | Thionin | Platinum plate SA=0.0009 $m^2$ | Ferricyanide | 0.305 | 560 Ω | Choi *et al.* (2003) |
| Platinum SA=0.019 $m^2$ | *Nocardia + Glucose* | MB | Platinum SA=0.019 $m^2$ | PBS + Glucose ($O_2$) | 0.03 V | 1000 Ω | Davis & Yarbrough (1962) |
| Carbon Felt SA=0.0004 $m^2$ | *Candida melibiosica* | MB | Carbon Felt SA=0.0004 $m^2$ | Ferricyanide | 0.036 | 1250 Ω | Hubenova *et al.* (2010) |
| Carbon fibre veil SA=0.018 $m^2$ | *Escherichia coli + glucose* | MB | Carbon fibre veil SA=0.018 $m^2$ | Ferricyanide | 0.0018 | 10 KΩ | Ieropoulos *et al.* (2005) |
| Carbon fibre veil SA=0.018 $m^2$ | *Escherichia coli + glucose* | HNQ | Carbon fibre veil SA=0.018 $m^2$ | Ferricyanide | 0.0017 | 10 KΩ | Ieropoulos *et al.* (2005) |
| Carbon fibre veil SA=0.018 $m^2$ | *Escherichia coli + glucose* | Thionin | Carbon fibre veil SA=0.018 $m^2$ | Ferricyanide | 0.0016 | 10 KΩ | Ieropoulos *et al.* (2005) |
| Carbon fibre veil SA=0.018 $m^2$ | *Escherichia coli + glucose* | MelB | Carbon fibre veil SA=0.018 $m^2$ | Ferricyanide | 0.0015 | 10 KΩ | Ieropoulos *et al.* (2005) |
| Carbon fibre veil SA=0.018 $m^2$ | *Escherichia coli + glucose* | Neutral Red | Carbon fibre veil SA=0.018 $m^2$ | Ferricyanide | 0.0007 | 10 KΩ | Ieropoulos *et al.* (2005) |
| RVC SA=0.00304 | *Proteus vulgaris* | Thionin | Platinum SA=0.0016 $m^2$ | Ferricyanide | 0.0526 | 1000 Ω | Kim *et al.* (2000) |

| | | | | | | | |
|---|---|---|---|---|---|---|---|
| RVC SA=0.00304 | *Proteus vulgaris* | Thionin | Platinum SA=0.0016 $m^2$ | Ferricyanide | 0.058 | 1000 Ω | Kim *et al.* (2000) |
| Graphite rod SA=0.00099 $m^2$ | *Enterobacter cloacae* | MV | Graphite plate SA=0.0015 $m^2$ | PBS ($O_2$) | 0.236 | 500 Ω | Mohan *et al.* (2008) |
| **Woven Graphite felt SA=5.64 $m^2$** | *Escherichia coli + glucose* | Neutral Red | **Woven Graphite felt SA=564 $m^2$** | Ferricyanide in Phosphate Buffer | 0.0005 | 120 Ω | Park & Zeikus (2000) |
| **Woven Graphite felt SA=5.64 $m^2$** | *Actinobacillus succinogenes* | Neutral Red | **Woven Graphite felt SA=564 $m^2$** | Ferricyanide in Phosphate Buffer | 0.0006 | 1000 Ω | Park & Zeikus (2000) |
| **Woven Graphite felt SA=5.64 $m^2$** | Sewage sludge | Neutral Red | **Woven Graphite felt SA=564 $m^2$** | Ferricyanide in Phosphate Buffer | 2E-05 | 1000 Ω | Park & Zeikus (2000) |
| Rod Anode SA=0.005 $m^2$ | *Pseudomonas Aerugenosa* | Pyocyanin | Graphite SA=0.005 $m^2$ | Ferricyanide | 0.0027 | 20 Ω | Rabaey *et al.* (2005) |
| Rod Anode SA=0.005 $m^2$ | *Escherichia coli* | Pyocyanin | Graphite SA=0.005 $m^2$ | Ferricyanide | 0.0002 | 20 Ω | Rabaey *et al.* (2005) |
| Rod Anode SA=0.005 $m^2$ | *Lactobacillus amylovorus* | Pyocyanin | Graphite SA=0.005 $m^2$ | Ferricyanide | 0.0011 | 20 Ω | Rabaey *et al.* (2005) |
| Rod Anode SA=0.005 $m^2$ | *Alcaligenes faecalis* | Pyocyanin | Graphite SA=0.005 $m^2$ | Ferricyanide | 0.0005 | 20 Ω | Rabaey *et al.* (2005) |
| Rod Anode SA=0.005 $m^2$ | *Enterococcus faecium* | Pyocyanin | Graphite SA=0.005 $m^2$ | Ferricyanide | 0.004 | 20 Ω | Rabaey *et al.* (2005) |
| Graphite rod with RVC SA=0.4 $m^2$ | *Klebsiella pneumoniae* | HNQ | Graphite rod with RVC SA=0.4 $m^2$ | *Leptothrix discophora* *($O_2$)* | 0.0039 | 50 Ω | Rhoads *et al.* (2005) |
| Graphite rod with RVC SA=0.4 $m^2$ | *Klebsiella pneumoniae* | HNQ | Graphite rod with RVC SA=0.4 $m^2$ | *Leptothrix discophora* *($Mn^{2+}$)* | 0.1267 | 50 Ω | Rhoads *et al.* (2005) |
| Graphite Disk SA=0.183 $m^2$ | *Desulfuromonas acetoxidans + Acetate* | AQDS | Graphite Disk SA=0.183 $m^2$ | Ocean water (O2) | 0.02 | 500 Ω | Tender *et al.* (2002) |
| RVC SA=0.08 $m^2$ | *Proteus vulgaris + Glucose* | Thionin | Platinum Foil SA=0.0004 $m^2$ | Ferricyanide | 0.015 | 100 Ω | Thurston *et al.* (1985) |

| | | | | | | | |
|---|---|---|---|---|---|---|---|
| Carbon SA=0.005 $m^2$ | Synechocystis PCC-6803 biofilm (Light) | HNQ | Carbon (+Pt) SA=0.00096 $m^2$ | Water ($O_2$) | 0.59 | 1000 Ω | Zou *et al.* (2009) |
| Carbon (Poly A) SA=0.005 $m^2$ | Synechocystis PCC-6803 biofilm (Light) | HNQ | Carbon (+Pt) SA=0.00096 $m^2$ | Water ($O_2$) | 1.47 | 1000 Ω | Zou *et al.* (2009) |
| Carbon (Poly P) SA=0.005 $m^2$ | Synechocystis PCC-6803 biofilm (Light) | HNQ | Carbon (+Pt) SA=0.00096 $m^2$ | Water ($O_2$) | 1.56 | 1000 Ω | Zou *et al.* (2009) |

Legend: Methylene Blue (MB), Neutral Red (NR), 2-hydroxy-1,4-naphthoquinone (HNQ), Meldola's blue (MelB).

# Appendix 4

**Single Chamber Microbial Fuel Cells**

| Anode | Inoculum | Liquid | Cathode | Power Density $Wm^{-2}$ | External Load Ω | Reference |
|---|---|---|---|---|---|---|
| Glassy Carbon SA=0.016 $m^2$ | Activated sludge blanket | Synthetic wastewater + Glucose | Glassy Carbon SA=0.016 $m^2$ | 0.0734 | 250 Ω | Aldrovandi *et al.* (2009) |
| Carbon Cloth SA=0.0002 $m^2$ | Acetate acclimatised consortium | Glucose | Carbon Cloth + PTFE + Pt SA=0.0007 $m^2$ | 2.16 | 120 Ω | Catal *et al.* (2008) |
| Carbon Cloth SA=0.0002 $m^2$ | Acetate acclimatised consortium | Galactose | Carbon Cloth + PTFE + Pt SA=0.0007 $m^2$ | 2.09 | 120 Ω | Catal *et al.* (2008) |
| Carbon Cloth SA=0.0002 $m^2$ | Acetate acclimatised consortium | Fructose | Carbon Cloth + PTFE + Pt SA=0.0007 $m^2$ | 1.81 | 120 Ω | Catal *et al.* (2008) |
| Carbon Cloth SA=0.0002 $m^2$ | Acetate acclimatised consortium | Fuctose | Carbon Cloth + PTFE + Pt SA=0.0007 $m^2$ | 1.76 | 120 Ω | Catal *et al.* (2008) |
| Carbon Cloth SA=0.0002 $m^2$ | Acetate acclimatised consortium | Rhamnose | Carbon Cloth + PTFE + Pt SA=0.0007 $m^2$ | 1.32 | 120 Ω | Catal *et al.* (2008) |
| Carbon Cloth SA=0.0002 $m^2$ | Acetate acclimatised consortium | Mannose | Carbon Cloth + PTFE + Pt SA=0.0007 $m^2$ | 1.24 | 120 Ω | Catal *et al.* (2008) |
| Carbon Cloth SA=0.0002 $m^2$ | Acetate acclimatised consortium | Xylose | Carbon Cloth + PTFE + Pt SA=0.0007 $m^2$ | 2.33 | 120 Ω | Catal *et al.* (2008) |
| Carbon Cloth SA=0.0002 $m^2$ | Acetate acclimatised consortium | Arabinose | Carbon Cloth + PTFE + Pt SA=0.0007 $m^2$ | 2.03 | 120 Ω | Catal *et al.* (2008) |

| | | | | | | |
|---|---|---|---|---|---|---|
| Carbon Cloth SA=0.0002 $m^2$ | Acetate acclimatised consortium | Ribose | Carbon Cloth + PTFE + Pt SA=0.0007 $m^2$ | 1.52 | 120 Ω | Catal *et al.* (2008) |
| Carbon Cloth SA=0.0002 $m^2$ | Acetate acclimatised consortium | Galacturonic acid | Carbon Cloth + PTFE + Pt SA=0.0007 $m^2$ | 1.48 | 120 Ω | Catal *et al.* (2008) |
| Carbon Cloth SA=0.0002 $m^2$ | Acetate acclimatised consortium | Glucuronic acid | Carbon Cloth + PTFE + Pt SA=0.0007 $m^2$ | 2.77 | 120 Ω | Catal *et al.* (2008) |
| Carbon Cloth SA=0.0002 $m^2$ | Acetate acclimatised consortium | Gluconic acid | Carbon Cloth + PTFE + Pt SA=0.0007 $m^2$ | 2.05 | 120 Ω | Catal *et al.* (2008) |
| Carbon Cloth SA=0.0002 $m^2$ | Acetate acclimatised consortium | Xylitol | Carbon Cloth + PTFE + Pt SA=0.0007 $m^2$ | 2.11 | 120 Ω | Catal *et al.* (2008) |
| Carbon Cloth SA=0.0002 $m^2$ | Acetate acclimatised consortium | Arabitol | Carbon Cloth + PTFE + Pt SA=0.0007 $m^2$ | 2.03 | 120 Ω | Catal *et al.* (2008) |
| Carbon Cloth SA=0.0002 $m^2$ | Acetate acclimatised consortium | Ribitol | Carbon Cloth + PTFE + Pt SA=0.0007 $m^2$ | 2.35 | 120 Ω | Catal *et al.* (2008) |
| Carbon Cloth SA=0.0002 $m^2$ | Acetate acclimatised consortium | Galactitol | Carbon Cloth + PTFE + Pt SA=0.0007 $m^2$ | 2.65 | 120 Ω | Catal *et al.* (2008) |
| Carbon Cloth SA=0.0002 $m^2$ | Acetate acclimatised consortium | Mannitol | Carbon Cloth + PTFE + Pt SA=0.0007 $m^2$ | 1.49 | 120 Ω | Catal *et al.* (2008) |
| Carbon Cloth SA=0.0002 $m^2$ | Acetate acclimatised consortium | Sorbitol | Carbon Cloth + PTFE + Pt SA=0.0007 $m^2$ | 1.69 | 120 Ω | Catal *et al.* (2008) |
| Carbon Cloth SA=0.0007 $m^2$ | N/A | Brewary Wastewater + PBS | Cabon Cloth SA=0.0075 $m^2$ (+Pt) | 0.528 | 1000 Ω | Feng *et al.* (2008) |

| | | | | | | |
|---|---|---|---|---|---|---|
| Carbon Cloth SA=0.01 $m^2$ | River Sediment | *River water* | Platinum coated RVC SA=0.0086m2 | 0.025 | 1000 Ω | He *et al.* (2007) |
| Carbon Paper SA=0.000706 $m^2$ | Wastewater | Bovine Serum Album | Carbon paper (+ Pt) | 0.354 | 1000 Ω | Heilmann & Logan (2006) |
| Carbon Paper SA=0.000706 $m^2$ | Wastewater | Peptone | Carbon paper (+ Pt) | 0.269 | 1000 Ω | Heilmann & Logan (2006) |
| Carbon paper SA=0.0005 $m^2$ | Anaerobic Sludge | Wastewater Biofilm ($O_2$) | Tory carbon paper + Pt SA=0.0005 $m^2$ | 0.3 | 1400 Ω | Hu (2008) |
| Carbon paper SA=0.0005 $m^2$ | Washed Sludge + glucose | Wastewater Biofilm ($O_2$) | Tory carbon paper + Pt SA=0.0005 $m^2$ | 0.129 | 1400 Ω | Hu (2008) |
| Graphite felt SA=0.0465 $m^2$ | *Activated sludge* | Artificial wastewater ($O_2$) | Graphite felt SA=0.0089 $m^2$ | 0.0013 | 200 Ω | Huang & Logan (2008) |
| Carbon Paper SA=0.0007 $m^2$ | *Anaerobic Sludge + Ethanol* | Ethanol + PBS ($O_2$) | Carbon Paper SA=0.0007 $m^2$ (+ Pt) | 0.976 | 1000 Ω | Jang *et al.* (2004) |
| Carbon Felt SA=0.00188 $m^2$ | Paper Wastewater | Wastewater ($O_2$) | Carbon cloth + Pt | 0.144 | 993 Ω | Kim *et al.* (2007) |
| Carbon Felt SA=0.00188 $m^2$ | Paper Wastewater + 0.1 M PBS | Wastewater ($O_2$) | Carbon cloth + Pt | 0.672 | 292 Ω | Kim *et al.* (2007) |
| Carbon Cloth SA= 0.0006 $m^2$ | N/A | Anaerobic treated Wastewater ($NO_3^-$) | Carbon Cloth SA= 0.0006 $m^2$ | 0.23 | 1000 Ω | Li *et al.* (2010) |
| Granular-activated carbon SA= 0.0006 $m^2$ | N/A | Anaerobic treated Wastewater ($NO_3^-$) | Carbon Cloth SA= 0.0006 $m^2$ | 0.784 | 1000 Ω | Li *et al.* (2010) |
| Carbon paper SA=0.0007 m2 | N/A | Wastewater ($O_2$) | Carbon paper SA=0.0007 m2 (+Pt) | 0.494 | 465 Ω | Liu & Logan (2004) |
| Graphite Rods SA=0.245 $m^2$ | | Wastewater ($O_2$) | Cathode/PEM | 0.125 | 69 Ω | Liu *et al.* (2004) |

| | | | | | | |
|---|---|---|---|---|---|---|
| Carbon paper SA=0.001 m2 | Domestic Wastewater + 0.4 mM NaCl | Wastewater ($O_2$) | Carbon paper + Pt | 1.33 | 79 Ω | Liu *et al.* (2005) |
| Carbon paper SA=0.001 m2 | Domestic Wastewater + Acetate | Carbon paper + Pt | Wastewater ($O_2$) | 0.661 | 218 Ω | Liu *et al.* (2005) |
| Carbon paper SA=0.001 m2 | Domestic Wastewater + butyrate | Carbon paper + Pt | Wastewater ($O_2$) | 0.349 | 1000 Ω | Liu *et al.* (2005) |
| Carbon paper SA=0.0025 $m^2$ | Starch processed wastewater | Wastewater ($O_2$) | Carbon paper + Pt SA=0.0017 $m^2$ | 0.2394 | 120 Ω | Lu *et al.* (2009) |
| Carbon paper SA=0.001125 $m^2$ | Swine Wastewater | Wastewater ($O_2$) | Carbon paper SA=0.001125 $m^2$ (+ Pt) | 0.261 | 200 Ω | Min *et al.* (2005) |
| Carbon paper SA=0.00071 $m^2$ | Cereal Wastewater | Proponate | Carbon paper SA=0.00071 $m^2$ (+ Pt) | 0.067 | 100 Ω | Oh & Logan (2005) |
| Neutral red woven graphite SA=1.27 $m^2$ (0.008 $m^2$) | *N/A* | *Shewanella putrefaciens* + *Lactate* | $Fe^{3+}$ graphite SA=0.05 $m^2$ | 0.00001 (0.015) | 1000 Ω | Park & Zeikus (2002) |
| $Mn^{4+}$ graphite SA=0.008 $m^2$ | *N/A* | *Shewanella putrefaciens* + *Lactate* | $Fe^{3+}$ graphite SA=0.05 $m^2$ | 0.000013 (0.021) | 1000 Ω | Park & Zeikus (2002) |
| woven graphite SA=1.27 $m^2$ (0.008 $m^2$) | Sewage sludge | Sewage sludge | woven graphite SA=1.27 $m^2$ (0.008 $m^2$) | 0.00017 (0.0255) | 1765 Ω | Park & Zeikus (2003) |
| woven graphite SA=1.27 $m^2$ (0.008 $m^2$) | Sewage sludge | Sewage sludge | $Fe^{3+}$ graphite SA=0.04 $m^2$ | 0.00065 (0.0975) | 462 Ω | Park & Zeikus (2003) |
| woven graphite SA=1.27 $m^2$ (0.008 $m^2$) | *N/A* | *Escherichia coli* | woven graphite SA=1.27 $m^2$ (0.008 $m^2$) | 0.0003 (0.045) | 1000 Ω | Park & Zeikus (2003) |
| woven graphite SA=1.27 $m^2$ (0.008 $m^2$) | *N/A* | *Escherichia coli* | $Fe^{3+}$ graphite SA=0.04 $m^2$ | 0.00044 (0.0656) | 233 Ω | Park & Zeikus (2003) |

| | | | | | | |
|---|---|---|---|---|---|---|
| Neutral red woven graphite SA=1.27 $m^2$ (0.008 $m^2$) | Sewage sludge | Sewage sludge | $Fe^{3+}$ graphite SA=0.04 $m^2$ | 0.00532 (0.8446) | 53 Ω | Park & Zeikus (2003) |
| $Mn^{4+}$ graphite SA=0.008 $m^2$ | Sewage sludge | Sewage sludge | $Fe^{3+}$ graphite SA=0.04 $m^2$ | 0.788 | 32 Ω | Park & Zeikus (2003) |
| Neutral red woven graphite SA=1.27 $m^2$ (0.008 $m^2$) | *Escherichia coli* | *Escherichia coli* | $Fe^{3+}$ graphite SA=0.04 $m^2$ | 0.0012 (0.1524) | 106 Ω | Park & Zeikus (2003) |
| $Mn^{4+}$ graphite SA=0.008 $m^2$ | *Escherichia coli* | *Escherichia coli* | $Fe^{3+}$ graphite SA=0.04 $m^2$ | 0.091 | 108 Ω | Park & Zeikus (2003) |
| Platinum mesh SA=0.002 $m^2$ | Marine sediment | Platinum mesh SA=0.002 $m^2$ | Ocean water (O2) | 0.014 | 1500 Ω | Reimers *et al.* (2001) |
| Graphite fibre brushes SA=0.000707 | *Chlorella vulgaris,* | Pt SA=0.000707 | $O_2$ | 0.98 | 350 Ω | Velasquez-Orta *et al.* (2009) |
| Graphite fibre brushes SA=0.000707 | *Ulva lactuca* | Pt SA=0.000707 | $O_2$ | 0.76 | 270 Ω | Velasquez-Orta *et al.* (2009) |
| Carbon Cloth SA=0.0256 $m^2$ | Manure | Wastewater ($O_2$) | Carbon Cloth SA=0.0256 $m^2$ | 0.005 | 350 Ω | Scott & Murano (2007) |
| Carbon Cloth SA=0.0256 $m^2$ | Manure | Wastewater ($O_2$) | Carbon Cloth SA=0.0256 $m^2$ (+Pt) | 0.011 | 350 Ω | Scott & Murano (2007) |
| Carbon Cloth SA=0.0006 $m^2$ | Anaerobic Sludge blanket + Glucose | Air ($O_2$) | Carbon Cloth SA=0.0006 $m^2$ (+Pt) | 0.401 | 1000 Ω | Sharma & Li (2010) |
| Carbon Cloth SA=0.0006 $m^2$ | anaerobic sludge blanket + Acetate | Air ($O_2$) | Carbon Cloth SA=0.0006 $m^2$ (+Pt) | 0.368 | 1000 Ω | Sharma & Li (2010) |
| Carbon Cloth SA=0.0006 $m^2$ | Anaerobic Sludge blanket + Ethanol | Air ($O_2$) | Carbon Cloth SA=0.0006 $m^2$ (+Pt) | 0.302 | 1000 Ω | Sharma & Li (2010) |
| Carbon paper SA=0.0036 $m^2$ | Anaerobic Sludge (Glucose) | Aerobic Sludge (Glucose) | Carbon Cloth + PTFE + Pt SA=0.0036 $m^2$ | 0.162 | 500Ω | Sun *et al.* (2009) |

| | | | | | | |
|---|---|---|---|---|---|---|
| Carbon paper SA=0.0036 $m^2$ | Anaerobic Sludge (Acetate) | Aerobic Sludge (Acetate) | Carbon Cloth + PTFE + Pt SA=0.0036 $m^2$ | 0.064 | 500Ω | Sun *et al.* (2009) |
| Carbon paper SA=0.0036 $m^2$ | Anaerobic Sludge (Sucrose) | Aerobic Sludge (Sucrose) | Carbon Cloth + PTFE + Pt SA=0.0036 $m^2$ | 0.139 | 500Ω | Sun *et al.* (2009) |
| Carbon paper SA=0.0036 $m^2$ | Anaerobic Sludge (Confectionery wastewater) | Aerobic Sludge (Confectionery wastewater) | Carbon Cloth + PTFE + Pt SA=0.0036 $m^2$ | 0.103 | 500Ω | Sun *et al.* (2009) |
| Graphite Disk SA=0.183 $m^2$ | *Desulfuromonas acetoxidans* + *Acetate* | Ocean water (O2) | Graphite Disk SA=0.183 $m^2$ | 0.02 | 500 Ω | Tender *et al.* (2002) |

# Appendix 5

**Environmental Microbial Fuel Cells**

| Anode composition and Surface Area (SA) | Anode Contents | Cathode composition and Surface Area (SA) | Cathode Contents | Power Density $Wm^{-2}$ | Notes | External Load Ω | Reference |
|---|---|---|---|---|---|---|---|
| AQDS modified Graphite disks SA=0.457$m^2$ | Marine sediment | Graphite disks SA=0.457 $m^2$ | Ocean water ($O_2$) | 0.098 | Immobilized Mediator | 5 Ω | Lowy *et al.* (2006) |
| GCC modified anode SA=0.183 $m^2$ | Marine sediment | Graphite disks SA=0.457 $m^2$ | Ocean water ($O_2$) | 0.105 | Immobilized Mediator | 5 Ω | Lowy *et al.* (2006) |
| Graphite Disk SA=0.183 $m^2$ | Marine sediment | Graphite Disk SA=0.183 $m^2$ | Ocean water (O2) | 0.028 | N/A | 14 Ω | Tender *et al.* (2002) |
| Carbon SA=0.005 $m^2$ | Synechocystis PCC-6803 biofilm | Carbon (+Pt) SA=0.00096 $m^2$ | Water ($O_2$) | 1.56 | Two chambered (HNQ) | 1000 Ω | Zou *et al.* (2009) |